
Earth Pressure Calculation

**according to 'Eurocode 7' using empiric
soil values and showing misinterpretations
in the calculation basics**

and

**a new 'Earth Pressure Theory'
with real soil characteristics,
and based on pure physics**

Issue
April 2015

Norbert Giesler
Schilfweg 11
D-34253 Lohfelden

Table of contents		Page
1	Introduction	1
1.1	General situation	2
1.2	Task in hand	3
1.3	Study structure	4
1.4	Materials and methods	6
2	Earth pressure theses and their appraisal	9
2.1	Definitions of earth pressure teachings	9
2.2	Definitions of New Earth Pressure Theory	10
2.3	Theses of teachings and New Theory in comparison	15
2.3.1	Physical values of inclined plane and wedge	16
2.3.2	Expansion of physical plane rules	19
2.3.3	Coulomb's earth pressure theory	23
2.3.4	Mohr-Coulomb failure criterion	24
2.3.5	Comparison: Coulomb's theory and failure criterion	28
2.3.6	Comparison: Mohr's stress theory and failure criterion	31
2.3.7	Force distribution acc. to physical plane and failure criterion	32
2.3.8	Earth pressure force acc. to failure criterion and Coulomb (calculation example)	34
2.4	Determining the natural inclination and shear angles of soils	37
2.4.1	Formation of a natural shear plane in sand, Test 1	38
2.4.2	Formation of a natural inclined plane in sand, Test 2	40
2.4.3	Compaction of dry sand by adding water, Test 3	41
2.5	Determination of inclination and shear angle under load	43
2.6	Determination of inclination and shear angle with soil loosening	47
2.7	Changed angles due to cohesion and/or wall friction	48
2.8	Flow condition and earth pressure, Tests 4 and 5	50
2.9	Silo theory and earth pressure	52
3	Calculation of soil properties	54
3.1	General information on soil properties	54
3.1.1	Calculating the properties of dry soils	57
3.1.2	Calculating the properties of wet soils	59
3.1.3	Calculating the properties of wet soils with soil compaction	62
3.1.4	Calculating the properties of moist soils	63
3.1.5	Formation of a shear plane in moist basalt grit, Test 6	64
3.2	General information on soils under water	67
3.2.1	Calculating the properties of wet soils under water	68
3.2.2	Experiment with wet basalt grit under water, Test 7	70
3.2.3	Calculating the properties of moist soils under water	76
3.2.4	Experiment with moist basalt grit under water, Test 8	79
3.3	Soil parameters summarized in a table	88
3.4	Conclusions for Chapter 3	90
4	Soil behaviour and force build-up according to the New Theory	92
4.1	General information on the New Earth Pressure Theory	92
4.2	Determining the load bearing capacity of soils – earth resistance	93

4.2.1	Load capacity of soils with one-sided force distribution	95
4.2.2	Load capacity of soils with polydirectional force distribution	97
4.2.3	Load capacity of foundations with permissible soil subsidence	99
4.2.4	Load capacity of foundations with anchoring depths	102
4.3	Earth pressure in soils with inclined surface	104
4.3.1	Shear plane in soils with inclined surface, Test 9	104
4.3.2	Forces in dry soils with inclined surface	114
4.3.3	Influence of loads on soils with inclined surface	117
4.3.4	Determination of forces and angles in Test 5	120
4.3.5	Conclusions for Section 4.3	126
4.4	Forces in soils with inclined surface under water	126
4.4.1	Properties of wet soil under water	127
4.4.2	Properties of dry soil above water	128
4.4.3	Determination of force against a fictitious perpendicular wall	131
4.5	Soil sliding on inclined/level rock layer, Test 10	133
4.6	Soil sliding on rock layer with continuous incline	137
4.7	Earth pressure on underground pipes and tunnels	142
4.8	Earth pressure on single piles	148
4.9	Conclusions for Chapter 4	158
5	Accidents caused by earth movements	160
5.1	Collapse of Cologne's Historic Archive in 2009	160
5.1.1	Assumptions on tunnel cross-section and substratum	161
5.1.1.1	Load assumptions about the archive and residential building	162
5.1.1.2	Assumptions for soil properties	165
5.1.2	Load on the substratum due to the building weights	167
5.1.3	Forces from the substratum against the tunnel cross-section	171
5.1.4	Forces from archive and substratum against right-hand slotted wall	174
5.1.5	Formation of earth blocks to determine the uplift forces	176
5.1.6	Determination of uplift forces against the tunnel floor	181
5.1.7	Determination of horizontal earth pressure forces under water	186
5.1.8	Balancing the uplift forces with the tunnel's weight pressures	188
5.1.9	Conclusions about collapse of the archive in Cologne	193
5.2	Landslide into the Concordia lake near Nachterstedt in 2009	195
5.2.1	Filling material and its properties	197
5.2.2	Adaptation of loads in soils under water	203
5.2.3	Location of shear planes in the respective Stations	204
5.2.4	Result and conclusions for the landslide in Nachterstedt	223
6	Summary	226
6.1	Basics of earth pressure teachings and New Theory	226
6.2	Force determination and force distribution	227
6.3	Soil properties and their determination	228
6.4	Applicability of the New Earth Pressure Theory	229
	Terminology of the New Earth Pressure Theory	231
	References	234
	Tables	238

List of illustrations

The list uses the terms 'figure' (Fig.) and 'picture' (Pict.), whereby the author's own diagrams and photographs are also described as 'Fig.'. Graphics that have been cited or taken from references [1] are described as 'Pictures'. Coulomb uses the term 'Fig.' in his sketch sheet.

	List of illustrations	Page
Fig. 1	Glass container with dimensions for the test series.	7
Fig. 2	Network of vertical and horizontal earth stresses.	12
Fig. 3	Earth blocks with active and reactive force areas.	12
Fig. 4	Inclined plane with force distribution [15].	17
Fig. 5	Physical wedge with force distribution [15].	17
Fig. 6	Location of centers of gravity S1 to S4 in the earth block or wedge area.	19
Fig. 7	Force descriptions and directions in the earth block or wedge area.	19
Fig. 8	Portrait of Monsieur de Coulomb.	23
Fig. 9	Sketch sheet with Coulomb's earth pressure theory.	23
Diagr. 7	Coulomb's force arrangement within an earth wedge.	25
Pict. P05.50	Section and force polygon at one point (earth pressure teaching).	25
Pict. I06.10	Mohr's stress circles in soil with cohesion (earth pressure teaching).	26
Pict. I06.40	Shear surface(s) and direction in triaxial test (earth pressure teaching).	26
Pict. I06.20	Relationship between shear and failure line (earth pressure teaching).	27
Pict. I01.40	Main stresses and their position to axis 0–B (earth pressure teaching).	27
Pict. I01.70	Physical plane and Mohr's stress circle (earth pressure teaching).	28
Fig. 10	Earth block with positions of active and reactive force areas A_o and A_u .	29
Fig. 11	Earth block with area of downhill force, and position of earth pressure force H_f .	29
Fig. 12	Earth block with force areas, forces, and their direction (New Theory).	29
Pict. I01.70a	Resolution of normal and downhill forces (Coulomb).	30
Pict. I01.70b	Stress circle with forces inserted by the author.	30
Pict. I03.20	Friction of a body on an inclined plane (earth pressure teaching).	33
Pict. I03.30	Overcoming friction on an inclined plane (earth pressure teaching).	33
Fig. 13	Area of earth pressure force H_f with thrust height h_v (new).	36
Fig. 14	Downhill force T rotated on inclined plane (teaching).	36
Fig. 15	Test 1: Determination of natural shear plane with sand	39
Fig. 16	Inclined plane with angle β , and assignment of areas A_o and A_u .	40
Fig. 17	Assignment of inclination and shear plane and their angles β and s .	40
Fig. 18	Test 2: Determination of natural inclined plane with sand.	41
Fig. 19	Test 3: Sand compaction by adding water.	42
Fig. 20	Test 3: Creation of voids in the compacted sand.	42
Fig. 21	Test 3: Loss of sand volume due to the addition of water.	42
Pict. P05.60	Convex curvature of fracture plane with positive wall friction.	43
Pict. P05.120	Earth pressure stresses from loaded ground surface (teaching).	44

	List of illustrations	Page
Fig. 22	Change of inclination angle due to load on surface (theory).	44
Fig. 23	Change of inclination angle due to horizontal rock layer (theory).	46
Fig. 24	Change of inclination angle due to pressure (theory).	46
Fig. 25	As above, with different height/side ratio of the cylinder.	46
Fig. 26	Change of shear angles due to soil loosening (volume increase).	48
Fig. 27	Change of inclination angle due to volume increase (New Theory).	48
Pict. P03.20	Inclined supporting area with angle α and stress σ_α (earth pressure teaching).	49
Fig. 28	Inclined supporting area and force distribution (New Theory).	49
Fig. 29	Test 4: Glass container filled with layered basalt grit.	50
Fig. 30	Test 4: Sliding of basalt grit – obstruction with paper strips.	50
Fig. 31	Test 4: Sliding of basalt grit without obstructions.	51
Fig. 32	Test 5: Sliding with alternate layers of basalt grit and sand.	51
Fig. 33	Semicircle of soil types and the soil's force meters (New Theory).	55
Fig. 34	Equilibrium in the ground due to opposing forces (New Theory).	56
Fig. 35	Soil properties with solids volume V_f and basic value $V_{f90} = 1,00 \text{ m}^3$.	58
Fig. 36	Soil properties with pore volume $V_l = 0,01 \dots 0,99 \text{ m}^3$.	58
Fig. 37	Soil properties through addition of $V_f + V_l$ and standardization.	58
Figs. 38/39	Change of soil properties due to water absorption.	60
Fig. 40	Volumes and angle β of soils in dry and wet states.	61
Fig. 41	Pore volume V_l divided into V_{lt} and V_{ln} .	63
Fig. 42	Test 6: Glass container filled with moist basalt grit.	65
Fig. 43	Test 6: Formation of shear plane in moist basalt grit.	66
Fig. 44	Cube of wet soil under water, with indication of volume.	69
Fig. 45	Volumes of wet soil under water after standardization.	70
Fig. 46	Test 7: Glass container with wet basalt grit under water.	71
Fig. 47	Test 7: Compaction of wet basalt grit due to water.	71
Fig. 48	Test 7: Location of shear plane in wet grit under water.	71
Fig. 49	Test 8: Location of inclined plane in wet grit under water.	73
Fig. 50	Test 8: Comparison: measured and calculated soil movement.	75
Fig. 51	Test 8: Behaviour of basalt grit after removal of water.	77
Fig. 52	Cube of soil with volumes of moist soil above water (New Theory).	78
Fig. 53	Soil band with volumes of moist soil under water (New Theory).	79
Fig. 54	Test 9: Glass container with moist basalt grit under water.	79
Fig. 55	Cube of soil with volumes of moist soil under water.	83
Fig. 56	Test 9: Shear plane location of the moist grit under water.	84
Fig. 57	Test 9: Dimensions of moist grit under water.	84
Fig. 58	Test 9: Dependence due to unoccupied pore volume.	85
Fig. 59	Test 9: Location of filling & removal areas after soil movement.	86
Fig. 60	Comparison of horizontal forces in dry and wet soils.	90
Fig. 61	Rock column with height h^* , width b^* , and inclination angle β^* .	94

	List of illustrations	Page
Fig. 62	Transition of the rock column into the force areas Aa' and Ar' of a soil.	94
Fig. 63	Force fields of different soil types in the ground (limit ranges).	94
Fig. 64	As a load, a soil column requires the same column in the ground for load transfer.	96
Fig. 65	Conversion of the soil column under angle β into a force area	96
Fig. 66	Load test conducted by Degebo [A] with quadrilateral force distribution.	97
Figs. 67 - 69	Plan views of different force distributions in the ground.	97
Fig. 70	Section shows force fields under load with bilateral spreading.	99
Fig. 71	Section shows force fields, as above, with permissible soil subsidence.	101
Fig. 72	Force fields, as above, on foundation with anchoring depth.	103
Fig. 73	Test 9.1: Starting basis: Sand body with horizontal surface.	106
Fig. 74	Test 9.1: Location of natural shear plane of the sand.	106
Fig. 75	Test 9.1: Filling & removal area after soil movement.	107
Fig. 76	Test 9.2: Sand body with partially inclined surface.	108
Fig. 77	Test 9.2: As above, after soil movement and with shear plane.	108
Fig. 78	Test 9.2: Characteristics for determining shear plane with loads.	110
Fig. 79	Test 9.3: Sand body with continuously inclined surface.	112
Fig. 80	Test 9.3: Shear plane with continuously inclined surface.	112
Fig. 81	Test 9.3: As above, characteristics for determining the shear plane.	113
Fig. 82	Test 9.3: As above, with force insertion with/without load.	115
Fig. 83	Load in rectangular form (distributed load) on an earth block.	117
Figs. 84/85	Load on an earth block with representation of forces and force areas.	118
Figs. 86/87	Wedge-shaped load in an earth block with upward-sloping surface.	119
Figs. 88/89	Wedge-shaped load in an earth block with downward-sloping surface.	119
Fig. 90	Treatment of loads with different soil beddings.	122
Fig. 91	Adaptation of inclined plane with different soil beddings.	123
Fig. 92	Surface loads through soil on soil layer in groundwater.	127
Fig. 93	As above, adaptation of surface load via soil densities.	129
Fig. 94	As above, location of shear plane and filling & removal area.	130
Fig. 95	As above, force areas and forces against the fictitious wall.	132
Fig. 96	Test 10: Sand body on inclined plane with horizontal surface.	133
Fig. 97	Test 10: As above, but after the sand has slipped.	135
Fig. 98	Test 10: Concave shear plane due to height offset on reference axis.	136
Fig. 99	Test 10: Lowering of shear plane with inclined basal plane.	138
Fig. 100	Shear plane with load on continuously inclined basal plane.	140
Fig. 101	Force areas and forces on continuously inclined basal plane.	141
Fig. 102	Force areas and forces against a pipe or tunnel cross-section.	142
Fig. 103	As above, force areas with reduced pipe or tunnel depth.	143
Fig. 104	As above, force areas with increased pipe or tunnel depth.	143
Fig. 105	Test 11: Behaviour of unequal soil types on a common wall.	144
Fig. 106	Force area to determine the mainly horizontal pipe load.	145

List of illustrations

Fig. 107	Force areas of vertical pipe load and pipe bedding.	147
Fig. 108	Soil column to determine force against pile, adapted to reference axis.	150
Fig. 109	Expansion of soil column due to adaptation of force fields on pile skin.	152
Fig. 110	Representation of force fields and forces against the pile skin.	155
Fig. 111	Street view of the archive and the neighbouring residential building.	162
Fig. 112	Force fields in the ground to disperse the weight of the archive.	168
Fig. 113	Force fields in soil to disperse the weight of the residential building.	170
Fig. 114	Force fields from the ground against slotted walls, without building loads.	171
Fig. 115	Force fields combined with building and earth loads against the tunnel.	174
Fig. 116	Earth blocks to determine uplift forces against the tunnel floor.	176
Fig. 117	Weight forces of the blocks (left/center) to determine A-force R_{vl} .	182
Fig. 118	Weight forces of the blocks (right/center) to determine A-force R_{vr} .	183
Fig. 119	Superposition of force areas of uplift forces R_{vl} and R_{vr} .	185
Fig. 120	Representation of forces and their locations against the tunnel cross-section.	189
Fig. 121	Representation of possible fractures in right-hand slotted wall.	192
Fig. 122	Open cast mine pit before flooding.	195
Fig. 123	Cube of soil of clay-sand mix in dry state.	197
Fig. 124	As above, but as moist soil with low water absorption.	198
Fig. 125	Cube of soil, as above, but after spreading due to water absorption.	198
Fig. 126	Cube of soil, as above, but volume of the moist compacted soil.	198
Fig. 127	Cube of wet soil with volume increase.	201
Fig. 128	Cube of wet soil with loss of height due to water absorption.	201
Fig. 129	As above, but volumes after compaction and water absorption.	201
Fig. 130	Band of wet soil under water before standardization.	202
Fig. 131	Cube of wet soil under water after standardization.	202
Fig. 132	Band of wet soil under water with load and uplift.	204
Fig. 133	Profile section of landslide in Nachterstedt (before/after).	205
Fig. 134	Location and angle se of shear plane under load in Stat. 2405.	208
Fig. 135	Location and angle se of shear plane under load in Stat. 2330.	211
Fig. 136	Slide-prone earth mass, with forces and force meters in Stat. 2330.	212
Fig. 137	Location and angle se of shear plane under load in Stat. 2230.	214
Fig. 138	Slide-prone earth mass, with forces and force meters in Stat. 2230.	216
Fig. 139	Location and angle se of shear plane under load in Stat. 2123.	218
Fig. 140	Slide-prone earth mass, with forces and force meters in Stat. 2123.	219
Fig. 141	Location and angle se of shear plane under load in Stat. 2030.	221
Fig. 142	Slide-prone earth mass, with forces and force meters in Stat. 2030.	222
Fig. 143	Terrain level after the landslide, and the calculated slide plane.	224

List of symbols

As various systems are examined in this study, the terminology used can quickly become confusing. Therefore, and in order to explain the new system (the New Earth Pressure Theory) clearly, a different nomenclature has been introduced, which is listed below as reference. Hereby, the conventional use of subscripts and superscripts is avoided, and the respective constituent parts are shown in *italics* to differentiate them clearly from current teaching, and are written consecutively as a kind of assembly set.

Name	Unit	Terminology
		Terms and/or letter extensions:
<i>t</i>		Dry soil (dried)
<i>i</i>		Moist soil (infiltrated with water, partially saturated)
<i>n</i>		Wet soil (pores completely filled with water)
<i>w</i>		Water in soil or soil under water (with uplift)
<i>o, u</i>		Localization top (o) and bottom (u)
<i>r, l</i>		Localization right and left
		Wedge dimensions
<i>a</i>	m	Calculation depth (e.g. in direction of trench)
<i>h</i>	m	Wedge height or calculation height
<i>he</i>	m	Height of a load or substitute load
<i>hl</i>	m	Calculation height plus load height
<i>ho</i>	m	Upper part of calculation height
<i>hu</i>	m	Lower part of calculation height
<i>hm</i>	m	Mean height
<i>b</i>	m	Wedge width or calculation width
<i>be</i>	m	Wedge width of a load or substitute load
<i>bo</i>	m	Upper width
<i>bor</i>	m	Right upper width
<i>bu</i>	m	Lower width
<i>bur</i>	m	Right lower width
$\Delta b, \Delta h$	m	Partial width/partial height
<i>bm</i>	m	Mean width
<i>l</i>	m	Length of inclined plane
		Wedge values
<i>A</i>	m ²	Wedge area
<i>Ae</i>	m ²	Area of load or substitute load
<i>Aa</i>	m ²	Active load area
<i>Ar</i>	m ²	Reactive load area
<i>Aae</i>	m ²	Active load area with load
<i>Are</i>	m ²	Reactive load area with load
<i>V</i>	m ³	Total volume
<i>Vo</i>	m ³	Initial volume
ΔV	m ³	Partial volume
ΣV	m ³	Sum of volumes
		Angles
β	°	Inclination angle (angle of internal soil friction)
β_e	°	Inclination angle under load

Name	Unit	Abbreviations, terms
β_t	°	Inclination angle of dry soil
β_i	°	Inclination angle of moist soil
β_n	°	Inclination angle of wet soil
β_w	°	Inclination angle of soil under water
β_{iw}		Inclination angle of moist soil under water
β_{nw}		Inclination angle of wet soil under water
μ		Friction value: $\mu = \tan \beta_t$
s	°	Shear angle: $\tan s = (\tan \beta)/2$
s'	°	Slope plane
s_t	°	Shear angle of dry soil
s_i	°	Shear angle of moist soil
s_n	°	Shear angle of wet soil
s_w	°	Shear angle of dry soil under water
s_{iw}		Shear angle of moist soil under water
s_{nw}		Shear angle of wet soil under water
β_s	°	Angle of repose
β_{st}	°	Angle of repose of dry soil
β_{sn}	°	Angle of repose of wet soil
β_{sw}	°	Angle of repose of soil under water
		Volumes
V_p	m ³	Volume of a soil cube ($V_p = 1,00 \text{ m}^3$)
V_{f90}	m ³	Volume of rock ($V_{f90} = 1,00 \text{ m}^3$)
V_f	m ³	Solids volume within a soil type
V_l	m ³	Pore volume within a soil type
V_{lt}	m ³	Pore volume, not filled with water (dry)
V_{li}	m ³	Pore volume, partially filled with water (moist)
V_{ln}	m ³	Pore volume, completely filled with water (wet)
V_w	m ³	Volume of water within a soil type
V_{nw}	m ³	Pore volume of wet soil under water
V_{fn}	m ³	Fictitious solids volume of a wet soil
V_{fi}	m ³	Fictitious solids volume of a moist soil
V_{fw}	m ³	Solids volume of soil $V_{fw} = 2 \cdot V_f/3$
V_{fa}	m ³	Volume of uplifts $V_{fa} = 1 \cdot V_f/3$
		Soil density / parts by weight
p_{90}	t/m ³	Density of rock without pores (hard basalt $p_{90} = 3,0 \text{ t/m}^3$)
p_w	t/m ³	Density of water ($p_w = 1,0 \text{ t/m}^3$)
P_b	t/m ³	Density of concrete ($P_b = 2,0$ up to $2,5 \text{ t/m}^3$)
p_{tg}	t/m ³	Density of dry soil (pores filled with gas/air)
p_{wg}	t/m ³	Parts by weight of water in pores
p_{ig}	t/m ³	Density of moist soil
p_{iwg}	t/m ³	Density of moist soil under water
p_{nwg}	t/m ³	Density of wet soil under water

Name	Unit	Abbreviations, terms		
<i>dB</i>	% by vol.	Compaction density of soil		
<i>g</i>	m/s ²	Gravity force → $g = 9,807 \text{ m/s}^2$		
		Forces in earth wedge	Force meter	
<i>gi</i>	kN/m ²	Force index (conversion factor of force to force meters)		
<i>G</i>	kN	Weight (subscripts: <i>t, n, w, l</i> and <i>r</i>)	<i>gh</i>	m (dm)
<i>Ga</i>	kN	Uplift force	<i>ga</i>	m
<i>Ge</i>	kN	Weight of a load	<i>he</i>	m
<i>Ee</i>	t	Substitute load	<i>e</i>	m
<i>FN</i>	kN	Normal force in <i>standing</i> earth wedge	<i>fn</i>	m
<i>FH</i>	kN	Downhill force in <i>standing</i> earth wedge	<i>fh</i>	m
<i>Nv</i>	kN	Vertical portion of normal force in <i>standing</i> earth wedge	<i>nv</i>	m
<i>Hv</i>	kN	Vertical portion of downhill force, else as above	<i>hv</i>	m
<i>Hn</i>	kN	Horizontal portion of normal force, else as above	<i>hn</i>	m
<i>Hf</i>	kN	Horizontal portion of downhill force, as above	<i>hf</i>	m
<i>FR</i>	kN	Frictional force	<i>fr</i>	m
<i>FT</i>	kN	Normal force in <i>lying</i> earth wedge	<i>ft</i>	m
<i>FL(FS)</i>	kN	Downhill force in <i>lying</i> earth wedge	<i>fl (fs)</i>	m
<i>Lv</i>	kN	Vertical portion of normal force in <i>lying</i> earth wedge	<i>lv</i>	m
<i>Ln</i>	kN	Vertical portion of downhill force, else as above	<i>ln</i>	m
<i>Lhn</i>	kN	Horizontal portion of normal force, else as above	<i>lhn</i>	m
<i>Lh</i>	kN	Horizontal portion of downhill force, as above	<i>lh</i>	m
<i>Hm</i>	kN	Mean horizontal forces (subscripts: <i>t, n, w, l</i> and <i>r</i>)	<i>hm</i>	m
<i>M</i>	kNm	Moment		
<i>Mb</i>	kNm	Moment around Point B		
		Location terms		
OKG		Top edge of terrain		
OK		Top edge		
UK		Bottom edge		
VK		Front edge		
HK		Rear edge		
WSp		Water plane		
Stat		Station		
		Institutions		
DLR		Deutsches Zentrum für Luft- und Raumfahrt		
DWA		Deutsche Vereinigung für Wasserwirtschaft, Abwasser und Abfall e.V.		
DVWK		Deutscher Verband für Wasserwirtschaft und Kulturbau		
LMBV		Lausitzer u. Mitteldeutsche Bergbau-Verwaltungsgesellschaft		

Legal reservation

The author reserves all rights of this document, also those of translations, reprints, and reproductions, in whole or in part. Without the author's consent, no part of this document may be processed, copied, reproduced or distributed in any form.

1 Introduction

DIN standards accompany many construction activities – from the draft, through execution and up to invoicing. They are seen as "generally accepted engineering practice" and are sometimes specified as legal rules, or their observance is compulsory in lists of services/construction contracts. Their technical specifications might be helpful when handling construction tasks, but the author's professional experience in the construction business also led to the realization that even the strictest adherence to the standards can lead to structural damage. Especially when investigating damage to newly laid sewage pipes – the author's own field of competence – it was frequently established that damage was often linked to deficiencies in the standards for earth pressure determination. Based on these findings, the author has pointed out the facts in corresponding trade journals [16 and 17] in the past. Unfortunately, the compilers of these specifications ignored these indications of possible deficiencies in the standards for earth pressure calculation. Consequently, there is good reason to point out the recognized discrepancies in current calculations based on Eurocode 7 (EC7) and DIN 4085, and to prepare a study for discussion by experts.

As both of the above standards are based on the writings of the chair for Soil Mechanics, Foundation Engineering, Rock Mechanics and Tunneling at the Institute for Construction and Geotechnology of the Technical University of Munich (TUM) [1] the study primarily points out the discrepancies in the current teachings. Regarding the content and structure of the standards, the chair points out the significant influence of the German Geotechnical Society (Deutsche Gesellschaft für Geotechnik e.V.) with its "Grundlagen geotechnischer Entwürfe und Ausführungen" (Basics of geotechnical drafts and execution) [1: page J.1f.].

The predominant doctrine states that earth pressure builds up as horizontal stress only when the soil is subjected to a vertical load, or if the wall supporting the soil moves. Usually, this horizontal stress is calculated as earth pressure force Ea by means of the soil's body or weight G (F). Force G encompasses the earth mass of the wedge area, which is limited by the perpendicular rear wall surface, the terrain surface, the soil's natural inclination or fracture plane, and calculation depth a . Currently, Mohr-Coulomb's failure criterion is used for stress determinations.

The teachings claim that this calculation method conforms to the theories of Coulomb (1736-1806), Christian Otto Mohr (1835-1918), and the basics of physics. As the teachings support their earth pressure calculations on empiric factors and empiric soil parameters – contrary to the New Theory – there is reason to review the analogies indicated by the teachings, and to replace the empiric values with provable soil parameters. In particular, these checks must be based on the basics of physics, on Newton's axioms, the specifications for determining spring force and frictional force, and the rules governing "inclined planes" and wedges.

1.1 General situation

Our geological environment includes countless structures that are subjected to earth pressure, e.g. supporting walls, underground pipes, tunnel runs, and many more. Moreover, the soil can absorb additional water, which can change its properties and thereby cause hillsides to slip. There are frequent reports in the media about structural and subsidence damage, whereby it can be assumed that only spectacular events find their way into the news. There is no literature containing official data about the amount of annual damage. Alone for the very small area of public sewage networks, the ATV-DVWK survey on the "Status of sewer systems in Germany – Summary" shows an annual renovation need of some 1,64 billion Euros, and an investment backlog of about 45 billion Euros. Considering that the privately operated sewage systems are estimated to be twice as long as the public networks [2], the need for renovation could also be twice as high. A survey by DWA in 2009 shows that the renovation costs for public sewers have remained at the same level [3]. As the above data on damage were collected on a voluntary basis, and as no department head will willingly admit damage in his area of responsibility, these figures could probably be several times higher. If one adds the costs for damage repair in the other sectors of construction work (civil engineering, road construction, and engineering construction) to the costs for sewer renewal, an annual damage sum of some 12 to 15 billion Euros can be assumed to be realistic. Who hasn't heard of the disconcerting accidents in 2009, in particular the collapse of the Historic Archive in Cologne and the huge landslide in Nachterstedt? Apart from the enormous material damage, the fatalities should be enough reason to critically question the reliability of current earth pressure calculations and the

associated rules and standards. This study examines both accidents, and shows that the causes can be determined entirely on the basis of pure physics, and without using empiric soil characteristics or factors.

1.2 Task in hand

Possible discrepancies in the rules and standards for earth pressure determination have already been pointed out in scientific papers [16] and [17]. Therefore, the task of explicitly naming the individual controversies in earth pressure teachings remains, and to show how construction and structural damage can be avoided to a great extent in future. During the preparatory work for this study, it became clear that it is simpler to abandon the originally intended selective examination of the doctrines due to the contradictions found in the basics of current teachings, and to work out a New Earth Pressure Theory instead. This New Theory is based on spatial force fields in the ground, which are under permanent stress. Natural or artificial interventions in the equilibrium of earth forces – e.g. the application of loads onto the earth surface, or excavations – change the stress pattern in the ground. In the course of re-establishing equilibrium, the properties of the affected soils, such as inclination angle β and density, are changed.

Because the advocates of current earth pressure teachings [1] claim that their calculation basics follow Coulomb's and Mohr's theories as well as the laws of physics (inclined plane), this study primarily examines the stated consensus with rules and standards. For this, facts from the multi-phase system of solid-state physics are also applied, with which the volumes of solids, liquids (water) and gases (air) are put into relation with the total volume [4: page 14ff.; 6: pages 2.2–1 and 8: page 5].

The involvement with solid-state physics led to an extension of this system, so that it is now possible to demonstrate the physical dependencies between the properties of soils and water. With the help of soil volume and weight, extension of the system permitted the density, inclination angle, shear angle and other properties of dry, moist (partially saturated) and wet (fully saturated) soils above and below a water plane to be determined. By means of the soil properties, changing force fields in the ground as well as soil movements can be verified and calculated. Another task was to investigate possible discrepancies in current earth pressure teachings by means of own experiments. For this

purpose, tests were carried out with different soil types and water in a glass container. Hereby, the following can be shown: If a soil property is changed through external interventions (compaction or loosening), also the other properties such as inclination angle, shear angle, and the load bearing capacity of soils are changed. The realization that every soil type forms its own inclination angle – which can lie between $\beta = 0,6^\circ$ and $\sim 89,4^\circ$ – gave reason to extend the physical plane's elevation angle by the range $\beta > 45^\circ$ [16]. Here one can see that soil resting on its inclined plane is clamped on all sides by the surrounding ground, and is therefore unable to slide or tip on the inclined plane. Solid bodies that are placed on an "inclined plane" do not fulfill the above properties, and will only start moving on a steeper plane. Time factors, thermal conditions, and water movements (waves) are not taken into account when determining soil properties.

After comparing the earth pressure teachings with the New Earth Pressure Theory, the task in hand was extended to prove that the results of the conducted experiments can be applied in all areas of construction engineering. To provide this proof, the calculations to determine the cause of damage that led to the collapse of the Historic Archive in Cologne and to the landslide in Nachterstedt in 2009 were selected. Both accidents have been dealt with extensively in the media and the Internet, whereby a newspaper recently admonished the absence of final conclusions about the causes [13]. The absence of the requested expert opinions on the cause of the accidents is understandable, if one considers the discrepancies in the specifications of earth pressure teachings. Insofar as expert opinions exist, they can only have been prepared using the knowledge provided by current rules, standards, and teachings. And finally, this study shows that the New Earth Pressure Theory can be represented as a closed calculation system, with which the pure basics of physics can be used to determine the soil properties as well as the forces in the ground [15].

1.3 Study structure

First, the definitions of earth pressure teachings and the New Earth Pressure Theory are described, and the different theses discussed and compared. Because the teachings and the New Theory both make use of the rules and standards for the distribution of earth stresses & forces in inclined planes, it should be noted that different soil types generate different inclination angles

from $\beta = 89,4^\circ$ up to $\beta = 0,6^\circ$. Consequently, it is not realistic to limit the elevation angle of the inclined plane to $\alpha < 45^\circ$ for earth pressure determination. While the teachings stick to the specifications for inclined planes, the New Theory cancels the limitation of $\alpha < 45^\circ$. Hereby, the New Theory shows that every soil type creates a fracture/inclined plane in the ground below its inclination angle β , but because of the polydirectional clamping effect within the ground, nothing can slide or tip on this plane. To enable the teachings to disassemble the major stresses and forces into vectorial components by means of the specifications for inclined planes, they rotate the stress pattern of the soil body into the position of the inclined plane. The demonstrated new approach to stress or force distribution permits the differences between Coulomb's earth pressure theory and Mohr-Coulomb's failure criterion as presented by the teachings to be examined. Similarly, the analogy between Mohr's stress theory and the failure criterion as presented by the teachings is discussed. While comparing the theories, the different descriptions of planes and linear slopes were found to be disturbing. As a remedial measure, test setups with different soil types and soil conditions were used to determine the natural position of the inclined plane and shear plane in the respective soil bodies. The plane angles change if the soil absorbs or discharges pore water, the soil is compacted or loosened, or stressed by external forces/loads. Also the significance and dependencies of the angles for the respective calculation systems of current earth pressure teachings and the New Earth Pressure Theory is examined as appropriate (see physical plane and failure criterion in Section 2.3.7, page 32ff, and the new terminology on page 231).

After comparing the different earth pressure theories, a possible extension for the current multi-phase system of solid-state physics prepared by the author is presented. This modification, which is backed by test setups, permits soil properties such as density and angles to be determined exactly by means of dry density and the water absorbed by the soil (see Chapter 3). The conformance of calculated and real soil properties of different soils is tested with the help of experiments in the glass container described below.

1.4 Materials and methods

Today's teachings define Coulomb's earth pressure theory and Mohr's stress theory as the Mohr-Coulomb failure criterion. This criterion forms the basis of previous earth pressure determinations in Germany [1: page I.3-5 and 1: page 7ff.]. Therefore, it must be clarified which part of the Mohr-Coulomb failure criterion obeys Coulomb's earth pressure theory (Section 2.3.3, page 23) and which part obeys Mohr's stress circle [7: page 385-412]. This clarification is considered to have top priority, because Coulomb and the teachings determine weight G – which is required for an earth pressure calculation – in the same way by means of the wedge area behind the perpendicular wall. But when calculating earth forces or stresses, different approaches are used. While Coulomb marks the earth forces in the surface of the weight (see Section 2.3.3, Fig. 9, page 23), the teachings rotate the earth wedge in order to calculate the earth stresses against the perpendicular wall. Moreover, the teachings see a stress equilibrium in the ground, which they try to eliminate by introducing the factor K_0 [1: page P.3ff.]. By mirroring the wedge area, the teachings obtain a concentration of forces G , Q and E_a at one point of the inclined plane (third point of failure line) and therefore claim to be able to calculate earth stresses from the inclined plane. The permissibility of stress rotation is justified with Mohr's stress theory, according to which main stresses can be varied by means of transformation equations, enabling the new values to be determined easily within the stress circle [1: page I.4ff.].

Additional stresses are seen by the teachings in a cohesion and in a wall friction between the wall and the soil behind the wall, which can define force flow, force value, and force direction in the ground. Current earth pressure calculation is described in DIN 4085. The factors K_0 , K_a and other empiric soil characteristics can be taken from the tables in DIN 18196, DIN 18300, and DIN 1054.

The study also examines the questions of whether the teachings' theses agree with Mohr-Coulomb's failure criterion, and whether earth pressure determination according to the failure criterion conforms to the physical law of the inclined plane [15: page 55ff.]. In order to provide well-founded answers to these questions, the previously mentioned experiments were carried out in the glass container shown below in Fig. 1.

The container, which can be divided into two chambers by a central glass pane, has the following inside dimensions: Overall height $hk = 2,95$ dm, overall width $b = 4,88$ dm, depth $a = 2,90$ dm, widths of chambers $bk_1 = 2,44$ dm and $bk_2 = 2,40$ dm, width of the removable glass pane $bg = 0,04$ dm (which is located between guides in the container). The joints between the separating pane and the glass container are not sealed, so that water filled into one chamber can seep into the other chamber. The time required for this infiltration can be influenced by raising the separating pane. With a total content of $V = 41,75$ dm³, the glass container provides several times the volume specified in DIN 18137-1 /-2 for soil body tests, with which measurements of shear strength and shear angle φ are conducted. The above DIN standard describes cylinders with volume $V = 0,87$ dm³ (\varnothing 1,05 dm and height 1,00 dm) and volume $V = 2,21$ dm³ (\varnothing 1,50 dm and height 1,25 dm). When comparing the volumes, the measurement results obtained with the test setup in Fig. 1 are likely to be more convincing than those obtained from experiments with smaller dimensions.

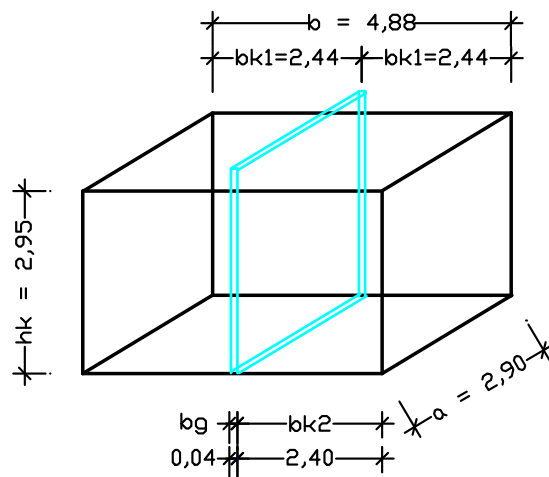


Fig. 1: Glass container and its dimensions.

The following materials were selected for the test setup in Fig. 1: Sand, loamy soil, bentonite granulate, basalt grit 0/3 mm, water, as well as cotton wool as easily formable soil. Volume and weight of the individual materials (except cotton wool) were determined before being inserted into the wider chamber. Soil mixtures were first prepared in a larger container, and then filled into the glass container. Before measuring the height, the soil surface was smoothed with a pointing trowel without applying any pressure. Hereby, the unavoidable formation of small unevennesses was accepted. As mentioned above, the water that was filled into the smaller chamber was able to infiltrate through the joints

between the container walls and the separating glass pane. During the experiments, the glass pane was removed abruptly. The planes created by the slipping soil were measured, and the measurement values compared with the heights, widths, and angles previously calculated from the volumes and weights of the soil.

To prove that the results are comparable, three tests per experiment were conducted with different soil types. After increasing evidence that the experimental results in the glass container coincided with the calculated results, subsequent experiments were usually limited to one test, and instead, the experiment was extended with different filling heights or soil body forms. About 50 tests were conducted in total, whereby unsuccessful photographs reduced the number of publishable test setups to 38. In particular, experiments enabled the natural inclination angle β of soils in dry, moist or wet state, as well as soils under water (groundwater level) to be determined. Moreover, by cross-linking the test results, i.e. transferring the properties of dry soils to moist or wet soils and vice-versa, additional data on general soil behaviour was collected.

In order to prove that the test results can be applied to larger earth construction projects, these basics were used to examine the causes of damage that might have led to the collapse of the Historic Archive in Cologne and to the landslide in Nachterstedt. Unfortunately, it was not possible to obtain documentation for these incidents from the responsible authorities. Only the Deutsche Zentrum für Luft- und Raumfahrt (DLR) [H] provided site plans and before/after sectional views to re-enact the landslide. Further information about the events was obtained from the media and photo galleries [11] and [12]. Regarding the subway excavation work in Cologne, constructional conclusions were drawn from the documentation [B, C, and D], and then used to calculate the probable cause of damage. Should the assumptions made require correction, they could be replaced with actual dimensions and/or facts, and the calculations repeated simply by third parties.

In order to represent the differences between current earth pressure teachings, Coulomb's and Mohr's theories, the physical laws, and the New Earth Pressure Theory, it was necessary to introduce new abbreviations and terminology for the New Theory, which differ from the existing terms. Following the hoped-for discussion about the New Earth Pressure Theory, the new terms can be adapted to the needs of geology, physics, and mathematics. As already mentioned, the new terminology is described on page 231ff.

2 Earth pressure theses and their appraisal

As an introduction to the subject of "earth pressure calculation", the basics of current teachings and the New Theory will first be described and then compared. Test setups will be used to show whether theory and practice can be harmonized.

2.1 Definitions of earth pressure teachings

The doctrine for earth pressure is summarized in the writings of the chair for Soil Mechanics, Foundation Engineering, Rock Mechanics and Tunneling at the Institute for Construction and Geotechnology of the Technical University of Munich (TUM) [1]. Accordingly, only one material stress – which is parallel to the perpendicular force direction – occurs in a soil on whose terrain surface loads or forces are applied, similar to a solid material such as rock, concrete, metal etc. Only if a yielding support is introduced, will a transverse contraction build up in the soil, i.e. in addition to the vertical stresses in the ground, also horizontal forces are generated. In order to mobilize the earth resistance of a soil behind a rigid wall, a parallel shift and an upper or base point rotation of the wall are assumed [1: page P.22ff.].

As opposed to a liquid, a soil that loses its lateral support from the wall will experience thrust stresses that reduce the soil's tendency to move accordingly [1: page P.1f.]. The horizontal pressure against the wall, which arises due to this mobilization of the ground, is described with the term "earth pressure". Normally, it does not act vertically on the loaded wall surface. Instead, and together with the surface normals, it forms an earth pressure inclination angle δ_a or δ_p that can – at best, and under optimum interlocking conditions between soil and wall – adopt the soil's friction angle φ' . As described in Janssen's silo theory, wall friction forces can arise between the soil and the wall surface, thereby reducing the earth pressure against the wall. If there is no relative shift between wall and soil, the resulting earth pressure is named minimum or active earth pressure E_a . The active earth pressure can be zero, if the soil (or rock) behind the wall exhibits an adequately high cohesion. The pressure required to shift the lateral support (wall) against the soil, is named maximum or passive earth pressure E_p . The at-rest earth pressure E_0 indicates the ground force of an undisturbed soil body, whose soil particles are not subject to any further struc-

tural changes after their sedimentation [1: page P.2]. The teachings do not see the equilibrium condition in the ground given only by soil density γ , particularly not in the horizontal stress plane. To compensate for this deficit, the teachings introduce limiting cases (such as active, increased active, and passive earth pressure), and assign an earth pressure factor K (K_a , K_0 , K_p) for the purpose of obtaining an equilibrium. Use of these limiting cases is reasoned by the previously described relative shift of the supporting wall, which accordingly must also create different earth pressures against the wall [1: page P.3ff.]. Apart from these limiting cases, the calculations of the teachings distinguish between cohesive and non-cohesive soils, whose properties are based on empirically established values (see DIN 18196:2006 [1: page J.3]). In this way, the teachings indicate that the soil value data (shear strength, influencing value, and density) are based on empiric vales [1: page I.19].

When determining forces, the teachings make use of the "Mohr-Coulomb failure criterion" and present this as a combination of Coulomb's and Mohr's theses. Moreover, the teachings point out the similarity of stress distributions according to the failure criterion and the physical plane. The thrust height of the earth pressure force against the loaded wall, as calculated from weight G , is fixed equally for all soil types at $1/3$ of wall height h by the teachings. The applied earth pressure inclination angle δ_a or δ_p can be influenced by the angle of the wall surface in contact with the soil, the wall friction angle, and soil cohesion (see [1: page I.4f. 1: page P.7ff. and page P.11f.]).

2.2 Definitions of New Earth Pressure Theory

The New Earth Pressure Theory is based on the multi-phase system of solid-state physics [4: S 14ff], [5: page 47ff], [6: page 2.2–1] and [8: page 5], whereby further findings are added to the previous representations for soil structure and soil behaviour, which resulted from the author's own experiments with different soils above and below water. As in the teachings, an idealized, pore-free rock material is assumed for the considerations, whose stress behaviour is the same as that of a solid material, e.g. concrete, metal etc. In to determine its properties, this rock material – which is only able to form stresses parallel to the perpendicular force direction when under load – is subjected to erosions that are intended to create pores in the rock. In natural surroundings, the rock particles removed by weather-based erosion would result in a reduction of rock

volume. But if one assumes that the rock particles and the resulting pores remain attached to the sound rock, the initial rock volume will be increased by the pore volume. If shown in time lapse, every erosion phase creates a new material structure, until the pore increase finally converts hard rock into the "dust/primordial dust" state. Consequently, all soil types can be considered as decomposition products of their original material, which differ from the original hard rock (e.g. basalt) due to pore formation. From the rock's initial volume and the respective pore increase, it is possible to calculate the friction value μ of dry soils by using the ratio between solid volume V_f and pore volume V_l (volume of soils), which thereby equals the tangent of inclination angle βt . If one formulates the dry density of the idealized basalt rock with $\gamma = G/V = 3,0 \text{ t/m}^3$ [6: page 2.2–2], the dry density and the inclination angle of this soil type can be calculated from the solid volume of a soil type, and can also be inserted steplessly between the angles $\beta t = 89,4^\circ$ and $\beta t = 0,6^\circ$ in the so-called "semi-circle of the soil type" (see Fig. 33, page 55).

If one considers the properties of rock and dust even further, it can be assumed that earth masses are embedded above and below the natural inclined plane, which – due to their own weight and gravity – are able to build up an urge to move within the masses. Therefore, in order to promote internal stresses or forces in the ground, no external mobilization of the soil is required through movement of the wall supporting the earth wedge. Because soil physics also do not view soils as a solid mass, it is not possible to follow the teachings when they only assign vertical forces to the soil behind an immovable rigid wall, i.e. without transverse contraction in the ground, and thereby negate the creation of horizontal forces in the soil. If one were to follow the teachings, soil resting against an immovable rock wall will not generate any horizontal stresses against this wall. The New Earth Pressure Theory cannot follow this thesis, as the ratio of solid volume to pore volume in the soil permanently influences the action of density and angle in the soil, thereby leading to continuous stresses in the ground. Moreover, these stresses/forces maintain the equilibrium in the ground. Smaller external forces acting on the soil can be absorbed by the inclined planes (Fig. 2). For larger events (earthquakes), the frictional forces in the inclined planes are no longer sufficient, so that the surplus force must be compensated by soil movements. The New Theory relies on a network of vertical

and horizontal forces in the ground (Fig. 2). This opposes the doctrine, which only sees a vertical force direction in the soil, without the external mobilization of a transverse contraction.

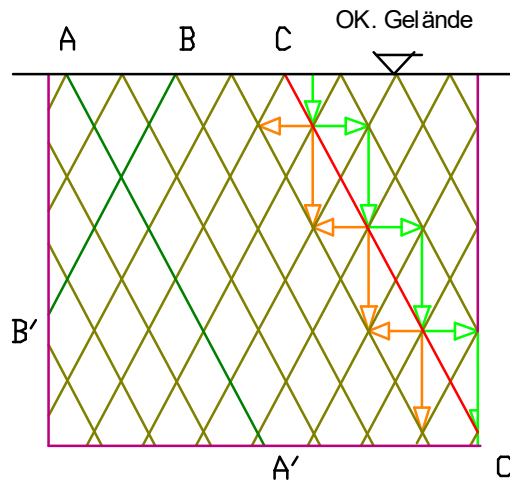


Fig. 2: Assumed network of inclined planes with vertical and horizontal earth stresses in the ground.

An equilibrium condition in the ground can be recognized if one places several earth blocks of the same soil type next to each other (Fig. 3). In the earth pressure theory, an earth block consists of a body of soil, whose height/width ratio corresponds to the tangent $\tan \beta$, whereby the inclined plane appears as a diagonal in the block's side view. The block's depth is designated as a .

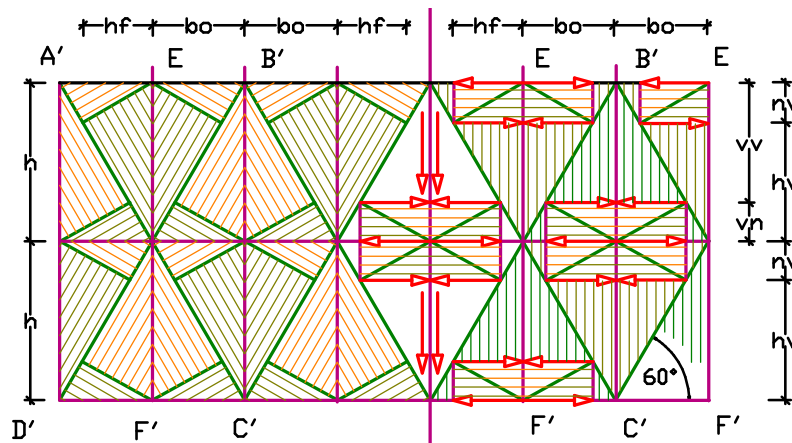


Fig. 3: Active and reactive force areas (left), and the vertical and horizontal force components of soil weight G (right).

In the author's view, a soil's urge to move depends mainly on its pore content. If the pore structure of a dry soil is filled with water, a soil with a low pore content is more likely to exhibit the stress behaviour of a pore-free rock, while the behaviour of a soil with a high pore content (primordial dust) will be more

like that of liquids. The unique description of a soil type by means of density and angle β permits the previous classification of soil types according to magmatic, metamorphic or sedimentary primary rock to be omitted, as well as the division into non-cohesive and cohesive soils. The above elimination of the classification of soil types can also be derived from the fact that the teachings and the New Theory make exclusive use of the weight/body force G of the earth wedge to determine earth pressure force Ea , i.e. particular features of the primary rock, such as grain size or the nature of the bedding, have previously been ignored in earth pressure determinations.

The New Theory follows the change of energy that is observed when operating an hourglass that consists of two vertically mirrored hollow cones, which are connected via an opening. If the bottom cone is filled with sand, the shear point of the filling material is formed in the lower third of the cone's height. The cone of sand remains passive. If the bottom cone is now rotated to the top, energy is applied to the mass, and the originally passive filling material becomes active. Its shear point is now located in the upper third of the cone's height.

If one also assumes that the inclination angle of the cone walls corresponds to the sand's shear plane ($\tan s = \tan \beta / 2$), the sand in the lower cone would neither be able to spread out nor generate horizontal forces against the cone wall. If the hourglass is rotated again so that the sand – with an equal filling amount – is on top, the filling height will change, but not the force acting against the cone's wall. This permits the conclusion that only the sand in the upper cone with its tip pointing downward is active and charged with energy. Conversely, this stored energy is lost when the filling material flows downwards and forms a cone with its tip pointing upwards.

Therefore, the orientation of the tip of an earth wedge also determines the force distribution in the earth body. If one were to place this earth wedge is placed behind a fictitious wall with its tip downwards, and the support from the wall is removed, only half of the wedge volume would slide down (see Test 1, Fig. 15, on page 39). Similarly, also the stored energy would be divided, thereby maintaining an equilibrium of forces in opposing directions to the left and right of the fictitious wall.

Usually, the calculation depth $a = 1,00$ m is specified when determining a force, so that the forces can be calculated from the soil's force area instead of the earth volume. The area Ao of a standing earth wedge, which leans against the perpendicular wall, is determined by the specified wall height h and the soil type's inclination angle β . Consequently, the earth wedge acting against the wall is standing on its tip, so that angle β must be measured between the horizontal and the rise of the inclined plane. With a specified calculation depth $a = 1,00$ m, weight G is determined from wedge area Ao , multiplied with soil density ptg ($png\dots$) and gravity force g . Weight G acts vertically, and occupies the space behind the wall surface supporting the soil. Distribution of the force area between areas of normal force and the downhill force is done according to the expanded physical plane rules. Thus the calculation of weight G , the weight's location in the earth wedge, and force distribution complies with the requirements of Coulomb's classical earth pressure theory (see Section 2.3.3, Fig. 9, page 23).

Regarding the force distribution within the earth wedges, it is shown that with the soil type put forward here, the normal force FN leads away from the perpendicular wall, and the downhill force FH runs towards the wall (see Fig. 7, page 19).

Moreover, it is shown that forces FN and FH stand in the same relationship to weight G as their wedge areas, i.e. the addition of force areas FN and FH results in the force area of weight G . The horizontal forces from the normal force Hn and downhill force Hf are always the same, but adopt opposite directions. When added, the vertical force component Nv of normal force FN and the vertical force component Hv of downhill force FH results in the weight G (see Section 2.3.5, Figs. 10 to 12, page 29). Other forces and their force meters will be described later.

If the support of the soil behind a perpendicular wall is removed, it will slide down the inclined plane, and – assuming that it does not loosen during the slide – will form the upper limit of its natural shear plane with shear angle s . The value of this angle is determined by half the inclination angle's tangent: $\tan s = (\tan \beta) / 2$. If one were to apply loads or forces to the terrain surface, as specified by the teachings for the mobilization of transverse contraction, the soil's natural inclination angle will change, and with it the size of the earth wedge, its weight, and all the other forces or stresses in the soil. In a similar

manner, also the soil properties change, if the soil is compacted or loosened. Determination of the inclination angles of moist and wet soils above and under water is described in Chapter 3.

2.3 Theses of teachings and New Theory in comparison

The earth pressure teachings view soils as solid bodies that are subjected to a material stress parallel to the perpendicular force direction. Only in the case of a resilient lateral support will a transverse contraction arise, whereby horizontal forces occur in the soil. Moreover, the teachings do not consider the equilibrium conditions in soil as given, and introduce the empiric earth pressure factor Ka as compensation [1: page P.3f.]. Contrary to this, the New Theory requires no rotation or parallel shift of the supporting wall to produce horizontal forces in the soil. It sees horizontal forces being generated by the diversion of vertical earth stresses onto the soil's inclined plane. These forces are always present, and they maintain the stress equilibrium in the earth layers. The proportions of vertical and horizontal forces are determined by the natural inclination angle of the respective soil type, which is directly dependent on the soil's density.

For their earth pressure calculations, the teachings use empiric values for soil density a , and reduce the wedge area of the stressed soil by applying the factor $K < 1,00$ so that a difference arises between weight G of the teachings and weight G of the New Theory. In the teachings, this reduced weight G leads to a lower earth pressure. Furthermore, the teachings set the earth pressure force at $1/3$ of the wall height h against the perpendicular wall for all soil types right from the start. They also see reductions of the force due to possible deviations of the angle from the horizontal position of the force due to the influence of wall inclination, wall friction, and soil cohesion [1: page P.2 and page P.10ff.]. The New Theory requires no empiric values for determining earth pressure, and considers the equilibrium of the earth forces as given. Due to the expansion of the multi-phase system of solid-state physics, if one soil property is known, all the others (density ρ , inclination angle β , and shear angles s and a) can be calculated. Experiments have shown that the angles change if external forces are applied to the soil body. From the experiments, this permits the conclusion that the soil's "natural" shear angle s cannot be the same as the shear angle φ' of the teachings, which is determined by means of shear tests with external forces applied to soil samples/soil bodies.

Likewise, influences on the direction of the earth pressure force due to wall friction or cohesion cannot be seen. According to physical laws, wall friction involves a movement, which normally is not present here, and soil cohesion can possibly slow down soil movements due to its adhesive effect, but it cannot stop them. In this respect it is known that cohesion cannot develop without water. Moreover, the teachings claim that Mohr-Coulomb's failure criterion is based on Coulomb's and Mohr's theses, and is suitable for determining earth stresses. This study proves that Coulomb's theory is ignored in the failure criterion, and that the teachings might have extended Mohr's theory in an impermissible manner by the inclusion of external stresses in the stress circle.

Also the thesis of alleged equality, which the teachings see between stress distribution according to the failure criterion, and the physical plane, cannot be followed, because the teachings rotate the original force or stress pattern in the inclined plane (see calculation and example on page 36ff, and Figs. 13 and 14 on page 36). Further detailed reasons for the possible misinterpretation when establishing the failure criterion are given later.

2.3.1 Physical values of inclined plane and wedge

In order to describe the physical principles of the inclined plane and the wedge, they will be cited literally from the "Taschenbuch der Physik" (Pocket book on physics) [15: 5.5.6-5.5.7]. Any increase of the "inclined plane" is limited by angle $\alpha < 45^\circ$, as it can normally be assumed that the frictional forces between body and surface cannot prevent even a rectangular body from sliding down a steeper plane (see Fig. 4 below).

These considerations do not include the fact that a body placed on an inclined plane still generates horizontal forces even if some kind of hindrance prevents it from sliding. As an example, one can imagine a vehicle standing on a slope, but with its bumper against a wall. Also in this case, the vehicle would exert a horizontal force against the wall, whereby the force value depends on the vehicle's weight and the inclination angle of the sloping terrain.

Regarding the "inclined plane", here are excerpts from the "Taschenbuch der Physik":

Section 5.5.6 Inclined plane

This is a plane that is angled from the horizontal.

Inclined plane	
G	Weight of the body
F_H	Downhill force
F_N	Normal force
b	Base of inclined plane
l	Length of inclined plane
h	Height of inclined plane
α	Inclination angle (new β)

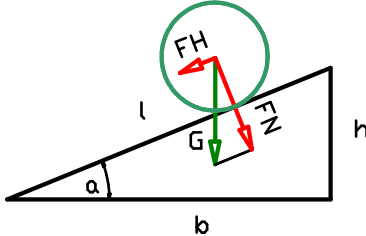


Fig. 4: An inclined plane.

$$F_H = G \cdot h/l = G \cdot \sin \alpha$$

$$F_N = G \cdot b/l = G \cdot \cos \alpha$$

Weight of a body on the inclined plane can be divided into two force components that form a right angle:

- the downhill force F_H parallel to the inclined plane, and
- a normal force F_N at right angles to the inclined plane.
- the slope is defined as the ratio $h/b = \tan \alpha$ (new β).

In this study, the physical plane of the natural inclined plane (soil's sliding plane) is adapted, and the angle β is measured from the horizontal up to the inclined plane.

Section 5.5.7 Wedge

The wedge consists of two inclined planes joined at their bases. The lateral forces exerted by the flanks stand vertically on the flanks (normal force).

If

F = force exerted on the wedge's back
 F_N = flank force of the wedge
 r = width of the wedge's back
 s = length of a flank
 α = half the wedge angle

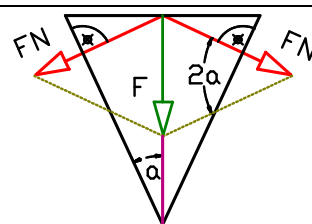


Fig. 5: The physical wedge.

then (M 5.18) $F_N = F / (2 \sin \alpha)$

The "Taschenbuch" describes friction as follows [15: page 98f.]:

Section 7.1.4 Frictional force

Apart from the resistance of the surrounding medium, friction appears as an energy-consuming resistance. It acts on the contact surfaces of two touching "solid bodies" and constrains the relative movement between the two bodies. Friction always acts in parallel with the contact surface, and opposes the movement and therefore also the force causing the movement.

Frictional force is smaller than the normal force.

If

frictional force = F_R , friction value = μ , and normal force = F_N ,

$$\text{then (M 7.8)} \quad F_R = \mu \cdot F_N$$

The frictional force is independent of the size of the contact surface.

The following friction types are distinguished:

Dynamic friction: *It acts where one body moves relative to another (mostly a substrate or similar) and is independent of speed.*

Static friction: *It acts on a resting body and is equal to the opposing external tractive force. The maximum value of static frictional force is always greatest with (M 7.8). If there is no external force, $F_R = 0$. The static friction value μ_o is larger than the dynamic friction value μ ($\mu_o > \mu$).*

Consequently:

If

μ is the friction value to be determined, and a is the angle of the inclined plane, then frictional force = downhill force.

then

$$\begin{aligned} \text{(M 7.8)} \quad & F_R = \mu F_N \\ & \mu G \cos a = G \sin a \\ & F_N = G \cos a, F_H = G \sin a \\ \text{(M 7.9)} \quad & \mu = \tan a \end{aligned}$$

It should be noted that the above rules and calculation approaches were adopted in the New Earth Pressure Theory – only the term "elevation angle α " was changed into "inclination angle β ".

2.3.2 Expansion of physical plane rules

As described, the physical plane rule are based on the conclusion that a solid, rectangular or cubic body, which is placed on an inclined plane with an elevation angle $\alpha > 45^\circ$ (Fig. 4), will slide down the plane or tip over. But because the soil of an earth block is supported on all sides by the surrounding ground, and its inclined plane passes diagonally through the earth block, other physical dependencies arise in the soil than those described for the classical inclined plane. It is therefore possible to cancel the previous calculation limit $\beta \leq 45^\circ$, and to use this extended inclination angle $\beta > 45^\circ$ to divide weight G of the soil directly into the vertical and horizontal forces.

This rearrangement leads to the following dependencies [16 and 17]:

1. Angle $\beta < 45^\circ$: Frictional force is smaller than normal force.
2. Angle $\beta = 45^\circ$: Frictional and normal forces are equal.
3. Angle $\beta > 45^\circ$: Frictional force is larger than normal force.

The following applies: $FH = -FR = G \cdot \sin \beta \rightarrow FN = G \cdot \cos \beta \rightarrow \mu = \tan \beta t$

Due to the diagonal position of the inclined plane in the earth block, the wedge areas $Ao = Au = h \cdot b/2$ are formed, whose active and reactive forces can be divided between the weight forces (soil's dead weight) of the wedge areas by applying the extended physical plane rules.

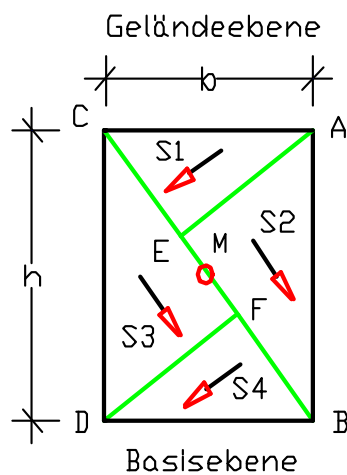


Fig. 6: Different force directions and their centers of gravity within the side view of an earth block.

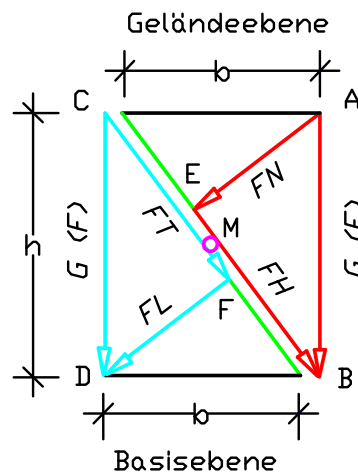


Fig. 7: Active (red) and reactive (cyan) forces, and their force directions within an earth block.

As shown in Fig. 7, normal force FN and downhill force FH as well as forces FT and FL have different directions. Weight G represents the vertical side of the respective earth wedge, so that force G can be seen in relation to wedge

height h . Moreover, it can be concluded that two centers of gravity can be assigned to each earth wedge Ao and Au , namely S1 and S2, and S3 and S4. If we now rotate the above forces around the common central point M, the equilibrium condition in the earth block is confirmed. Taking the positions of the forces, their directions, and their centers of gravity, one could conclude that the "third point in the failure line" used by the earth pressure teachings to distribute weight G , actually doesn't exist (1: page P10, Pict. P05.50).

In the same way that weight G is determined from volume V of the earth wedge or its area $A = V/a$, it is possible to calculate the individual forces by means of their partial areas. If one pursues the division of weight area Ao into the areas of normal force FN and downhill force FH , it is possible to further split these areas into the areas of the vertical and horizontal components. In this way, the areas of vertical force component Nv and horizontal component Hn are developed from the normal force area. The area of downhill force FH is divided into the areas of vertical force component Hv and horizontal component Hf . Similarly, the earth pressure force Hf is formed from the horizontal component's area. The horizontal forces Hn and Hf adopt opposing directions, but as they have equal areas a , they are also equal. An addition of all the partial areas leads to the wedge area of weight G again.

The above areas with the standard depth $a = 1,00$ m can be used to determine the forces of objects subjected to soil pressures, e.g. walls, strip foundations, underground pipes, and tunnel cross-sections. For the force determination of single foundations and single piles according to the New Theory, the corresponding volumes can generally be used.

Regarding the above expansion of the inclined plane rules, it must be noted that in his Figs. 5 and 7, Coulomb already showed the inclined plane/fracture plane under the elevation angle $x = \beta \sim 60^\circ$, and used this angle for force distribution in the earth wedge (see Fig. 9, page 23).

This study uses the expansions of the physical plane, and thereby follows Coulomb's force distribution. Hereby, all forces generated in the earth wedge above the inclined plane are described as active. Reason: if the soil in this wedge loses its hold on the wall supporting it, the ground becomes active and slides down. The soil in the earth wedge below the inclined plane remains at rest and is therefore described as reactive. Both force pairs maintain the equilibrium in the earth block. It is also assumed that the active and reactive forces

change their positions in the respective adjacent block, thereby forming a network of vertical and horizontal forces in the ground (see Figs. 2 and 3, page 12).

As there is good reason to compare Coulomb's theory with the basics of the Mohr-Coulomb failure criterion, the figures in Coulomb's sketch sheet will be named "Fig.", and graphics taken from the references [1: I or 1: P] will be named "Pict."

As already described, Coulomb and the New Theory determine weight G via the wedge area $Ao = Vo/a$ of an earth block, and multiply these areas with depth a , density (t/m^3), and gravity force $g = 9,807 \text{ m/s}^2$. Position and direction of forces FN , FH , Hv , and Hf are shown in Figs. 10 to 12 on page 29 (also see the list of symbols on page viii ff).

Due to the demonstrated dependence of force area and forces, it was possible to derive that weight G of the active earth wedge can be put into relation with height h of the earth wedge. The resulting quotient is introduced into earth pressure determination as new "force index" gi (git , gin , ...). The force index permits the true-to-scale conversion of earth forces into force meters, i.e. in the same way as addition of the vertical forces $Nv + Hv$ returns weight G , the calculation height h results from the sum of force meters $nv + hv$. In the same way, dividing the horizontal force Hf through force index gi results in force meter hf . Conversely, this procedure permits the force index to be used to determine forces within the earth wedge from force meters. To help understand the dependencies of different soil types from angle, density, forces, and force meters, Tables 1 to 3 have been prepared, see pages 238ff.

The described force build-up within an earth block changes if its earth mass loses its hold on the perpendicular wall. One part of the soil slides downwards on the inclined plane and forms the natural shear plane under angle s as the upper limit. The tangent of the shear angle under load is calculated via $\tan se = (\tan \beta) / 2$. More detailed information on angle conversion will be given later.

Determination of individual forces

It should be noted that the unit t/m^3 was selected for densities.

Weight G

$$G = A_o \cdot a \cdot \text{ptg} \cdot g \text{ (analogous: } \text{pig, png, etc.)} \quad \text{kN} \quad 2.1$$

Force FN

$$FN = G \cdot \cos \beta \quad \text{kN} \quad 2.2$$

Force FH

$$FH = G \cdot \sin \beta \quad \text{kN} \quad 2.3$$

Force Nv

$$Nv = G \cdot \cos^2 \beta \quad \text{kN} \quad 2.4$$

Force Hv

$$Hv = G \cdot \sin^2 \beta \quad \text{kN} \quad 2.5$$

Force $Hf = -Hn$

$$Hf = -Hn = G \cdot \sin \beta \cdot \cos \beta \quad \text{kN} \quad 2.6$$

For a true-to-scale representation of the above forces, they will be converted into force meters by means of the force index.

Force index $gi' \rightarrow$ via the earth volume V

$$gi' = a \cdot b \cdot \text{ptg} \cdot g/2 \quad \text{kN/m}^2 \quad 2.7$$

Force index $gi \rightarrow$ simplified via the load area A

$$gi = b \cdot \text{ptg} \cdot g/2 \quad \text{kN/m} \quad 2.8$$

Calculation depth = a Dry density = ptg

Wedge width = b Gravity force = g

Force meter h

$$h = G/gi \quad \text{m} \quad 2.9$$

Force meter fn

$$fn = FN/gi \quad \text{m} \quad 2.10$$

Force meter fh

$$fh = FH/gi \quad \text{m} \quad 2.11$$

Force meter nv

$$nv = Nv/gi \quad \text{m} \quad 2.12$$

Force meter hv

$$hv = Hv/gi \quad \text{m} \quad 2.13$$

Force meter $hf = -hn$

$$hf = -hn = Hf/gi \quad \text{m} \quad 2.14$$

The force index must be adapted to the respective wedge width b and soil density.

2.3.3 Coulomb's earth pressure theory

In order to represent Coulomb's earth pressure theory, his own sketch sheet (Fig. 9 below) will be used. Until a few years ago, the sketch sheet was freely accessible on the website of the Technische Universität Dresden.



Fig. 8: Portrait of Monsieur de Coulomb.

Particularly Fig. 7 of the sketch shows that Coulomb places an earth wedge behind a supporting wall, which is described by (C–a–B). He also assigned the inclined plane (C–M) under the inclination angle $\alpha \sim 57^\circ$ to this earth wedge. The earth wedge was loaded with a weight P , and to divert this load, the wedge area of the column height is increased by area (a–a'–B'–B). Due to the increased area, also the calculation height h (C–B) is increased by the distance of point B to B'. Coulomb transfers the force directions of Fig. 5 into the wedge area (C–a–B), and thereby shows that the normal force runs in plane (φ –G), and the downhill force adopts plane (G–B). Depending on the angle, the normal force plane will be shorter than the angled downhill plane. Because of the possible relation between force length and force, it can be stated that the normal force is smaller than the downhill force.

The horizontal force (G–F), which is exerted against the supporting wall by the earth wedge, is opposed by reactive force A . In this way it can be shown in Coulomb's Fig. 7 that the indicated thrust height of the earth pressure force against the perpendicular wall can neither be aligned with the center of gravity of wedge area (C–a–B), nor with $1/3$ of wedge height h .

Moreover, the weight of column height G lies directly behind the perpendicular wall (C–B), and not – as stated by present earth pressure teachings – on the third point of the failure line/inclined plane.

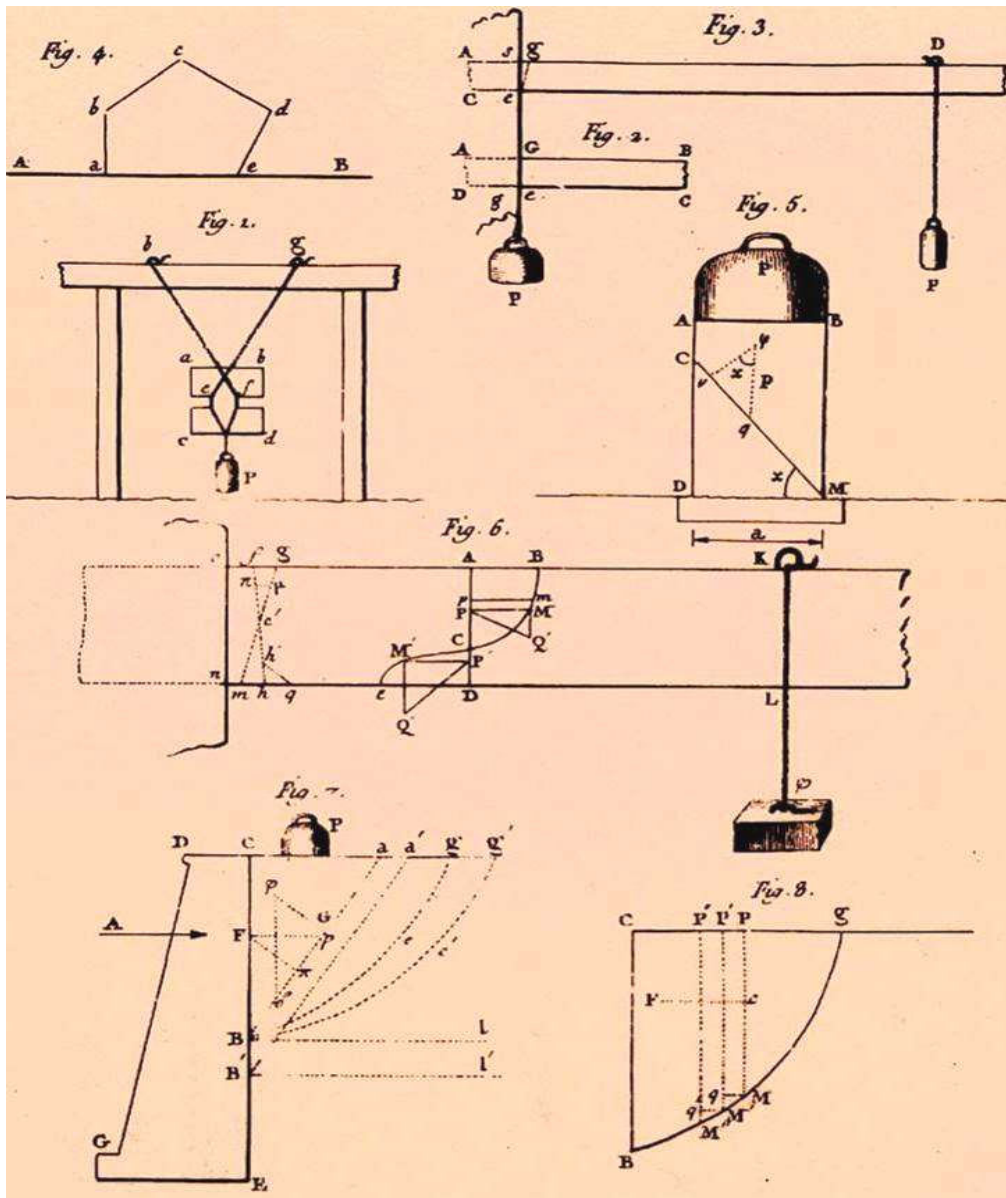


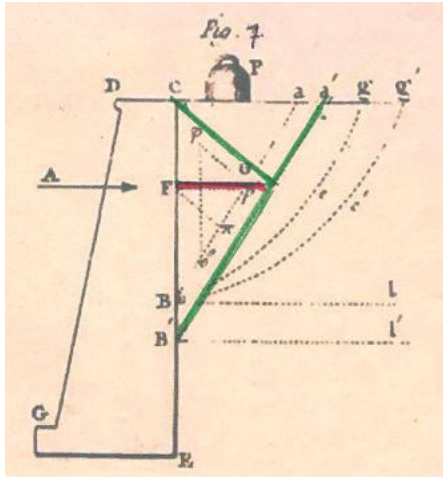
Fig. 9: Sketch sheet with figures showing Coulomb's earth pressure theory.

What's more, neither the force area (C–a–B) nor the value for weight show a reduction, which would justify the application of an earth pressure factor $K < 1$, as inserted by the teachings for force calculations. While Coulomb projects all forces in the earth wedge, the teachings rotate Coulomb's force system in order to place the downhill force in the physical plane under Coulomb's angle φ (see Pict. I06.40, page 28).

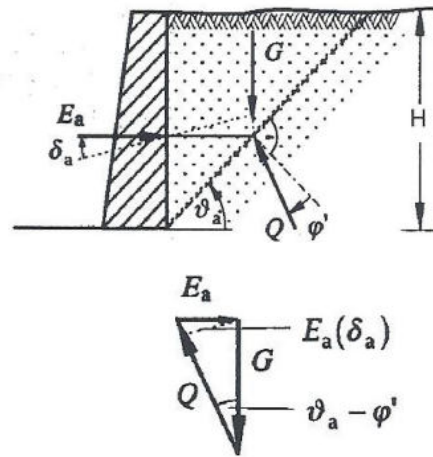
Also not comprehensible is the reference made by the earth pressure teachings on the one hand, that Coulomb states *“for the base case with a perpendicular wall face and level ground [...] the stress distribution is unknown with this approach”*, but on the other hand uses “Mohr-Coulomb's failure criterion” for their calculation method (see [1: page P.10]).

2.3.4 Mohr-Coulomb failure criterion

Although the earth pressure teachings use the shape of Coulomb's load area $A = b \cdot H/2$, they present the forces resulting from the weight in a modified way (see Coulomb's Diagr. 7 and Pict. P05.50 [1: page P.10] below).



Diagr. 7 Coulomb's force arrangement in an earth wedge



Pict. P05.50: Section and force polygon at one point

Moreover, the teachings shift the position of the weight force from the rear wall surface to the third point of the failure line and – as already mentioned – rotate Coulomb's force system in order to match them to the physical plane guidelines (see Pict. I01.70, page 28).

The teachings justify this shift of the weight and the different stress distribution of Coulomb's diagram, and state the following in the references [1: page P.10]:
“If one [...] assumes that all forces acting on the earth wedge are integrals of stresses that increase linearly with depth, G, Q and Ea intersect at a point (third point of the fracture), and if $\delta = 0$ (simplification), this leads to:

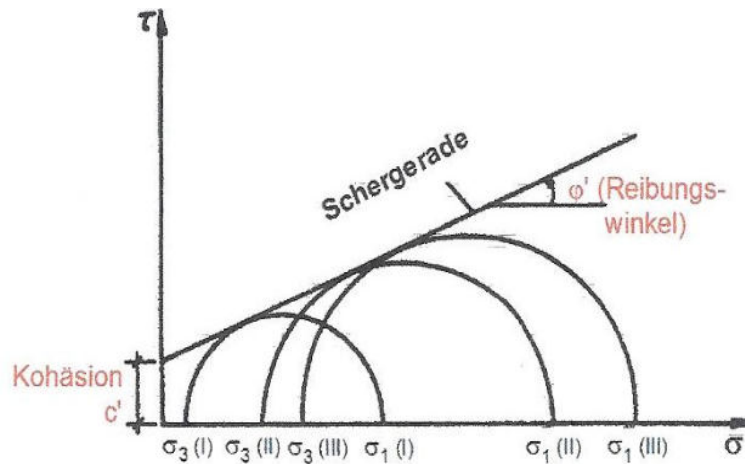
$$G = \frac{1}{2} \gamma \cdot H^2 \cdot \cot \theta \text{ and } E_a = G \cdot \tan (\theta - \varphi).”$$

The friction angle φ' is calculated using [1: page I.15]

$$\sin \varphi' = \tan \alpha = \tan (90^\circ - \beta)$$

In accordance with these specifications, the teachings fix the horizontal action of earth pressure force E_a against the wall equally for all soil types at 1/3 of the wall height h , insofar as the earth pressure inclination angle $\delta_a = 0$ [1: page P10]. Moreover, regarding the above Pict. P05.50, the teachings indicate that the Mohr-Coulomb fracture condition applies when calculating and distributing the stresses due to weight. The fracture condition is intended to permit the determination of normal and thrust stresses caused by load forces or moments

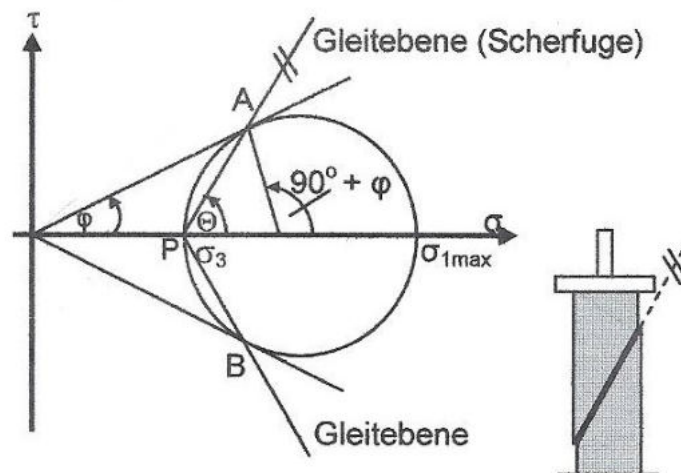
in supporting structures or solid bodies. For this, the values σ_x , σ_y and τ_{xy} are applied along the σ -axis, whose intersecting angles generate points on the circle, which enable the stress condition to be displayed graphically. With uniaxial tension or pure thrust, the highest thrust stresses occur under an angle of 45° to the x-axis.



Pict. I06.10: Mohr's stress circles for the fracture condition of a soil with cohesion

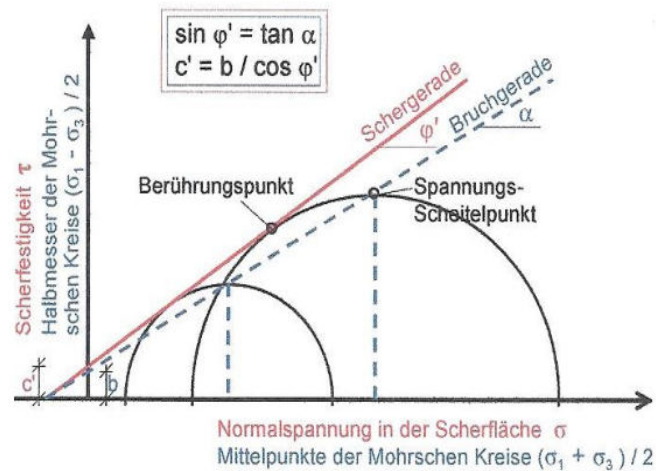
Another citation involving the fracture condition is [from 1: page I.14]:

“If one enters the stress conditions $\sigma_3 / \sigma_{1,max}$ obtained with different triaxial tests on the same material, but with different lateral pressures σ_3 into Mohr's representation as stress circles, one sees that the circles share a common tangent (see Pict. I06.10). It defines the Mohr-Coulomb fracture condition that has a central function in soil mechanics (shear straight).”



Pict. I06.40: Directions of shear surface(s) in the triaxial test; $\theta = 45^\circ + \phi/2$

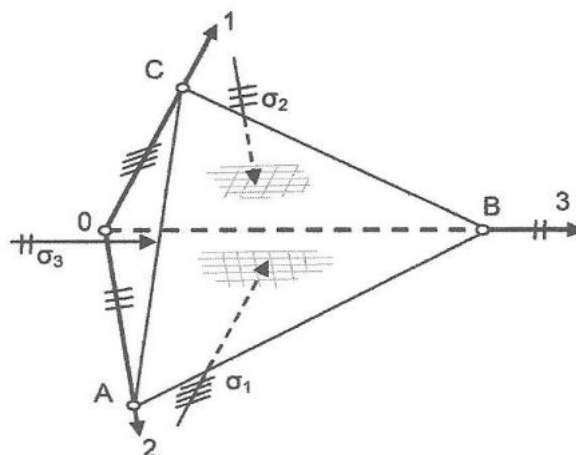
In the above Pict. I06.40 [1: page I.15] the teachings show the fracture plane (A–P) with angle θ , sliding plane (shear plane) with internal friction angle φ and the third point A or B on the failure line. By means of the triaxial test, the directions of the shear surfaces are determined as $\theta = 45^\circ + \varphi/2$.



Pict. I06.20: Relationship between shear and failure lines

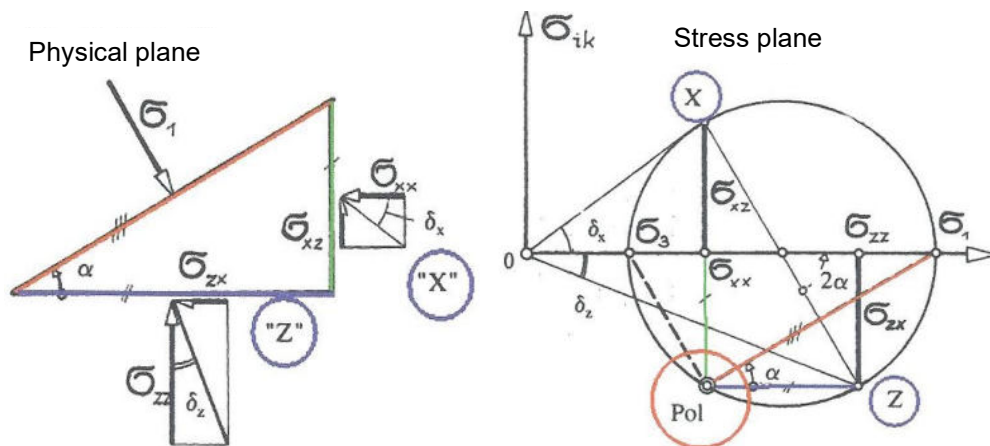
The cohesion of an over-consolidated binding soil is shown as thrust stress c' on the ordinate in Pict. I06.10 [1: page I.14]. The stress point on the failure line indicates the peak stress point in the limit state, whereby the fracture straight under angle α intersects the ordinate at value b . The relationships shown in Pict. I06.20 are used for converting the stress paths shown with their stress points in the p - q diagram.

For every stress condition, the main stress invariants can be determined via three mutually orthogonal main stress areas, in which no stresses occur. The normal stresses acting on these areas are named primary stresses σ_1 , σ_2 , σ_3 (Pict. I01.40) [1: page I.3].



Pict. I01.40: Primary stresses

Indices 1, 2, and 3 have been selected so that $\sigma_1 > \sigma_2 > \sigma_3$. Consequently, the normal stresses σ_{xx} , σ_{zz} , $\sigma_{x'x'}$, $\sigma_{z'z'}$, σ_1 and σ_3 can be entered on the abscissa, and the thrust stresses σ_{xxi} , σ_{zzz} , $\sigma_{x'x'}$ and $\sigma_{z'z'}$ on the ordinate. With soil in the state of rest, the known stresses σ_{xx} , σ_{zz} and $\sigma_{xz} = \sigma_{zx}$ in the x, y coordinate system can be assigned as vertical stress σ_{zz} or horizontal stress $\sigma_{xx} = K_o \cdot \sigma_{zz}$. In the case of wall friction, the above stresses can change. In this respect, the teachings assume that horizontal wall movements will reduce or increase the horizontal stress, whereby the limits of change can be indicated by stress circles in Mohr's representation. Hereby, the circle size is defined when it reaches the limiting straight, whose position is determined by friction angle φ' and cohesion C' .



Pict I01.70: Mohr's stress circle

By means of Pict. I01.70, the teachings relate the "inclined plane" of the Mohr-Coulomb fracture condition to Mohr's stress circle for an even stress condition [1: page I.5]. Into this stress circle, they insert the vertically mirrored force polygon of Pict. P05.50 [1: page P.10] and show it as stress area (X-Z-Pol) in Pict. I01.70. Hereby, the transverse force Q is converted into primary stress σ_1 . Weight G is assigned to plane (X-Pol), and the earth pressure force E_a to plane (Pol-Z). The same normal stress σ_1 is placed on the inclined plane at an angle. The inclined plane appears again in the stress circle, where it rises from Pol up to the abscissa with elevation angle α . The teachings then determine the partial stresses in the circle by means of stress σ_{ik} – which acts outside the circle – and angles δ_x and δ_z .

2.3.5 Comparison: Coulomb's theory and failure criterion

The teachings see an analogy between Coulomb's teachings and the failure criterion, and describe it in the references [1: page P.10]. Hereby, the teachings

assume “that all the forces acting on the earth wedge are integrals of stresses that increase linearly with depth”, and that the resulting stresses (G , E_a and Q) will intersect at the third point of the failure line/inclined plane, provided that angle $\delta_a = 0$ (see Pict. P05.05).

Consequently, only the forms of the wedge areas for determining the weight are comparable in Coulomb's theory and the failure criterion. All other characteristics of Coulomb's theory, as described in Section 2.3.3, are not found in the failure criterion. Therefore, an analogy between Coulomb's theory and the failure criterion of the teachings cannot be seen. In contrast, and as already described, the New Earth Pressure Theory applies Coulomb's force distribution unchanged (see force distribution in Figs. 10 to 12 below).

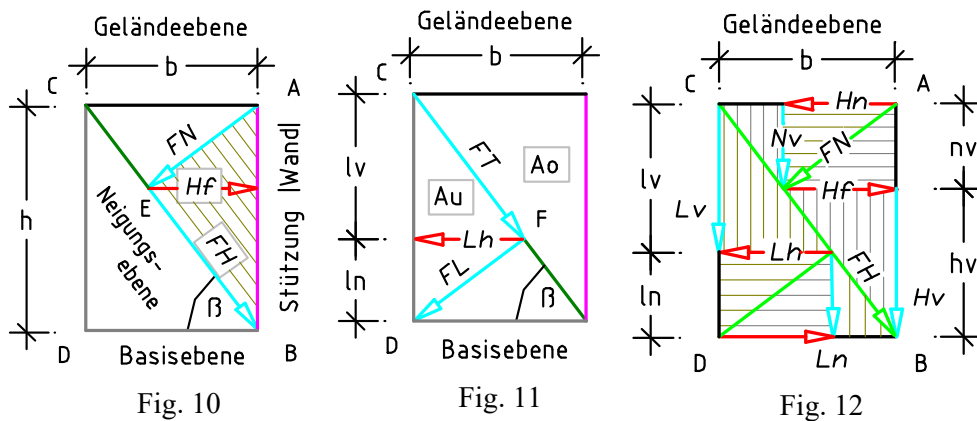


Fig. 10: The hatched area of downhill force FH with earth pressure force Hf within active force area Ao , and above that the area of normal force FN .

Fig. 11: Force areas Ao and Au within an earth block, together with normal force FT , and downhill force FL in the reactive area Au .

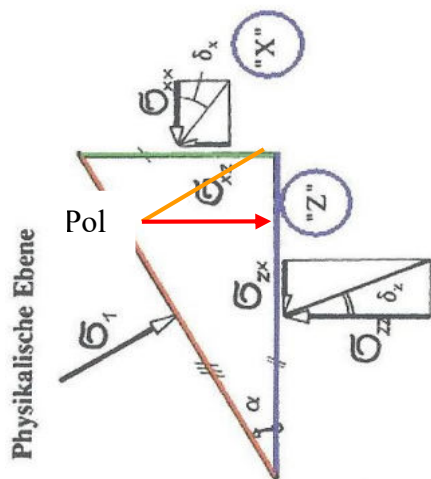
Fig. 12: Hatched force areas of an earth block with the vertical and horizontal force components of normal force FN , as well as the downhill force FH and its force directions.

While the forces shown in Fig. 10 must be regarded as active and be assigned to area Ao , the reactive forces are developed in area Au . The earth block in Fig. 12 shows the projection areas of the forces as well their respective areas of origin, position, and direction. In particular, the area of normal force FN permits the deduction that neither the vertical nor the horizontal force component of normal force FN have any influence on wall loading. Consequently, the only forces against the supporting wall originate from the earth mass, which must be assigned to the area of downhill force FH . Moreover, the values of downhill force FH and frictional force $-FR$ (R) are identical. Therefore, the earth pressure force Hf at thrust height h_v is generated by the area of the downhill

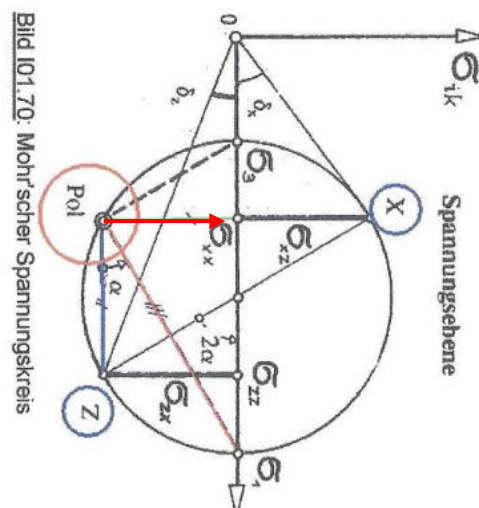
force (see Fig. 12). In the same way that the weight forces G can be derived from areas $A_o = V_o/a$ and $A_u = V_u/a$, all other forces – including their vertical and horizontal force components – can be calculated from their respectively assigned partial areas (see Fig. 13, page 36).

The force distributions also prove that Coulomb's calculation systems and the earth pressure teachings are not equal. In the following, the shift of weight G from the perpendicular wall surface (Coulomb) to the lower third point of the failure line/inclined plane (teaching) will be examined. As already mentioned, the teachings show a force polygon in Pict. P05.50, whose hypotenuse they assign to transverse force Q . The teachings assume that friction occurs in the entire fracture plane, which in turn generates transverse force Q . Coulomb however, limits soil friction to the length/force meter fh of downhill force FH , and thereby sees no larger force around the earth wedge than weight G . Moreover, transverse force Q would be lacking an earth mass or an area from which it could develop.

The representation of Coulomb's different force systems (Diagr. 7) and the teachings can be simplified if Pict. I01.70 is divided into Pict. I01.70a and Pict. I01.70b, and these are rotated so that weight G is returned to its perpendicular position. Moreover, the position of earth pressure force Hf (red) has been entered in both Pictures.



Pict. I01.70a: Stress distribution acc. to Coulomb's Fig. 7



Pict. I01.70b: Stress distribution acc. to Mohr's stress circle

Simply the different positions of the earth pressure forces in the two Pictures indicate the different approaches of Coulomb and the current teachings. While Coulomb calculates the earth pressure force from the wedge area of downhill

force FH (Fig. 10), the teachings determine earth pressure force from the total wedge area (Fig. 11) and then place transverse force Q , weight G , and earth pressure force E_a into the lower third point of the failure line. Obviously, by placing the force at a single point, the teachings ignore the fact that earth forces build up within a soil body and this is where they must take up their fixed position. As the equilibrium condition in the soil is given, the New Theory considers the inclusion of earth pressure factor K_a , earth pressure inclination angles δ_a and/or δ_p , and wall friction angle just as superfluous as soil cohesion C or c' .

Conclusions:

In their references [1: page I.14ff.], the teachings point out that the Mohr-Coulomb failure criterion is based on Coulomb's flow condition. Therefore, when regarding the force behaviour in an hourglass, it must be established that the stress distribution of the teachings cannot be brought into line with Coulomb's force distribution [1: 0I.5], as there is no original drawing showing his flow condition, comparable with that of his earth pressure theory (Fig. 9).

Also the determination of the position of earth pressure force E_a within Mohr's stress circles by means of an external stress σ_{ik} and the angles δ_x and δ_z does not lead to results that can be confirmed with the "calculation example" on Page 35 or by the following tests (see Section 2.8, page 50ff).

2.3.6 Comparison: Mohr's stress theory and failure criterion

Also here, the teachings state that an analogy exists between Mohr's stress theory for a level stress condition and the failure criterion. This thesis will be examined in the following.

The University of Bremen is one of the sources that have presented a short summary of Mohr's theory [7]. In a stress circle with radius r , the center point coordinates $(\sigma_M, 0)$ and the values σ_x and σ_y on its main axis σ must be marked. The thrust stress τ_{xy} lies above the value σ_x , and the same stress with inverted sign lies above value σ_y . In this way, two points are created on the arc, whose connecting line passes through the circle's center [7: page 391]. If an additional point is marked on the stress circle, its coordinates can be used to directly read the change of the primary stresses and the main thrust stresses [7: page 392].

In this respect, the mentioned short summary of Mohr's theory shows that the primary stresses as well as the main thrust stresses lie within the arc, i.e. the

stresses cannot leave the circular area. In the author's opinion, the teachings modify Mohr's theory by placing stress σ_{ik} outside the arc, and use the distance of this stress to the diameter in order to determine angles (δ_x and δ_z , see Pict. I01.70b). The teachings justify an exit from the stress circle by taking a soil cohesion into account, which would influence the earth stresses (see the defined fracture condition that is presented as Mohr-Coulomb's fracture condition in Pict. I06.10 [1: page I.14]).

The author is convinced that a force (stress σ_{ik}) can only develop from its associated mass, i.e. one must be able to determine this mass by means of an area ($A_o = V_o/a$) within the arc. Because, according to Coulomb, weight G accounts completely for the mass of the earth wedge behind the supporting wall, the corresponding mass required for generating a cohesive force is missing. Consequently, cohesion can only be a moderate portion of weight G , which cannot stop soil movements, but can delay them for a short time. Therefore, the internal friction and cohesion forces can only act in the soil's inclined plane, and cannot adopt different directions or angles, as represented by the teachings with Pict. I.06.20 [1: page I.15].

The difference between frictional/inclined plane and shear plane in soils will be discussed later in this study.

Conclusions:

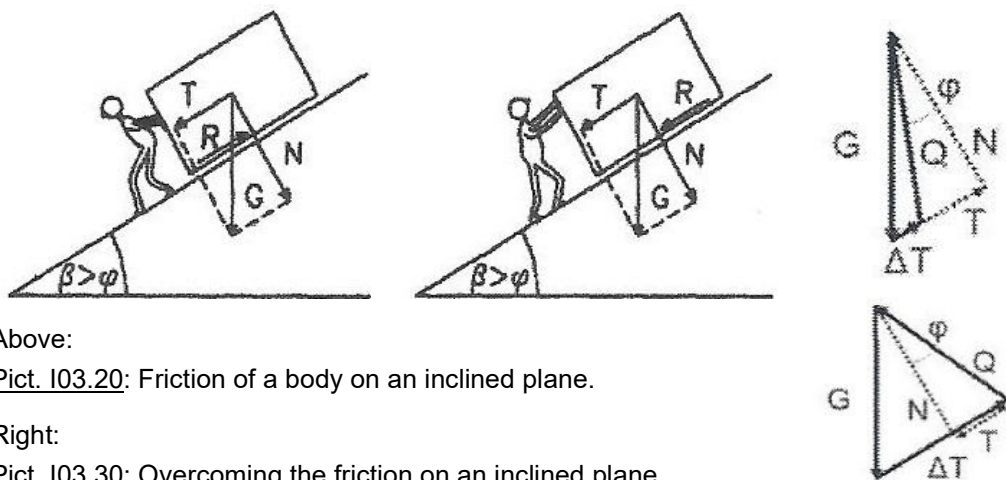
The above comparison of Mohr's stress theory with the Mohr-Coulomb failure criterion shows that the inclusion of an external stress σ_{ik} into the stress circle Picture represents an impermissible transformation of Mohr's theory. Hence, also here, an analogy between the two theses is not discernible (see Pict. I01.70b, page 32). Simply by rotating the Pict. through 90° one can see that the teachings use Mohr's stress theory in order to move the vertical force of the soil's own weight into a new direction (see Pict. I01.70b, page 32). It is unlikely that a structural engineer would follow the failure criterion and place a building at an angle before dimensioning the walls and ceilings in this position. The rotation of forces or stresses as practiced by the teachings for earth pressure calculations can only lead to faulty results (see the force distribution in the calculation example in Section 2.3.8, and Figs. 13 + 14, page 36).

2.3.7 Force distribution acc. to physical plane and failure criterion

Finally, the teachings describe an equivalence between the force distribution according to the physical plane, and Mohr-Coulomb's failure criterion. To explain this parity, the teachings show the Pictures I01.70, I03.10, I03.20 [1: page I.8], and P01.30 [1: page P.1].

In order to explain the calculation requirements for determining earth pressures from the teachings, the physical plane, and Coulomb in a simple manner, the conventional force descriptions will be assigned to the descriptions used by the New Theory. The descriptions and positions of the forces within an earth block are shown in Figs. 10 to 12 (page 29).

Normal force N (FT) rests on the inclined plane at an angle, and downhill force T (FL) lies on the inclined plane. In the event that neither wall friction nor cohesion is applied to reduce weight G , weight G represents the hypotenuse in the force wedge, and elevation angle α of the inclined plane is equal to the contact friction angle φ . Therefore, angle $\beta = 90^\circ - \alpha$ must be seen as being supplementary to angle α . If wall friction and cohesion are applied via friction angle δ in order to reduce weight G , the latter changes into the smaller transverse force Q . In the Pictures, the contact friction angle φ between transverse force and normal force is measured. Earth pressure force E_a (Lh) rests on the inclined plane at the starting point of inclination force N (FT), and (without wall friction) it leads in a horizontal direction to the soil supporting the rear wall surface (plane of weight G). Possibly, the analogy to Pict. P05.50, page P10 is missing in the description of the position of the weight force.



Above:

Pict. I03.20: Friction of a body on an inclined plane.

Right:

Pict. I03.30: Overcoming the friction on an inclined plane.

To determine the force, the teachings state [1: page I.9] that if the soil's dead weight G is placed on an inclined plane, this force will be divided into downhill force T (FL) and normal force N (FT), whereby the following is true:

$$N = G \cdot \cos \beta \text{ and } T = G \cdot \sin \beta$$

The soil body could start moving, if the inclined plane's angle becomes greater than the contact friction angle φ , so that:

$$R = N \cdot \tan \varphi = G \cdot \cos \beta \cdot \tan \varphi < G \cdot \sin \beta$$

According to the teachings, the proportionality factor $f = \mu$ corresponds to the ratio of downhill force T and normal force N .

The angle between the resultant and the normal is described as friction angle δ – also called contact friction angle φ .

Insofar as the body placed on the inclined plane remains at rest, $T < N \cdot \tan \varphi$ will apply, i.e. the body can be held with a small force ΔT (Pict. I03.20). Opposing the downhill force T is the frictional force R , which must be overcome to move the body. According to the teachings, *“the frictional force R is only first mobilized and its direction determined by an attacking force”*.

The teachings introduce a wall movement as mobilizing force, which is intended to generate the friction angle φ' :

$$\sin \varphi' = \tan \alpha = \tan (90^\circ - \beta); [\text{Pict. I06.20: page I.15}].$$

Without this mobilization, the contact friction angle φ between the vertical and the plane of the transverse force is measured (Pict. I03.10). Regarding the mobilizing force, the teachings state that the value of the earth pressure force also depends on movements between soil and wall. The earth pressure will then be greater, if the wall moves towards the adjacent soil. If the wall moves away from the soil, the earth pressure force is reduced. Consequently, an analogy to the possible force exists in the direction of movement, which can additionally move a body on the inclined plane (see Pict. P01.30 [1: page P.1]).

It can be established that stress distribution according to the Mohr-Coulomb failure criterion does not agree with Coulomb's classical earth pressure theory (Fig. 9, page 23). To show the difference, the forces will first be calculated according to the earth pressure theory, after which they will be assigned to the failure criterion locations (see Figs. 13 and 14, page 36). Fig. 14 shows that the teachings rotate the downhill force FH of the standing earth wedge into the "inclined plane" as force T .

2.3.8 Earth pressure force according to failure criterion and Coulomb

Calculation example

The determination of force is based firstly on the teaching's specifications (see P.5.3.1 Basics [1: page P.10 and page I.15]), and secondly on Coulomb's Fig. 7 for classical earth pressure theory. Wall friction and cohesion are not taken into account.

For the soil resting behind a 5,00 m high wall, firmly bedded detritus with a dry density $\rho_{tg} = 2,046 \text{ t/m}^3$ and an inclination angle $\beta = 65^\circ$ ($\alpha = \varphi = 25^\circ$) is assumed. Weight $G = 116,9 \text{ kN}$ of the earth wedge was determined using the calculation depth $a = 1,00 \text{ m}$. Details about the dependencies between soil density and inclination angle are given in Chapter 3, page 54.

A) Determination according to the teachings, whereby proof of $\varphi = \alpha$ is omitted (see the Pictures P01.30 and P03.20 [1: page P.1 and P.5]).

The specifications for the calculation of forces N , T , and R are shown in [1: I.3.1; page I.8f.].

Weight G_I	$G = 116,9 \text{ kN} \rightarrow \varphi = \alpha = 25^\circ$
Factor K_a	$K_a = \tan^2 (45 - \varphi/2) = 0,406$
Earth pressure force E_a	$E_a = \frac{1}{2} \cdot K_a \cdot \gamma \cdot g \cdot h^2 \cdot \cot \theta \rightarrow \theta = \beta = 65^\circ$
$H = h$	$E_a = 0,5 \cdot 0,406 \cdot 2,046 \cdot 9,807 \cdot 5,0^2 \cdot 0,466$ $E_a = 47,5 \text{ kN}$
Normal force N (FT)	$N = G \cdot \cos \beta = 116,9 \cdot 0,423 = 49,4 \text{ kN}$
Downhill force T (FL)	$T = G \cdot \sin \beta = 116,9 \cdot 0,906 = 105,9 \text{ kN}$
Friction value / detritus	$\mu = T / N = 105,9 / 49,4 = 2,144$
Frictional force / detritus	$-R = N \cdot \tan \varphi = 49,4 \cdot 0,466 = 23,0 \text{ kN}$
Moment M_B of force Hf	$M_{B1} = E_a \cdot h/3 = 47,5 \cdot 1,67 = 79,3 \text{ kNm}$

B) Determination according to Coulomb and based on his Fig. 7:

Weight G	$G = 116,9 \text{ kN} \rightarrow \beta = 65^\circ$
Normal force FN (N)	$FN = G \cdot \cos \beta = 116,9 \cdot 0,423 = 49,4 \text{ kN}$
Downhill force FH (T)	$FH = G \cdot \sin \beta = 116,9 \cdot 0,906 = 105,9 \text{ kN}$
Earth pressure force Hf	$Hf = FH \cdot \cos \beta = 105,9 \cdot 0,423 = 44,8 \text{ kN}$
Vertical portion of FH	$Hv = G \cdot \sin^2 \beta = 116,9 \cdot 0,821 = 96,0 \text{ kN}$
Frictional force / detritus	$-FR = FH = 105,9 \text{ kN}$
Friction value / detritus	$\mu = FH / FN = \tan \beta \rightarrow \tan 65^\circ = 2,145$
Force index gi (new)	$gi = G / h = 116,9 / 5,00 = 23,38 \text{ kN/m}$
Force meter	$fn = FN / gi = 49,4 / 23,38 = 2,11 \text{ m}$

$$fh = FH / gi = 105,9 / 23,38 = 4,53 \text{ m}$$

$$hf = Hf / gi = 44,8 / 23,38 = 1,92 \text{ m}$$

$$hv = Hv / gi = 96,0 / 23,38 = 4,11 \text{ m}$$

$$\text{Moment } M_B \text{ of force } Hf \quad M_{B2} = Hf \cdot hv = 44,8 \cdot 4,11 = 184,1 \text{ kNm}$$

The difference in the calculations becomes particularly clear if one compares the moments $M_{b1} = 79,3 \text{ kNm}$ and $M_{b2} = 184,1 \text{ kNm}$. Also the equality of forces T and FH as well as N and FN decreases in value, because the forces occupy completely different positions in the system. While Coulomb's Fig. 7 inserts weight G , downhill force FH , and normal force FN into the wedge area Ao with inclination angle β (Fig. 13), the teachings rotate Coulomb's forces so that the downhill force T is located on the inclined plane with angle $\alpha = 25^\circ$. Normal force N rests on the plane of force T at an angle, and weight G runs along plane $(A'-B')$. These planes exhibit neither a parallelism with the natural inclination plane $(C-B)$ nor with the shear plane $(C-F)$. As the forces can be converted into force meters using the force index, their values and positions can be shown in Figs. 13 and 14 below.

The teachings refer to Mohr's stress theory in order to justify their force rotation, but misperceive that the vertically acting weight cannot be rotated.

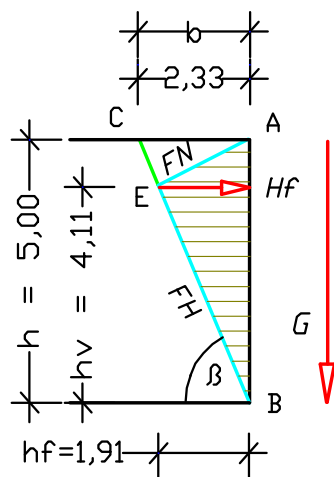


Fig. 13: Hatched area of downhill force acc. to Coulomb, with earth pressure force Hf and thrust height h_v as lever (diagram of moments).

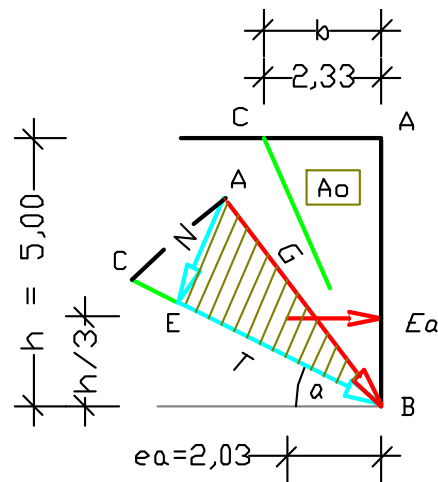


Fig. 14: Downhill force T rotated on the inclined plane, force N resting on this plane at an angle, and the angled position of weight G .

While Coulomb also places the earth pressure force Hf in the wedge area Ao , and assigns thrust height h_v to this force, the teachings determine earth pressure force E_a and its thrust height $h/3$. Obviously, the teachings do not see that a third point on the failure line and the corresponding assignment

to weight G simply does not exist, as shown when comparing Coulomb's Fig. 7 with Pict. P05.50 (page 25). Also if the load area is mirrored around plane $C'-B'$, neither the value nor the assignment of the moments would be changed. Even the different centers of gravity $S1$ to $S4$ and the force directions in Fig. 6 as well as the position of weight G in Fig. 7, page 19 indicate shortcomings in the calculation specifications of the teachings.

Conclusions:

Moreover, the teachings state that the value of earth pressure force Ea also depends on movements between soil and wall, whereby this wall movement is viewed as a mobilizing force. Similarly, earth pressure is supposed to increase if the wall moves towards the adjacent soil. If the wall moves away from the soil, the earth pressure force is reduced. In the direction of movement, the teachings see an analogy with a possible force that can impart additional movement to a body on the inclined plane (see Pict. P01.30 [1: page P.1]). The author cannot follow this view, because otherwise there would neither be a mobilization of horizontal forces nor an earth pressure force against the wall in the soil behind an immovable, nonrotatable wall. Once again, he points out that the New Earth Pressure Theory sees permanent horizontal stresses in the ground, which maintain the equilibrium in the ground. Simply a hard, pore-free rock (basalt) is unsuited to develop horizontal forces against the wall. All other soil types and water can create frictional planes – and thereby also internal frictional forces – without a particular mobilization of the soil.

Furthermore, and to a great extent, the calculations made in the teachings ignore the fact that different soil types also create different inclination angles for $\beta = 0,6^\circ$ to $\sim 89,4^\circ$. If the forces are to be calculated according to the physical plane rules, the elevation angle must first be adapted to the planes of the respective soils' inclination angles. The teachings see such an adaptation when applying the Mohr-Coulomb failure criterion, and point out that their calculations are based on Coulomb's yield criterion [1: S. I.14ff.]. However, the test setups 4 and 5 (see page 50ff) prove that Coulomb's Fig. 7 on earth pressure theory and the yield criterion describe two different physical facts. Coulomb's yield criterion is not a modification of his earth pressure theory!

In summary, one can say that Mohr-Coulomb's failure criterion follows neither Coulomb's Fig. 7 on classical earth pressure theory, nor Mohr's stress theory, nor the physical plane rules. Also the thesis of the teachings cannot be confirmed, that a mobilizing force is required to raise horizontal forces in the ground and to determine the direction of the frictional force.

Regarding the enormous differences in the calculated moments $M_{b1} = 79,3$ kNm and $M_{b2} = 184,1$ kNm it must be noted that if a wall is dimensioned according to moment M_{b1} , damage, tipping or shifting of the wall must be expected within a short time.

2.4 Determining the natural inclination and shear angles of soils

From Pictures I06.20 to I06.40 [1: page I.15] one could deduce that angle φ of the failure line, and elevation angle α of the inclined plane are identical. More explicitly, in Pict. I06.20, the teachings derive the shear straight angle φ' using $\sin \varphi' = \tan \alpha$. Shear angle φ is determined by means of shear tests, whereby the shear strength of soil samples is measured under the application of axial or tri-axial pressure [1: page I.9, Pict. I03.30]. A wide spectrum of soil parameters and angles is specified in DIN 1055–2 for earth pressure determination (see [1: page I.19f. and 5: page 7ff.]). With the knowledge that only a few soil types are suitable for conducting shear tests, and for the implementation according to DIN 18137–1 /–2, only cylinder sizes of $\varnothing i = 1,05$ dm, height 1,00 dm, $V = 0,87$ dm³ or $\varnothing i = 1,50$ dm, height 1,25 dm, $V = 2,21$ dm³ are permissible, the author's doubts about the applicability of the specified tabulated values are increased. Thus, most of the soil parameters listed in DIN 1055–2 have probably been found empirically, and therefore cannot be identical with the real densities and angles of soils in nature. Moreover, the freehand selection of soil values from DIN 1055–2 [1: page I.19] promotes the possible "massaging" of earth pressure forces and thereby the readiness to accept underdimensioned components. In order to exclude unspecific tabulated values for earth pressure determinations in future, the multi-phase system of solid-state physics was expanded accordingly. This extension permits soil properties and angles to be calculated, regardless of whether the soil is in a dry, moist or wet state [5: page 47ff.; 6: page 2.2–1 and 8: page 5ff.].

Chapter 3 contains experiments to determine soil parameters, such as the value of the natural inclination angle β , soil density, and compression strength σ_D . First, only the positions of the angles in the soil bodies are determined, because the teachings mention other angles, which cannot be determined in nature. Subsequently, three tests are conducted with sand and water in the glass container (Fig. 1, page 7).

2.4.1 Formation of a natural shear plane in sand, Test 1

This experiment was devised to determine the natural position of the inclined plane and the shear plane in dry sand. Hereby, observation of the natural soil behaviour stood in the foreground, not the measurement of empiric values. 27,0 kg of dry sand were filled (uncompressed) and evenly distributed in the left-

hand chamber with width $bk_l = 2,44$ dm. The surface was then levelled and the filling height $ht = 2,33$ dm measured. Following the abrupt removal of the separating glass pane, the sand slipped down into the right-hand chamber. The shear plane formed in this way is indicated by a green line, and the inclined plane by a red line. Slight deviations between real and indicated planes depend on the respective resolution (pixel size) of the image, and are accepted (see Fig. 15).

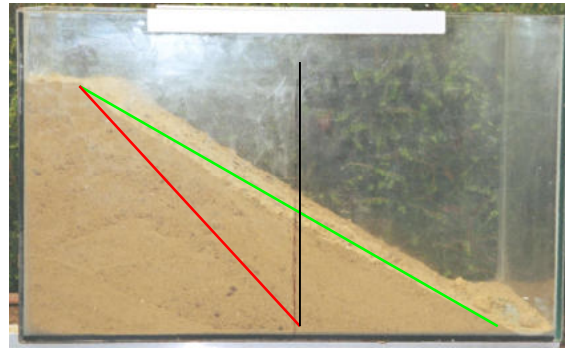


Fig. 15: Spreading of the sand with indicated shear plane (green) and inclined plane (red).

Deposits of the filling medium (sand) can occur in the upper part of the shear plane, because only the vertical force component Nv of normal force FN acts here ($nn \cdot nv/2$), i.e. horizontal forces, which could assist the sand's sliding motion, are missing in this part of the normal force area, (see Fig. 12, page 29). For force determination, the filling height h of the filling medium is measured, and the widths $bo = bu$ calculated from inclination angle β of the soil type. Width bo runs from the top of the container's center down to the sand's break line. At the bottom, width bu fills the distance between the container's center and the shear plane's base point. Width of the natural shear plane is described with $bue = bo + bu$, and its angle with s . The double tangent of the shear angle corresponds to the tangent of inclination angle β ($2 \tan s = \tan \beta$). If the soil is loosened during the slide, widths bo and bu become unequal, thereby changing the angle. Details about the consequences of loosened or compacted will be given later.

Inclination angle β

$$\tan \beta = h/b \rightarrow \tan \beta = 2,33/1,91 = 1,220 \quad 2.15$$

$$\beta = 50,7^\circ \quad [-] \quad 2.16$$

Shear angle s

$$\tan s = (\tan \beta) / 2 \rightarrow \tan s = 1,220/2 = 0,610 \quad 2.17$$

$$s = 31,4^\circ \quad [-] \quad 2.18$$

The test setup can be shown graphically as follows:

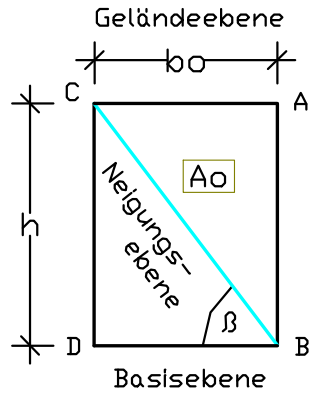


Fig. 16: Wedge areas A_o and A_u , which are divided by the inclined plane with its angle β .

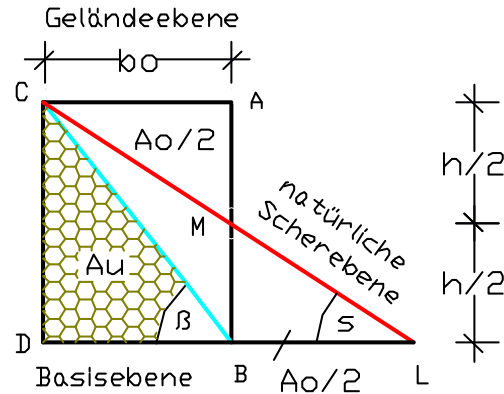


Fig. 17: "Reclining earth wedge" (C-L-D), inclined plane, and the shear plane under angle s .

In this study, area A_o is described as active, because its earth mass slides down along the inclined plane as soon as its lateral support is removed. There is no tendency to slide in reactive area A_u , because the earth mass is held by the adjacent earth block. The lengths of the inclined and shear planes can be calculated from height h and angle β or s . Density – and thereby the angles – of this soil type are changed if the soil loosens as it slides or is compacted by an external force. Both modifications result in a new soil type.

2.4.2 Formation of a natural inclined plane in sand, Test 2

Also for this experiment, 27 kg of sand were filled loosely into the left-hand chamber, and the surface levelled. The filling height $h_t = 2,36$ dm was measured. Subsequently, the right-hand chamber was filled with water up to a height of 2,75 dm. After about 2 hours, the water was suctioned off via a thin tube with an internal diameter $\varnothing_i = 6$ mm. On the next day, after the sand had consolidated, the separating glass pane was pulled out and the experiment left for 10 days, in order for the sand body to dry out naturally. As the expected fracture line did not develop in the sand body along the presumed inclined plane after this time, a cut was made with a fine saw blade in order to relieve a possible transverse stress in the sand body. The cut was made centrally through the consolidated sand body, parallel to the container's long sides. After applying a slight pressure on the separated surface, the sand wedges formed (Fig. 18). The ratio of height $hb = 2,11$ dm to measured width $b - b_o = 1,35$ dm indicates the tangent of the fracture plane's inclination angle β in the consolidated sand body.

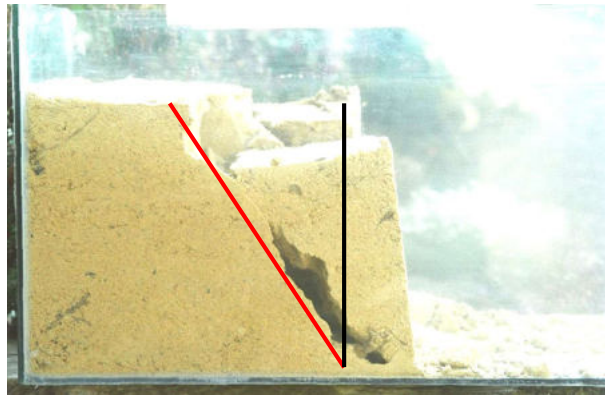


Fig. 18: Consolidated sand body with its inclined plane (red).

The following was calculated:

Inclination angle β

$$\tan \beta = 2,11/1,35 = 1,563 \quad 2.19$$

$$\beta = 57,4^\circ \quad [-] \quad 2.20$$

Compaction factor λ

$$\lambda = ht/hb \rightarrow \lambda = 2,36/2,11 = 1,12 \rightarrow 12\% \text{ by vol.} \quad 2.21$$

For the following description of the test results, reference is made to the previous calculation approaches and equations with corresponding brackets (). The test setup showed that the water compacted the dry sand with filling height $ht = 2,36$ dm by the amount of 12% by vol., and that this compaction resulted in an increase of inclination angle from $\beta = 50,7^\circ$ (2.16) to $\beta = 57,4^\circ$ (2.20). To validate the sand's compaction factor λ , which resulted in a value of 12% by vol. simply through the addition of water, the following supplementary test was conducted with sand and water.

2.4.3 Compaction of dry sand by adding water, Test 3

For the test, a glass cylinder with an interior height 2,97 dm and an internal diameter $\varnothing_i = 1,41$ dm was used. First, 7,6 kg of dry sand were loosely filled into the cylinder, and then 2,0 liters of water were carefully added. Following a waiting period of about 10 hours, the sand filling height $ht = 2,97$ dm had dropped to height $hb = 2,60$ dm. Therefore, simply the addition of water had compacted the dry sand by factor λ .



Fig. 19: Cylinder and filling height ht .



Fig. 20: Voids in the compacted sand



Fig. 21: Compacted sand with height hb .

The following was calculated:

Compaction factor λ

$$\lambda = 2,97/2,60 = 1,142 \rightarrow 14,2 \quad \% \text{ by vol.} \quad 2.22$$

Dry density ptg

$$ptg = kg/V = 7,6 \cdot 4 / (2,97 \cdot 1,41^2 \cdot \pi) = 1,639 \text{ kg/dm}^3 \quad 2.23$$

Dry density ptg'

$$ptg' = kg/V' = 7,6 \cdot 4 / (2,60 \cdot 1,41^2 \cdot \pi) = 1,872 \text{ kg/dm}^3 \quad 2.24$$

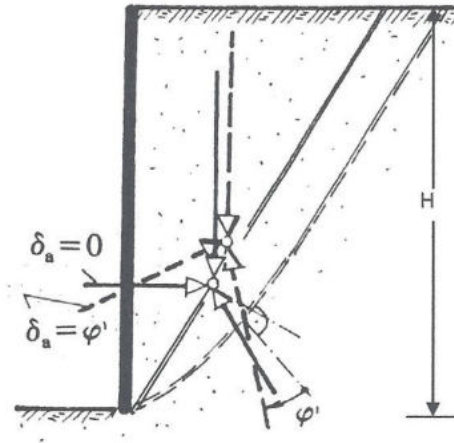
Even though there is a slight difference in the compaction factors established in Tests 2 and 3 ($\lambda = 12,0\%$ by vol. and $\lambda = 14,2\%$ by vol.), which can be due to different dry densities and minimal measurement inaccuracies, the following remains true:

If one were to dry the wet sand again, height hb would remain constant, and the dry density ptg of the loose sand would change into the dry density ptg' of the dry compacted sand. From this it can be derived that water can only reduce the volume of dry soil if the latter is first subjected to a liquid. If the compacted soil were to be dried and then flooded again with water, possibly with different levels, the dry density would simply change to a wet density, but the soil's volume would not change.

Summary:

The following can be derived from Tests 1 to 3:

1. The natural shear plane in a body of soil (sand) will be found, if the soil shifts from a “standing” into a “lying” earth wedge, without loosening in the process (see Figs. 15 to 17, page 41ff).
2. Shear plane and inclined plane form a straight line, and not a convex curvature, as represented by the teachings with the following Pict. P05.60 [1: page P.11].



Pict. P05.60: Convex curvature of the fracture plane caused by positive wall friction

It must be noted that during the author's own numerous experiments with different soil types, a convex curvature of the fracture plane never occurred.

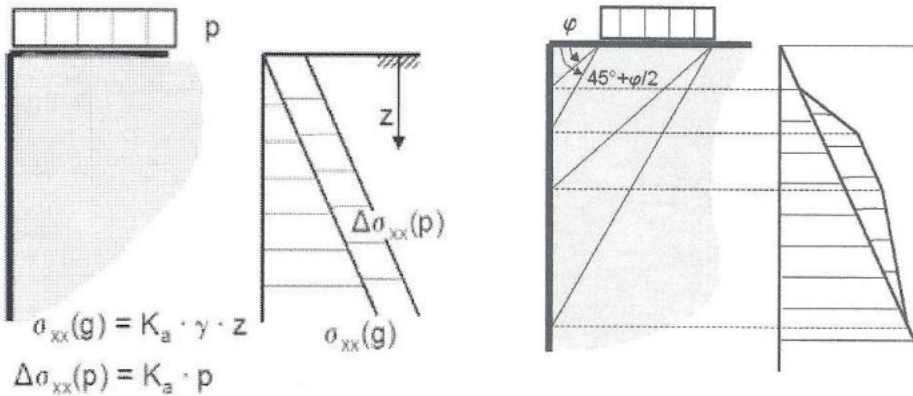
3. Shear angle s stands in a direct relationship with the inclination angle β of a soil: $\tan s = (\tan \beta) / 2$ (2.17).
4. Water is able to compact dry sand up to 14,2% by vol. (2.22).
5. As observed, voids are formed in the wet compacted sand, only to collapse and reform in another location (see Fig. 21, page 42).

2.5 Determination of inclination and shear angle under load

Coulomb and the teachings use different approaches for the dispersal into the ground of loads or external forces that are applied to a terrain area. These differences will be examined.

In his Fig. 7, Coulomb shows load p as an expansion of earth wedge (a-a'). The teachings use the expanded area from Fig. 7, but mirror it vertically into the stress field acc. to Pict. P05.120 [1: page P.15]. Regarding possible influ-

ences from adjacent loads, this modification is described as *appropriate* and *coherent* by the teachings [1: page P.14f.].



Pict. P05.120: Earth pressure stresses due to a load on terrain surface

While with Coulomb the load changes the width and height of the earth wedge behind the wall, the teachings only see an expansion of the earth wedge. In both approaches, the inclination angle of the loaded soil remains constant. If one adds the author's observations on soil behaviour to these explanations, a loaded earth wedge will slide faster than an unloaded wedge, and will thereby have an influence on the position of the inclined plane and its angle.

The New Theory recognizes that loads or external forces acting on a terrain area are dispersed into the ground via active and reactive force fields. Consequently, a longer frictional/inclined plane is formed in the ground for dispersing the force. In general, and if deeper soil layers permit this force dispersal, the changed calculation height shown by Coulomb is used (see Diagr. 7, page 25, and Fig. 22 below).

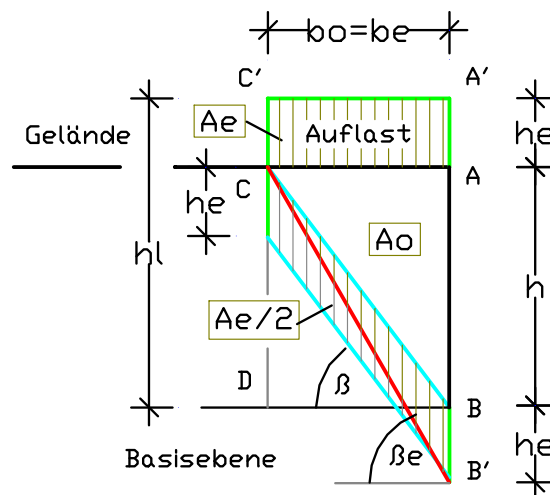


Fig. 22: Unloaded earth wedge (C–A–B), the load's active force area (C–B–B'), and the steeper inclined plane (C–B') due to the load.

The interaction between an external force and its dispersal within the ground is shown above in Fig. 22. For better understanding of the changes, the "unloaded" force distribution is shown with a blue inclined plane, and the "loaded" distribution with a red inclined plane.

The original wedge area Ao with wedge height h and wedge width b is stressed by load area Ae . In order to disperse the load, the equally sized area Ae (C–B–B'–D) is formed in the ground. This area is divided into the active partial area (C–B–B') and the reactive partial area (C–B'–D), thereby forming the steeper inclined plane (C–B'). Addition of the active wedge areas $Ao + Ae/2$ creates the wedge area (C–A–B'), which enables weight Ge to be determined and distributed.

External forces, which must be treated as distributed load q in kN/m, are introduced into the calculation system via height he . Height he is calculated from distributed load q divided by dry density ptg (new term) and gravity force $g = 9,807 \text{ m/s}^2$. The dry density is used, because liquids/water escape under pressure, so that water is unable to absorb and disperse loads (see calculation of soil properties in Chapter 3, page 54).

Addition of load height he and height h permits the steeper inclination angle βe and the new force area Aae to be determined from overall height hl and wedge width b .

Height he

$$he = q/ptg \cdot g \quad \text{m} \quad 2.25$$

Height h

$$h = b \cdot \beta \quad \text{m} \quad 2.26$$

Height hl

$$hl = he + h \quad \text{m} \quad 2.27$$

Angle βe

$$\tan \beta e = hl/be \rightarrow \beta e \quad [-] \quad 2.28$$

Area Ae

$$Ae = be \cdot he \quad \text{m}^2 \quad 2.29$$

Area Aa

$$Aa = b \cdot h/2 \quad \text{m}^2 \quad 2.30$$

Area Aae

$$Aae = Aa + Ae/2 \quad \text{m}^2 \quad 2.31$$

The change of inclination angle (from β to βe) and the value of force area (Aa to Aae) show that a load or external force applied to a soil body will influence the force or stress behaviour in this body. If the vertical force build-up in the soil is prevented by a rock or concrete layer, any undispersed vertical forces are

converted into horizontal forces along the barrier layer. This force conversion reduces the angle of the "loaded inclination plane".

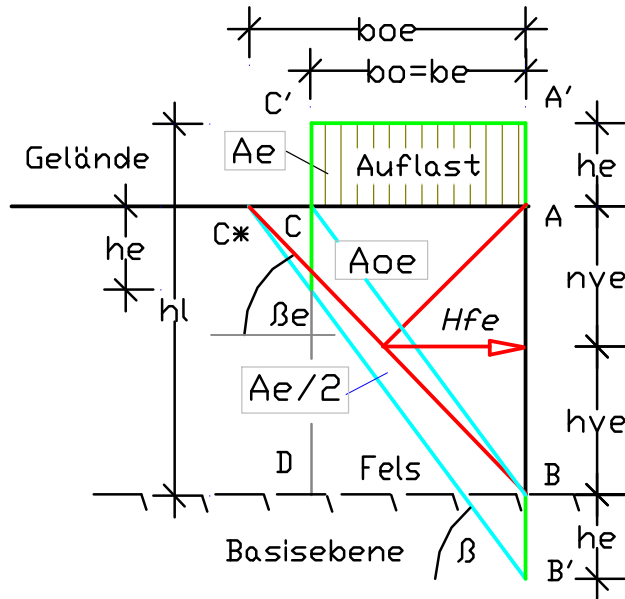


Fig. 23 Earth wedge (C*-A-B) with flattened inclination angle under load (red) due to a rock or concrete layer in the soil.

The figures above show that a soil body under load will form different inclination planes if a barrier layer (container bottom) prevents the dispersal of its vertical forces. Consequently, the locally measured natural shear angle s (see Fig. 15, page 39), which stands in a direct relationship with the inclination angle [$\tan s = (\tan \beta) / 2$], cannot be identical with shear angle φ , which is measured in the sample body/earth sample under axial or triaxial pressure according to DIN 18137-2 [1: page I.11ff.].

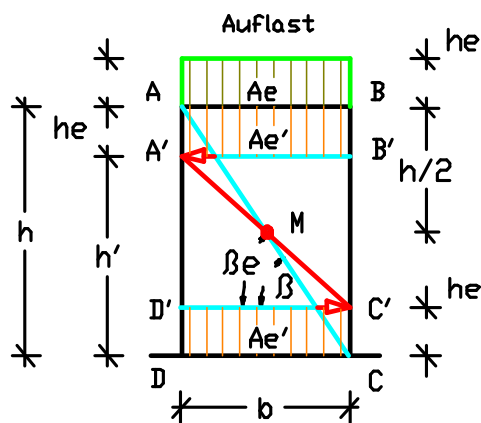


Fig. 24

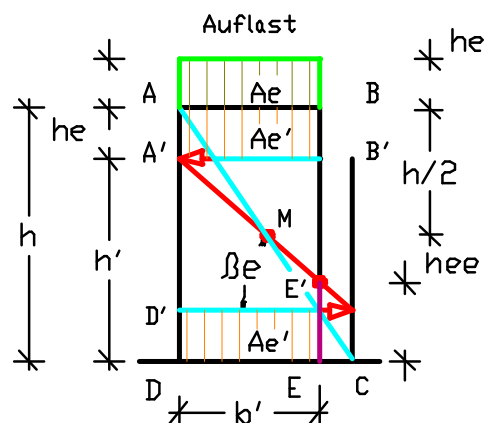


Fig. 25

Fig. 24: Changed position of inclined plane in the soil body due to the applied external force/load.

Fig. 25: Soil body, whose inclined plane (A-C) deviates from the cylinder's height/side ratio.

Force dispersal under restriction of the vertical force flow is shown above in Figs. 24 and 25. The earth blocks (sample bodies) shown have the same height, but have different widths b and b' . The height/side ratio in Fig. 24 has been selected so that the natural inclined plane (A–C) is accommodated as the diagonal in the soil body. In the narrower earth block in Fig. 25, the same inclined plane as shown in Fig. 24 ends in plane (D'–C'). Due to the vertical pressure applied to the sample body, the position of the inclined plane changes from (A–C) to (A'–C') within the body, and the angles change from β to βe . Because angle βe remains constant under equal pressure, the inclined plane already exits from the narrower body at the height of point E' (see Fig. 25).

Conclusions:

Figs. 22 to 25 show different force behaviours during the dispersion of external forces or loads in the soil body. This also depends on whether the vertical force flow is able to expand unrestricted or is impeded e.g. by a rock layer. Figs. 24 and 25 represent the changes of shear planes within sample bodies, which have been clamped in a device for the purpose of measuring shear strength, whereby the device exerts a pressure on the bodies. Consequently, the angle determined via the soil's shear strength can never be identical to the natural inclination angle β of soils that occurs without external pressure. Therefore, the New Theory distinguishes between the "inclination angle βe under load" and the natural "inclination angle β without load" (see compression strength test acc. to DIN EN 1926 as well as the Figs. in [6: page 5.2–1ff. and 10: page 25]).

2.6 Determination of inclination and shear angles with soil loosening

Figs. 26 and 27 below show that the angles in the earth block are also influenced by the soil's loosening or compaction.

With a soil that does not loosen as it slides down, the shear plane divides the active area Aa into area $Aa/2$ to the left, and area $Aa/2$ to the right of the reference axis. However, if the soil loosens as it slides, the pore increase becomes apparent in the soil's wedge area (C–L'–L) with height h and width bx . Due to the soil's loosening, the plane (C–L') no longer passes through the central point of the perpendicular reference axis, so that plane (C–L') is described as the "slope plane". If one shifts the reference axis to the right by the amount $bx/2$ (Fig. 27), the widths $bo + bx/2 = bu + bx/2$ are created. Under this condition,

the "slope plane" once again becomes the "natural shear plane" of the loosened soil type with shear angle s' .

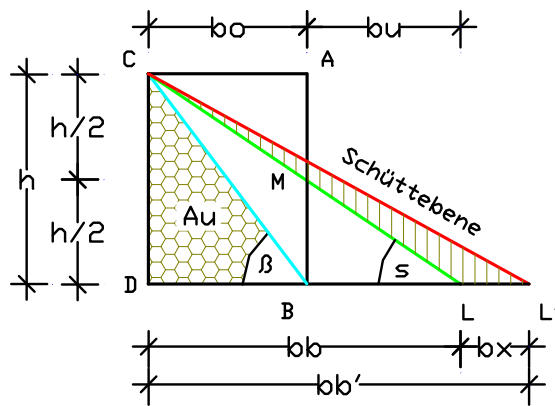


Fig. 26: Volume increase due to soil loosening (C-L'-L).

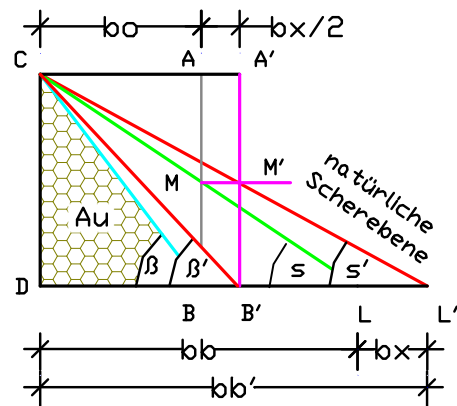


Fig. 27: Increase of wedge width by amount bx , and block width by $bx/2$.

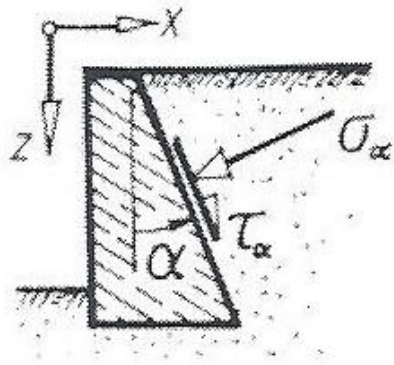
If the loosened soil is now formed back into an earth block of the same height h , the block will have a width of $b + bx/2$ and an inclination angle β' . Because of the direct dependence between inclination angle β' and shear angle s' , the approach $\tan s' = (\tan \beta') / 2$ will remain. Compacting of soils runs contrary to soil loosening, and increases the inclination angle.

2.7 Changed angles due to cohesion and/or wall friction

The teachings say that cohesion (adhesive strength of cohesive soils) and wall friction (between wall surface and adjacent soil) can influence failure angle α and shear angle φ' (see [1: page P.8ff.] and table in [1: page I.19]). Moreover, with Pict. P03.20 [1: page P.5] the teachings show that a soil in the stress-free condition below a sloping wall surface with angle α will develop a maximum shear stress σ_α , and the wall friction τ_α will occur between wall and soil (see [1: page P.5 and page P.22ff.]).

It must be noted that the wall friction on a sloping wall surface as well as the skin friction of a pile shaft – as shown by the teachings in [1: page P.11 and page P.25ff.] – does not show any reference to physical friction. Physics describe friction as a force between two solid bodies moving in different directions [15: page 98f.]. According to the rules of physics, either the wall or the soil behind the wall must be in continuous motion in order to generate a wall friction.

As such movements are undesirable in earth construction – the so-called wall friction – can neither generate a force in the static state, nor influence the direction of other forces or stresses in the ground.



Pict. P03.20: Sloping wall with angle α , and the position of stress σ_α against it.

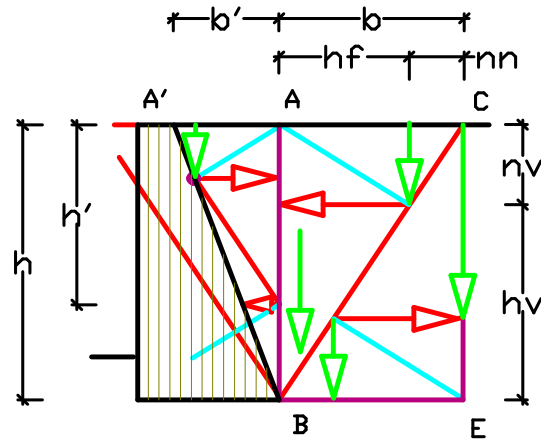


Fig. 28: Sloping wall, and behind it the new method of force distribution.

The same applies for the skin friction on a pile shaft. This could be imaginable where the pile "sinks" due to an overload, i.e. it loses its hold in the ground, and therefore moves. Contrary to this, the New Theory sees permanently active force fields in the ground, whose horizontal forces exert a pressure against the wall or the pile shaft. With a pile, the forces act radially on the pile skin, and disperse the forces bearing down on the pile in the same way as the pile's foot (see Section 4.8, page 148ff). Consequently, it is denied that the inclination of a wall surface or its roughness can influence the angle and the value of stress σ_α (see Pict. P03.20). The conducted experiments show that it is the type of the adjacent soil that determines the force value, its angle, and its direction – not the wall's inclination (see Section 4.4, page 126ff).

Contrary to this, the teachings describe *cohesion* as the adhesive force of moist, cohesive soils, and gives it the ability to influence forces and force directions in the ground (see [1: I.5–I.8 and 1: page P.11]). The New Theory recognizes the adhesive effect of cohesion, but doubts its ability to influence forces or force directions. But rather, cohesion is seen as a component of weight, which can slow down soil movements, but cannot stop them (see soil properties and soil behaviour of moist or wet soils in Chapter 3).

Similarly, a slight shift or rotation of the wall – as described by the teachings for the mobilization of horizontal forces in the ground – can influence neither the inclination angle β nor the earth pressure force. Only the clear movement of a perpendicular wall away from the adjacent soil or a serious skewing of the wall can lead to a loosening of the soil behind the wall, thereby changing soil density and inclination angle. This issue is discussed in detail in Chapter 4.

2.8 Flow condition and earth pressure, Tests 4 and 5.

As the author has no possibility of comparing Coulomb's original version of flow condition with the graphics used by current earth pressure teachings on flow condition [1: page I.14ff.], various tests were carried out in the glass container. In particular, the tests were intended to demonstrate the sliding of soils from a standing earth wedge to a lying wedge. One test was conducted with layers of basalt grit and another test with layers of sand and basalt grit.

Setup for Test 4

The left chamber of the glass container was filled with layers of dry basalt grit, topped with a layer of wet grit. The layers were separated with paper strips to visualize the grit's sliding movement from a standing wedge to a lying wedge.



Fig. 29 Layers of basalt grit in the glass container.



Fig. 30 Basalt grit and paper strips after removing the separating glass pane.



Fig. 31 Basalt grit after pulling out the paper strips from the two upper layers.

When the grit had slipped down after pulling out the glass pane, the paper strips of the three upper layers had bent down in the sliding direction. For further observation of the basalt grit's sliding movement, the paper strips under the upper three layers were carefully pulled out of the material horizontally. Subsequently, the shear plane of the grit came to rest at angle s ($\tan s = \tan \beta / 2$), as shown in Fig. 15, page 39. Not confirmed was a deformation in accordance with the Mohr-Coulomb 'flow condition' [1: S. I.14ff.] with development of a horizontal force in the lower third of the filling height.

Setup for Test 5

The left chamber of the glass container was loosely filled with differently high layers of sand and basalt grit. No separating paper strips were used. Fig. 32 below shows the material distribution after pulling out the glass pane.



Fig. 32 Inclination plane of the sand, and shear plane of the grit after the filling material had slipped down.

Conclusions:

Test 4 with basalt grit as filling material shows that the friction angle φ' described by the earth pressure teachings for the sliding process did not occur, i.e. also not a "flow of the brittle material" (see Picture I06.20, page 27).

If, on the one hand, the soil does not exhibit the indicated "flow condition" as it slides down from a standing earth wedge (Figs. 29 to 32), and on the other hand the *stress distribution* in Coulomb's classical earth pressure theory (Fig. 9, page 23) *is unknown* to the teachings, there is no basis for using the Mohr-Coulomb failure criterion for determining and distributing earth stresses.

Test 5 with different heights of sand and basalt grit layers produced the same result. Also here, no material flow was observed, which follows the description of the failure criterion in the earth pressure teachings even in the most rudimentary form. On the contrary: The tests confirmed that the flow condition

does not represent a modification of Coulomb's earth pressure theory, but that the flow condition and Coulomb's earth pressure theory obviously describe two different issues.

Regarding Test 5, it should be noted that by means of Coulomb's earth pressure theory the force distribution in the soil bodies (Fig. 9, page 23) before and after removing the separating glass pane was proved to be true (see Section 4.3.4, page 120ff). Here, the planes, angles, and forces are calculated, which explain the sliding behaviour of the filling materials in Fig. 32. Proof of a "flow of the filling materials", as described by the teachings for their fracture condition [1: page I.14ff.], could not be found – neither with Tests 4 and 5, nor by means of the calculations (see Figs. 30 to 32).

If, on the one hand, current earth pressure teachings claim that – regarding Coulomb – *“for the base case with a perpendicular wall face and level ground [...] the stress distribution is unknown with this approach”* (Fig. 9, page 23), and on the other hand it has been shown that natural soil behaviour does not exhibit the “flow condition” suggested by the teachings (Figs. 29 to 32), there is no longer any basis for the Mohr-Coulomb failure criterion. Consequently, earth pressure measurements carried out according to the teachings' specifications can only lead to faulty results.

2.9 Silo theory and earth pressure

The teachings refer to a relationship between Mohr-Coulomb's failure criterion and the silo theory. This is done to justify the statement that the friction between the rear wall surface and the adjacent soil, as assumed by the teachings, is able to reduce the earth pressure force against the wall [1: page P.2]. In addition, the teachings indicate that Janssen's investigations of grain silos can be used to determine the arching effect, and that these specifications were modified by Terzaghi and Houska for the stress conditions of the tunnel shell [1: page 3.5]. Hereby, factor K_0 is defined from the ratio of effective horizontal and effective vertical stress.

Based on pure physics, such a friction can only occur on the silo wall if the filling media starts moving down the silo wall. If grain is removed from a silo via a central opening in the silo floor, a funnel-shaped depression will soon show on the upper surface of the grain filling. This funnel indicates that the

grains tend to move away from the silo wall towards the center, whereby they are no longer available to create wall friction. Such a hollow cone is also created if one fills loose, dry sand into a funnel, and allows it to run out at the lower end. The same phenomenon appears when water is drained from a sink. Also here, it is more likely that a hollow cone appears in the water above the drain, than that the water simply runs down the sink walls to the drain.

Consequently, there is good reason to doubt that the wall friction proposed by the teachings exists at all, and that this friction is able to reduce the earth pressure force.

Conclusions:

If, according to pure physics, friction can only be generated by the opposite movement of two solid bodies [15: page 98ff.], neither wall friction nor skin friction can occur between resting bodies. Therefore, it is up to the teachings to justify the introduction of factor K_0 in their earth pressure determination. Equally questionable is the use of the same factor when determining a tunnel shell (see [1: page 3.3]).

3 Calculation of soil properties

3.1 General information on soil properties

Currently, there is a large number of rules, regulations, and DIN standards that provide tables with empiric soil parameters for earth pressure determinations – frequently with considerable differences in the values [1: page J.2f.]. If characteristic values are selected from these tables, which differ from the real soil values, the discrepancies in the earth pressure calculations become larger with increasing calculation height h . Ultimately, this deficiency can lead to underdimensioned constructions, structural damage and even to severe or fatal injuries. As a solution for this dilemma, the New Earth Pressure Theory is based on soil parameters that can be determined on-site very easily by means of the water content and the dry density of the adjacent soil. The experiments conducted with different soils resulted in the author's own expansion of the multi-phase system used in solid-state physics. By taking volume and weight proportions of soils into account, this innovation permits soil density ρ_{tg} (ρ_{ig} , ρ_{ng} , ...), friction value μ , inclination angle β , and shear angle s of all soil types to be determined unambiguously.

As already described, different soil types are seen as decomposition products of their respective primary rock. Continuous erosion converts hard rock into dust, and pressure converts dust back into rock. Every decomposition or compaction phase increases or reduces the pore volume in the mass, thereby creating a new soil type with new properties. Consequently, dry erosive rock or dry soil consists of solid matter and pores, whereby all voids in the rock or soil structure are seen as 'pores', regardless of whether they can absorb water or not. In the medium term, water (liquid) penetrating the pore structure cannot change either the volume of the pore or the solids, but can only influence the soil properties, e.g. density, inclination angle and soil behaviour. Because only the soil density and the inclination angle are required to determine earth pressure, all other influences on the soil characteristics such as type of primary rock, structure of the rock composite, as well as the grain, direction, and distribution structure [9: page 3f.] can be ignored. This applies particularly in the case of increasing calculation height. Similarly, possible time factors as well as thermal effects on soils have been ignored when calculating the soil properties, which encourages further studies.

Calculation of soil properties is based on density and inclination angle β of an ideal rock (basalt), which should be pore-free and only permit vertical stresses. A value of $\rho_{90} = 3,0 \text{ t/m}^3$ was selected for dry density [6: page 2.2–2 and 15: page 605], and friction value $\mu = 100$ was selected as the tangent of inclination angle β . In this way, the selected friction value enables a rock column with inclination angle $\beta = 89,4^\circ \sim 90^\circ$, height $h^* = 100 \text{ m}$, depth $a = 1,00 \text{ m}$, and width $b^* = 1,00 \text{ m}$ to be represented. Moreover, using a basalt rock with density ρ_{90} as an example, the index 90 can be used to indicate inclination angle $\beta_{90} = 90^\circ$. In addition, it was necessary to introduce new terms and abbreviations for the representation of the New Earth Pressure Theory (see page 231).

For a simplified understanding of the calculation results, this study makes use of the unit t/m^3 for density. Because soil density and inclination angle describe the same soil type, the types can be classified in the 'semicircle of soil types' by means of their angles, which range from $\beta = 0,6^\circ$ (primordial dust) up to $\beta = 89,4^\circ$ (basalt). Current descriptions were assigned to angles and planes of the soil types. By means of the force meters n_v , h_v and h_f measured or calculated within the circle – and multiplied with the respective force index g_i – it is possible to determine the earth forces FN , N_v , FH , H_v and H_f (see Section 2.3.2, page 19ff).

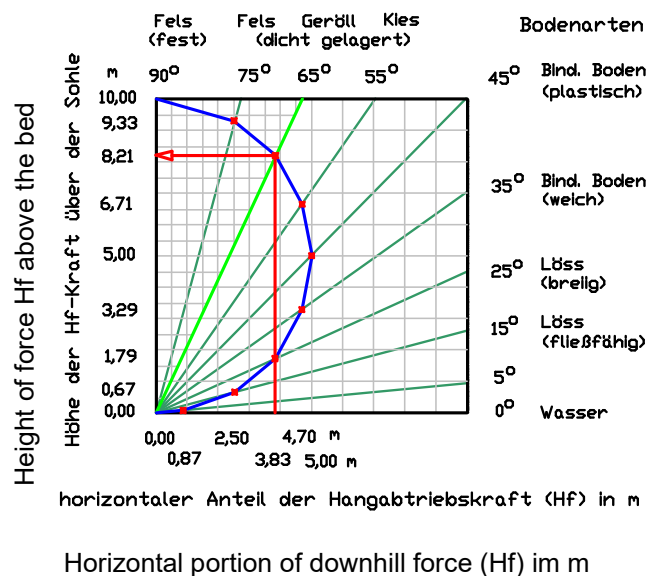


Fig. 33: Soil force meters in the 'semicircle of soil types', whereby the 'primordial dust' with a value of $\beta = 0,6^\circ$ must be located above the water.

For the 'semicircle of soil types', the height ordinate $h = 10,0 \text{ m}$ was selected, and the dry soil's inclination angle was marked from the zero point. At the point

where the soil type's inclined plane cuts the circle's arc, the normal force plane rises to the upper point of the ordinate, and the downhill plane drops back to the zero point. The horizontal plane – from the intersection to the ordinate – corresponds to force meter hf . The horizontal plane divides the ordinate – and thereby the wedge height – into force meter n (vertical component Nv of normal force FN), and below into force meter hv (vertical component Hv of downhill force FH). Force meters $hv = 8,21$ m and $hf = 3,83$ m have been drawn into the semicircle for the selected soil type, with angle $\beta t = 65^\circ$. Before determining the forces by means of force meters, the force index gi (2.7) must be calculated from wedge width $bo = h/\tan \beta_{65}$, soil density ptg_{65} , and gravity force g .

If one horizontally mirrors the earth wedge shown in the semicircle, together with its forces, the force distribution shown in Fig. 34 results. If one also draws an arc around the marked central point (M), so that points C, C', D', and D lie on the arc, this diagram shows a stress distribution according to Mohr's theory.

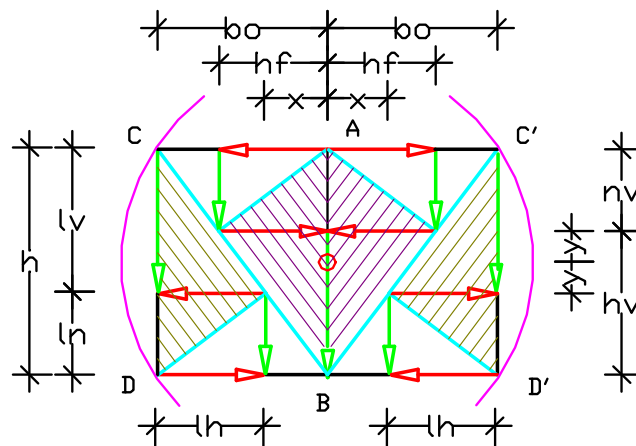


Fig. 34: Opposing earth blocks with height h , width bo , plus horizontal (hf) and vertical (nv and hv) force meters.

Figs. 33 and 34 prove that it is possible to classify 'dry' soil by means of density $ptg_{90} = 3,00$ t/m³ and friction value $\mu = 100$ of the idealized hard rock, and that the force distribution according to the New Earth Pressure Theory follows Coulomb's earth pressure theory unmodified, as well as Mohr's stress theory, and the calculation method according to the physical plane.

3.1.1 Calculating the properties of dry soils

Soil classifications regarding solid substances (solid phase), pore quantity (gaseous phase) as well as the amount of liquid absorbed by the soil (liquid phase) are derived by means of the multi-phase system of solid-state physics. Currently, the multi-phase system is used in particular to graphically represent the measurement results of the examined soil types in the individual phases [4: 1.4–1.8; 6: page 2.2–2.3 and 8: page 2–6], and to develop their properties.

This multi-phase system has been extended by the author so that the different changes of soil properties above and below water remain reproducible and calculable. Hereby, the basis is a rock cube (basalt) in the dry state, with height $h = 1,00$ m, width $b = 1,00$ m, and depth $a = 1,00$ m. As already described, the pore-free rock should have a density $\rho_{90} = 3,0$ t/m³ under the inclination angle $\beta \sim 90^\circ$. In this way, the rock cube's volume $V_{p90} = 1,00$ m³ equals the volume of solid substances or, using the new terminology, "solid substance volume V_{f90} ". It is also assumed that 'pores' with volume V_l are formed in the rock due to erosion processes, and that the pores penetrate the rock. In this way, a new soil type is created with every pore increase, until the hard rock is finally converted into dust. This process is described with the volumes $V_{p'} = V_{f90} + V_l$. If one were to permit the pore increase only in the axial direction, volume V_l could be determined via width Δb : $V_{p'} = h \cdot a \cdot (b + \Delta b)$. The final limit of rock dissolution is indicated by the term 'primordial dust'. Following the standardization to volume $V_p = 1,00$ m³, the solids volume should be $V_f = 0,01$ m³, and the pore volume $V_l = 0,99$ m³. By means of ratio V_f to V_l , friction value $\mu = \tan \beta = 0,01$ and thereby inclination angle $\beta_t = 0,6^\circ$ are calculated for the primordial dust. In spite of the indicated pore increase of $V_l = 99$ m³ with primordial dust, the initial volume of solid substance $V_{f90} = 1,00$ m³ remains unchanged.

As an example, the change of the rock will be investigated, which extends its original cube size $V_{p90} = 1,00$ m³ by the amount of width $\Delta b = 0,70$ m due to linear erosion caused by the pore increase. In order to determine all the other properties of the new soil type using the calculated soil volume $V = h \cdot a \cdot (b + \Delta b) = 1,70$ m³, the ratio V_f to V_l in volume $V_{p_n} = 1,00$ m³ must first be illustrated by means of standardization.

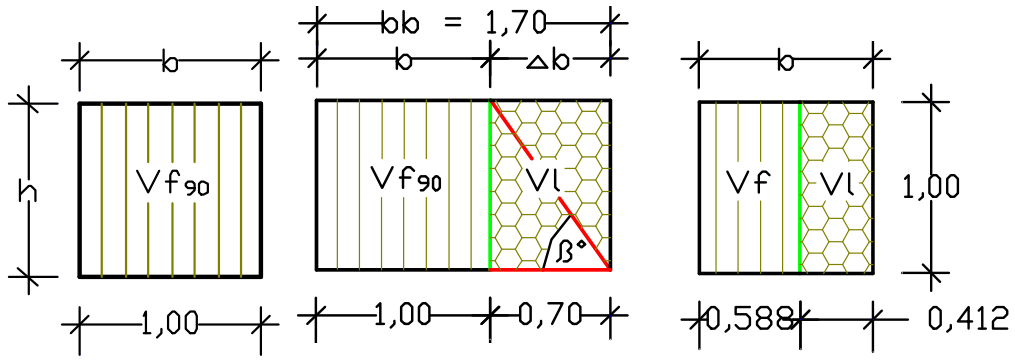


Fig. 35: Rock with volume Vf_{90} .

Fig. 36: Rock adhesion after the erosion phases.

Fig. 37: Volume $Vp_n = Vf + VL$ of a soil with angle $\beta t = 55^\circ$.

Figs. 35 to 37 show this change into volume Vp_n .

Calculation:

Solids volume Vf_n of the new soil type

$$Vf_n = Vf_{90} \cdot Vp/Vp'$$

$$Vf_n = 1,00 \cdot 1,00/1,70 = 0,588 \quad \text{m}^3 \quad 3.1$$

Pore volume VL_n of the new soil type

$$VL_n = Vf_{90} - Vf_n \rightarrow 1,00 - 0,588 = 0,412 \quad \text{m}^3 \quad 3.2$$

Inclination angle βt

$$\tan \beta t = \mu = Vf_n/VL_n \rightarrow 0,588/0,412 = 1,428 \quad 3.3$$

$$\beta t = 55,0^\circ \quad [-] \quad 3.4$$

or inclination angle βt

$$\tan \beta t = \mu = b/\Delta b \rightarrow 1,00/0,70 = 1,428 \quad 3.5$$

$$\beta t = 55,0^\circ \quad [-] \quad 3.6$$

Shear angle st

$$\tan st = (\tan \beta t) / 2 = 1,428/2 = 0,714 \quad 3.7$$

$$st = 35,5^\circ \quad [-] \quad 3.8$$

In order to identify the volumes during calculation, they can first be marked with n and then replaced with the respective angle value, e.g. $Vf_n = Vf_{55}$ or $VL_n = VL_{55}$.

Dry density ptg_{55} can be calculated from solids volume $Vf_{55} = 0,588 \text{ m}^3$ (3.1), rock density $ptg_{90} = 3,00 \text{ t/m}^3$, pore volume $VL_{55} = 0,412 \text{ m}^3$, and gas density $p_l = 0,00 \text{ t/m}^3$.

Dry density ptg_{55}

$$ptg_{55} = (Vf_{55} \cdot ptg_{90} + VL_{55} \cdot p_l) / Vp_{90} \quad (3.1)$$

$$ptg_{55} = (0,588 \cdot 3,00 + 0,0) / 1,00 = 1,764 \text{ t/m}^3 \quad 3.9$$

Result:

For the dry soil with volumes $Vf_{55} = 0,588 \text{ m}^3$ (3.1) and $VL_{55} = 0,412 \text{ m}^3$ (3.2), the inclination angle $\beta t = 55,0^\circ$ (3.4), shear angle $st = 35,5^\circ$ (3.8), and density ptg_{55}

= 1,764 t/m³ (3.9) have been calculated. This method for calculating volumes, angles, and dry density can be applied for all soil types – from hard rock up to primordial dust. The inclination angle forms the system's basis, via which all soil types can be classified continuously (see also Fig. 28, page 49).

3.1.2 Calculating the properties of wet soils

According to the New Theory, a soil whose pore structure Vln ($n = \text{wet}$) is completely filled with water is defined as 'wet'. If pressure is applied to this wet soil, at least part of the absorbed pore water will escape. Consequently, it is possible to derive that within a wet soil, only the solids structure of the loaded soil can serve for dispersing the forces, i.e. the solids in the dry soil. However, when calculating the force area for force dispersal, the inclination angle of the wet or moist soil remains unchanged. Experiments carried out by the author showed that a dry soil, which has once been completely flooded with water and thereby been compacted, will not be compacted further by renewed water absorption (see Test 3, page 41ff, and Section 3.1.3 below).

As the mobility of 'dry' soil depends on the 'solids to pore volume' ratio, and therefore also on its inclination angle βt , it should also be possible to calculate the inclination angle βn of a 'wet' soil under similar conditions. All that needs to be taken into account is the driving effect of the water absorbed by the dry soil. Similar to the determination of slump of fresh concrete [DIN 1045–2], it is likely that the amount of water in the soil has an influence on whether the inclination angle βn of a 'wet' or a 'moist' soil will result.

When calculating the angle of dry soil, the solids volume Vf takes the position of the numerator, and pore volume Vl takes the position of the denominator. Because the solid material cannot absorb any water, the lateral force of the water on the denominator side of the fraction must be taken into account when determining the inclination angle βn of wet soil. If one further assumes that only the pore volume Vl can be filled with water, and the densities of rock $ptg_{90} = 3,00 \text{ m}^3$ and water $pwg = 1,00 \text{ m}^3$ must be aligned, the 'fictitious' solids volume $Vfn = Vl \cdot pwg/ptg$ is included in the angle calculation of dry soil in order to take these facts into account. The following dependencies result for the fictitious solids volume Vfn of wet soil:

$$Vfn = Vln \cdot pwg/ptg_{90} \rightarrow Vln/3 = Vl/3 \quad \text{m}^3 \quad 3.10$$

By means of the previously calculated soil parameters $Vf_{55} = 0,588 \text{ m}^3$ (3.1) and $Vl_{55} = 0,412 \text{ m}^3$ (3.2), the inclination angle βn for the same soil type in the wet state can be determined as follows:

Inclination angle βn

$$\tan \beta n = Vf / (Vl + Vfn) \quad 3.11$$

$$\tan \beta n_{55} = 0,588 / (0,412 + 0,412/3) = 1,071$$

$$\beta n_{55} = 47,0^\circ \quad [-] \quad 3.12$$

Shear angle sn

$$\tan sn = (\tan \beta t) / 2 = 1,071/2 = 0,536 \quad 3.13$$

$$st = 28,2^\circ \quad [-] \quad 3.14$$

In this respect, also see the determination of inclination angle βt of the same soil in the dry state (3.3), and compare Fig. 36 with Figs. 38 and 39. The volumes of the wet soil are illustrated in the extended soil cubes below.

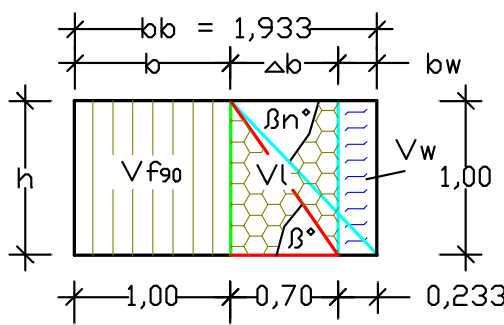


Fig. 38: Expansion of soil body in Fig. 36 due to water volume V_w , and with new inclination angle βn° .

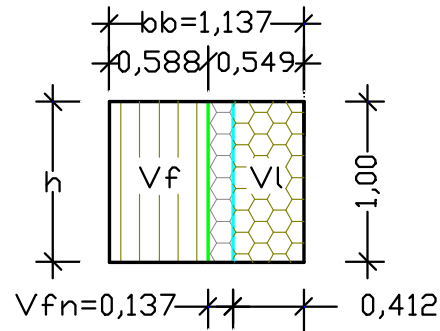


Fig. 39: Expansion of soil body in Fig. 37 due to the fictitious solids volume Vfn .

Wet soil density png is calculated by means of dry density $ptg_{55} = 1,764 \text{ t/m}^3$ (3.9) plus the weight of the pore water, whereby $V_w = Vl$ describes the water volume.

Wet density png

$$png = (Vf_{55} \cdot ptg_{90} + Vl_{55} \cdot pwg) / Vp_{90}$$

$$png = (0,588 \cdot 3,00 + 0,412 \cdot 1,0) / 1,0 = 2,176 \quad \text{t/m}^3 \quad 3.15$$

Results:

It has been shown that the inclination angle of the wet soil $\beta n = 47,0^\circ$ (3.12) can be calculated by means of the solids volume $Vf_{55} = 0,588 \text{ m}^3$ (3.1) and the pore volume $Vl_{55} = 0,412 \text{ m}^3$ (3.2) of the dry soil. To determine the tangent of inclination angle βn , the fictitious solids volume Vfn with $Vl/3$ was included on the denominator side of the fraction. The wet density $png = 2,176 \text{ t/m}^3$ (3.15) is derived from the addition of dry density $ptg = 1,764 \text{ t/m}^3$ (3.9) and weight of the absorbed pore water.

For the wet soil, the system of order shown in Fig. 40. In dependence of the densities ptg and pwg , it shows the solids volume Vf , the fictitious solids volume Vfn , and the pore volume Vl . It must be noted that also the properties of a wet soil stand in a direct relationship with each other, i.e. if density changes, also the angle will change, and vice versa. Every change creates a different soil type.

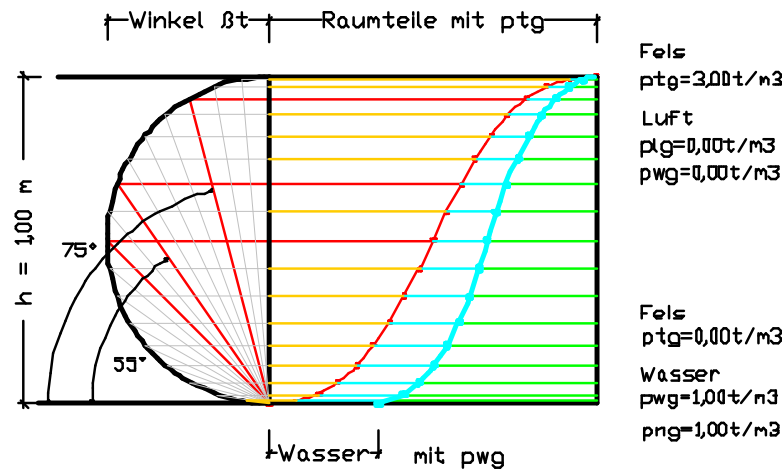


Fig. 40: With increasing angles, the pore volumes Vl and Vfn are reduced, and the solids volume Vf increases.

Fig. 40 shows a system of coordinates. To the left of the ordinate, the inclined planes of the dry soil types increase under their angle βt from the zero point up to the semicircle. To the right of the axis is the side view of a soil cube with height $h = 1,00$ m and width $b = 1,00$ m. If one draws horizontal lines from the intersections of the inclined planes with the semicircle to the right side of the cube, the volumes Vf and Vl as well as Vfn can be entered as widths on these planes. By connecting the end points of the widths, the curves shown in Fig. 40 are created. The red curve shows the separating line between the solids and pore volumes, and the blue curve combines the solids volume Vf and the fictitious solids volume Vfn . In the side view, the rock occupies the upper edge with volume $Vf_{90} = 1,00$ m³ and dry density $ptg_{90} = 3,00$ t/m. The lower edge is occupied by the pore volume. The so-called primordial dust – consisting of solids volume $Vf_{0,6} = 0,010$ m³ and pore volume $Vl = 0,990$ m³ – would be located slightly above this level. Moreover, Fig. 40 shows that the densities of dry and wet soils can be determined graphically.

3.1.3 Calculating the properties of wet soils with soil compaction

This example is based on Test 3, page 41, where loose sand with a dry density $ptg = 1,639$ kg/dm³ (2.23) is compacted simply by the addition of water.

The following values are used for calculation:

$Vf_{55} = 0,588 \text{ m}^3$ (3.1)	$Vl_{55} = 0,412 \text{ m}^3$ (3.2)
Angle $\beta t = 55,0^\circ$ (3.4)	Density $ptg_{55} = 1,764 \text{ t/m}^3$ (3.9)
Angle $\beta n = 47,0^\circ$ (3.12)	Density $png = 2,176 \text{ t/m}^3$ (3.15)
$Vp_{90} = 1,00 \text{ m}^3$ and degree of compaction $\lambda = 14,2\%$ by vol. (2.22)	

Calculation:

Pore volume Vl'

$$Vl' = Vl_{55} - Vp \cdot \lambda = 0,412 - 1,00 \cdot 0,147 = 0,265 \quad \text{m}^3 \quad 3.16$$

Total volume Vp'

$$Vp' = Vf_{55} + Vl' = 0,588 + 0,265 = 0,853 \quad \text{m}^3 \quad 3.17$$

Solids volume Vf^* → standardized to $Vp_{90} = 1,00 \text{ m}^3$

$$Vf^* = Vf_{55} \cdot Vp_{90} / Vp'$$

$$Vf^* = 0,588 \cdot 1,000 / 0,853 = 0,689 \quad \text{m}^3 \quad 3.18$$

Pore volume Vl^* → standardized to $Vp = 1,00 \text{ m}^3$

$$Vl^* = Vl' \cdot Vp_{90} / Vp'$$

$$Vl^* = 0,265 \cdot 1,000 / 0,853 = 0,311 \quad \text{m}^3 \quad 3.19$$

Inclination angle βt^* → after drying the soil

$$\tan \beta t^* = Vf^* / Vl^* = 0,689 / 0,311 = 2,215 \quad 3.20$$

$$\beta t^* = 65,7^\circ \quad [-] \quad 3.21$$

Inclination angle βn^* → of the wet and compacted soil

$$\tan \beta n^* = Vf^* / 1,333 \cdot Vl^* \quad 3.22$$

$$\tan \beta n^* = 0,689 / 1,333 \cdot 0,311 = 1,662 \quad 3.22$$

$$\beta n^* = 59,0^\circ \quad [-] \quad 3.23$$

Parts by weight of water pwg^*

$$pwg^* = Vl^* \cdot p_w / Vp_{90} = 0,311 \cdot 1,0 / 1,0 = 0,311 \quad \text{t/m}^3 \quad 3.24$$

Wet density png^*

$$png^* = Vf^* \cdot ptg / Vp_{90} + pwg^*$$

$$png^* = 0,689 \cdot 3,0 / 1,0 + 0,311 = 2,378 \quad \text{t/m}^3 \quad 3.25$$

Result:

By applying the compaction factor of 14,2% by vol. (2.22), the specified soil has changed its volume and thereby its properties.

Before compaction (dry)	After compaction (wet)
Angle $\beta t = 55,0^\circ$ (3.4)	Angle $\beta t^* = 65,7^\circ$ (3.21)
Angle $\beta n = 47,0^\circ$ (3.12)	Angle $\beta n^* = 59,0^\circ$ (3.23)
Density $png = 2,176 \text{ t/m}^3$ (3.15)	Density $png^* = 2,378 \text{ t/m}^3$ (3.25)

3.1.4 Calculating the properties of moist soils

Soils, whose pore structure does not permit complete water absorption, are defined as 'moist'. In these cases, the structure of the rock or the soil does not allow

all pores to be completely filled with water. Consequently, and depending on their water content, moist soils can be classified between 'dry' and 'wet'. The pore volume Vl is divided into volume Vlt , which is not occupied by water, and volume Vln containing water. The inclination angle β_i and density p_{ig} are assigned to moist soils or soils infiltrated by water.

The actual amount of water absorbed by the soil, as well as the minimum & maximum values for water absorption capacity, can be determined from undisturbed soil samples under laboratory conditions [DIN 18121-1/-2].

The following values are used for calculation:

$Vf_{55} = 0,588 \text{ m}^3$ (3.1)	$Vl_{55} = 0,412 \text{ m}^3$ (3.2)
Angle $\beta_t = 55,0^\circ$ (3.4)	Density $p_{tg} = 1,764 \text{ t/m}^3$ (3.9)

Moreover, it is specified that 75% by vol. of pore volume Vl can be filled with water, i.e. 25% by vol. of the pore volume remain dry.

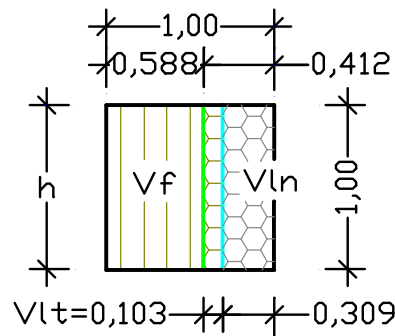


Fig. 41: Pore volume Vl divided into Vlt and Vln .

Pore volume $Vlt \rightarrow$ not occupied by water \rightarrow 25% by vol.

$$Vlt = Vl \cdot 0,25 = 0,412 \cdot 0,25 = 0,103 \quad \text{m}^3 \quad 3.26$$

Pore volume $Vln \rightarrow$ occupied by water \rightarrow 75% by vol.

$$Vln = Vl \cdot 0,75 = 0,412 \cdot 0,75 = 0,309 \quad \text{m}^3 \quad 3.27$$

Fictitious solids volume Vfn

$$Vfn = Vln \cdot p_{wg}/p_{tg90} = 0,309 \cdot 1/3 = 0,103 \quad \text{m}^3 \quad 3.28$$

Inclination angle β_i

$$\tan \beta_i = Vf / (Vl + Vfn) = 0,588 / (0,412 + 0,103) = 1,142 \quad 3.29$$

$$\beta_i = 48,8^\circ \quad [-] \quad 3.30$$

Parts by weight of water p_{wg}

$$p_{wg} = Vln \cdot p_w/Vp_{90} = 0,309 \cdot 1,0/1,0 = 0,309 \quad \text{t/m}^3 \quad 3.31$$

Wet density p_{ig}

$$p_{ig} = Vf \cdot p_{tg}/Vp_{90} + p_{wg}$$

$$p_{ig} = 0,588 \cdot 3,0/1,0 + 0,309 = 2,073 \quad \text{t/m}^3 \quad 3.32$$

Results:

By means of partial volumes $V_{lt} = 0,103 \text{ m}^3$ (3.26) and $V_{ln} = 0,309 \text{ m}^3$ (3.27) it was possible to calculate angle β_i and density p_{ig} for the moist soil.

Before water absorption	After water absorption
Angle $\beta_t = 55,0^\circ$ (3.4)	Angle $\beta_i = 48,8^\circ$ (3.30)
Density $p_{tg} = 1,764 \text{ t/m}^3$ (3.9)	Density $p_{ig} = 2,073 \text{ t/m}^3$ (3.32)

If one considers the different densities and inclination angles formed by a dry soil due to the absorption of more or less pore water one the one hand, and compares them with the generalized empiric tabulated values of current standards on the other, an earth pressure calculation based on the tabulated values must lead to a result that is not in accordance with theory. It remains a mystery, how one is supposed to obtain unambiguous soil characteristics by means of a “finger test”, a “kneading test”, or the current descriptions for soil states (firm, stiff, soft, pasty, liquid, silty, etc.). It can be demonstrated that with a dry soil, an angular difference of $60^\circ - 55^\circ = 5^\circ$ results in a deviation of some 8% for weight G . With lower calculation heights of $h < 3,0 \text{ m}$, this force difference might still be acceptable, but with increasing height h , it could possibly lead to structural damage. The tabulated values mentioned above are found in the standards [DIN 18196], [DIN 18300], [DIN 18301] and in [1: E.6ff. and 1: I.19].

In conclusion, one can say that using the extended multi-phase system of solid-state physics to calculate soil properties makes the tabulated values superfluous to a great extent.

3.1.5 Formation of a shear plane in moist basalt grit, Test 6

The following experiment was selected as Test 6. First, dry basalt grit 0/3 mm and water were mixed in another container, and then loosely filled into the left-hand chamber of the glass container, and the surface of the mixture smoothed without applying pressure. For the tests in the glass container, the unit of density was changed from t/m^3 to kg/dm^3 .

The following values are used for calculation:

$G_t = 30,5 \text{ kg basalt grit 0/3 mm}$	Density $p_{tg} = 1,808 \text{ kg/dm}^3$
$G_w = 3,0 \text{ kg water}$	Filling height $h_i = 2,34 \text{ dm}$

Next, the properties of the dry soil were determined, followed by determination of the moist soil properties after the addition of water. Using inclination angle β_i and shear angle si of the moist soil, it is then possible to calculate widths b_o and b_u , which are reached after the separating glass pane has been pulled out, and the basalt grit has slipped down.



Fig. 42: Glass container filled with moist basalt grit.

Calculation:

Base area A_{k1} → left-hand chamber with width $b_{k1} = 2,44$ dm

$$A_{k1} = a \cdot b = 2,90 \cdot 2,44 = 7,08 \quad \text{dm}^2 \quad 3.33$$

Volume V_{kt} → of the dry basalt grit

$$V_{kt} = G_t / p_{tg} = 30,5 / 1,808 = 16,87 \quad \text{dm}^3 \quad 3.34$$

Filling height h_t → of dry basalt grit

$$h_t = V_{kt} / A_{k1} = 16,87 / 7,08 = 2,38 \quad \text{dm} \quad 3.35$$

Volume V_{ki} → of moist basalt grit → $h_i = 2,34$ dm (measured)

$$V_{ki} = A_{k1} \cdot h_t = 7,08 \cdot 2,34 = 16,57 \quad \text{dm}^3 \quad 3.36$$

Compaction factor λ

$$\lambda = V_{kt} / V_{ki} = 16,87 / 16,57 = 1,017 \quad \% \text{ by vol.} \quad 3.37$$

Parts by weight of water p_{wg}

$$p_{wg} = G_w / V_{ki} = 3,0 / 16,57 = 0,181 \quad \text{kg/dm}^3 \quad 3.38$$

Wet density p_{ig}

$$p_{ig} = (G_t + G_w) / V_{ki} = 33,5 / 16,57 = 2,022 \quad \text{kg/dm}^3 \quad 3.39$$

Fictitious solids volume V_{fn}

$$V_{fn} = p_{wg} \cdot V_{p90} / p_{tg90} = 0,181 \cdot 1,0 / 3,0 = 0,060 \quad \text{dm}^3 \quad 3.40$$

Solids volume V_f → of dry basalt grit

$$V_f = G_t \cdot V_{p90} / V_{ki} \cdot p_{tg90}$$

$$V_f = 30,5 \cdot 1,0 / 16,58 \cdot 3,0 = 0,613 \quad \text{dm}^3 \quad 3.41$$

Pore volume V_l → of dry basalt grit

$$V_l = V_{p90} - V_f = 1,000 - 0,613 = 0,387 \quad \text{dm}^3 \quad 3.42$$

Inclination angle β_i

$$\tan \beta_i = V_f / (V_l + V_{fn}) = 0,613 / (0,387 + 0,060) = 1,371 \quad 3.43$$

$$\beta_i = 53,9^\circ \quad [-] \quad 3.44$$

Shear angle si

$$\tan si = (\tan \beta i) / 2 = 1,371/2 = 0,686 \quad 3.45$$

$$si = 34,4^\circ \quad [-] \quad 3.46$$

Wedge width $bo = bu \rightarrow$ of measured filling height $hi = 2,34$ dm

$$bo = hi / \tan \beta i = 2,34/1,371 = 1,71 \quad \text{dm} \quad 3.47$$

Width bue

$$bue = bo + bu = 2 \cdot bo = 2 \cdot 1,71 = 3,42 \quad \text{dm} \quad 3.48$$

Width bue indicates the shear plane's horizontal level, formed by widths bo and bo from the center of the glass container. If the soil is not loosened as it slides from a standing to a lying earth wedge, widths bo and bo as well as the lateral distances to the container walls bl and br are equal (see Section 2.4, page 37ff). For the following calculation it is assumed that the basalt grit hardly loosens as it slides down.

Width $bl = br \rightarrow$ container width $b = 4,88$ dm.

$$bl = (b - bue)/2 = (4,88 - 3,42)/2 = 0,73 \quad \text{dm} \quad 3.49$$

Widths $bl' = 0,70$ dm and $br' = 0,68$ dm were measured from Fig. 43 below, so that the new width bue' results. Using height $hi = 2,34$ dm and width bue' it is then possible to determine shear angle si' of the moist basalt grit.

Width bue'

$$bue' = b - bl' - br' = 4,88 - 0,70 - 0,68 = 3,50 \quad \text{dm} \quad 3.50$$



Fig. 43: Position of shear plane of the moist basalt grit.

Shear angle si'

$$\tan si' = hi/bue' = 2,34/3,50 = 0,669 \quad 3.51$$

$$si' = 33,8^\circ \quad [-] \quad 3.52$$

Inclination angle $\beta i'$

$$\tan \beta i' = 2 \cdot \tan si' = 2 \cdot 0,669 = 1,337 \quad 3.53$$

$$\beta i' = 53,2^\circ \quad [-] \quad 3.54$$

Results:

Test 6 showed that the author's extension of the multi-phase system of solid-state physics can be applied to determine soil properties. The slight difference between calculated and measured angles can be due to a slight loosening of the mixture as it slides down.

Calculated	Measured
Inclination angle $\beta_i = 53,9^\circ$ (3.44)	Inclination angle $\beta_i' = 53,2^\circ$ (3.54)
Shear angle $si = 34,4^\circ$ (3.46)	Shear angle $si' = 33,8^\circ$ (3.52)
Width $bue = 3,42$ dm (3.48)	Width $bue' = 3,50$ dm (3.50)

In an earth pressure calculation using specified wedge height $h = 5,00$ m and wedge widths bo and bo' , the difference between inclination angles $\beta_i = 53,9^\circ$ (3.44) and $\beta_i' = 53,2^\circ$ (3.54) would result in the following deviation:

Wedge width bo with $h = 5,00$ m

$$bo = h / \tan \beta_i = 5,00 / 1,371 = 3,65 \quad \text{m} \quad 3.55$$

Wedge width bo' with $h = 5,00$ m

$$bo' = h / \tan \beta_i' = 5,00 / 1,337 = 3,74 \quad \text{m} \quad 3.56$$

With height $h = 5,00$ m, the wedge widths bo and bo' differ by 0,09 m. This result is perfectly acceptable – even for dimensioning a supporting wall.

3.2 General information on soils under water

The experiments conducted for this complex show that the illustrated dependencies between density, angles, and volumes of soils above water can also be applied for wet and moist soils under water. The extensions used in the previously described formulas can be derived from the soil's buoyancy according to the Archimedean principle [15: page 148f.]. As shown in Section 3.1.2, the pore volume Vl of a wet soil is filled with water, and is then described as volume Vln . Moreover, the pore water pressure in volume Vln is opposed by the hydrostatic pressure, thereby reducing the wet soil's tendency to spread.

Because the hydrostatic pressure has the shape of a wedge under the 45° angle, the water volume $Vw = h \cdot a \cdot b/2$ in the side view $Aw = Vw/a$ of the 'soil band' is represented as a rectangle, whereby the soil band is understood as an extension of the soil cube. Also with wet soils under water, the tangent β_{nw} represents the ratio of solids volume to pore volume. But with soils under water, and in accordance with the densities p_w to ptg_{90} , the uplift divides the solids volume Vf into the uplift volume $Vfa = Vf/3$ and the remaining solids volume under water

$V_{fw} = 2 \cdot V_f/3$, which forms the numerator. On the denominator side of the fraction we have the pore volume V_l and the pore volume $V_{ln} = V_l$ occupied by water. By means of the densities p_w/ptg_{90} , volume V_{ln} must be converted back into the fictitious solids volume $V_{fn} = V_{ln} \cdot 1,0/3,0$. Consequently, the 'earth pressure under water' is formed by the fictitious solids volume V_{fn} and volume $V_w = V_{ln}/2$ of the sideways-acting force of wet soils under water. Opposing the earth pressure is the water pressure with volume $V_w = V_{ln}/2$ of the water column.

By means of the above volumes, the tangent of the wet soil under water can be calculated as follows:

$$\tan \beta_{nw} = 2/3 \cdot V_f / (V_l + V_{fn} - V_w) = 2/3 \cdot V_f / V_l \cdot 5/6$$

Because earth pressure in the 'soil under water' force system usually exceeds the water pressure, the earth pressure becomes decisive for the static calculation of components. In the same way, therefore, loads on soils under water can only be dispersed via the soil structure. Regarding the densities p_{nwg} and p_{iwg} of wet and moist soils under water, it must be noted that because of the apparent loss of weight due to uplift, they are only valid for determining forces under water.

3.2.1 Calculating the properties of wet soils under water

For this calculation of soil properties, it is assumed that the soil has already been compacted by the water, and is therefore not subjected to any further loss of volume by the water.

The following values are used:

Solid substance $V_{f_{55}} = 0,588 \text{ m}^3$ (3.1)	Pore volume $V_{l_{55}} = 0,412 \text{ m}^3$ (3.2)
Angle $\beta_t = 55,0^\circ$ (3.4)	Density $ptg = 1,764 \text{ t/m}^3$ (3.9)

Calculation:

Solids volume $V_{fw} \rightarrow$ under uplift

$$V_{fw} = 2 \cdot V_f/3 = 2 \cdot 0,588/3 = 0,392 \quad \text{m}^3 \quad 3.57$$

Water volume V_w

$$V_w = V_{ln}/2 = 0,412/2 = 0,206 \quad \text{m}^3 \quad 3.58$$

Occupied pore volume $V_{ln} \rightarrow$ with wet soil

$$V_{ln} = V_l = 0,412 \quad \text{m}^3 \quad 3.59$$

Fictitious solids volume V_{fn}

$$V_{fn} = V_{ln} \cdot p_w/ptg_{90} = 0,412 \cdot 1/3 = 0,137 \quad \text{m}^3 \quad 3.60$$

Inclination angle $\beta_{nw} = 48,8^\circ$ (3.62)
Shear angle $s_{nw} = 29,7^\circ$ (3.64)
Wet density $\rho_{nw} = 1,588 \text{ t/m}^3$ (3.66)

Due to standardization, the volumes shown in the soil band in Fig. 39 are converted into the volumes of the new soil type cube (see Fig. 40), whereby volumes $V_{ln/3}$ and V_w in the wet soil under water represent opposing water pressures.

The volume $V_{nw} = V_{ln/3} - V_w = 0,137 - 0,206 = -0,069 \text{ dm}^3$ indicates that when determining angle β_{nw} (see 3.61), volume V_{nw} might have to be entered with a negative sign.

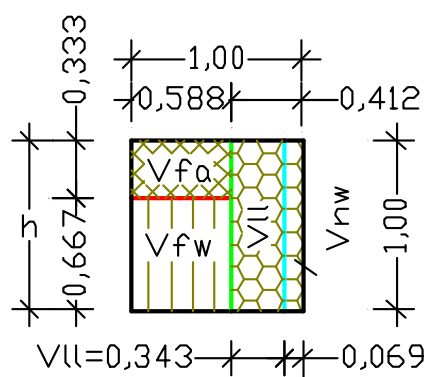


Fig. 45: Volume of wet soil under water after standardization.

3.2.2 Experiment with wet basalt grit under water, Test 7

The experiment in Test 7 was intended to check the angles and densities of wet soils under water calculated by means of the volume and weight portions.

The following values are used:

Basalt grit, $G_t = 30,0 \text{ kg}$	Filling height $h_t = 2,34 \text{ dm}$
Water, $G_w = 22,0 \text{ kg}$	Filling height $h_w = 2,28 \text{ dm}$
Measured height $h_b = 2,14 \text{ dm}$ (see Figs. 46 to 48).	

Dry grit 0/3 mm was filled into the left-hand chamber of the glass container up to filling height $h_t = 2,34$. After smoothing the grit's surface, the right-hand chamber was carefully filled with water.

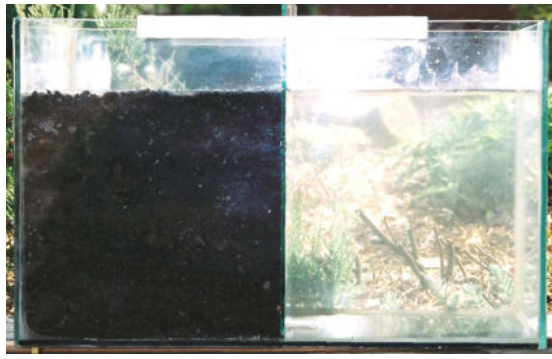


Fig. 46: Height $hw = 2,28$ dm of the water level reached at the end of the filling procedure.

As the water was able to seep into the basalt grit through the joints between the container walls and the separating glass pane, it was assumed after four hours that all the pores of the basalt grit had been filled with water. Subsequently, the height $hw = 2,28$ dm of the water level, and height $hb = 2,14$ dm of the compacted wet basalt grit under water were measured, and the separating glass pane pulled out. The 4-hour waiting period was chosen, because similar tests with basalt grit under water had shown that no further compaction occurred after this time.

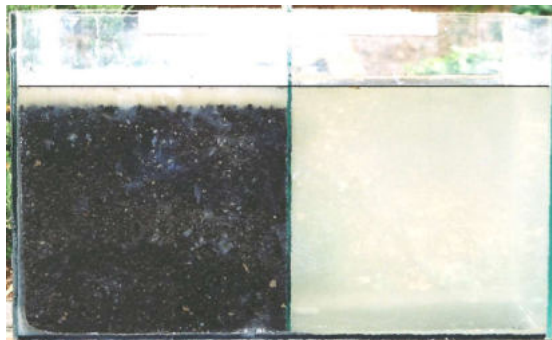


Fig. 47: Measured height $hb = 2,14$ dm of the grit compacted by water before pulling out the separating glass plane.

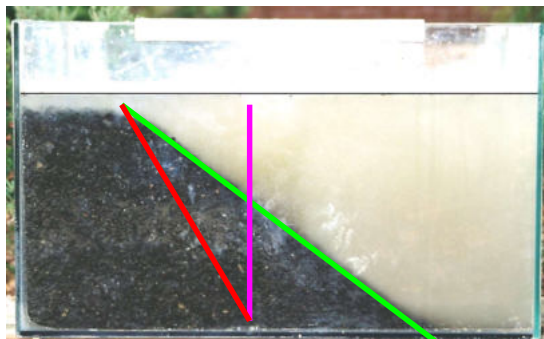


Fig. 48: Shear plane of the basalt grit under water.

After the wet basalt grit had slipped down into the right-hand chamber, widths $bl = 1,06$ dm and $br = 1,06$ dm were measured, and width bue calculated.

$$bue = b - bl - br = 4,88 - 1,06 - 1,06 = 2,76 \quad \text{dm} \quad 3.67$$

Width *bue* corresponds to the horizontal plane of the basalt grit's inclined surface. It is divided into width *bo* to the left of the vertical central axis, and width *bu* to the right of the axis. If widths *bo* and *bu* adopt different shapes after the filling material has slipped down, the width difference *bx* indicates a loosening of the material.

Width *bo* → measured on the glass container

$$bo = bk_l - bl = 2,44 - 1,06 = 1,38 \quad \text{dm} \quad 3.68$$

Width *bu* → measured

$$bu = bk_l - br = 2,44 - 1,06 = 1,38 \quad \text{dm} \quad 3.69$$

Width *bx* → loosening width

$$bx = bo - bu = 1,06 - 1,06 = 0,00 \quad \text{dm} \quad 3.70$$

In order to calculate the properties of the wet grit under water, the properties of the dry basalt grit must be determined first.

Properties to be calculated for dry basalt grit

Volume *Vkt* → $ht = 2,34$ dm, $Ak_l = 7,08$ dm³ (3.33)

$$Vkt = ht \cdot Ak_l = 2,34 \cdot 7,08 = 16,57 \quad \text{dm}^3 \quad 3.71$$

Dry density *ptg*

$$ptg = Gt/Vkt = 30,0/16,57 = 1,811 \quad \text{kg/dm}^3 \quad 3.72$$

Solids volume *Vfn* → Index *n* can be replaced with angle βt .

$$Vfn = Vf_{90} \cdot ptg/ptg_{90} = 1,0 \cdot 1,811/3,0 = 0,604 \quad \text{dm}^3 \quad 3.73$$

Pore volume *VL_n*

$$VL_n = Vp_{90} - Vfn = 1,000 - 0,604 = 0,396 \quad \text{dm}^3 \quad 3.74$$

Inclination angle βt

$$\tan \beta t = Vfn/VL_n = 0,604/0,396 = 1,525 \quad 3.75$$

$$\beta t = 56,7^\circ \quad [-] \quad 3.76$$

Shear angle *st*

$$\tan st = (\tan \beta t) / 2 = 1,525/2 = 0,763 \quad 3.77$$

$$st = 37,3^\circ \quad [-] \quad 3.78$$

The dry mass with volume *Vkt* in the glass container is composed of the solids volume $\sum Vf_{57}$ and pore volume $\sum VL_{57}$, which are calculated below.

Solids volume $\sum Vf_{57}$

$$\sum Vf_{57} = Vkt \cdot Vfn/Vp_{90} = 16,57 \cdot 0,604/1,0 = 10,01 \quad \text{dm}^3 \quad 3.79$$

Pore volume $\sum VL_{57}$

$$\sum VL_{57} = Vkt \cdot VL_n/Vp_{90} = 16,57 \cdot 0,396/1,0 = 6,56 \quad \text{dm}^3 \quad 3.80$$

Partial result:

Properties of dry basalt grit (uncompacted)	
Solids volume $V_f = 0,604 \text{ dm}^3$ (3.73)	Pore volume $V_l = 0,396 \text{ dm}^3$ (3.74)
Volume $V_{kt} = 16,57 \text{ dm}^3$ (3.71)	Density $\rho_{tg} = 1,811 \text{ kg/dm}^3$ (3.72)
Total $\sum V_f = 10,01 \text{ dm}^3$ (3.79)	Angle $\beta_t = 56,7^\circ$ (3.76)
Total $\sum V_l = 6,56 \text{ dm}^3$ (3.80)	Angle $\beta_s = 37,3^\circ$ (3.78)

Properties to be calculated for wet basalt grit under water

Apart from the values of the dry basalt grit determined above, the properties of the wet grit under water must be determined by means of the amount of water = 22,0 l (equal to volume $\sum V_w = 22,0 \text{ dm}^3$), height $h_w = 2,28 \text{ dm}$ of the water, and height $h_b = 2,14 \text{ dm}$ of the basalt grit compacted by the water.

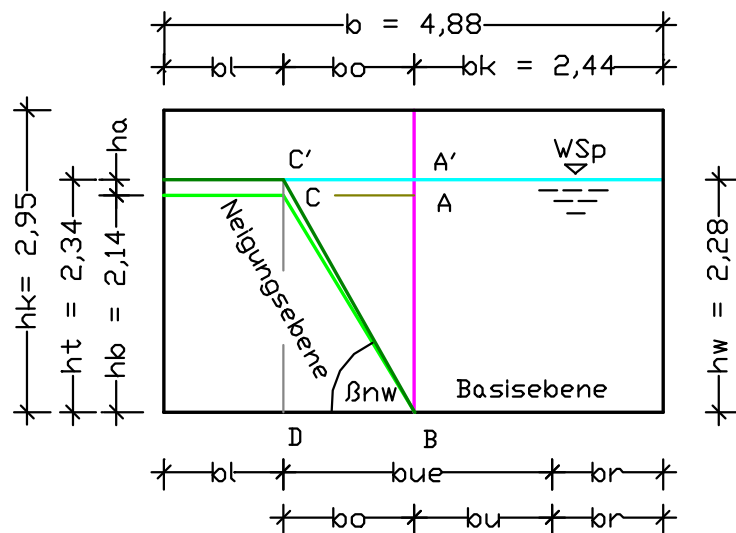


Fig. 49: Filling height of grit $h = h_t = 2,34 \text{ dm}$, height of water $h_w = 2,28 \text{ dm}$, and height of the compacted grit $h_b = 2,14 \text{ dm}$.

Because height h_w of the water plane was measured before removing the glass pane, height h_w is now reduced by the amount corresponding to volume V_g of the glass pane (see Fig. 49). The new height is given the description h_w' .

Volume V_g of the glass pane, with $b_g = 0,04 \text{ dm}$ and height $h_w = 2,28 \text{ dm}$

$$V_g = h_w \cdot a \cdot b_g = 2,28 \cdot 2,90 \cdot 0,04 = 0,26 \quad \text{dm}^3 \quad 3.81$$

Height h_w'

$$h_w' = h_w - V_g/a \cdot b = 2,28 - 0,26/2,90 \cdot 4,88 = 2,26 \quad \text{dm} \quad 3.82$$

The water distribution can be reconstructed as follows:

- Left chamber: The pore water in the compacted grit with volume V_{wl} can be calculated from height difference ($h_w' = 2,26 \text{ dm}$ minus $h_b = 2,14 \text{ dm}$), depth $a = 2,90 \text{ dm}$, and pore volume $\sum V_l$ compacted by the water.

b) Right chamber: Water volume V_{W2} can be determined from width $bk_l = 2,44$ dm, height $hw' = 2,26$ dm, and depth $a = 2,90$ dm.

The following is determined after compaction of the grit:

Volume $V_{kn} \rightarrow hb = 2,14$ dm, $Ak_l = 7,08$ dm³ (3.33)

$$V_{kn} = hb \cdot Ak_l = 2,14 \cdot 7,08 = 15,15 \quad \text{dm}^3 \quad 3.83$$

Total pore volume $\sum V_{l57}^*$

$$\sum V_{l57}^* = V_{kn} - \sum V_{f57} = 15,15 - 10,01 = 5,14 \quad \text{dm}^3 \quad 3.84$$

Volume $V_{W1} \rightarrow$ water in the left-hand chamber

$$V_{W1} = (hw' - hb) \cdot a \cdot bk_l + \sum V_{l57}^*$$

$$V_{W1} = (2,26 - 2,14) \cdot 2,90 \cdot 2,44 + 5,14 = 5,99 \quad \text{dm}^3 \quad 3.85$$

Volume $V_{W2} \rightarrow$ water in the right-hand chamber

$$V_{W2} = hw' \cdot a \cdot bk_l = 2,26 \cdot 2,90 \cdot 2,44 = 15,99 \quad \text{dm}^3 \quad 3.86$$

The following calculation is used to check whether the filling quantity of water = 22,0 l corresponds to height $hw' = 2,26$ dm, and how many basalt pores V_{ln} have actually been filled with water.

Volume $\sum V_{ln}$

$$\sum V_{ln} = V_{W1} + V_{W2} = 5,99 + 15,99 = 21,98 \quad \text{dm}^3 \quad 3.87$$

Volume $\sum V_{lt}$

$$\sum V_{lt} = \sum V_w - \sum V_{ln} = 22,00 - 21,98 = 0,02 \quad \text{dm}^3 \quad 3.88$$

The excess of pore volume $\sum V_{lt} = 0,02$ dm³ can be due either to measurement inaccuracies, to soil loosening while sliding down, or to a pore volume V_{lt} that could not be occupied by water. Volume $\sum V_{lt}$ is not taken into account when determining the properties of the wet basalt grit.

Calculation:

Pore volume V_{l}^*

$$V_{l}^* = \sum V_{l57}^* / V_{kn} = 5,14 / 15,15 = 0,339 \quad \text{dm}^3 \quad 3.89$$

Solids volume V_{f}^*

$$V_{f}^* = V_{p90} - V_{l}^* = 1,00 - 0,339 = 0,661 \quad \text{dm}^3 \quad 3.90$$

Solids volume $V_{fw} \rightarrow$ under uplift

$$V_{fw} = 2 \cdot V_{f}^* / 3 = 2 \cdot 0,661 / 3 = 0,441 \quad \text{dm}^3 \quad 3.91$$

Water volume V_w

$$V_w = V_{l}^* / 2 = 0,339 / 2 = 0,170 \quad \text{dm}^3 \quad 3.92$$

Occupied pore volume $V_{ln} = V_{l}^* \rightarrow$ with water and wet soil

$$V_{ln} = V_{l}^* = 0,339 \quad \text{dm}^3 \quad 3.93$$

Fictitious solids volume V_{fn}

$$V_{fn} = V_{ln} \cdot p_w / ptg_{90} = 0,339 \cdot 1/3 = 0,113 \quad \text{dm}^3 \quad 3.94$$

Inclination angle β_{nw}

$$\tan \beta_{nw} = Vf_w / (Vl^* + Vfn - V_w)$$

$$\tan \beta_{nw} = 0,441 / (0,339 + 0,113 - 0,170) = 1,564 \quad 3.95$$

$$\beta_{nw} = 57,4^\circ \quad [-] \quad 3.96$$

Shear angle snw

$$\tan snw = (\tan \beta_{nw}) / 2 = 1,564/2 = 0,782 \quad 3.97$$

$$snw = 38,0^\circ \quad [-] \quad 3.98$$

Parts by weight of water p_{wg}

$$p_{wg} = Vln \cdot p_w / Vp_{90} = 0,339 \cdot 1/1 = 0,339 \quad \text{kg/dm}^3 \quad 3.99$$

Wet density p_{nwg}

$$p_{nwg} = Vf_w \cdot p_{t90} / Vp_{90} + p_{wg}$$

$$p_{nwg} = 0,441 \cdot 3,0/1,0 + 0,339 = 1,662 \quad \text{kg/dm}^3 \quad 3.100$$

Volume $V_{kt} = 16,57 \text{ dm}^3$ (3.71) of the dry grit in relation to volume $V_{kn} = 15,15 \text{ dm}^3$ (3.83) of the wet grit indicates the compaction ratio due to the addition of water.

Compaction density d_{Bt}

$$d_{Bt} = V_{kt}/V_{kn} = 16,57/15,15 = 1,094 \quad [-] \quad 3.101$$

Compaction factor λ in % by vol.

$$\lambda = (d_{Bt} - 1,0) \cdot 100 = 9,4 \quad \% \text{ by vol.} \quad 3.102$$

After pulling out the separating glass pane, the wet compacted basalt grit under water slid from the left-hand standing earth wedge to the right-hand lying earth wedge, thereby forming the slope plane C-L (see Fig. 50).

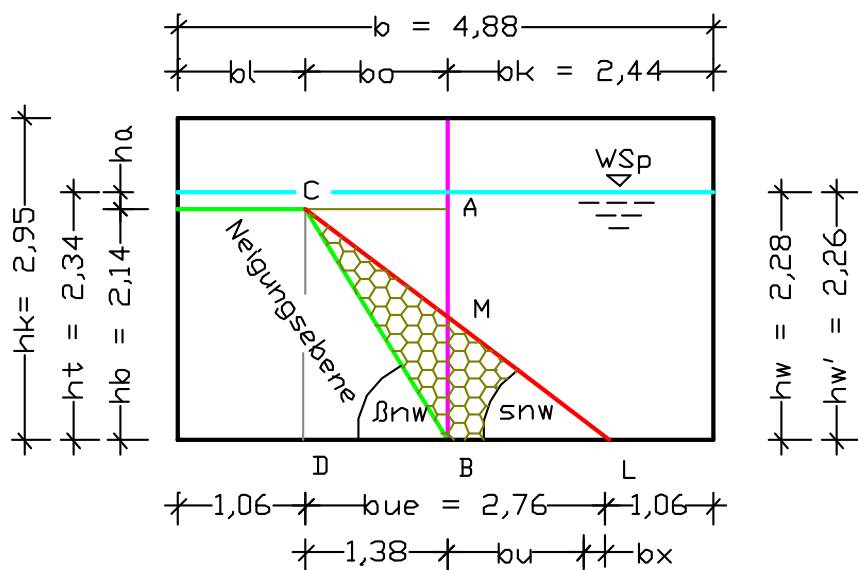


Fig. 50. Earth wedge (C-L-B) after sliding, and its dimensions.

Representation of calculated slope plane (C-L)

by means of the previously calculated soil properties:

Width bo^* → using height $hb = 2,14$ dm and angle $\beta_{nw} = 57,0^\circ$ (3.96)

$$bo^* = hb / \tan \beta_{nw} = 2,14 / 1,564 = 1,37 \quad \text{dm} \quad 3.103$$

Width bue^*

$$bue^* = 2 \cdot bo^* = 2 \cdot 1,37 = 2,74 \quad \text{dm} \quad 3.104$$

Width bl^*

$$bl^* = (bk_l - bo^*) = (2,44 - 1,37) = 1,07 \quad \text{dm} \quad 3.105$$

Width br^*

$$br^* = b - bl^* - bue^* = 4,88 - 1,07 - 2,74 = 1,07 \quad \text{dm} \quad 3.106$$

Results:

The measured heights were transferred into the calculation of soil values. In the result, the measured widths $bl + bue + br = 1,06 + 2,76 + 1,06 = 4,88$ dm are confronted by the calculated widths $bl^* + bue^* + br^* = 1,07 + 2,74 + 1,07 = 4,88$ dm. The slight deviations are acceptable for earth construction. The change of the dry basalt grit properties to those of wet basalt grit under water can be followed by means of the tabulated values below.

Table

Before water absorption (dry)	After water absorption (wet)
Solids volume $Vf_{57} = 0,604$ dm ³ (3.73)	Solids volume $Vf^* = 0,661$ dm ³ (3.90)
Pore volume $Vl_{57} = 0,396$ dm ³ (3.74)	Pore volume $Vl^* = 0,339$ dm ³ (3.89)
Volume $Vkt = 16,57$ dm ³ (3.71)	Volume $Vkn = 15,15$ dm ³ (3.83)
Total $\sum Vf_{57} = 10,01$ dm ³ (3.79)	Total $\sum Vf^* = 10,01$ dm ³ (3.79)
Total $\sum Vl_{57} = 6,56$ dm ³ (3.80)	Total $\sum Vl^* = 5,14$ dm ³ (3.84)
Angle $\beta_{t57} = 56,7^\circ$ (3.76)	Angle $\beta_{nw} = 57,4^\circ$ (3.96)
Angle $s_{t57} = 37,3^\circ$ (3.78)	Angle $s_{nw} = 38,0^\circ$ (3.98)
Density $ptg = 1,811$ kg/dm ³ (3.72)	Density $pnwg = 1,662$ kg/dm ³ (3.100)

It can be shown that by means of calculation, the properties of a dry soil can be converted to those of a wet soil under water.

3.2.3 Calculating the properties of moist soils under water

Soils are considered as moist, if their structure prevents their pores being completely filled with water (gas inclusions) or where the available water supply is inadequate to fill all the soil pores. Consequently, the pore volume Vl of a moist soil is divided into the pore volume Vln occupied by water, and pore volume Vlt , which is free of water. While with a wet soil under water, only 1/3 of the solids

volume V_f is subjected to uplift, the pore volume V_{lt} enriched with gas increases the uplift considerably. If the volumes of the wet soil under water are selected as the basis, they must be supplemented with the volumes that take uplift and partial pore filling into account. Affected by these changes are:

$$\text{Uplift volume } V_{fa} = (V_f + V_{lt}) / 3$$

$$\text{Solids volume } V_{fw} = (2 \cdot V_f - V_{lt}) / 3$$

$$\text{Pore volume } V_{ln} = V_l - V_{lt} \text{ und}$$

$$\text{Fictitious solids volume } V_{fn} = V_{ln}/6.$$

As shown in the above calculations, the pore volume V_{lt} not occupied by water will increase the uplift, reduces the solids volume V_f and the occupied pore volume V_{ln} , and to a great extent cancels the expansion tendency of the pore water $V_{fn} = V_{ln}/6$. For moist soil under water, the tangent of inclination angle β_{iw} is calculated via:

$$\tan \beta_{iw} = V_{fw} / (V_l - V_{fn}) \text{ or } \tan \beta_{iw} = V_{fw} / (V_l - V_{ln}/6).$$

In order to investigate how the fully saturated basalt grit behaves when water is removed, the free water was extracted from the glass container by means of a tube with an internal diameter of 6 mm.

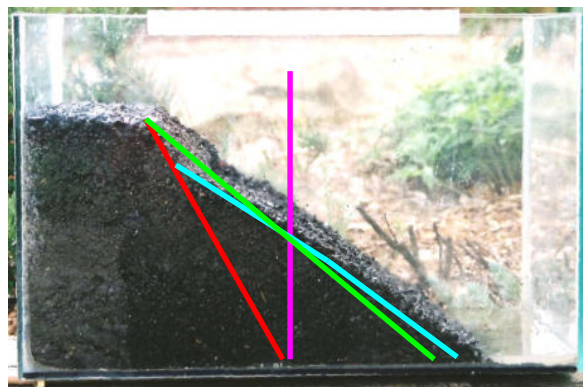


Fig. 51: Spreading of the grit after removal of free water.

During water extraction, the shear plane (green) of the basalt grit changed (Fig. 48, page 71), and partially adopted the flatter shear plane (cyan) of the moist soil above water (Fig. 43, page 66). Obviously, this change of the soil body is due to removal of the free water pressure from the basalt grit (see Fig. 51).

For further illustration of the behaviour of moist soils under water, a calculation example with soil, and an experiment with basalt grit under water are carried out and described.

The following values are used for the calculation example with soil:

Solid substance $V_{f_{55}} = 0,588 \text{ m}^3$ (3.1)	Pore volume $V_{l_{55}} = 0,412 \text{ m}^3$ (3.2)
Angle $\beta_t = 55,0^\circ$ (3.4)	Density $\rho_{tg} = 1,764 \text{ t/m}^3$ (3.9)
Pore volume $V_{lt} = 5,8\%$ by vol. of pore volume $V_{l_{55}}$ (3.2)	

Unoccupied pore volume $V_{lt} \rightarrow$ selected with 5,8% by vol. of $V_l = 0,412 \text{ m}^3$

$$V_{lt} = V_l \cdot 0,058 = 0,412 \cdot 0,058 = 0,024 \quad \text{m}^3 \quad 3.107$$

Occupied pore volume V_{ln}

$$V_{ln} = V_l - V_{lt} = 0,412 - 0,024 = 0,388 \quad \text{m}^3 \quad 3.108$$

Uplift volume V_{fa}'

$$V_{fa}' = (V_f + V_{lt}) \cdot \rho_{wg} / \rho_{tg_{90}} = (0,588 + 0,024) / 3 = 0,204 \text{ m}^3 \quad 3.109$$

Solids volume V_{fw}

$$V_{fw} = (2 \cdot V_f - V_{lt}) / 3 = (2 \cdot 0,588 - 0,024) / 3 = 0,384 \text{ m}^3 \quad 3.110$$

Fictitious solids volume $V_{fn} \rightarrow V_w = V_{ln} / 2$

$$V_{fn} = V_{ln} / 3 - V_{ln} / 2 = 0,388 / 6 = 0,065 \quad \text{m}^3 \quad 3.111$$

Inclination angle β_{iw}

$$\tan \beta_{iw} = V_{fw} / (V_l - V_{fn}) = 0,384 / (0,412 - 0,065) = 1,107 \quad 3.112$$

$$\beta_{iw} = 47,9^\circ \quad [-] \quad 3.113$$

Shear angle siw

$$\tan siw = (\tan \beta_{iw}) / 2 = 1,107 / 2 = 0,553 \quad 3.114$$

$$\beta_{iw} = 29,0^\circ \quad [-] \quad 3.115$$

Density ρ_{iwg}

$$\rho_{iwg} = V_{fw} \cdot \rho_{tg_{90}} / V_{p_{90}} + V_{ln} \cdot \rho_w / V_{p_{90}}$$

$$\rho_{iwg} = 0,384 \cdot 3,0 / 1,0 + 0,388 \cdot 1,0 / 1,0 = 1,540 \quad \text{t/m}^3 \quad 3.116$$

Results:

The calculated volumes are shown as a soil cube in Fig. 52, and as a soil band in Fig. 53, with the expansion of the soil cube by volumes V_{ln} and V_w (before standardization).

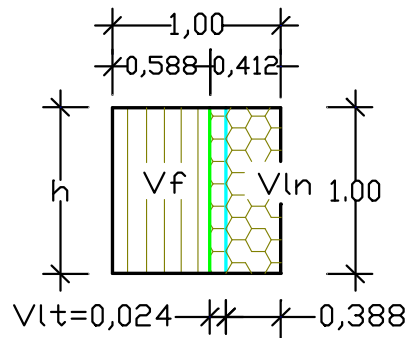


Fig. 52: Volume of a moist soil above water.

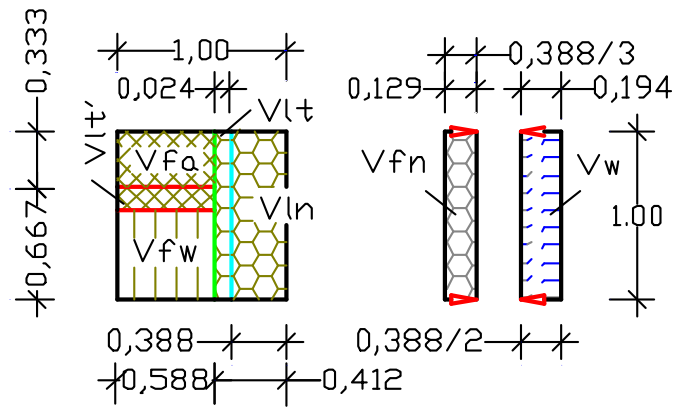


Fig. 53: Volume change of a moist soil above water to a moist soil under water.

The most important properties of the moist basalt grit are shown in the table:

Inclination angle $\beta_{iw} = 47,9^\circ$ (3.113)
Shear angle $s_{iw} = 29,0^\circ$ (3.115)
Wet density $\rho_{iwg} = 1,540 \text{ t/m}^3$ (3.116)

3.2.4 Experiment with moist basalt grit under water, Test 8

The experiment in Test 8 was carried out to check the validity of the previously calculated properties of moist basalt grit above and below water. To obtain a moist basalt grit under water, the necessary measurements were carried out immediately after the addition of water into the glass container, and about 30 minutes later, the separating glass pane was pulled out. This procedure ensured that not all the pores of dry basalt grit could be filled with water.

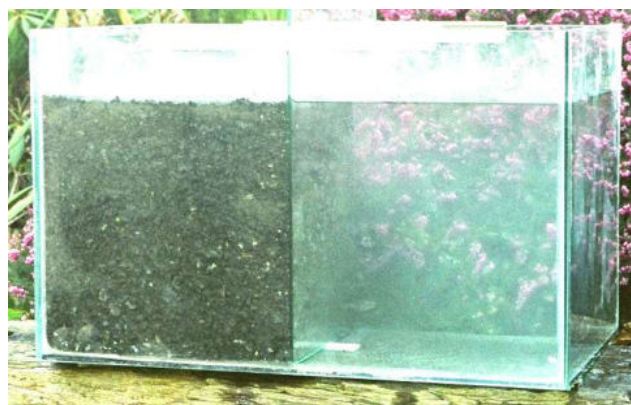


Fig. 54: Same filling heights hb of basalt grit and water before pulling the glass plane.

The dry grit 0/3 mm was filled into the left-hand chamber of the glass container up to the filling height $ht = 2,56 \text{ dm}$ and the surface smoothed. Next, 20 liters of water were filled into the right-hand chamber. Due to the addition of water, the

basalt grit was compacted up to height $hb = 2,35$ dm, and the water plane levelled off at the same height $hw = 2,35$ dm. After pulling out the glass pane, the water plane dropped by 2 mm, resulting in height $hw' = 2,33$ dm.

The test is based on the following values:

Basalt grit $G_t = 33,0$ kg	Filling height $h_t = 2,56$ dm
Water $G_w = 20,0$ kg	Filling height $h_w = 2,35$ dm
Measured height $h_b = 2,35$ dm (see Figs. 53 and 57).	

Properties to be calculated for dry basalt grit

Volume $V_{kt} \rightarrow h_t = 2,56$ dm, $A_{k1} = 7,08$ dm³ (3.33)

$$V_{kt} = h_t \cdot A_{k1} = 2,56 \cdot 7,08 = 18,12 \quad \text{dm}^3 \quad 3.117$$

Dry density ptg

$$ptg = G_t / V_{kt} = 33,0 / 18,12 = 1,821 \quad \text{kg/dm}^3 \quad 3.118$$

Solids volume $V_{fn} \rightarrow$ Index n can be replaced with angle $\beta t = 57^\circ$.

$$V_{fn} = V_{f90} \cdot ptg / ptg_{90} = 1,0 \cdot 1,821 / 3,0 = 0,607 \quad \text{dm}^3 \quad 3.119$$

Pore volume V_{ln}

$$V_{ln} = V_{p90} - V_{fn} = 1,000 - 0,607 = 0,393 \quad \text{dm}^3 \quad 3.120$$

Inclination angle βt

$$\tan \beta t = V_{fn} / V_{ln} = 0,607 / 0,393 = 1,544 \quad 3.121$$

$$\beta t = 57,0^\circ \quad [-] \quad 3.122$$

Shear angle st

$$\tan st = (\tan \beta t) / 2 = 1,544 / 2 = 0,772 \quad 3.123$$

$$st = 37,7^\circ \quad [-] \quad 3.124$$

The dry mass in the glass container with volume V_{kt} consists of solids volume $\sum V_{f57}$ and pore volume $\sum V_{l57}$.

Solids volume $\sum V_{f57}$

$$\sum V_{f57} = V_{kt} \cdot V_{fn} / V_{pf90} = 18,12 \cdot 0,607 / 1,0 = 11,00 \text{ dm}^3 \quad 3.125$$

Pore volume $\sum V_{l57}$

$$\sum V_{l57} = V_{kt} \cdot V_{ln} / V_{p90} = 18,12 \cdot 0,393 / 1,0 = 7,12 \text{ dm}^3 \quad 3.126$$

Partial result:

Properties of the dry basalt grit	
Solid substance $V_f = 0,607$ dm ³ (3.119)	Volume $V_{kt} = 18,12$ dm ³ (3.117)
Pore volume $V_l = 0,393$ dm ³ (3.120)	Density $ptg = 1,821$ kg/dm ³ (3.118)
Total $\sum V_f = 11,00$ dm ³ (3.125)	Angle $\beta t = 57,0^\circ$ (3.122)
Total $\sum V_l = 7,12$ dm ³ (3.126)	Angle $st = 37,7^\circ$ (3.124)

Properties to be calculated for moist, compacted basalt grit

First of all, the subsidence of the water plane after pulling out the separating glass plane must be determined.

Volume Vg of the glass pane with width $bg = 0,04$ dm and height $hw = 2,35$ dm

$$Vg = hw \cdot a \cdot bg = 2,35 \cdot 2,90 \cdot 0,04 = 0,27 \quad \text{dm}^3 \quad 3.127$$

Height hw'

$$hw' = hw - Vg/(a \cdot b) = 2,35 - 0,27/(2,90 \cdot 4,88) = 2,33 \text{ dm} \quad 3.128$$

For the compacted basalt grit under water, height $hb = 2,35$ dm remains, while the height of the original water plane hw is reduced to height $hw' = 2,33$ dm by height $hoo = 0,02$ dm. Moreover, it is assumed that the water will permeate through the entire pore volume $\sum Vl^*$ by means of capillary action, and not only within volume (Vw_1) below the water plane.

Volume $\sum Vkn \rightarrow hb = 2,35$ dm, base area $Ak_1 = 7,08$ dm³ (3.33)

$$\sum Vkn = hb \cdot Ak_1 = 2,35 \cdot 7,08 = 16,64 \quad \text{dm}^3 \quad 3.129$$

Total pore volume $\sum Vl_{57}^* \rightarrow$ after grit compaction

$$\sum Vl^* = Vw_1 = Vkn - \sum Vf = 16,64 - 11,00 = 5,64 \quad \text{dm}^3 \quad 3.130$$

The distribution of the water can be reconstructed in the left-hand chamber by means of volume $\sum Vl^*$ of the compacted grit, and in the right-hand chamber by means of base area $Ak_1 = 7,08$ dm³ (3.33) and water plane height hw' .

Volume Vw_2

$$Vw_2 = hw' \cdot Ak_1 = 2,33 \cdot 7,08 = 16,50 \quad \text{dm}^3 \quad 3.131$$

The next step determines whether the filling quantity of water corresponds to the measured height $hw' = 2,33$ dm, and how many basalt pores $\sum Vln$ have actually been filled with water.

Volume $\sum Vln$

$$\sum Vln = \sum Vl^* + Vw_2 = 5,64 + 16,50 = 22,14 \quad \text{dm}^3 \quad 3.132$$

Volume $\sum Vlt \rightarrow$ addition of water $Gw = 20,00$ kg

$$\sum Vlt = \sum Vw - \sum Vln = 20,00 - 22,14 = -2,14 \quad \text{dm}^3 \quad 3.133$$

For complete filling of the pores, 2,14 dm³ of water are missing, i.e. the basalt grit can be classified as moist, and the soil properties can be determined using the above values.

Pore volume Vl^*

$$Vl^* = \sum Vl^*/Vkn = 5,64/16,64 = 0,339 \quad \text{dm}^3 \quad 3.134$$

Solids volume Vf^*

$$Vf^* = Vp_{90} - Vl^* = 1,000 - 0,339 = 0,661 \quad \text{dm}^3 \quad 3.135$$

Pore volume $V_{lt} \rightarrow$ without water

$$V_{lt} = \sum V_{lt}/V_{kn} = 2,14/16,64 = 0,129 \quad \text{dm}^3 \quad 3.136$$

Occupied pore volume $V_{ln} = V_{l^*} - V_{lt} \rightarrow$ with moist soil

$$V_{ln} = V_{l^*} - V_{lt} = 0,339 - 0,129 = 0,210 \quad \text{dm}^3 \quad 3.137$$

Solids volume $V_{fa} \rightarrow$ subjected to uplift

$$V_{fa} = (V_{f^*} + V_{lt}) / 3 = (0,661 + 0,129) / 3 = 0,263 \quad \text{dm}^3 \quad 3.138$$

Solids volume $V_{fw} \rightarrow$ with moist soil subjected to uplift

$$V_{fw} = (2 \cdot V_{f^*} - V_{lt}) / 3$$

$$V_{fw} = (2 \cdot 0,661 - 0,129) / 3 = 0,398 \quad \text{dm}^3 \quad 3.139$$

Water volume $V_w \rightarrow V_{ln}/2$

$$V_w = V_{ln}/2 = 0,210/2 = 0,105 \quad \text{dm}^3 \quad 3.140$$

Fictitious solids volume V_{fn}

$$V_{fn} = V_{ln} \cdot p_w / p_{tg90} - V_{ln}/2$$

$$V_{fn} = 0,210 \cdot 1/3 - 0,210/2 = -0,035 \quad \text{dm}^3 \quad 3.141$$

Inclination angle $\beta_{iw} \rightarrow$ moist grit

$$\tan \beta_{iw} = V_{fw} / (V_{l^*} - V_{fn})$$

$$\tan \beta_{iw} = 0,398 / (0,339 - 0,035) = 1,309 \quad 3.142$$

$$\beta_{iw} = 52,6^\circ \quad [-] \quad 3.143$$

Shear angle siw

$$\tan siw = (\tan \beta_{iw}) / 2 = 1,309/2 = 0,655 \quad 3.144$$

$$siw = 33,2^\circ \quad [-] \quad 3.145$$

Inclination angle $\beta_{nw} \rightarrow$ wet, compacted grit

$$\tan \beta_{nw} = 2/3 \cdot V_{f^*} / (V_{l^*} \cdot 5/6)$$

$$\tan \beta_{nw} = (2/3 \cdot 0,661) / (0,339 \cdot 5/6) = 1,560 \quad 3.146$$

$$\beta_{nw} = 57,3^\circ \quad [-] \quad 3.147$$

Shear angle $snw \rightarrow$ wet, compacted grit

$$\tan snw = (\tan \beta_{nw}) / 2 = 1,560/2 = 0,780 \quad 3.148$$

$$snw = 38,0^\circ \quad [-] \quad 3.149$$

Parts by weight of water p_{wg}

$$p_{wg} = V_{ln} \cdot p_w / V_{p90} = 0,210 \cdot 1,0 / 1,0 = 0,210 \quad \text{kg/dm}^3 \quad 3.150$$

Moist density p_{iwg}

$$p_{iwg} = V_{fw} \cdot p_{tg90} / V_{p90} + p_{wg}$$

$$p_{iwg} = 0,398 \cdot 3,0/1,0 + 0,210 = 1,404 \quad \text{kg/dm}^3 \quad 3.151$$

When placed in relation to volume $V_{kn} = 16,64 \text{ dm}$ (3.129) of the moist compacted grit, volume $V_{kt} = 18,12 \text{ dm}^3$ (3.117) of the dry grit indicates the compaction ratio caused by the addition of water.

Compaction density dBt

$$dBt = Vkt/Vkn = 18,12/16,64 = 1,089 \quad [-] \quad 3.152$$

Degree of compaction λ

$$\lambda = (dBt - 1,0) \cdot 100 = 8,9 \quad \% \text{ by vol.} \quad 3.153$$

The properties of moist basalt grit under water are shown in Fig. 55, and are summarized in the table below.

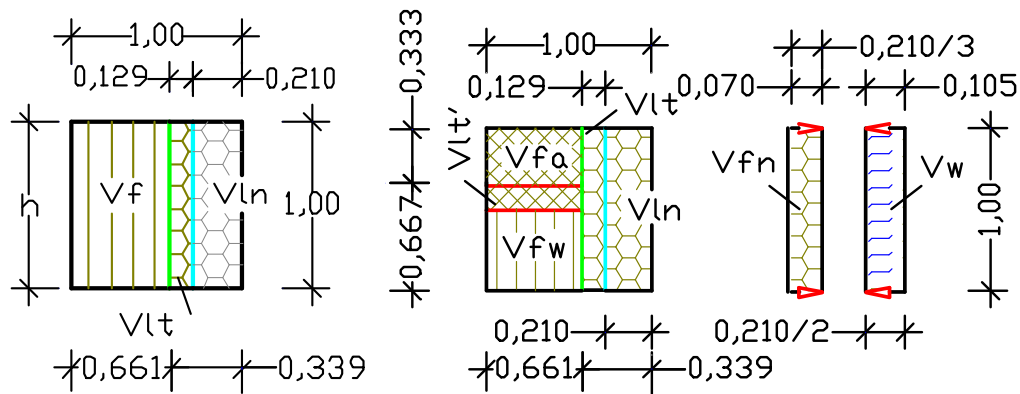


Fig. 55: Volume formation of a moist soil under water.

Partial result:

Before water absorption (dry)	After water absorption (moist)
Solids vol. $Vf_{57} = 0,607 \text{ dm}^3$ (3.119)	Solids vol. $Vf^* = 0,661 \text{ dm}^3$ (3.135)
Pore volume $Vl_{57} = 0,393 \text{ dm}^3$ (3.120)	Pore volume $Vl^* = 0,339 \text{ dm}^3$ (3.134)
Volume $Vkt = 18,12 \text{ dm}^3$ (3.117)	Volume $Vkn = 16,64 \text{ dm}^3$ (3.129)
Total $\sum Vf_{57} = 11,00 \text{ dm}^3$ (3.125)	Total $\sum Vf^* = 11,00 \text{ dm}^3$ (3.125)
Total $\sum Vl_{57} = 7,12 \text{ dm}^3$ (3.126)	Total $\sum Vl^* = 5,64 \text{ dm}^3$ (3.130)
Angle $\beta_{t57} = 57,0^\circ$ (3.122)	Angle $\beta_{iw} = 52,6^\circ$ (3.143)
Angle $s_{t57} = 37,7^\circ$ (3.124)	Angle $s_{iw} = 33,2^\circ$ (3.145)
Density $ptg = 1,821 \text{ kg/dm}^3$ (3.118)	Angle $\beta_{nw} = 57,3^\circ$ (3.147)
Compaction $\lambda = 8,9\%$ by vol. (3.153)	Density $piwg = 1,404 \text{ kg/dm}^3$ (3.151)

Representation of measured slope plane (C-L)

When the basalt grit had slipped down, the slope plane was measured (Fig. 56) and the dimensions were transferred to Fig. 57. Measurements included width $bl = 0,38 \text{ dm}$, height $hb = 2,35 \text{ dm}$, the container's center height $hmu = 0,99 \text{ dm}$, the distance of width $bru = 0,45 \text{ dm}$ from the right-hand container wall, height $hri = 0,31 \text{ dm}$, and height $hs = 0,20 \text{ dm}$. In the photos, the coloured lines marking the planes can deviate slightly from the real planes due to the pixel spacing. But these deviations have no influence on the evaluation of the experiment.

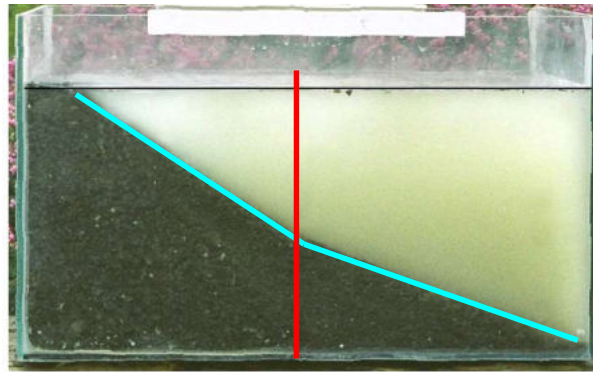


Fig. 56: Test setup after pulling the glass pane.

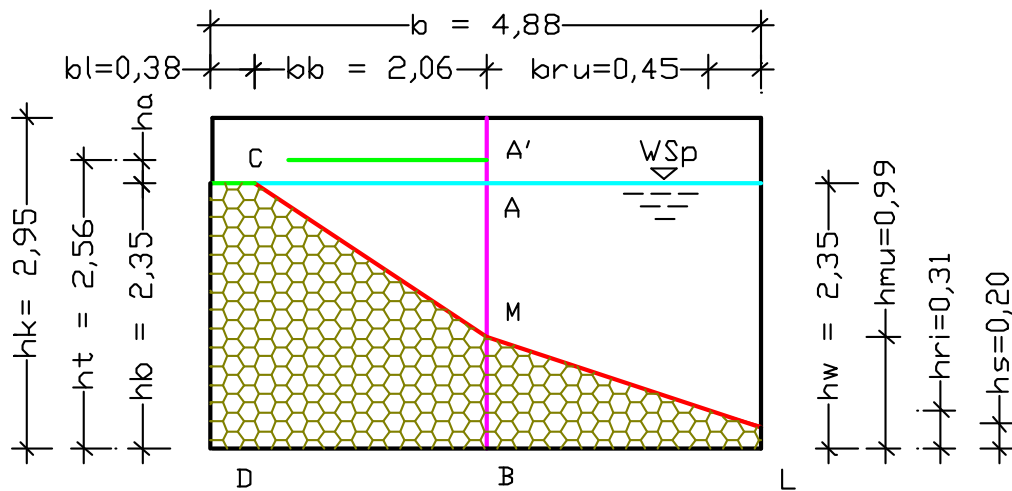


Fig. 57: Dimensions measured on the glass container.

First of all, by means of volume $Vkn = 16,64 \text{ dm}^3$ (3.129), it must be checked whether the basalt grit has loosened during the slide. Loosening has occurred, if the volume of the slid-down soil to the right of the central axis differs from the volume of the backed-up soil to the left of the axis.

Area $Akn' \rightarrow Vkn = 16,64 \text{ dm}^3$ (3.129)

$$Akn' = Vkn/a = 16,64/2,90 = 5,74 \quad \text{dm}^2 \quad 3.154$$

Left-hand area Akn^*

$$Akn^* = bl \cdot hb + (bk_l - bl) \cdot (hb + hmu) / 2$$

$$Akn^* = 0,38 \cdot 2,35 + (2,44 - 0,38) \cdot (2,35 + 0,99) / 2$$

$$Akn^* = 0,89 + 3,44 = 4,33 \quad \text{dm}^2 \quad 3.155$$

Consequently, the following amount has entered the right-hand chamber:

$$Akn_l = Akn' - Akn^* = 5,74 - 4,33 = 1,41 \quad \text{dm}^2 \quad 3.156$$

Right-hand area Akn_r

$$Akn_r = (bk_l - bru) \cdot (hmu + hru) + bro \cdot (hru + hs) / 2$$

$$Akn_r = (2,44 - 0,45) \cdot (0,99 + 0,31) / 2 \dots$$

$$\dots + 0,45 \cdot (0,31 + 0,20) / 2 = 1,40 \quad \text{dm}^2 \quad 3.157$$

Regarding area $A_{knl} = 1,41 \text{ dm}^2$ (3.156), it cannot be determined whether the measured width bl indicates the basalt grit's tear-off edge or whether the width includes a small amount of material that was unable to slide down due to the lack of horizontal forces in the force area N_v (also see Fig. 15, page 39).

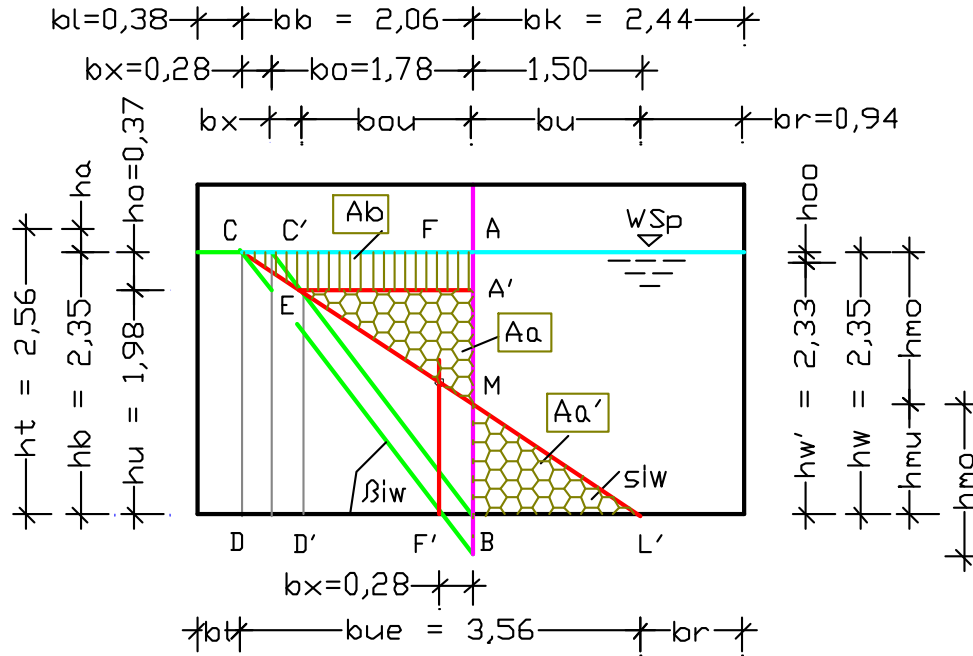


Fig. 58: Area Ab of the unoccupied pore volume A_{knl} that caused the shift of the inclined plane by the amount of width bx .

Measured width $bb = bk_l - bl = 2,44 - 0,38 = 2,06 \text{ dm}$ and height $h_{mo} = 1,36 \text{ dm}$ are used to determine shear angle siw^* and the other dimensions.

Shear angle $siw^* \rightarrow$ moist grit, via the measured height and width

$$\tan siw^* = h_{mo}/bb = 1,36/2,06 = 0,660 \quad 3.158$$

$$siw^* = 33,4^\circ \quad [-] \quad 3.159$$

Inclination angle β_{iw}^*

$$\tan \beta_{iw}^* = 2 \cdot \tan siw^* = 2 \cdot 0,660 = 1,320 \quad 3.160$$

$$\beta_{iw}^* = 52,9^\circ \quad [-] \quad 3.161$$

By means of the dimensions below, it is possible to determine the soil's behaviour as it slides down from the standing earth wedge to the lying wedge.

Width bue

$$bue = hb / \tan siw^* = 2,35/0,660 = 3,56 \quad \text{dm} \quad 3.162$$

Width bo

$$bo = hp / \tan \beta_{iw}^* = 2,35/1,320 = 1,78 \quad \text{dm} \quad 3.163$$

Width bx

$$bx = bb - bo = 2,06 - 1,78 = 0,28 \quad \text{dm} \quad 3.164$$

Width bou

$$bou = bo - bx = 1,78 - 0,28 = 1,50 \quad \text{dm} \quad 3.165$$

Width bu

$$bu = hmu / \tan siw^* = 0,99 / 0,660 = 1,50 \quad \text{dm} \quad 3.166$$

Width br

$$br = b - bl - bue = 4,88 - 0,38 - 3,56 = 0,94 \quad \text{dm} \quad 3.167$$

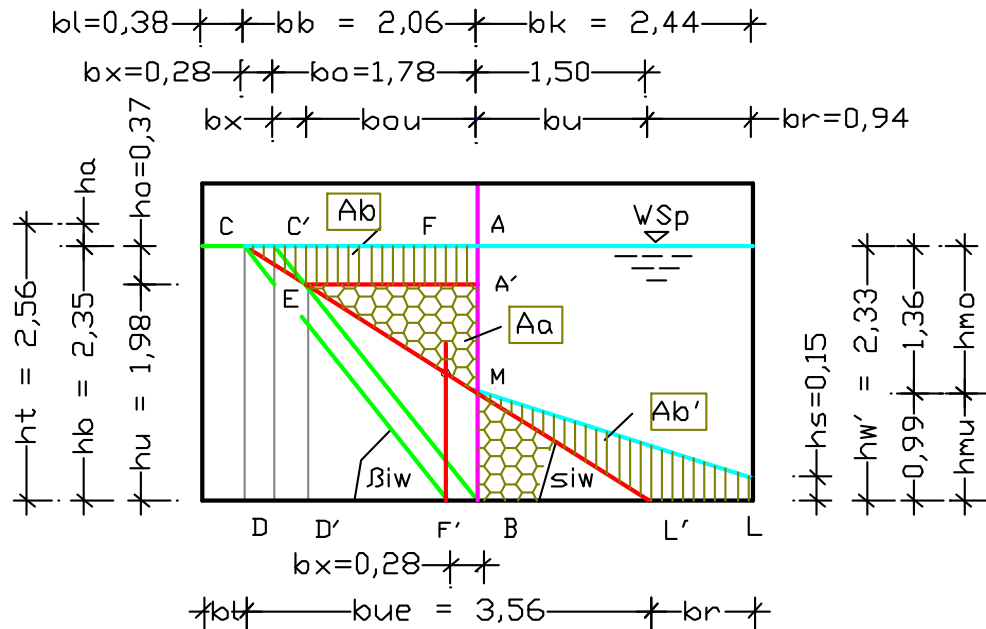


Fig. 59: Distribution of areas after the soil has slipped down (area Ab).

Height ho

$$ho = bx \cdot \tan \beta_{iw}^* = 0,28 \cdot 1,320 = 0,37 \quad \text{dm} \quad 3.168$$

Height hu

$$hu = bou \cdot \tan \beta_{iw}^* = 1,50 \cdot 1,320 = 1,98 \quad \text{dm} \quad 3.169$$

Area Ac

$$Ac = hmo \cdot bb / 2 = 1,36 \cdot 2,06 / 2 = 1,40 \quad \text{dm}^2 \quad 3.170$$

Area $Aa = Aa'$

$$Aa = hmu \cdot bu / 2 = 0,99 \cdot 1,50 / 2 = 0,74 \quad \text{dm}^2 \quad 3.171$$

Area $Ab = Ab'$

$$Ab = Ac - Aa' = 1,40 - 0,74 = 0,66 \quad \text{dm}^2 \quad 3.172$$

Representation of the calculated slope plane (C-L)

For the purpose of graphical representation of soil movements in the glass container, additional dimensions for the moist soil under water are determined by means of height $hb = 2,35$ dm and the calculated angles $\beta_{iw} = 52,6^\circ$ (3.144) with $\tan \beta_{iw} = 1,309$ as well as $siw = 33,2^\circ$ (3.146) with $\tan siw = 0,655$ (3.145), as in the previous section.

Height ho^*	\rightarrow volume $Vlt = 0,129 \text{ dm}^3$ (3.137)		
	$ho^* = hb \cdot Vlt/Vp = 2,35 \cdot 0,129/1,00 = 0,30$	dm	3.173
Height hu^*			
	$hu^* = hb - ho^* = 2,35 - 0,30 = 2,05$	dm	3.174
Width bo^*			
	$bo^* = hb / \tan \beta_{iw} = 2,35/1,309 = 1,80$	dm	3.175
Width bx^*			
	$bx^* = ho^* / \tan \beta_{iw} = 0,30/1,309 = 0,23$	dm	3.176
Width bb^*			
	$bb^* = bo^* + bx^* = 1,80 + 0,23 = 2,03$	dm	3.177
Width bl^*			
	$bl^* = bk_l - bb^* = 2,44 - 2,03 = 0,41$	dm	3.178
Width bue^*			
	$bue^* = hb / \tan siw = 2,35/0,655 = 3,59$	dm	3.179
Width bou^*			
	$bou^* = bo^* - bx^* = 1,80 - 0,23 = 1,57$	dm	3.180
Width bu^*			
	$bu^* = bue^* - bo^* = 3,59 - 2,03 = 1,56$	dm	3.181
Width br^*			
	$br^* = bk_l - bu^* = 2,44 - 1,56 = 0,88$	dm	3.182
Height hmo^*			
	$hmo^* = bb \cdot \tan siw = 2,03 \cdot 0,665 = 1,35$	dm	3.183
Height hmu^*			
	$hmu^* = hb - hmo^* = 2,35 - 1,35 = 1,00$	dm	3.184
Area Ac^*			
	$Ac^* = bb \cdot hmo^*/2 = 2,03 \cdot 1,35/2 = 1,37$	dm ²	3.185
Area Aa^*			
	$Aa^* = bu^* \cdot (hp - hmo^*) / 2$		
	$Aa^* = 1,56 \cdot (2,35 - 1,35) / 2 = 0,78$	dm ²	3.186
Area Ab^*			
	$Ab^* = Ac - Aa' = 1,37 - 0,78 = 0,59$	dm ²	3.187

Results:

The measured and calculated dimensions of the moist basalt grit under water are summarized in the table below. The table is divided into the dimensions that can be measured on the soil body, and those required to follow the conversion of the soil properties from a dry to a moist soil under water. With the latter dimensions, there are slight differences between the experimental values and those calculated by means of the basalt grit volumes. The deviations can possibly be explained by the procedure used to convert a dry grit into a moist soil simply by adding water, i.e. without previous mixing. The slight inaccuracies in the calculations might

also have occurred even if the grit and water had been previously mixed, because further water enrichment of the moist basalt grit was possible due to filling the water into the right-hand chamber. But ultimately, this experiment shows that the behaviour of moist soil under water can be determined by means of its volume and weight proportions.

Tabulated results:

Dimensions measured on glass container	Calculated dimensions
Width $bl = 0,39$ dm Width $bo = 1,78$ dm (3.164) Height $hmo = 1,36$ dm	Width $bl^* = 0,41$ dm (3.178) Width $bo^* = 1,80$ dm (3.175) Height $hmo = 1,35$ dm (3.182)
Dimensions within soil body Height $ho = 0,37$ dm (3.169) Width $bx = 0,28$ dm (3.165) Width $bb = 2,05$ dm Width $bue = 3,56$ dm (3.163) Width $bou = 1,50$ dm (3.166) Width $bu = 1,50$ dm (3.167) Width $br = 0,94$ dm (3.168) Area $Ac = 1,40$ dm ² (3.170) Area $Aa = 0,74$ dm ² (3.171) Area $Ab = 0,66$ dm ² (3.172)	Dimensions within soil body Height $ho^* = 0,30$ dm (3.173) Width $bx^* = 0,23$ dm (3.176) Width $bb^* = 2,03$ dm (3.177) Width $bue^* = 3,59$ dm (3.179) Width $bou^* = 1,57$ dm (3.180) Width $bu^* = 1,56$ dm (3.181) Width $br^* = 0,88$ dm (3.182) Area $Ac^* = 1,37$ dm ² (3.184) Area $Aa^* = 0,78$ dm ² (3.185) Area $Ab^* = 0,59$ dm ² (3.186)

3.3 Soil parameters summarized in a table

A table was prepared for simplified following of the described changes of the soil parameters dry, wet, and wet under water. The calculation results for the soil with inclination angle $\beta t = 45^\circ$ are marked red (see Table 1, page 238).

Column 1 of the table contains the different soil types with their conventional descriptions, whereby the soil description 'loam, aqueous' is often subscripted with 'primordial dust under water'. This multiple nomination is used to assign different solid material portions V_f to the soil/water mixture.

Column 2: Shows the inclination angle βt assigned to the soil types.

Column 3: Shows the tangent of inclination angle βt .

Columns 4 and 5: Contain the shear angle st and the corresponding tangent.

Columns 6 and 7: Show the height and width of the soil cube, whereby the calculation depth $a = 1,00$ m is taken into account.

Column 8: Shows width Δb , by means of which the volume increase ΔV is calculated from depth $a = 1,00$ m (Column 10).

Column 9: Initial volume $V_0 = 1,00$ m³ plus volume ΔV gives total volume V_p (Column 11).

Columns 12 and 13: Contain the solids and pore volumes (V_f and V_l) of the respective soil types.

Columns 14 to 18: List the weight portions of the soils below the corresponding calculation methods.

Columns 19 to 24: Here, the angles of wet soils and wet soils under water are assigned to the soil types.

Column 25: Contains the gravity force g .

Similar to the table in Enclosure 1, the following graphical representation of forces in dry and wet soils are intended to help follow the force changes within dry soils due to water absorption. For the diagram shown below in Fig. 60, the calculated values of soil types with inclination angles β_t (75° , 65° , 55° to 5°) were taken from Tables 2 and 3. All other values were calculated from the inclination angle β_t or β_t of the respective soil type (see Tables, page 238ff).

Wall height $h = 10,00$ m and thrust height h_v of the earth pressure were entered on the Y-axis. Horizontal force H_f and its force meter h_f were entered on the X-axis. For this, the height/weight ratio 1 : 50 was selected.

The red curve is created by connecting the entered earth pressure forces H_f of the dry soil, and the blue curve shows the earth pressure forces of the wet soil. No empiric factors or assumed soil densities are required for this calculation method.

The demonstrated difference between the earth pressure forces of dry and wet soils clearly shows that the water content of a soil is decisive when determining soil angles and densities. In order to obtain reliable values for an earth pressure calculation, it would be enough to take undisturbed soil samples in the construction area, and to determine their water content and the dry density. With the help of these two factors, all the other soil properties and possible changes to the properties – which might result e.g. from compaction, loads, excessive loads, etc. – can be reproduced.

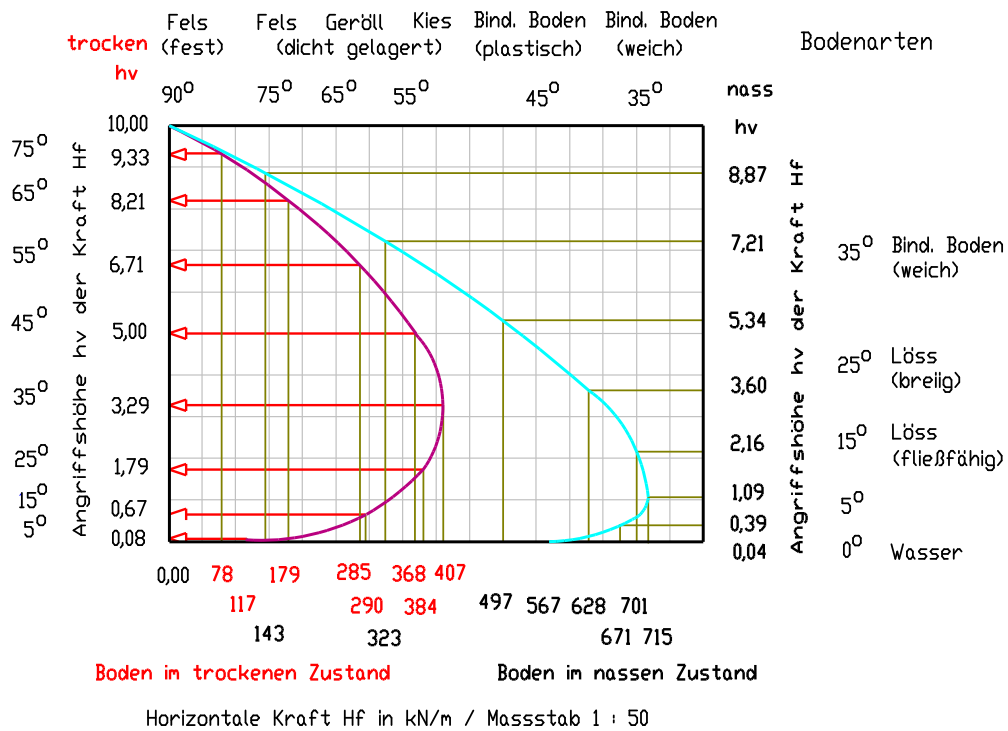


Fig. 60: Earth pressure forces of the same soil types in the dry (red) and wet (cyan) states, with a wall height $h = 10,0$ m.

3.4 Conclusions for Chapter 3

Currently, the multi-phase system of solid-state physics uses the solids volume V_f (solid phase), pore volume V_l (gaseous phase), and water volume V_n (liquid phase) is used to graphically represent the volumes of a soil type. For his New Theory, the author selected rock density $\rho_{t90} = 3,00$ t/m³, and friction value $\mu = \tan \beta t = 100$ for the idealized pore-free basalt, by means of which the volume and weight portions of all soil types can be calculated. Hereby, it was shown that with dry soils the friction value μ , the internal friction, and the tangent of inclination angle βt correspond to the proportionality factor V_f/V_l . With this finding, it was possible to create a system of order that is free from empiric factors, and which is applicable for all soil types – from weathered rock down to 'primordial dust' – steplessly via the inclination angle, from $\beta = 89,4^\circ$ to $0,6^\circ$. Another order was established using the soil's pore volume V_l as a water reservoir, which permits moist soils to be classified between the options 'dry soil' and 'wet soil' according to their water content. With a wet soil, all pores are completely filled with water. Contrary to this, with a moist soil, either the soil's grain structure or the lack of water in its surroundings prevents a complete absorption of water. Consequently, the pore volume V_l of a wet soil corresponds to

the volume V_{ln} occupied by water, whilst in a moist soil the pore volume is divided into volume V_{lt} not occupied by water, and volume $V_{ln} = V_l - V_{lt}$ occupied by water. This division of pore volumes assists the calculation of angles and the determination of soil densities, as shown in the previous sections.

Moreover, the numerous tests carried out in the glass container with moist (partially saturated) and wet soils (fully saturated), and with soils under water showed that:

- Soil volume is reduced, if dry soil is loosely filled into a container, and water is added;
- Soil volume remains constant, if a dry soil compacted by water is dried and then submerged in water again, i.e. like soils in free nature, which are repeatedly subjected to groundwater, and do not reduce their volume any further;
- Soil behaviour is calculable, and a wet soil under water generates less horizontal forces than a moist soil under water;
- Soil resting on an inclined rock layer does not change its shear angle when it slides down into a horizontal plane. However, this finding changes as soon as loads are applied to the soil, whose vertical forces have not been dispersed completely when the rock layer is reached, and are therefore converted into horizontal forces.

4 Soil behaviour and force build-up acc. to New Theory

In Chapter 2 it was shown that current earth pressure teachings promote Mohr-Coulomb's failure criterion for determining earth stresses. They state that this procedure complies with Coulomb's earth pressure teachings, Mohr's stress theory, and the physical plane rules. The indicated analogy between the calculation methods was investigated, with the result that the author was unable to find a theory-compliant connection between the failure criterion and the other rules and standards. Moreover, the teachings are based on empirically found soil parameters, which – like Mohr-Coulomb's failure criterion – can lead to inaccurate earth pressure determinations and thereby to subsequent structural damage. Within the scope of the above discussions, the basics of the New Earth Pressure Theory were introduced, which follow Coulomb's earth pressure teachings in all essential points.

In order to dispense completely with empiric values for earth pressure determination, the author developed a new method, which was described in Chapter 3. This New Theory enables the soil characteristics, densities, and angles of all soil types to be calculated in the dry, moist, and wet states, above and below water. The calculation method is seen as an extension of the multi-phase system of solid-state physics.

Following a short introduction of the New Earth Pressure Theory, this Chapter describes various application examples, some of them backed by corresponding experiments. Included in the examples are calculations using the properties of different soil types.

4.1 General information on the New Earth Pressure Theory

The New Earth Pressure Theory observes the basics of physics, and is based on the behaviour of soils in free nature. By means of the author's extension of the multi-phase system of solid-state physics, all soil types can be steplessly assigned in the semicircle of soil types according to their angles $\beta = 89,4^\circ$ to $\beta = 0,6^\circ$. Consequently, there is no further need for the previous sub-division of soils according to their magmatic, metamorphous or sedimentary primary rock, nor for the classification in non-cohesive and cohesive soils. What's more, calculation of the soil parameters enables the load capacities of soils to be determined.

4.2 Determining the load bearing capacity of soils (earth resistance)

Determination of the load bearing capacity of soils is carried out analogously to the calculation of soil properties using the fictitious, stress-free dry rock with density $\rho_{\text{rock}} = 3,00 \text{ t/m}^3$. But instead of the cube, a square rock column is used here, with height $h^* = 100 \text{ m}$, 'footprint' $A_d = b \cdot a = 1,00 \text{ m}^2$, and volume $V^* = 100 \text{ m}^3$. When placed on a rock massif, the rock column generates the permissible pressure $\sigma_{D \text{ zul}}$ by means of weight G on footprint A_d , whereby

$$\sigma_{D \text{ zul}} = G/A_d \quad \text{in kN/m}^2.$$

The calculation method to determine $\sigma_{D \text{ zul}}$ would remain unchanged, if one were to mount a soil column onto the terrain plane instead of the rock column. Only the soil's lower density would lead to a reduction of weight G and thereby to a lower pressure. As the soil – contrary to the rock – can change its outer form and expand into all directions under the shear angle, the column height will be reduced with increasing width.

Should one be able to dig a hole into the ground under the terrain area, and insert an equally large rock column, the soil surrounding the column would develop horizontal forces that would firmly clamp the column in the soil. This situation would change, if a soil column could be inserted in the ground instead of the rock column. The soil in the column would use its own abilities to generate horizontal forces against the surrounding soil. In the same way, the surrounding soil would generate horizontal forces against the soil column, thereby creating an equilibrium between the opposing forces. As described earlier, horizontal forces are generated because the vertical forces due to column height and gravitation are converted into horizontal forces via the soil's inclined planes. This play of forces maintains the equilibrium in the ground.

If, when determining the load capacity of soils, and all other conditions remaining the same, one assumes that a soil column placed on a terrain surface cannot change its form, only an equally high column below the terrain surface will be able to support the load. If the lower column is now permitted to disperse its load via a lateral force, a diagonal inclination plane will initially be established in the column. This plane divides the column's projection area $A = V^*/a$ into an active and a reactive wedge area, so that both areas have the same size $A_a = A_r = A/2$. Fig. 61 shows a rock column with height $h_x = 100 \text{ m}$, width $b_x = 1,00 \text{ m}$, and calculation depth $a = 1,00 \text{ m}$.

If one replaces the rock column with a soil column with the same volume, and permits a one-sided force distribution, width b_x will change into width b , and the soil type's inclination angle will reduce height $hx = 100$ m to height h (see Figs. 62 and 63).

The dimensions of the new force area are calculated from:

$$\text{Height } h = \sqrt{A \cdot \tan \beta} \text{ and width } b = \sqrt{A / \tan \beta}.$$

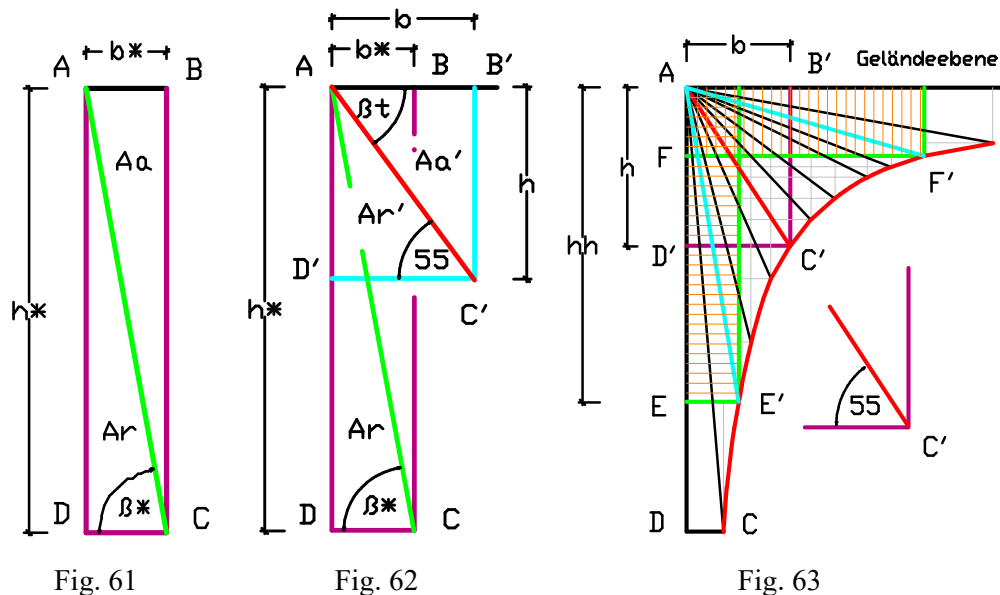


Fig. 61: Rock column with height h^* , width b^* , and inclined plane.

Fig. 62: Conversion of load area A into force areas $A_{a'}$ and $A_{r'}$.

Fig. 63: Change of the vertical rock column into columns of the soil types.

The two wedge areas $A_{a'}$ and $A_{r'}$ generate opposing horizontal forces, which maintain the equilibrium in the rock or earth block according to the principle actio = reactio. Fig. 62 shows a one-sided force in the hard rock with inclination angle $\beta = 89,4^\circ \rightarrow \mu = 100$, and in the soil with inclination angle $\beta = 55,0^\circ$. Fig. 63 shows how a vertical rock column with its inclination angle is converted via the soil types into a lying column of primordial dust with inclination angle $\beta = 0,6^\circ$.

In the same way that height h reduces the soil column in favour of its width b via the inclination angle, the load, and thereby also the permissible pressure $\sigma_{Dzul} = G/Ad$ is reduced when referred to the square meter. If the load, which has been distributed over width b via the inclination angle, is pushed back onto the square with width $b^* = 1,00$ m, the original load of the 100 m high soil column above the square is restored. Soil type with inclination angle $\beta = 55,0^\circ$ is

selected to calculate the permissible pressure $\sigma_{D\ zul}$. Its parameters have already been determined (page 58) and are used here:

$V_{f55} = 0,588\text{ m}^3$ (3.1)	$V_{l55} = 0,412\text{ m}^3$ (3.2)
Angle $\beta_t = 55,0^\circ$ (3.4)	Density $ptg_{55} = 1,764\text{ t/m}^3$ (3.9)
Area $A = 100\text{ m}^2$	Area $Ad = 1,00\text{ m}^2$

Calculation:

Height h

$$h = \sqrt{A \cdot \tan \beta} = \sqrt{100 \cdot 1,428} = 11,95 \quad \text{m} \quad 4.1$$

Width b

$$b = \sqrt{A / \tan \beta} = \sqrt{100 / 1,428} = 8,37 \quad \text{m} \quad 4.2$$

Volume V_{t55}

$$V_{t55} = Ad \cdot h = 1,00 \cdot 11,95 = 11,95 \quad \text{m}^3 \quad 4.3$$

Weight $Gt \rightarrow$ with $g = 9,807\text{ m/s}^2$

$$Gt = V_{t55} \cdot ptg_{55} \cdot g = 11,95 \cdot 1,764 \cdot 9,807 = 206,7 \quad \text{kN} \quad 4.4$$

Soil pressure $\sigma_{D\ zul}$

$$\sigma_{D\ zul} = Gt/Ad = 206,7/1,00 = 206,7 \quad \text{kN/m}^2 \quad 4.5$$

Results:

The calculation example also shows that according to the New Earth Pressure Theory, the permissible soil pressure $\sigma_{D\ zul} = 206,7\text{ kN/m}^2$ (4.5) can be calculated exactly for every soil type via inclination angle $\beta_t = 55^\circ$, column height $h = 11,95\text{ m}$ (4.1), and dry density $ptg_{55} = 1,764\text{ t/m}^3$ (3.9). Contrary to this, DIN 1054 "Permissible loading of substratum" uses empiric data for soil pressures, which are assigned to the different soils according to their consistency 'firm', 'semi-solid', and 'solid'. Therefore, a direct comparison of the calculated permissible soil pressures with the corresponding tabulated DIN values is not possible [see 1: page K.4]. In particular, the DIN standard does not make any reference to the soil's inclination angle, its density, or its water content.

4.2.1 Load capacity of soils with one-sided force distribution

After calculating the permissible load bearing capacity of soils, the force distribution in the soil, which results from the application of loads or forces on the terrain surface, is investigated. Also here, for a simplified understanding of force distribution in the ground, only a one-sided force distribution is permitted. To load the terrain surface, the previously determined soil column with height $h = 11,95\text{ m}$ (4.1), width $b^* = 1,00\text{ m}$, square footprint $Ad = 1,00\text{ m}^2$, and force $Gt = 206,7\text{ kN}$ (4.4) is used (see Fig. 64 below).

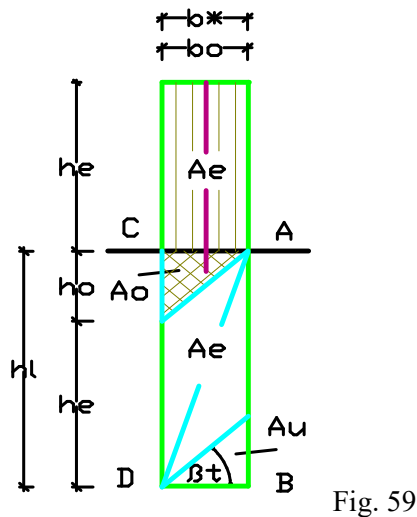


Fig. 59

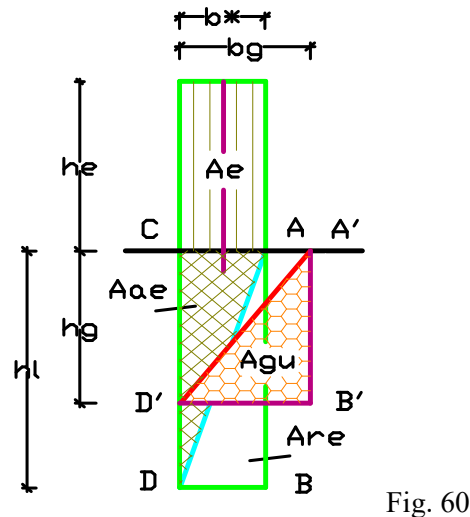


Fig. 60

Fig. 64: Load area Ae below the terrain plane, the areas Ao and Au for the soil's dead weight, and column height hl .

Fig. 65: One-sided force distribution with conversion of force areas Ae , Ao and Au into areas Aae and Agu with height hg .

To avoid confusion regarding the terminology used to determine soil pressure and to represent force dispersal in the ground, height h is renamed height he , width b^* is renamed foundation width bf , and weight Gt is renamed Ge . Volume V with depth a , width bo or bu , and height ho are assigned to the soil's dead weight below load area Ad . The inclined plane divides volume V into active volume Vo and reactive volume Vu . Volumes Vo and Vu divided by calculation depth $a = 1,00$ m enables the side views $Ao = Au = V/a$ to be created. The addition of areas Ao , Au , and Ae forms a square soil column with height $hl = ho + he$ below the footprint $Ad = 1,00$ m² (see Figs. 64 and 65).

If one applies the maximum earth load with height $he = h = 11,95$ m (4.1) for the soil type with density $ptg_{55} = 1,764$ t/m³ (3.9), a soil column is formed below the footprint Ad . If one now uses depth $a = 1,00$ m for calculation, the weight force can be assigned to area Ae , and the soil's dead weight to areas Ao and Au . Because the permissible soil pressure occurs in the footprint, the foundation's own weight Gf must be subtracted from the permissible weight Ge . What remains is payload $Ee = (Ge - Gf) / g$. The load-dispersing force area in the adjacent ground is increased due to the load. The force must be divided into the active $Ago = Ao + Ae/2$ and the reactive force area $Agu = Au + Ae/2$. Because of the force area's horizontal expansion under the natural inclination angle βt , width b^* becomes width bg , and height hl becomes height hg . The surface area remains unchanged (see Fig. 65).

4.2.2 Load capacity of soils with polydirectional force distribution

If more than one force direction is permitted, weight Ge for the force build-up in the ground must also be determined here by means of the permissible pressure σ_{Dzul} of the loaded soil, multiplied with footprint Ad .

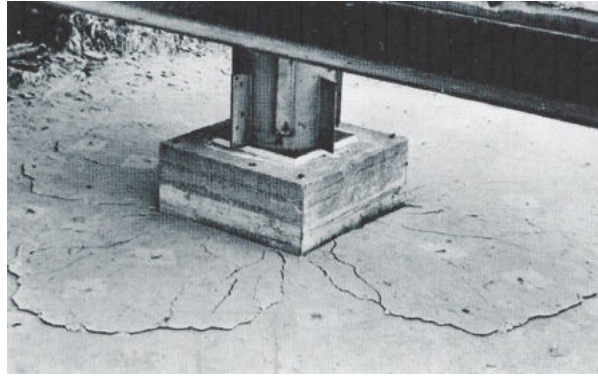


Fig. 66: Visible signs of a polydirectional force distribution in the ground following the Degebo load test [A].

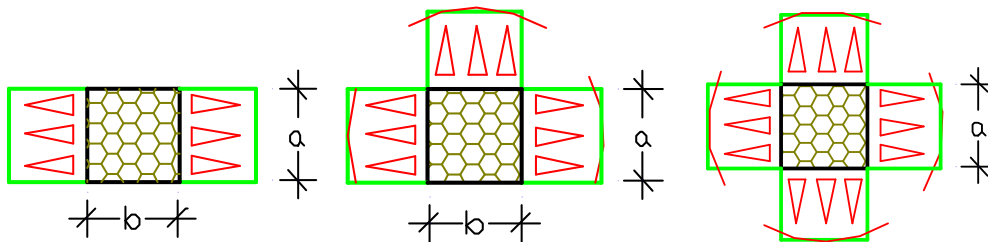


Fig. 67: Bilateral force distribution.

Fig. 68: Three-sided force distribution.

Fig. 69: Quadrilateral force distribution.

The number of permissible force directions is not freely selectable, but is specified by local conditions. Walls or inadequate foundation spacing can limit the force distribution in the ground, and lead to a reduction of the soil's load bearing capacity. Figs. 67 to 69 show plan views of different force distributions in the ground.

If payloads Ee or weight forces Ge are named for dispersal into the adjacent substratum, they must be converted into fictitious soil body by means of the loaded soil's density, and their volumes used in the subsequent force determinations. The dry density ptg of the loaded soil must be selected for conversion, because with moist or wet soils, although the absorbed pore water increases the soil's density, it will escape under pressure. Consequently, water is unsuitable for load dispersal. In the ground, every force direction contributes to load dispersal by means of volumes $V = a \cdot b \cdot h$. With a single square foundation with quadrilateral force distribution, and based on the example with dry density

$\rho_{tgs55} = 1,764 \text{ t/m}^3$ (3.9), height $h = 11,95 \text{ m}$ (4.1), and width $b = 8,37 \text{ m}$ (4.2), the maximum footprint $Ad = 4 \cdot 8,37 = 33,48 \text{ m}^2$ or side length $bf = \sqrt{(Ad/a)} = \sqrt{(33,48/1,0)} = 5,78 \text{ m}$ could be permitted. If area $Ad = 33,48 \text{ m}^2$ is multiplied with permissible height $h = 11,95 \text{ m}$ (4.1), the result is volume $V^* = 100 \text{ m}^3$ for each of the four soil columns.

Every time the maximum area Ad is exceeded, the soil's load bearing capacity is reduced. In order to maintain the balance of forces in the ground, the permissible load would have to be calculated using $E = Ad \cdot \sigma_{D \text{ zul}}/Ad'$, whereby Ad' describes the new foundation size.

The example of a strip foundation will be used to describe a bilateral force distribution in the ground. For force dispersal below the foundation, a vertical axis must be inserted at the center of foundation width $bf = 1,00 \text{ m}$, and force areas A with height h and width b applied on both sides. By means of the permissible soil pressure $\sigma_{D \text{ zul}} = 206,7 \text{ kN/m}^2$ (4.5) of the selected soil, the maximum applied weight $Gt = 206,7 \text{ kN}$ (4.4) can be dispersed in equal halves via the soil to the left and right of the reference axis (see Fig. 67, page 97, and Fig. 70, page 99).

Calculation example: Strip foundation, the following values are used:

$V_{f55} = 0,588 \text{ m}^3$ (3.1)	$V_{l55} = 0,412 \text{ m}^3$ (3.2)
Angle $\beta t = 55,0^\circ$ (3.4)	Density $\rho_{tgs55} = 1,764 \text{ t/m}^3$ (3.9)
Width $b = 8,37 \text{ m}$ (4.2)	Height $h = h_e = 11,95 \text{ m}$ (4.1)
Area $Ad = 1,00 \text{ m}^2$	Foundation width $bf = 1,00 \text{ m}$
Weight $G_e = G_t = 206,7 \text{ kN}$ (4.4)	

Calculation:

Area A_e

$$A_e = h_e \cdot bf/2 = 1,00 \cdot 11,95/2 = 5,98 \quad \text{m}^2 \quad 4.6$$

Width b_o

$$b_o = bf/2 = 1,00/2 = 0,50 \quad \text{m} \quad 4.7$$

Height h_o

$$h_o = b_o \cdot \tan \beta = 0,50 \cdot 1,428 = 0,71 \quad \text{m} \quad 4.8$$

Area $A_o = A_u$

$$A_o = b_o \cdot h_o/2 = 0,50 \cdot 0,71/2 = 0,18 \quad \text{m}^2 \quad 4.9$$

Area $A_{go} = A_{gu}$

$$A_{go} = A_o + A_e/2 = 0,18 + 5,98/2 = 3,17 \quad \text{m}^2 \quad 4.10$$

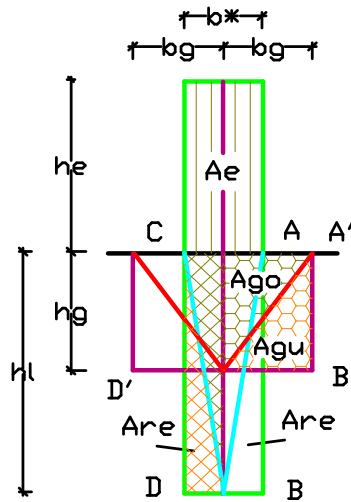


Fig. 70: Load dispersal with biaxial force distribution in the ground, and depth $a = 1,0$ m in areas Aae , Are , Ago , and Agu

Wedge areas $Ago = Agu$ represent the load-dispersing active and reactive areas. By means of these areas and the inclination angle β , it is possible to determine height hg and width bg of the force area required for force dispersal.

Height hg

$$g = \sqrt{2 \cdot Ago \cdot \tan \beta_{t55}} = \sqrt{2 \cdot 3,17 \cdot 1,428} = 3,01 \quad \text{m} \quad 4.11$$

Width bg

$$bg = \sqrt{2 \cdot Ago / \tan \beta_{t55}} = \sqrt{2 \cdot 3,17 / 1,428} = 2,11 \quad \text{m} \quad 4.12$$

Results:

Force dispersal under a strip foundation	
Inclination angle $\beta_t = 55,0^\circ$ (3.4)	Height $hg = 3,01$ m (4.11)
Weight $Gt = 206,7$ kN (4.4)	Width $bg = 2,11$ m (4.12)
Area $Ago = Agu = 3,17$ m ² (4.10)	

For the purpose of force dispersal in the ground, the area $Ago = Agu = 3,17$ m² (4.10) with height $hg = 3,01$ m (4.11) and width $bg = 2,11$ m (4.12) is formed to the left and right of the reference axis. As weight $Ge = Gt = 206,7$ kN (4.4) is within the permissible load limit (payload plus foundation weight), there will be no soil subsidence under the foundation. To illustrate the force fields in the soil in the case of an overload on the foundation, soil subsidence will be permitted in the following example.

4.2.3 Load capacity of foundations with permissible soil subsidence

Soil subsidence, regardless of whether under foundations or piles, represents excessive ground loading. Within its range of influence, subsidence reduces the soil's pore volume, thereby changing its properties, such as inclination angle,

friction value, and density. This change of the soil's structure is not subjected to any time limit, i.e. soil subsidence as well as its consequences can also occur many years later.

In the following, weight Ge for a strip foundation with width $bf = 1,00$ m and the above soil parameters will be determined, which causes subsidence by the amount of $\Delta h = 0,08$ m.

The following values are used:

Angle $\beta_t = 55,0^\circ$ (3.4)	Density $\rho_{tg_{55}} = 1,764$ t/m ³ (3.9)
Width $bg = 2,11$ m (4.12)	Foundation width $bf = 1,00$ m
Height $hg = 3,01$ m (4.11)	Height $\Delta h = 0,08$ m
Soil pressure $\sigma_{D_{zul}} = 206,7$ kN/m ² (4.5)	

In Fig. 70, active area Ago and reactive area Agu are shown to the left of the perpendicular reference axis: Weight $Ge = Gt = 206,7$ kN (4.4) is dispersed via these areas without any subsidence of the foundation. However, if the soil is loaded with a higher weight $Ge' = Ge + \Delta Ge$, thereby exceeding the permissible soil pressure, the ground under the foundation will subside by the assumed height Δh .

Two calculation methods are possible to determine the payload increase ΔG – which will be described in more detail later by means of calculation examples. The first method, with somewhat approximated results, is based on area $As = bg \cdot \Delta h$, which lies between the force areas Ago and Ags , and increases them proportionately. With this approach, the soil parameters remain constant. The areas are shown to the right of the axis in Fig. 71.

The second method to determine force ΔGe is based on soil compaction in the load-dispersing soil column, i.e. it uses the changes of inclination angle and volumes in the soil under the foundation.

Shown to the left of axis (A–B) in Fig. 71 below, are force areas Ago and Agu , which are formed if the permissible soil pressure is not exceeded. Shown to the right of the axis is the load penetration into the ground by the amount Δh . Via width bg , height Δh leads to force area As , which must be distributed proportionally between force areas Ago and Agu . For the calculation method using soil compaction, the angle of the inclined plane (C'–B') must be determined first, and then the other characteristics of the compacted soil. In Fig. 71, height he is shown with a different scale than the heights below the terrain plane.

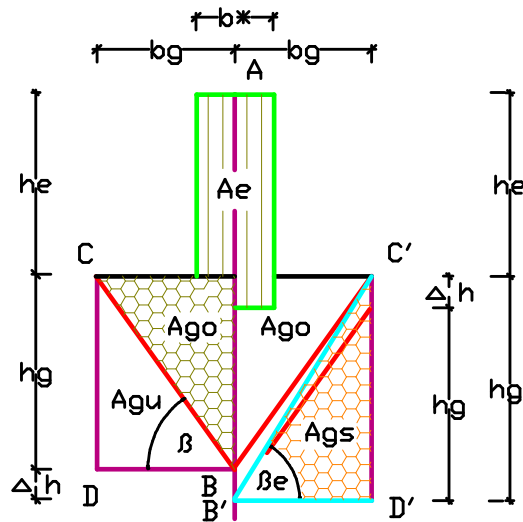


Fig. 71: Force areas – the axis with permissible (left) and exceeded soil pressure (right) with soil subsidence by amount Δh .

Calculation of weight ΔGe via increased areas

Height hg'

$$hg' = hg + \Delta h = 3,01 + 0,08 = 3,09 \quad \text{m} \quad 4.13$$

Area $Ago' = Agu' \rightarrow$ with width $bg = 2,11$ m (4.12)

$$Ago' = bg \cdot hg' / 2 = 2,11 \cdot 3,09 / 2 = 3,26 \quad \text{m}^2 \quad 4.14$$

Area Ae'

$$Ae' = 2 \cdot (Ago' - Ao) = 2 \cdot (3,26 - 0,18) = 6,16 \quad \text{m}^2 \quad 4.15$$

Weight $Ge \rightarrow ptg_{55} = 1,764$ t/m³ (3.9)

$$Ge = 2 \cdot Ae' \cdot ptg \cdot g = 2 \cdot 6,16 \cdot 1,764 \cdot g = 213,1 \quad \text{kN} \quad 4.16$$

Weight $\Delta Ge \rightarrow Gt = 206,7$ kN (4.4)

$$\Delta Ge = Ge - Gt = 213,1 - 206,7 = 6,4 \quad \text{kN} \quad 4.17$$

Calculation of weight ΔGe via soil compaction

If one uses weight $Ge = Gt = 206,7$ kN (4.4) for the column of the selected soil type with height $h = 11,95$ m, and permits a subsidence value of $\Delta h = 0,08$ m, the column height h will be reduced by $2 \cdot \Delta h = 0,16$ m (active and reactive portions). Therefore, the reduction of height also changes the solids volume $Vf = 0,588$ m³ (3.1) and pore volume $Vl = 0,412$ m³ (3.2) of the selected soil type.

Volume $\sum Vf \rightarrow$ within the volume $Ve = Ad \cdot h = 11,95$ m³

$$\sum Vf = Ve \cdot Vf / V_{90} = 11,95 \cdot 0,588 = 7,027 \quad \text{m}^3 \quad 4.18$$

Volume $Ve^* \rightarrow$ of compacted soil column

$$Ve^* = Ad \cdot (h - 2 \cdot \Delta h) = 1 \cdot (11,95 - 0,16) = 11,79 \quad \text{m}^3 \quad 4.19$$

Volume $Vf^* \rightarrow$ new

$$Vf^* = \sum Vf \cdot V_{90} / Ve^* = 7,027 / 11,79 = 0,596 \quad \text{m}^3 \quad 4.20$$

Inclination angle βe^*

$$\tan \beta e^* = Vf^* / (1,00 - Vf^*) = 0,596 / (1,00 - 0,596) = 1,475 \quad 4.21$$

$$\beta e^* = 55,9^\circ \quad [-] \quad 4.22$$

Density ptg^*

$$ptg^* = Vf^* \cdot ptg_{90} / V_{90} = 0,596 \cdot 3,00 / 1,0 = 1,788 \quad t/m^3 \quad 4.23$$

By means of the inclination angle βe^* , height h of the new soil column can be determined (see Section 4.2, Fig. 57).

Height h

$$h = \sqrt{V^* \cdot \tan \beta e^* / a} = \sqrt{100 \cdot 1,475 / 1,0} = 12,14 \quad m \quad 4.24$$

Weight $Ge^* \rightarrow$ with ptg^* and $g = 9,807m/s^2$.

$$Ge^* = Ad \cdot h \cdot ptg^* \cdot g = 12,14 \cdot 1,788 \cdot g = 212,9 \quad kN \quad 4.25$$

Weight ΔGe^*

$$\Delta Ge^* = Ge^* - Ge = 212,9 - 206,7 = 6,2 \quad kN \quad 4.26$$

Results:

Weight forces $\Delta Ge = 6,4$ kN (4.17) and $\Delta Ge^* = 6,2$ kN (4.26) show that even a slight soil overload will lead to significant subsidence $\Delta h = 0,08$ m of the foundation. Moreover, the soil parameters are changed as follows (see table below):

With permissible load, without subsidence	With permissible load and selected subsidence
Inclination angle $\beta_{t55} = 55,0^\circ$ (3.4)	Inclination angle $\beta e' = 55,9^\circ$ (4.22)
Weight $Gt = 206,7$ kN (3.9)	Weight $Ge^* = 212,9$ kN (4.25)

4.2.4 Load capacity of foundations with anchoring depths

For foundations with anchoring depths, DIN 1054 permits an increase of the bearing pressures σ_D specified in the tables. In the author's opinion, this increase of the permissible substratum loading is highly questionable, because loads are generally dispersed into the substratum via load area Ad below the foundation, and to a lesser extent via horizontal forces of the adjacent soil. If the horizontal forces are to be included in load dispersal, it must be ensured that the soil next to the foundation is able to generate and maintain a horizontal pressure against the foundation sides – similar to a bench vise. Subsequent excavations as well as vibrations around the foundation must be prevented. The foundation in Fig. 72 below is shown without anchoring in the surrounding ground to the left of the axis, and with anchoring to the right.

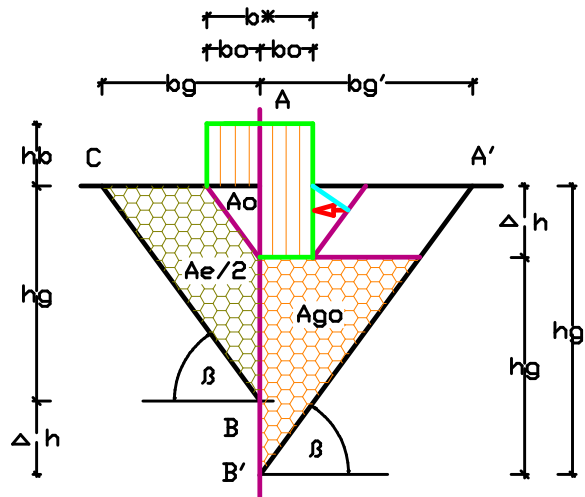


Fig. 72: Strip foundation with active force areas – without (left) and with anchoring depth Δh (right).

Calculation example: Foundation with anchoring depth

The following values are used:

Angle $\beta t = 55,0^\circ$ (3.4)	Density $ptg_{55} = 1,764 \text{ t/m}^3$ (3.9)
Force $Ge = 206,7 \text{ kN}$ (4.4)	Foundation width $bf = 1,00 \text{ m}$

Specified is the foundation's anchoring depth $\Delta h = 1,00 \text{ m}$. To be calculated is weight ΔGt from the force areas Ao next to the foundation. Force ΔGt corresponds to the vertical force components Hv of downhill force FH , which must be applied on both sides of the axis (see Fig. 72).

Calculation:

Width bo

$$bo = \Delta h / \tan \beta_{55} = 1,00 / 1,428 = 0,70 \quad \text{m} \quad 4.27$$

Area Ao

$$Ao = bo \cdot \Delta h / 2 = 0,70 \cdot 1,00 / 2 = 0,35 \quad \text{m}^2 \quad 4.28$$

Weight $\Delta Gt \rightarrow$ from the soil's dead weight with its dry density

$$\Delta Gt = Ao \cdot ptg_{55} \cdot g = 0,35 \cdot 1,764 \cdot 9,807 = 6,0 \quad \text{kN} \quad 4.29$$

Force Hf

$$Hf = \Delta Gt \cdot \sin \beta_{55} \cdot \cos \beta_{55} = 6,0 \cdot 0,470 = 2,8 \quad \text{kN} \quad 4.30$$

Force Hv

$$Hv = \Delta Gt \cdot \sin^2 \beta_{55} = 6,0 \cdot 0,671 = 4,0 \quad \text{kN} \quad 4.31$$

Weight $\Delta Gt \rightarrow$ double the force Hv

$$\Delta Gt = 2 \cdot Hv = 2 \cdot 4,0 = 8,0 \quad \text{kN} \quad 4.32$$

Weight ΣGt

$$\Sigma Gt = Gt + \Delta Gt = 206,7 + 8,0 = 214,7 \quad \text{kN} \quad 4.33$$

Results:

For strip foundation with anchoring depth $\Delta h = 1,00$ m.

Force dispersal under the strip foundation
Inclination angle $\beta_{t_{55}} = 55,0^\circ$ (3.4)
Weight $G_t = 206,7$ kN (4.4)
Weight $\Delta G_t = 8,0$ kN (4.32)
Weight $\sum G_t = 214,7$ kN (4.33)

Force $\sum G_t$ includes the foundation's dead weight. If weight G_t is to be increased by the amount of force ΔG_t , a force-locked transition from the adjacent soil to the foundation is required. Moreover, vibrations in the foundation area must be excluded.

4.3 Earth pressure in soils with inclined surface

The rising or falling terrain plane of a soil body is described as an inclined surface. Also included in this description is a soil body that is supported by a perpendicular wall (reference axis), and whose terrain plane rises with angle x .

In order to determine the earth pressure that such bodies apply against the wall, and to evaluate the sliding of earth masses from a slope, knowledge about the positions of inclination and shear planes in soil bodies with inclined surface is required. For this, the teachings use diagrams by means of which they deduce angle φ' and value K_{ah} [1: page P.12ff. Pictures P05.70, P05.80, P05.90, P08.10, and P08.30].

The New Theory sees other relationships for the formation of angles, and demonstrates them in the following tests with sand in the glass container. Force determinations are carried out after the experiments.

4.3.1 Shear plane in soils with inclined surface, Test 9

In the previous sections, examinations were carried out on earth blocks with horizontal surfaces that are supported by a real or fictitious wall (reference axis). In this test, the horizontal terrain plane will be replaced by an inclined surface. Consequently, the side view of a soil body consists of a rectangular base area and a wedge-shaped load area. Because it must be assumed here that the soil in the wedge area acts on the lower soil body as a load, this load will change the natural angles of the inclination and shear planes, similar to what happens with rectangular load areas. This change of angles in soil bodies with a

horizontal surface was investigated in Section 2.5, page 43ff (see Fig. 22, page 44).

Fig. 22 shows a soil body and a rectangular load area with height he and calculation depth $a = 1,00$ m. For load dispersal, an equally large area was located below the terrain plane, with its diagonal divided into active and reactive load portions. This division determines the position of the 'inclination plane under the load'. As above, the inclination angle βe of a wedge-shaped load can also be determined by means of width bx and height $he = hx/4$. Height hx must be specified in advance, or be calculated from slope angle s' . Quartering of height hx results from halving the rectangular load area, and dividing the load into active and reactive load portions. If a soil layer is applied as a load, it must be established whether load dispersal starts in the load dispersing soil or already in the load area, i.e. in the wedge area above the earth block.

If one selects block height hm , height hx , and width $bo = bx = hm/\tan \beta$, angle βe under load is calculated using $\tan \beta e = (hm + hx/4) / bo$.

Test 9 was conducted with sand and basalt grit in the glass container to confirm the above assumptions, and to detect possible differences when the soil slides down from an earth block (Fig. 15: page 39), and to recognize an earth block with wedge-shaped load. Three tests out of the series using dry sand were described, whereby Experiment 9.1 was designed to collect basic data for Tests 9.2 and 9.3. The experiments were carried out with equal sand quantities, but with different heights and different inclinations. For the calculations, a reference axis was located at the bottom wall surface of the removable glass pane, and a horizontal plane inserted where the inclined surface intersects the reference axis. The sand in the wedge area with height hx and width bx is seen as the load on the earth block below it.

Test setup 9.1

For the test 26,5 kg dry sand were filled into the left-hand chamber of the glass container up to height $ht = 2,28$ dm, and the sand's surface smoothed horizontally before the separating glass pane was removed. After the sand had slipped down, width $bl' = 0,56$ dm was measured between the inclined surface and the left-hand glass wall, and width $br' = 0,54$ dm to the right-hand glass wall. The

practically identical widths indicate that the terrain plane can be described as the sand's 'natural shear plane' (see Section 2.4, page 37ff).



Fig. 73: Sand filling with horizontal surface as starting basis.



Fig. 74: Shear plane (green) and the sand's shear angle s .

The following basic data were determined:

Volume V_{kt} → Base area $A_{k1} = 7,08 \text{ dm}^2$ (3.33)

$$V_{kt} = A_{k1} \cdot ht = 7,08 \cdot 2,28 = 16,14 \quad \text{dm}^3 \quad 4.34$$

Dry density ptg

$$ptg = Gt/V_{kt} = 26,5/16,14 = 1,642 \quad \text{kg/dm}^3 \quad 4.35$$

Solids volume V_f

$$V_f = ptg \cdot V_{p90}/ptg_{90} = 1,642 \cdot 1,0/3,0 = 0,547 \quad \text{dm}^3 \quad 4.36$$

Pore volume V_l

$$V_l = V_{p90} - V_f = 1,000 - 0,547 = 0,453 \quad \text{dm}^3 \quad 4.37$$

Inclination angle βt

$$\tan \beta t = V_f/V_l = 0,547/0,453 = 1,208 \quad 4.38$$

$$\beta t = 50,4^\circ \quad [-] \quad 4.39$$

Shear angle st

$$\tan st = (\tan \beta t) / 2 = 1,208/2 = 0,604 \quad 4.40$$

$$st = 31,1^\circ \quad [-] \quad 4.41$$

Width $bo = bu$

$$bo = ht / \tan \beta t = 2,28/1,208 = 1,89 \quad \text{dm} \quad 4.42$$

Width bl

$$bl = bk_1 - bo = 2,44 - 1,89 = 0,55 \quad \text{dm} \quad 4.43$$

Width bue

$$bue = ht / \tan st = 2,28/0,604 = 3,77 \quad \text{dm} \quad 4.44$$

Width br

$$br = bk_1 - bue/2 = 2,44 - 3,77/2 = 0,56 \quad \text{dm} \quad 4.45$$

Height $hmu = hmo$

$$hmu = hmo = ht/2 = 2,28/2 = 1,14 \quad \text{dm} \quad 4.46$$

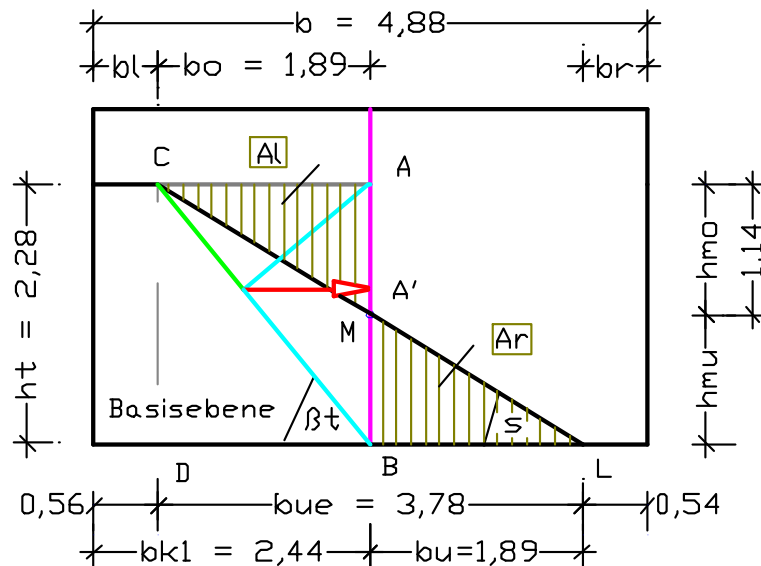


Fig. 75: Natural shear plane (C-L), along which the soil slides down from area Al to area Ar.

The angles determined above from the sand volume (4.39) and (4.41) are comparable with the angles that were calculated from measured height $ht = 2,28$ dm and wedge width $bue = 3,78$ dm.

Shear angle st'

$$\tan st' = ht/bue' = 2,28/3,78 = 0,603 \quad 4.47$$

$$st' = 31,1^\circ \quad [-] \quad 4.48$$

Inclination angle $\beta t'$

$$\tan \beta t' = 2 \cdot \tan st' = 2 \cdot 0,603 = 1,206 \quad 4.49$$

$$\beta t' = 50,3^\circ \quad [-] \quad 4.50$$

The calculated and measured angles are considered to be equal. Angles (4.39) and (4.41) are used for the further experiments.

Force determinations for Test 9.1:

Wedge area (C-A-B) and the following values are used to determine earth pressure force Hf and its thrust height hv :

Filling height $ht = 2,28$ dm	Width $bo = 1,89$ dm (4.42)
Angle $\beta t = 50,4^\circ$ (4.39)	Density $ptg_{50} = 1,642$ kg/dm ³

Calculation:

Volume $Vo \rightarrow$ by means of calculation depth $a = 2,90$ dm

$$Vo = ht \cdot bo \cdot a/2 = 2,28 \cdot 1,89 \cdot 2,9/2 = 6,25 \quad \text{dm}^3 \quad 4.51$$

Weight Gt

$$Gt = Vo \cdot ptg_{50} \cdot g = 6,25 \cdot 1,642 \cdot 9,807 = 100,6 \quad \text{N} \quad 4.52$$

Force $N_v \rightarrow$ with inclination angle $\beta_t = 50,4^\circ$ (4.39)

$$N_v = G_t \cdot \cos^2 \beta_t = 100,6 \cdot 0,406 = 40,8 \quad \text{N} \quad 4.53$$

Force H_v

$$H_v = G_t \cdot \sin^2 \beta_t = 100,6 \cdot 0,594 = 59,8 \quad \text{N} \quad 4.54$$

Earth pressure force H_f

$$H_f = G_t \cdot \sin \beta_t \cdot \cos \beta_t = 100,6 \cdot 0,491 = 49,4 \quad \text{N} \quad 4.55$$

Force index g_{it}

$$g_{it} = b_o \cdot a \cdot \text{ptg}_{50} \cdot g/2 = 15,2$$

$$g_{it} = 1,89 \cdot 2,90 \cdot 1,642 \cdot 9,807/2 = 44,1 \quad \text{N/dm}^2 \quad 4.56$$

Thrust height h_v of force H_f against the wall

$$h_v = H_v/g_{it} = 59,8/44,1 = 1,35 \quad \text{dm} \quad 4.57$$

Fig. 75 shows force $H_f = 49,4$ N as a red arrow.

Test setup 9.2

For this test, the sand used in Test 7.1 was loosely filled into the left-hand chamber of the glass container up to height $h_t = 2,58$ dm. Possible scatter losses and sand adhesions to the glass panes were not followed up. If necessary, this can be calculated by means of the measured soil body before and after the sand has slipped down and then deducted from the original filling weight.



Fig. 76: Sand body with partially inclined surface.



Fig. 77: Shear plane after the sand has slipped down.

As shown in Fig. 76, a wedge area to the right of the separating plane was not filled. The horizontal and angled soil surfaces were carefully smoothed with a trowel, after which wedge height $h_x = 1,02$ dm and wedge width $b_x = 1,54$ dm were measured. After pulling out the glass pane, widths $b_l = 0,21$ dm, $b_{ue} = 3,77$ dm, and $b_r = 0,90$ dm were established with the filling height $h_t = 2,58$ dm. Hereby, the shear plane moved from the central position by the amount b_m to the left (see Fig. 77 below, and Fig 78, page 110). For the adaptation of the natural inclination and shear plane into the new sand body form, and to

calculate the angles under load, the sand volume Vkt' is first calculated from filling height $ht = 2,58$ dm and the removed wedge area $Ax = hx \cdot bx / 2$.

Calculation:

Projection plane $A \rightarrow$ of measured sand body with height ht

$$A = bk_l \cdot ht = 2,44 \cdot 2,58 = 6,295 \quad \text{dm}^3 \quad 4.58$$

Projection plane $Ax \rightarrow$ sand-free area

$$Ax = bx \cdot hx/2 = 1,54 \cdot 1,02/2 = 0,785 \quad \text{dm}^3 \quad 4.59$$

Volume $Vkt' \rightarrow a = 2,90$ dm container depth

$$Vkt' = (A - Ax) \cdot a = (6,295 - 0,785) \cdot 2,9 = 15,98 \quad \text{dm}^3 \quad 4.60$$

As the volume reduction from Vkt to Vkt' is not due to compaction, but to scatter losses, density $ptg = 1,653$ kg/dm³ (4.35) and the angles $\beta t = 50,4^\circ$ (4.39) and $st = 31,1^\circ$ (4.41) remain unchanged. To determine the 'inclination angle βe under load', an earth block with width bx and height hm' must first be prepared.

Height hm'

$$hm' = bx \cdot \tan \beta t = 1,54 \cdot 1,208 = 1,86 \quad \text{dm} \quad 4.61$$

Height $hx/4$ must be added to height hm' for calculating the angle.

Inclination angle βe

$$\tan \beta e = (hm' + hx/4) / bx = (1,86 + 1,02/4) / 1,54 = 1,373 \quad 4.62$$

$$\beta e = 53,9^\circ \quad [-] \quad 4.63$$

Shear angle se

$$\tan se = (\tan \beta e) / 2 = 1,373 / 2 = 0,687 \quad 4.64$$

$$se = 34,5^\circ \quad [-] \quad 4.65$$

When the sand's restraining wall has been removed by pulling out the separating glass pane, it slides down along the 'shear plane under load', and forms a lying earth wedge (see Fig. 77). Hereby, a volume equalization (removal = filling) takes place between the sand sliding down and the sand build-up, which results in a lowering of the shear plane by height hy . The following are already known for calculation: heights $hx = 1,02$ dm, and $hm = ht - hx$, area $Ax = 0,785$ dm² (4.59), and angle $se = 34,5^\circ$ (4.65).

Height hm

$$hm = ht - hx = 2,58 - 1,02 = 1,56 \quad \text{dm} \quad 4.66$$

Height hy

$$(hx + hy)^2 / (2 \cdot \tan se) = (hm - hy)^2 / (2 \cdot \tan se) + Ax$$

$$(1,02 + hy)^2 / (2 \cdot 0,687) = (1,56 - hy)^2 / (2 \cdot 0,687) + 0,785$$

$$hy^2 + 2,04 hy + 1,04 = hy^2 - 3,12 hy + 2,42 + 1,08$$

$$hy = 2,46 / 5,16 = 0,48 \quad \text{dm} \quad 4.67$$

Height h_o

$$h_o = h_x + h_y = 1,02 + 0,48 = 1,50 \quad \text{dm} \quad 4.68$$

Height h_u

$$h_u = h_t - h_o = 2,58 - 1,50 = 1,08 \quad \text{dm} \quad 4.69$$

Width b_o

$$b_o = h_o / \tan se = 1,50 / 0,687 = 2,18 \quad \text{dm} \quad 4.70$$

Width $b_{l'}$

$$b_{l'} = b_{k_l} - b_o = 2,44 - 2,18 = 0,26 \quad \text{dm} \quad 4.71$$

Width b_u

$$b_u = h_u / \tan se = 1,08 / 0,687 = 1,57 \quad \text{dm} \quad 4.72$$

Area $A_l \rightarrow$ of the soil that has slipped down

$$A_l = (b_o' \cdot h_o) / 2 - A_x =$$

$$A_l = (2,18 \cdot 1,50) / 2 - 0,785 = 0,85 \quad \text{dm}^2 \quad 4.73$$

Area $A_r \rightarrow$ of the built-up soil

$$A_r = b_u \cdot h_u / 2 = 1,57 \cdot 1,08 / 2 = 0,85 \quad \text{dm}^2 \quad 4.74$$

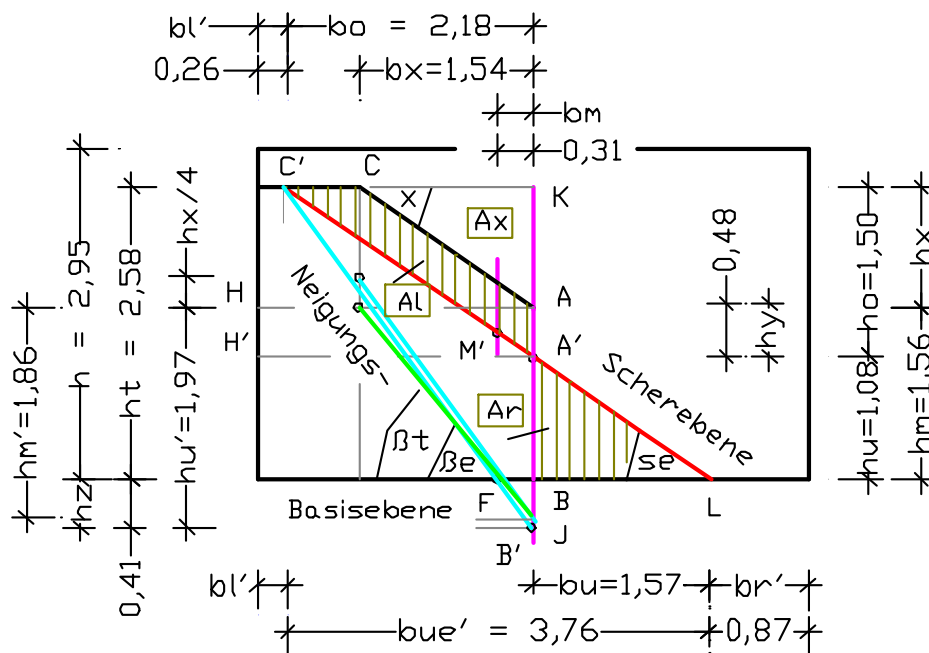


Fig. 78: Soil load in area A_l , which slides down along the shear plane under load after losing its restraining wall on the central axis.

Width $b_{r'}$

$$b_{r'} = b_{k_l} - b_u = 2,44 - 1,57 = 0,87 \quad \text{dm} \quad 4.75$$

Width b_m

$$b_m = (b_o' - b_u) / 2 = (2,18 - 1,57) / 2 = 0,31 \quad \text{dm} \quad 4.76$$

Width $b_{ue'}$

$$b_{ue'} = h_t / \tan se = 2,58 / 0,687 = 3,76 \quad \text{dm} \quad 4.77$$

Height h_s

$$h_s = b_o \cdot \tan \beta_e = 2,18 \cdot 1,373 = 2,99 \quad \text{dm} \quad 4.78$$

Height hz

$$hz = hs - ht = 2,99 - 2,58 = 0,41 \quad \text{dm} \quad 4.79$$

Height hu'

$$hu' = hs - hx = 2,99 - 1,02 = 1,97 \quad \text{dm} \quad 4.80$$

Before comparing the measured and calculated values, the measured heights and widths of shear angle se' and height hu' at the reference axis must first be determined.

Shear angle se'

$$\tan se' = ht / bue' = 2,58 / 3,77 = 0,684 \quad 4.81$$

$$se' = 34,4^\circ \quad [-] \quad 4.82$$

Height hu'

$$hu' = (bk_l - br) \cdot \tan se'$$

$$hu' = (2,44 - 0,90) \cdot 0,684 = 1,05 \quad \text{dm} \quad 4.83$$

Result of test 9.2:

The table summarizes the measured and calculated dimensions before and after the sand has slipped down.

Measured dimensions	Calculated dimensions
Width $bl = 0,21$ dm	Width $bl' = 0,26$ dm (4.71)
Width $bue = 3,77$ dm	Width $bue' = 3,76$ dm (4.77)
Width $br = 0,90$ dm	Width $br' = 0,87$ dm (4.75)
Height $hu' = 1,05$ dm	Height $hu = 1,08$ dm (4.69)
Shear angle $se' = 34,4^\circ$	Shear angle $se = 34,5^\circ$ (4.65)

Small differences in the heights and widths of the soil body can occur due to measurement inaccuracies, sliding resistances caused by the limited container width or loosening during sliding, as well as rounded calculation values. Nonetheless, the comparison between measured and calculated dimensions shows a high level of conformity. The method demonstrates that the sliding of earth masses from a slope can be calculated.

Test setup 9.3

In order to consolidate the results of Test 9.2, this experiment was carried out with the same amount of sand, but with a different shape of the sand body. When the sand had been filled into the container, filling height $ht = 2,95$ dm, width $bx = 2,34$ dm, and height $hx = 1,48$ dm were measured. After pulling out the glass pane, a sand wedge was formed with height $hd = 2,75$ dm at the left-

hand container wall, and widths $bue = 3,96$ dm and $br = 0,92$ dm on the container floor.



Fig. 79: Sand body with completely inclined surface.

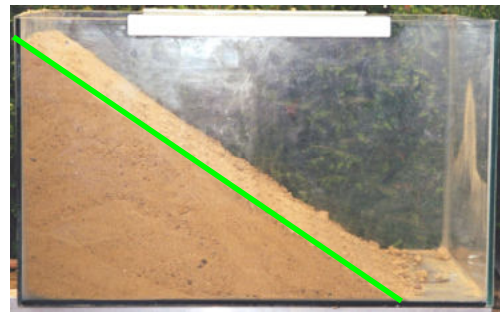


Fig. 80: Shear plane after the sand had slipped down.

The following calculations were carried out:

Projection plane $A \rightarrow$ of measured sand body with height $ht = 2,95$ dm

$$A = bk_l \cdot ht = 2,44 \cdot 2,95 = 7,198 \quad \text{dm}^2 \quad 4.84$$

Projection plane $Ax \rightarrow$ sand-free area

$$Ax = bx \cdot hx/2 = 2,34 \cdot 1,48/2 = 1,732 \quad \text{dm}^2 \quad 4.85$$

Volume $Vkt' \rightarrow a = 2,90$ dm container depth

$$Vkt' = (A - Ax) \cdot a = (7,198 - 1,732) \cdot 2,9 = 15,85 \quad \text{dm}^3 \quad 4.86$$

The angles $\beta_t = 50,4^\circ$ (4.39) and $st = 31,1^\circ$ (4.41) determined in Test 9.1 were used for the following calculations. Also here, the inclination angle β_e under load was determined from block width bx and heights $hx/4$ and hm' (see Fig. 81 below).

Height hm'

$$hm' = bx \cdot \tan \beta_t = 2,34 \cdot 1,208 = 2,83 \quad \text{dm} \quad 4.87$$

Inclination angle β_e

$$\tan \beta_e = (hm' + hx/4) / bx = (2,83 + 1,48/4) / 2,34 = 1,368 \quad 4.88$$

$$\beta_e = 53,8^\circ \quad [-] \quad 4.89$$

Shear angle se

$$\tan se = (\tan \beta_e) / 2 = 1,368 / 2 = 0,684 \quad 4.90$$

$$se = 34,4^\circ \quad [-] \quad 4.91$$

Height hm

$$hm = ht - hx = 2,95 - 1,48 = 1,47 \quad \text{dm} \quad 4.92$$

Height hy

$$(hx + hy)^2 / (2 \cdot \tan se) = (hm - hy)^2 / (2 \cdot \tan se) + Ax$$

$$(1,48 + hy)^2 / (2 \cdot 0,684) = (1,47 - hy)^2 / (2 \cdot 0,684) + 1,732$$

$$hy^2 + 2,96 hy + 2,19 = hy^2 - 2,94 hy + 2,16 + 2,37$$

$$hy = 2,34 / 5,90 = 0,40 \quad \text{dm} \quad 4.93$$

Height h_o

$$h_o = h_x + h_y = 1,48 + 0,40 = 1,88 \quad \text{dm} \quad 4.94$$

Height h_u

$$h_u = h_t - h_o = 2,95 - 1,88 = 1,07 \quad \text{dm} \quad 4.95$$

Width $b_o \rightarrow$ determines width b_l'

$$b_o = h_o / \tan se = 1,88 / 0,684 = 2,75 \quad \text{dm} \quad 4.96$$

Width b_l'

$$b_l' = b_{k_l} - b_o = 2,44 - 2,75 = -0,31 \quad \text{dm} \quad 4.97$$

Width b_u

$$b_u = h_u / \tan se = 1,07 / 0,684 = 1,56 \quad \text{dm} \quad 4.98$$

Area A_l

$$A_l = (b_o' \cdot h_o) / 2 - A_x =$$

$$A_l = (2,75 \cdot 1,88) / 2 - 1,732 = 0,85 \quad \text{dm}^2 \quad 4.99$$

Area A_r

$$A_r = b_u \cdot h_u / 2 = 1,56 \cdot 1,07 / 2 = 0,84 \quad \text{dm}^2 \quad 4.100$$

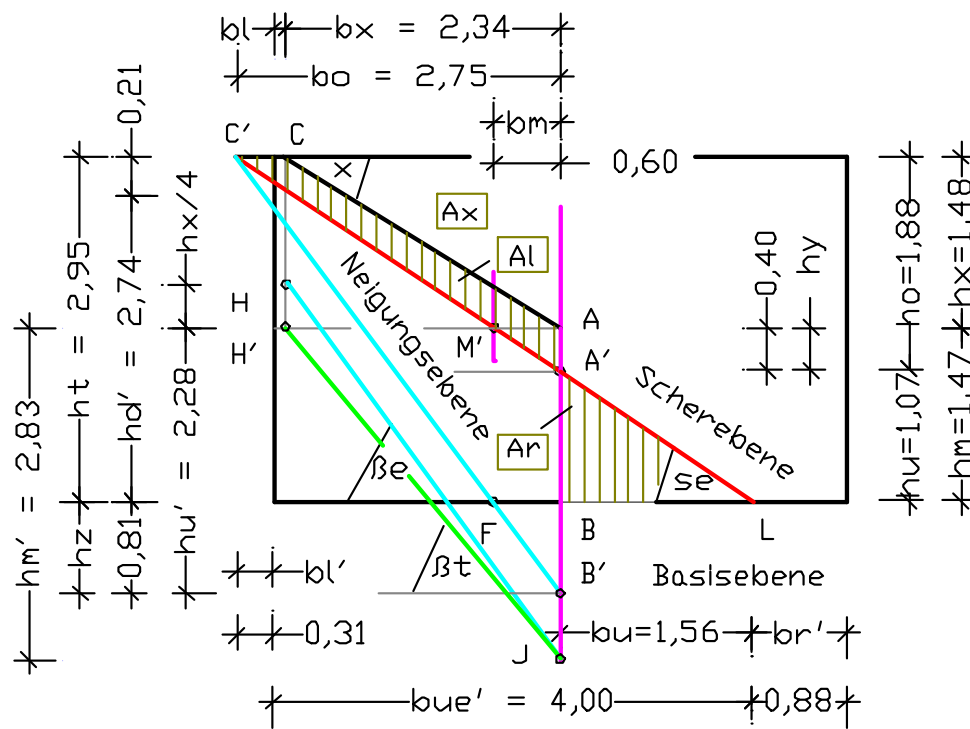


Fig. 81: Natural inclined plane (H'-J), inclined plane under load (H-J) and (C'-B'), and shear plane under load (C'-L).

Width $b_{r'}$

$$b_{r'} = b_{k_l} - b_u = 2,44 - 1,56 = 0,88 \quad \text{dm} \quad 4.101$$

Width b_m

$$b_m = (b_o' - b_u) / 2 = (2,75 - 1,56) / 2 = 0,60 \quad \text{dm} \quad 4.102$$

Width b_{ue}'

$$b_{ue}' = h_t / \tan se + b_l' = 2,95 / 0,684 - 0,31 = 4,00 \quad \text{dm} \quad 4.103$$

Height hd'

$$hd' = bue' \cdot \tan se = 4,00 \cdot 0,684 = 2,74 \quad \text{dm} \quad 4.104$$

Height hs

$$hs = bo \cdot \tan \beta e = 2,75 \cdot 1,368 = 3,76 \quad \text{dm} \quad 4.105$$

Height hz

$$hz = hs - ht = 3,76 - 2,95 = 0,81 \quad \text{dm} \quad 4.106$$

Height hu'

$$hu' = hs - hx = 3,76 - 1,48 = 2,28 \quad \text{dm} \quad 4.107$$

Before comparing the measured and calculated values, the measured heights and widths of shear angle se' and height hu' at the reference axis must first be determined.

Shear angle se'

$$\tan se' = hd / bue' = 2,75 / 3,96 = 0,694 \quad 4.108$$

$$se' = 34,8^\circ \quad [-] \quad 4.109$$

Height hu^*

$$hu^* = (bk_l - br) \cdot \tan se'$$

$$hu^* = (2,44 - 0,88) \cdot 0,694 = 1,08 \quad \text{dm} \quad 4.110$$

Result of Test 9.3:

The table summarizes the measured and calculated dimensions before and after the sand has slipped down.

Measured dimensions	Calculated dimensions
Width $br = 0,92$ dm	Width $br' = 0,88$ dm (4.101)
Height $hd = 2,75$ dm	Height $hd' = 2,74$ dm (4.104)
Width $bue = 3,96$ dm	Width $bue' = 4,00$ dm (4.103)
Height $hu' = 1,08$ dm	Height $hu = 1,07$ dm (4.95)
Shear angle $se' = 34,8^\circ$	Shear angle $se = 34,4^\circ$ (4.91)

Also here, the comparison between measured and calculated dimensions shows a high level of conformity. This confirms that inclination angle βe under load can be calculated from the wedge-shaped load area with height hx .

4.3.2 Forces in dry soils with inclined surface

Following Test 9.3, the earth forces before and after the sand had slipped down from the left-hand chamber are determined as Versions A and B. The determinations are based on the calculated soil properties and on the soil body's dimensions.

The force areas to be determined – with / without load – their position within the earth wedge, and their horizontal forces can be taken from Fig. 82 below.

The following values are available for the calculation:

Density $\rho_{tg} = 1,653 \text{ kg/dm}^3$	Filling height $ht = 2,95 \text{ dm}$
Calculation depth $a = 2,90 \text{ dm}$	Height $hx = 1,48 \text{ dm}$
Width $bk_l = 2,44 \text{ dm}$	Height $hm = 1,47 \text{ dm}$ (4.92)
Width $bx = 2,34 \text{ dm}$	Height $hu = 1,07 \text{ dm}$ (4.95)
Width $bo = 2,75 \text{ dm}$ (4.96)	Height $hz = 0,81 \text{ dm}$ (4.106)
Angle $\beta_e = 53,8^\circ$ (4.89)	Height $hu' = 2,28 \text{ dm}$ (4.107)
	$\tan \beta_e = 1,368$ (4.88)

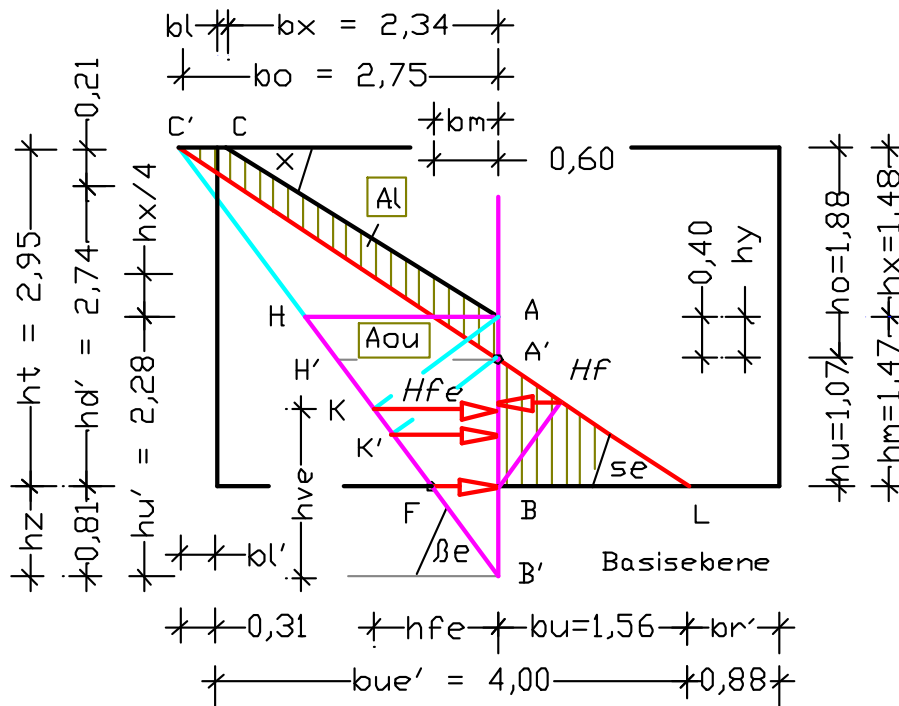


Fig. 82: Force area Aou below plane (H-A), out of which the earth pressure force Hfe acts against the reference axis (A-B').

Version A: Forces in the earth wedge before the sand slides down

For this load condition, load area (H-A-B') is valid, which can be determined by means of the above values.

Area $bo' \rightarrow$ angle $\beta_e = 53,8^\circ$ (4.89)

$$bo' = hu' / \tan \beta_e = 2,28 / 1,368 = 1,67 \quad \text{dm}^2 \quad 4.111$$

Volume Ve

$$Ve = hu' \cdot a \cdot bo' / 2 = 2,28 \cdot 2,90 \cdot 1,67 / 2 = 5,52 \quad \text{dm}^3 \quad 4.112$$

Weight Ge

$$Ge = Ve \cdot \rho_{tg} \cdot g = 5,52 \cdot 1,653 \cdot 9,807 = 89,5 \quad \text{N} \quad 4.113$$

Force Nve

$$Nve = Ge \cdot \cos^2 \beta_e = 89,5 \cdot 0,349 = 31,2 \quad \text{N} \quad 4.114$$

Force Hve

$$Hve = Ge \cdot \sin^2 \beta_e = 89,5 \cdot 0,652 = 58,4 \quad \text{N} \quad 4.115$$

Earth pressure force Hfe

$$Hfe = Ge \cdot \sin \beta e \cdot \cos \beta e = 89,5 \cdot 0,477 = 42,7 \quad \text{N} \quad 4.116$$

Force index git

$$git = bo' \cdot a \cdot ptg \cdot g/2$$

$$git = 1,67 \cdot 2,90 \cdot 1,653 \cdot 9,807/2 = 39,25 \quad \text{N/dm}^2 \quad 4.117$$

Height nv'

$$nv = Nve/git = 31,2 / 39,25 = 0,79 \quad \text{dm} \quad 4.118$$

Thrust height $hv \rightarrow$ of earth pressure force Hfe

$$hv = Hve/git = 58,4/39,25 = 1,49 \quad \text{dm} \quad 4.119$$

Because the bottom of the glass container – similar to a rock layer – prevents the vertical force dispersal in the sand, the undispersed vertical force of area Ae is converted into horizontal force Hf^* (F–B).

Earth pressure force Hfe^*

$$Hfe^* = Hfe \cdot hz/hv' = 42,7 \cdot 0,81/1,49 = 23,2 \quad \text{N} \quad 4.120$$

Results:

While force $Hfe^* = 23,2 \text{ N}$ (4.120) acts at the height of the container floor, earth pressure force $Hfe = 42,7 \text{ N}$ (4.116) acts against the reference axis at height $hv = 1,49 \text{ dm}$ (4.119).

Version B: Forces in the earth wedge after the sand slides down

When the soil has slipped down, the shear plane intersects the reference axis at Point A', so that weight Ge' for force determination can be derived from earth wedge area (H'–A'–B'). It is advisable to first determine heights nv and hv , and then the earth pressure forces Hf by means of the height ratios.

Height $Hfe^* = 23,2 \text{ N}$ (4.120) does not change.

Height $nv' \rightarrow$ angle $\beta e = 53,8^\circ$ (4.89)

$$nv' = (hu' + hz) \cdot \cos^2 \beta e = (1,07 + 0,81) \cdot 0,349 = 0,66 \quad \text{dm} \quad 4.121$$

Thrust height hv'

$$hv' = (hu' + hz) \cdot \sin^2 \beta e = 1,88 \cdot 0,651 = 1,22 \quad \text{dm} \quad 4.122$$

Force meter hf'

$$hf' = (hu' + hz) \cdot \sin \beta e \cdot \cos \beta e = 1,88 \cdot 0,477 = 0,90 \quad \text{dm} \quad 4.123$$

Earth pressure force $Hf \rightarrow$ by means of force $Hfe = 42,7 \text{ N}$ (4.116)

$$Hf = Hfe \cdot (hu' + hz)/hu' = 42,7 \cdot 1,88/2,28 = 35,2 \quad \text{N} \quad 4.124$$

or:

Earth pressure force Hf

$$Hf = hf' \cdot git = 0,90 \cdot 39,25 = 35,3 \quad \text{N} \quad 4.125$$

Results:

Earth pressure force $Hf = 35,2 \text{ N}$ (4.124) acts against the reference axis at height $h v' = 1,22 \text{ dm}$ (4.122), and force $Hfe^* = 23,2 \text{ N}$ (4.120) at the container floor remains unchanged.

4.3.3 Influence of loads on soils with inclined surface

In the previous sections, tests were conducted to illustrate how sand slides in a body with inclined surface. Hereby it was shown that the sand located above the natural shear plane must be seen as a load. As soon as the sand loses its support when the separating glass pane is pulled out, it slides down and forms the steeper 'shear plane under load'. The shear plane's position under load is influenced by angle x of the terrain slope or by height hx (see Figs. 78 and 81). The earth pressure teachings use Pictures P.05.80 and P.05.100 [1: P.13] to show a graphical earth pressure determination with an arbitrary surface form. Changes of angles due to loads in earth blocks with 'horizontal surface' were described in Section 2.5. for the New Theory. In Tests 9.2 and 9.3, loads resting on the natural shear plane were investigated. Hereby, it was shown that in spite of different load forms, the changed angles can be reproduced, regardless of whether the loads act on the shear plane of a 'standing earth wedge' (center of gravity in $2 \cdot h/3$) or a 'lying earth wedge' (center of gravity in $h/3$). Based on these tests, Figs. 83 to 89 were prepared, showing the forms of possible loads. Similar to the way in which an earth wedge on a horizontal plane can be a load, distributed loads or groundfill on horizontal terrains can become loads.

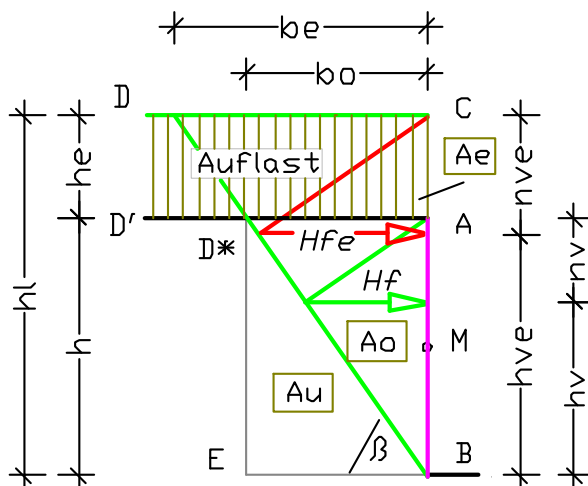


Fig. 83: Earth block with groundfill as a rectangular load area, and its force distribution.

In both cases, the load value can be determined by means of gravity and the density of the load-dispersing earth body. However, there is a difference in

load dispersal: In the case of a groundfill, load dispersal already starts in the groundfill above the terrain level. If the properties of the groundfill and the load-dispersing soil were equal, force dispersal would even occur along the same inclination angle. In Fig. 83, the groundfill is represented by area (D–C–A–D'). The effect is that the position of earth pressure force Hf (green) is shifted upwards and is turned into force Hfe (red).

However, if one places a force on an earth block (Figs. 84 and 85), and converts the force into the load area (D–C–A–D'), the area must be located below the natural inclined plane (D'–B). Hereby, the area is divided into the active part (D'–B–B') and the reactive part named area Ar . The active area Aa must be added to area Ao of the soil's dead weight, so that total area $Aae = Ao + Aa$ is created. Block height h is increased by amount he due to load dispersal in the soil, resulting in total height hl . Also shown in the block are natural shear plane (D'–M), shear plane under load (D'–A'), the position of the natural inclined plane with angle β , and the inclined plane under load with inclination angle β_e .

Fig. 85 shows the distribution of earth pressure force Hf without load (green) and earth pressure force Hfe under load (red). Hereby, it becomes clear that deeper lying ground is involved for load dispersal. If rock or concrete layers prevent a vertical force dispersal, undispersed vertical forces in the ground can be converted into horizontal forces. This is discussed in more detail in Section 4.6. page 137.

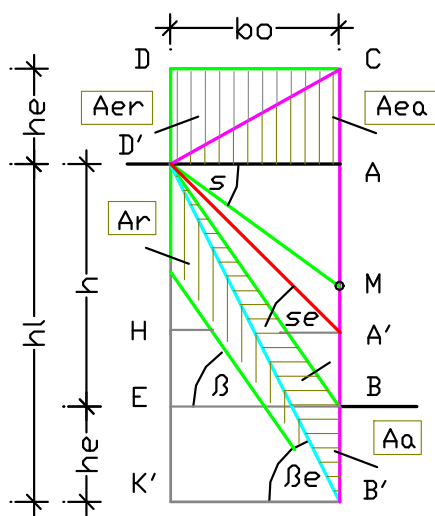


Fig. 84: Earth block with rectangular load area and its inclination and shear planes without / with load.

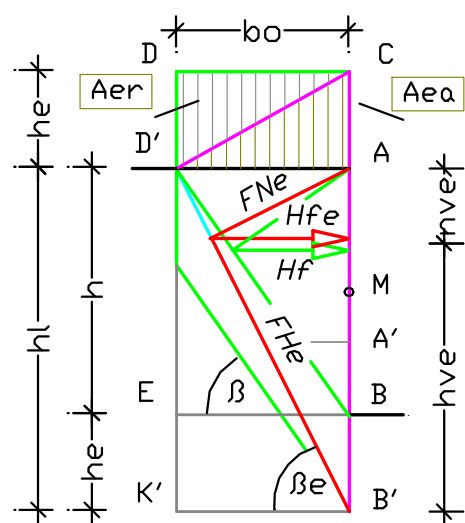


Fig. 85: Earth block with rectangular load area and its force distribution in wedge area (D'–A–B')

On the following pages, wedge-shaped force areas as loads on earth blocks will be examined.

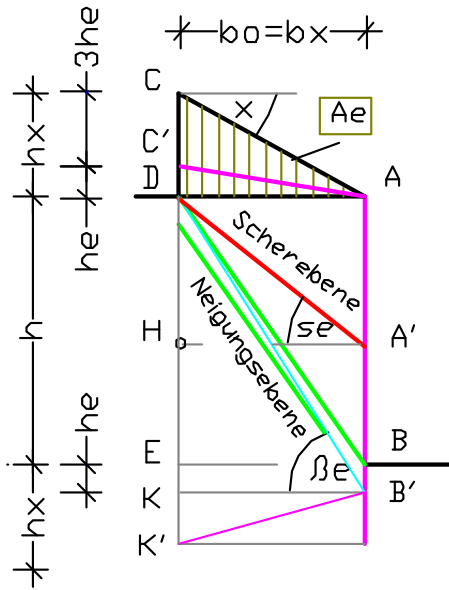


Fig. 86: Earth block with rising surface (A-C), and changed angles due to the load.

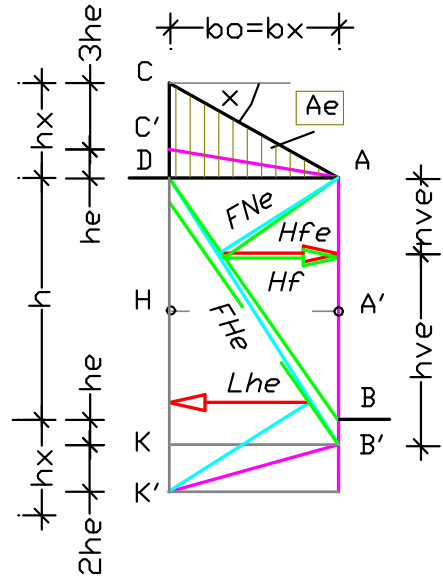


Fig. 87: Earth block with rising surface, and force distribution within the wedge area (D-A-B')

The use of height he to determine the inclined plane under load by means of angle β_e is based on the results of Tests 9.2 and 9.3.

Shown below is the determination of inclined plane under load and force distribution in a soil body with falling inclined surface.

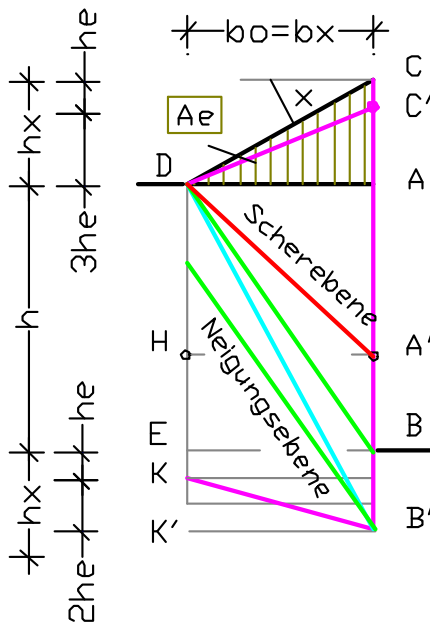


Fig. 88: Earth block with falling terrain surface, and inclination & shear planes under load.

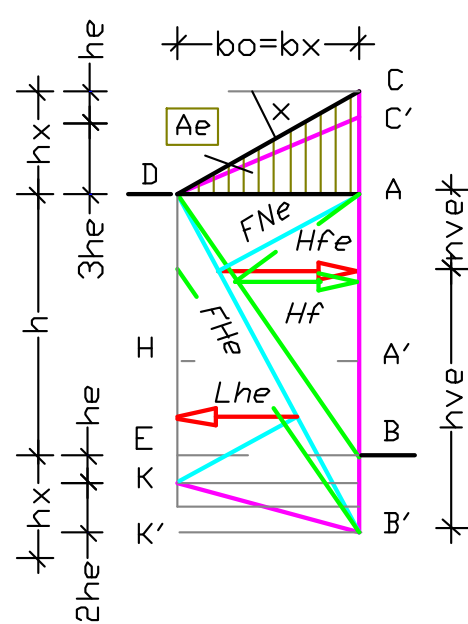


Fig. 89: Earth block with falling terrain surface, and force distribution within the wedge area (D-A-B').

4.3.4 Determining forces and angles from Test 5

To demonstrate that soils sliding from a standing to a lying earth wedge are subjected neither to a flow condition nor to the Mohr-Coulomb failure criterion, tests were conducted in Section 2.8, page 50ff.

Test 5 (Fig. 32, page 51) showed that the resulting planes and angles in the slid down material can be calculated by means of the soil characteristics (Chapter 3), and the forces by means of Coulomb's classical earth pressure theory and his Fig. 7. Moreover, force determination complies with the specifications in Section 4.3.3, Fig. 83, page 117. Value $a' = 1,00$ dm is selected as calculation depth.

For Test 5, dry sand with density $ptg_1 = 1,638$ kg/dm³ and weight $E_1 = 22,0$ kg was filled into the left-hand chamber of the glass container, and its surface smoothed. After that, dry basalt grit with density $ptg_2 = 1,846$ kg/dm³ and weight $E_2 = 13,5$ kg was filled into the container.

First, the properties of the filling material were calculated, and then the locations of the planes as well as their angles and earth forces.

Properties of sand:

Volume V_1

$$V_1 = E_1 / ptg_1 = 22,0 / 1,638 = 13,43 \quad \text{dm}^3 \quad 4.126$$

Height $h_1 \rightarrow$ via the chamber's base area $Ak_1 = 7,08$ dm² (3.33).

$$h_1 = V_1 / Ak_1 = 13,43 / 7,08 = 1,90 \quad \text{dm} \quad 4.127$$

Solids volume

$$Vf_1 = Vp \cdot ptg_1 / ptg_{90} = 1,0 \cdot 1,638 / 3,0 = 0,546 \quad \text{dm}^3 \quad 4.128$$

Pore volume

$$Vl_1 = Vp - Vf_1 = 1,0 - 0,546 = 0,454 \quad \text{dm}^3 \quad 4.129$$

Inclination angle β_1

$$\tan \beta_1 = Vf_1 / Vl_1 = 0,546 / 0,454 = 1,203 \quad 4.130$$

$$\beta_1 = 50,3^\circ \quad [-] \quad 4.131$$

Shear angle s_1

$$\tan s_1 = \tan \beta / 2 = 1,203 / 2 = 0,601 \quad 4.132$$

$$s_1 = 31,0^\circ \quad [-] \quad 4.133$$

Properties of basalt grit:

Volume V_2

$$V_2 = E_2 / ptg_2 = 13,5 / 1,846 = 7,31 \quad \text{dm}^3 \quad 4.134$$

Height h_2

$$h_2 = V_2 / Ak_1 = 7,31 / 7,08 = 1,03 \quad \text{dm} \quad 4.135$$

Solids volume

$$Vf_2 = Vp \cdot ptg_2 / ptg_{90} = 1,0 \cdot 1,846 / 3,0 = 0,615 \quad \text{dm}^3 \quad 4.136$$

Pore volume

$$Vl_2 = Vp - Vf_2 = 1,0 - 0,615 = 0,385 \quad \text{dm}^3 \quad 4.137$$

Inclination angle β_2

$$\tan \beta_2 = Vf_1 / Vl_1 = 0,615 / 0,385 = 1,597 \quad 4.138$$

$$\beta_2 = 58,0^\circ \quad [-] \quad 4.139$$

Shear angle s_2

$$\tan s_2 = \tan \beta_2 / 2 = 1,597 / 2 = 0,799 \quad 4.140$$

$$s_2 = 38,6^\circ \quad [-] \quad 4.141$$

Due to the different densities ptg_1 and ptg_2 , the basalt grit represents a load on the sand. For all further calculations, it is recommended to convert the layer height h_2 of the basalt grit into layer height h_3 by means of factor ptg_2/ptg_1 .

Height h_3

$$h_3 = h_2 \cdot ptg_2 / ptg_1 = 1,03 \cdot 1,846 / 1,638 = 1,16 \quad \text{dm} \quad 4.142$$

Following the adaptation of densities, weight force Ge , downhill force Fhe , and earth pressure force Hfe against the wall can be calculated by means of height $hl' = h_1 + h_3$, inclination angle β_1 , and wedge volume $Voe = Aoe \cdot a'$.

Calculation height $hl \rightarrow$ filling height $h = h_1 + h_2 = 2,93 \text{ dm}$

$$hl = h_1 + h_3 = 1,90 + 1,16 = 3,06 \quad \text{dm} \quad 4.143$$

Wedge width be

$$be = hl / \tan \beta_1 = 3,06 / 1,203 = 2,54 \quad \text{dm} \quad 4.144$$

Load wedge $Voe \rightarrow$ referred to depth $a' = 1,00 \text{ dm}$

$$Voe = hl \cdot be \cdot a' / 2 = 3,06 \cdot 2,54 \cdot 1,00 / 2 = 3,89 \quad \text{dm}^3 \quad 4.145$$

Weight force Ge

$$Ge = Voe \cdot ptg_1 \cdot g = 3,89 \cdot 1,638 \cdot 9,807 = 62,5 \quad \text{N} \quad 4.146$$

Downhill force $FHe \rightarrow$ with $\beta_1 = 50,3^\circ$

$$FHe = Ge \cdot \sin \beta_1 = 62,5 \cdot 0,769 = 48,1 \quad \text{N} \quad 4.147$$

Earth pressure force Hfe

$$Hfe = Ge \cdot \sin \beta_1 \cdot \cos \beta_1 = 62,5 \cdot 0,769 \cdot 0,639 =$$

$$Hfe = 30,7 \quad \text{N} \quad 4.148$$

Force meter hfe

$$hfe = hl \cdot \sin \beta_1 \cdot \cos \beta_1 = 3,06 \cdot 0,491 = 1,50 \quad \text{dm} \quad 4.149$$

Thrust height hve

$$hve = hl \cdot \sin^2 \beta_1 = 3,06 \cdot 0,592 = 1,81 \quad \text{dm} \quad 4.150$$

Regarding thrust height $hve = 1,81 \text{ dm}$ (4.150) of the earth pressure force Hfe against the vertical wall, it must be noted that this height is also subjected to the

adaptation of densities, i.e. it would be real to reduce height h_{ve} according to the ratio of heights h_l to $h = 3,08 / 2,93$. Fig. 90 shows the position of earth pressure force H_{fe} calculated by means of height h_l .

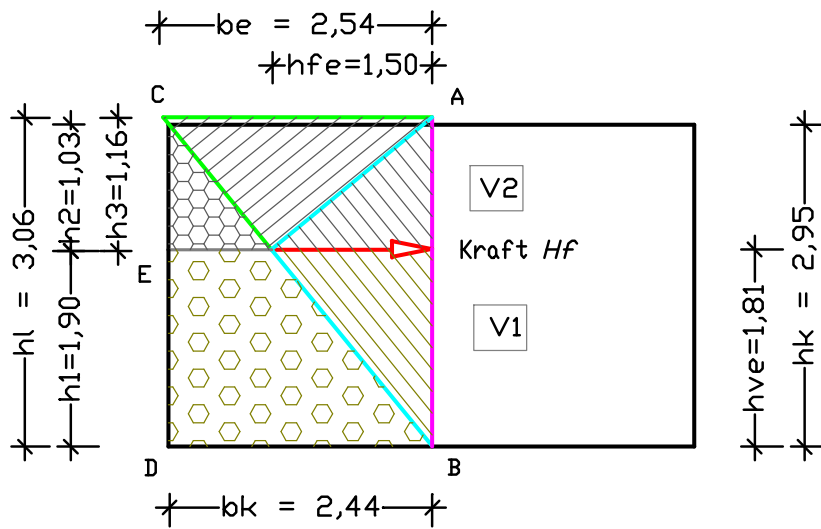


Fig. 90 Wedge area Ao and earth pressure force H_f acting against the glass pane (A–B) at height h_v .

When the glass pane has been removed, and the filling material has slid down, the standing earth wedge (Fig. 90) changes into a lying earth wedge (Fig. 91). Its planes, angles, and earth forces are determined below. Due to the height adaptation with factor ptg_2/ptg_1 , the earth body can be seen as a coherent mass, so that height $h_l = 3,06$ dm (4.143), inclination angle $\beta_l = 50,3^\circ$, and shear angle $s_l = 31,0^\circ$ (4.133) of the sand can be used. In order to determine the earth load to the left of reference axis (A–B), and the forces according to Figs. 86 and 87, plane (H–A') must be inserted in height $h_l/2 = 1,53$ dm (see Fig. 91).

An earth wedge with height h_x and width b_x rests on plane (H–A'), and is supported by the earth wedge with height $h_l/2$ and width b_x below the plane. As the load is dispersed via active and reactive forces, wedge height h_x must be adapted to the active load proportion by means of height $h_x/4 = h_e$. Height h_e describes the distance between Points J and H. Height h_x is calculated from width b_x and shear angle $s_l = 31,0^\circ$ (4.133).

The inclination angle under load is applied at Point J and leads to the intersection of reference axis and container bottom. In order to include the wedge-shaped load in the earth wedge below plane (H–A'), the inclination angle under load must be moved vertically and parallel at Point H, so that Point B is created below the basal plane on the reference axis.

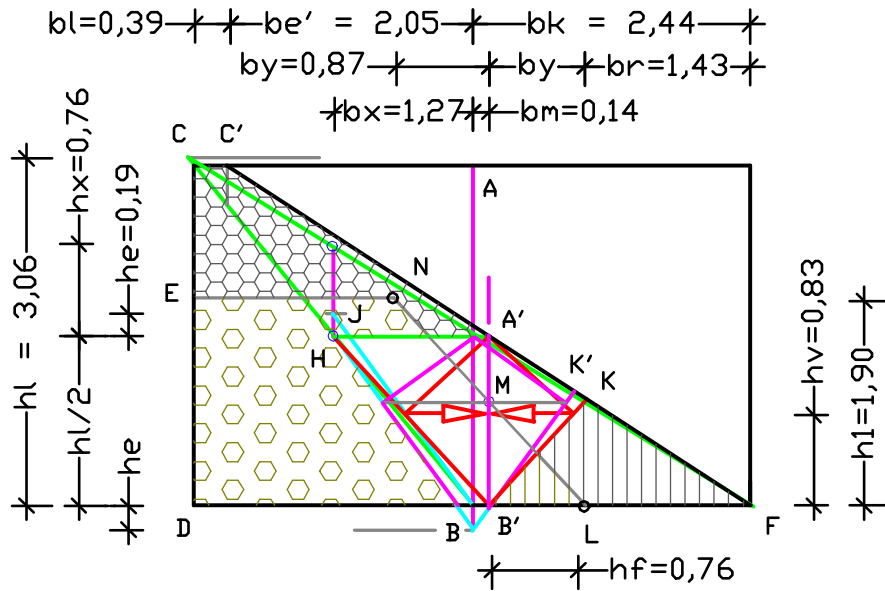


Fig. 91 Wedge areas (H–A–B) and (H–A'–B'), with earth pressure force H_f (red) acting against axis (A'–B') at thrust height h_v .

Because force dispersal in the inclination angle under load is prevented by the glass bottom, the undispersed vertical force is converted into a horizontal force. When the separating glass pane is removed, this horizontal force becomes active, and shifts the reference axis (A–B) by the amount of width bm into the position of reference axis (A'–B'). Consequently, the inclination angle under load (red) moves to plane (H–B'). The tangent of angle $\beta_{e'}$ can now be calculated by dividing $hl/2$ by width $bx' = bx + bm$. Due to the shifted reference axis (A–B) into plane (A'–B'), the wedge areas (H–A–B) and (H–A'–B') and thereby two load cases are created. Wedge area (H–A'–B) is used to determine the positions, angles, and forces of the individual planes (see Fig. 91). Because sand and basalt grit behave differently as they slide down, slight deviations between the measured and calculated values can occur.

The following values are calculated:

Wedge width $bx \rightarrow$ with angle $\beta_l = 50,3^\circ$ (4.131) and height $hl' = 3,06$ dm.

$$bx = hl / (2 \cdot \tan \beta_l) = 3,06 / (2 \cdot 1,203) = 1,27 \quad \text{dm} \quad 4.151$$

Height hx

$$hx = bx \cdot \tan s_l = 1,27 \cdot 0,602 = 0,76 \quad \text{dm} \quad 4.152$$

Height he

$$he = hx / 4 = 0,76 / 4 = 0,19 \quad \text{dm} \quad 4.153$$

Inclination angle β_{e_l}

$$\tan \beta_{e_l} = (hl/2 + he) / bx = (3,06/2 + 0,19) / 1,27 = 1,354 \quad 4.154$$

$$\beta_{e_l} = 53,6^\circ \quad [-] \quad 4.155$$

Shear angle se_l

$$\tan se_l = \tan \beta_e / 2 = 1,354 / 2 = 0,677 \quad 4.156$$

$$se_l = 34,1^\circ \quad [-] \quad 4.157$$

Shift width bm

$$bm = he / \tan \beta_e = 0,19 / 1,354 = 0,14 \quad \text{dm} \quad 4.158$$

Inclination angle β_e'

$$\tan \beta_e' = hl/2 \cdot (bx + bm) = 1,53 / (1,27 + 0,14) = 1,085 \quad 4.159$$

$$\beta_e' = 47,3^\circ \quad [-] \quad 4.160$$

Shear angle se' of the basalt grit can be determined from height $hl/2$ and width $be = 2,52$ dm (4.144) minus width $bm = 0,14$ dm.

Shear angle se'

$$\tan se' = hl/2 \cdot (be - bm) = 1,53 / (2,54 - 0,14) = 0,638 \quad 4.161$$

$$se' = 32,5^\circ \quad [-] \quad 4.162$$

The shear plane of the basalt grit intersects the earth body at the real height $h = h_1 + h_2 = 1,90 + 1,03 = 2,93$, where widths be' and bl are created, as well as widths by , br , and br' below at the basal plane.

Width be'

$$be' = [(h_1 + h_2) / \tan se'] - be =$$

$$be' = (2,93 / 0,638) - 2,54 = 2,05 \quad \text{dm} \quad 4.163$$

Width bl

$$bl = bk_1 - be' = 2,44 - 2,05 = 0,39 \quad \text{dm} \quad 4.164$$

Width by

$$by = h_1 / (2 \cdot \tan \beta_e') = 1,90 / (2 \cdot 1,085) = 0,87 \quad \text{dm} \quad 4.165$$

Width br'

$$br' = be - by - bm = 2,54 - 0,87 - 0,14 = 1,53 \quad \text{dm} \quad 4.166$$

Width br

$$br = bk_1 - by - bm = 2,44 - 0,87 - 0,14 = 1,43 \quad \text{dm} \quad 4.167$$

Force determination

Volume $Vou \rightarrow$ for determining the force against reference axis (A–B)

$$Vou = (hl/2 + he) \cdot bx \cdot a' / 2 =$$

$$Vou = (1,53 + 0,19) \cdot 1,27 \cdot 1,00 / 2 = 1,09 \quad \text{dm}^3 \quad 4.168$$

To determine the force acting against the reference axis (A'–B'), volume Vou' must first be determined by means of inclination angle β_e' , height $hl/2$, and width $bx' = bx + bm$.

Volume $Vou' \rightarrow$ for determining the force against reference axis (A'–B')

$$Vou' = (hl/2) \cdot (bx + bm) \cdot a' / 2 =$$

$$Vou' = 1,53 \cdot (1,27 + 0,14) \cdot 1,00 / 2 = 1,08 \quad \text{dm}^3 \quad 4.169$$

Weight force $Ge \rightarrow$ with $Voe' = 1,08 \text{ dm}^3$ (4.168)

$$Ge = Voe' \cdot \rho_{tg1} \cdot g = 1,08 \cdot 1,638 \cdot 9,807 = 17,3 \quad \text{N} \quad 4.170$$

Downhill force $FHe \rightarrow$ with $\beta e' = 47,3^\circ$ (4.160)

$$FH = Ge \cdot \sin \beta e' = 17,3 \cdot 0,737 = 12,7 \quad \text{N} \quad 4.171$$

Earth pressure force Hf

$$Hf = Ge \cdot \sin \beta e' \cdot \cos \beta e' = 17,3 \cdot 0,737 \cdot 0,678 =$$

$$Hf = 8,6 \quad \text{N} \quad 4.172$$

Force meter hf

$$hf = hl \cdot \sin \beta e' \cdot \cos \beta e' / 2 = 1,53 \cdot 0,500 = 0,76 \quad \text{dm} \quad 4.173$$

Thrust height hv

$$hv = hl \cdot \sin^2 \beta e' / 2 = 1,53 \cdot 0,540 = 0,83 \quad \text{dm} \quad 4.174$$

Fig. 91 also shows the horizontal force Hf' that is created by the earth wedge in the right-hand chamber against reference axis A–B, but this force is not used for further calculations.

The following table shows the heights, widths, and angles measured after removing the glass pane opposite the calculated values.

Measured values	Calculated values
Height $h_1 = 1,89 \text{ dm}$	Height $h_1 = 1,90 \text{ dm}$ (4.127)
Height $h_2 = 1,05 \text{ dm}$	Height $h_2 = 1,03 \text{ dm}$ (4.135)
Height $h = 2,94 \text{ dm}$	Height $h = 2,93 \text{ dm}$
Width $bk_1 = 2,44 \text{ dm}$	Width $bk_1 = 2,44 \text{ dm}$
Width $be' = 2,02 \text{ dm}$	Width $be' = 2,05 \text{ dm}$ (4.163)
Width $bl = 0,42 \text{ dm}$	Width $bl = 0,39 \text{ dm}$ (4.164)
Width $byl = 0,74 \text{ dm}$	Width $bm = 0,14 \text{ dm}$ (4.158)
Width $byr = 0,98 \text{ dm}$	Width $by = 0,87 \text{ dm}$ (4.165)
Width $br = 1,46 \text{ dm}$	Width $br = 1,43 \text{ dm}$ (4.167)
Incl. angle $\beta e' = 47,7^\circ$	Incl. angle $\beta e' = 47,3^\circ$ (4.160)
Shear angle $se' = 33,0^\circ$	Shear angle $se' = 32,5^\circ$ (4.162)

Result: It can be shown that after the filling material has slid down, the positions of their planes and angles can be calculated by means of their volumes and weights. Moreover, the force values and their assignments confirm that they can be determined in the standing earth wedge (Fig. 90) and also in the lying earth wedge (Fig. 91) using Coulomb's classical earth pressure theory (Fig. 7, page 19). The author cannot imagine how the Mohr-Coulomb failure criterion can be used to calculate the results shown in the table (see calculation example and Figs. 13 and 14, page 36).

4.3.5. Conclusions for Section 4.3.

The Test Series 9 showed that earth masses resting on a natural inclined plane create a steeper internal friction angle, thereby promoting the sliding of earth masses down a slope. Determination of angle β_e under load depends on angle x of the inclined surface or the load height hx , which is located above the earth block. In general, height h or width bo as well as angle β of an earth block are specified or are determined by local conditions. In the side view of an earth block, the natural inclined plane is represented by a diagonal. To obtain the tangent of the inclination angle under load, a partial load height hx must be added to block height h , and divided by block width bo . The partial height hx to be applied depends on the direction of the inclined surface (see Figs. 84 to 89).

Changing the angles does not affect soil density, but creates new force fields for force dispersal in the ground. With earth masses resting on a rock layer, it must be remembered that undispersed vertical forces can be converted into horizontal forces. Moreover, Tests 9.2 and 9.3 show that according to the New Earth Pressure Theory, a landslide can be calculated in advance.

Regarding the changed angles and forces due to imposed loads, Tests 4 and 5 show that the sliding of filling materials can be calculated by means of their volumes, weights, and forces in accordance with Coulomb's earth pressure theory (see Fig. 9, page 23). Neither the planes and angles shown in Figs. 90 and 91, nor the arrangement and values of the forces exhibit any similarity with Pictures I06.10 to I06.70 [1: page I14ff.].

The results of Test 4 and 5 prove that natural soil behaviour cannot be subordinated to any flow condition – whichever kind. Consequently, only Coulomb's classical earth theory can be used to determine earth pressures.

4.4 Forces in soils with inclined surface under water

In the previous tests, dry sand was used as soil to demonstrate the changes of angles and force areas. In order to illustrate the changes due to the load in layers of different soil types and inclined surfaces, an example was selected, in which wet soil under water is covered with dry soil above water. No provision was made for an intermediate layer, in which the dry soil can adapt to the wet soil.

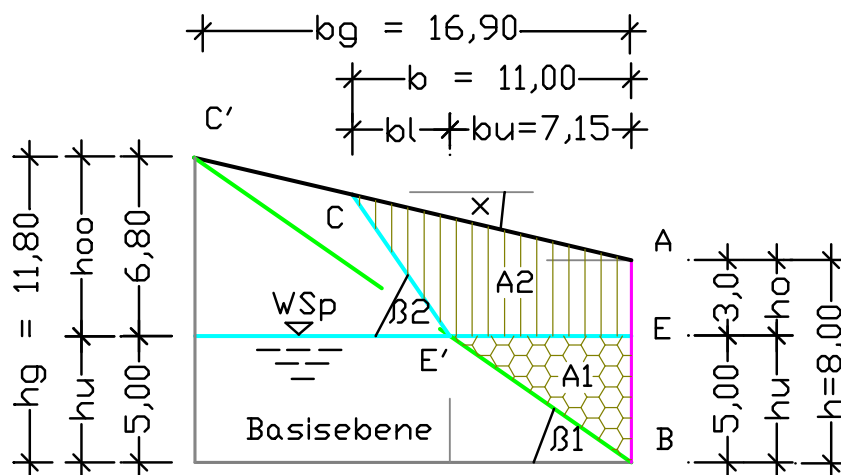


Fig. 92: Basic values to determine the 'force field under load' with layers of different soil types.

The wet soil below the groundwater level (WSp) forms the inclination angle $\beta_1 = \beta_{nw} = 35^\circ$. Its wedge area, described as $A1$, is limited by the inclined plane and height $h_u = 5,00$ m. The dry soil resting above it forms the inclination angle $\beta_2 = \beta_t = 55^\circ$, with height $h_o = 3,00$ m at the perpendicular reference axis. For this soil layer, with area $A2$, the surface is to slope upwards with angle $x = 12,8^\circ$. The supplementary dimensions are shown in Fig. 92.

To be calculated are the force field under load, earth pressure force H_{fe} against the reference axis, and all properties required to determine the selected soil type. In the previous section, determination of the force field under load was examined for only one soil type. To solve the new task, it is advisable to match the properties of the upper soil layer to those of the lower layer, and then follow the calculation sequence in Section 4.3. To match the soil properties, the parameters of both soil types are determined first.

4.4.1 Properties of wet soil under water

Inclination angle $\beta_{nw} = 35^\circ$ is specified. By means of this angle, the natural shear angle snw , volumes V_f and V_l , and density p_{nwg} can be calculated (see Section 3.2. page 67). Because the volume V_{ln} occupied by water in wet soil corresponds to total pore volume V_l , and the solids volume equals $V_f = V_p - V_l$, the tangent $\tan \beta_{nw}$ of inclination angle $\beta_{nw} = 35,0^\circ$ can be used to calculate the volumes below. The approach using the solids volumes under water with $2/3 \cdot V_f$ is derived from the reduction due to uplift (see Section 3.2.1. page 68).

$$\tan \beta_{nw} = 2/3 \cdot V_f / (V_l + V_{fn} - V_w) = 2/3 \cdot V_f / V_l \cdot 5/6$$

Calculation:

Volume $V_f \rightarrow$ determined using volume $V_p = 1,00 \text{ m}^3$

$$\tan \beta_{nw} \cdot 5 \cdot 3 \cdot (1,0 - V_f) = 12 \cdot V_f$$

$$0,700 \cdot 15 \cdot (1,0 - V_f) = 12 \cdot V_f \rightarrow 10,5 - 10,5 V_f = 12,0 V_f$$

$$V_f = 10,5 / 22,5 = 0,467 \quad \text{m}^3 \quad 4.175$$

Volume V_l

$$V_l = V_p - V_f = 1,00 - 0,467 = 0,533 \quad \text{m}^3 \quad 4.176$$

Solids volume $V_{fw} \rightarrow$ under uplift

$$V_{fw} = 2 \cdot V_f / 3 = 2 \cdot 0,467 / 3 = 0,311 \quad \text{m}^3 \quad 4.177$$

Wet density $p_{nwg} \rightarrow$ under water

$$p_{nwg} = (V_{fw} \cdot p_{tg90} + V_l \cdot p_w) / V_p$$

$$p_{nwg} = (0,311 \cdot 3,0 + 0,533 \cdot 1,0) / 1,0 = 1,466 \quad \text{t/m}^3 \quad 4.178$$

Results:

Angle $\beta_{nw} = 35,0^\circ$, $\tan = 0,700$	Shear angle $s_{nw} = 19,3^\circ$
Solids volume $V_f = 0,467 \text{ m}^3$ (4.175)	Pore volume $V_l = 0,533 \text{ m}^3$ (4.176)
Fictitious $V_{fw} = 0,311 \text{ m}^3$ (4.177)	Density $p_{nwg} = 1,466 \text{ t/m}^3$ (4.178)

4.4.2 Properties of dry soil above water

The properties of the soil with inclination angle $\beta_t = 55^\circ$ have already been calculated (see Section 3.1.1, page 57).

The following values are transferred from Section 3.1.1:

Angle $\beta_t = 55,0^\circ$ / $\tan \beta_t = 1,428$	Density $p_{tg} = 1,764 \text{ t/m}^3$ (3.9)
Solids volume $V_{f2} = 0,588 \text{ m}^3$ (3.1)	Pore volume $V_{l2} = 0,412 \text{ m}^3$ (3.2)

Adaptation of area A_2 to the properties of wet soil

For further calculations, the dry soil (layer 2) must be adapted to the wet soil (layer 1) by means of area increase. The new area can be determined by means of heights h_o and h_o' of layer 2, multiplied with the proportionality factor V_{f2}/V_{f1} .

Calculation:

Width $bg \rightarrow$ by means of angles $\beta_{nw} = 35^\circ$ and $x = 12,8^\circ$ (specified)

$$bg = h / (\tan \beta_{nw} - \tan x)$$

$$bg = 8,00 / (0,700 - 0,227) = 16,90 \quad \text{m} \quad 4.179$$

Height h_o'

$$h_o' = h_o \cdot V_{f2}/V_{f1} = 3,00 \cdot 0,588/0,467 = 3,80 \quad \text{m} \quad 4.180$$

Shear angle se

$$\tan se = (\tan \beta_e) / 2 = 0,771 = 0,385 \quad 4.191$$

$$se = 21,1^\circ \quad [-] \quad 4.192$$

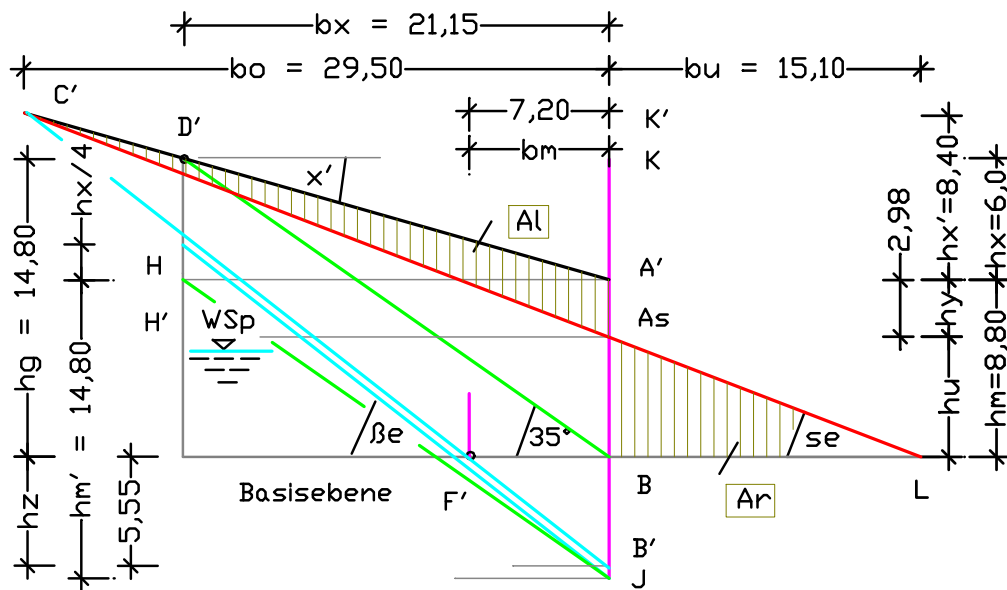


Fig. 94: Natural shear plane (D'-L), shear plane (E-L') under load, and area (E-D'-A'-A*) of the soil body forming the load.

The position of shear plane under load is determined by height hy , whereby the latter can be calculated by means of shear angle se , angle of slope $x' = 15,9^\circ$ (4.184), and height $hm = 8,80$ m (4.188).

Height hy

$$hy^2 / [2 \cdot (\tan se - \tan x')] = (hm - hy)^2 / (2 \cdot \tan se)$$

$$hy^2 / [2 \cdot (0,385 - 0,284)] = (8,80 - hy)^2 / (2 \cdot 0,385)$$

$$hy^2 = (8,80 - hy)^2 \cdot 0,202 / 0,770 \quad hy = \sqrt{0,262} \cdot (8,80 - hy)$$

$$hy + 0,512 hy - 4,51 = 0 \quad hy = 4,51 / 1,512 = 2,98 \text{ m} \quad 4.193$$

Height hu'

$$hu' = hm - hy = 8,80 - 2,98 = 5,82 \text{ m} \quad 4.194$$

Width bo

$$bo = hy / (\tan se - \tan x') =$$

$$bo = 2,98 / (0,385 - 0,284) = 29,50 \text{ m} \quad 4.195$$

Width bu

$$bu = hu' / \tan se = 5,82 / 0,385 = 15,12 \text{ m} \quad 4.196$$

Height hx'

$$hx' = bo \cdot \tan x' = 29,50 \cdot 0,284 = 8,38 \text{ m} \quad 4.197$$

Height hg'

$$hg' = bo \cdot \tan \beta_e = 29,50 \cdot 0,771 = 22,74 \text{ m} \quad 4.198$$

Height hz

$$hz = hg' - hx' - hm = 22,74 - 8,38 - 8,80 = 5,56 \quad \text{m} \quad 4.199$$

Width bm

$$bm = hz / \tan \beta_e = 5,56 / 0,771 = 7,21 \quad \text{m} \quad 4.200$$

Area Al

$$Al = (bo \cdot hy) / 2 = (29,5 \cdot 2,98) / 2 = 43,96 \quad \text{m}^2 \quad 4.201$$

Area Ar

$$Ar = (bu \cdot hu') / 2 = (15,12 \cdot 5,82) / 2 = 44,0 \quad \text{m}^2 \quad 4.202$$

Area $Al = 43,96 \text{ m}^2$ (4.201) defines the earth mass resting on the shear plane under load. If the soil loses its hold at the reference axis, it will slide down the shear plane with angle $se = 21,1^\circ$ (4.192) and form a soil body with area $Ar = 44,0 \text{ m}^2$ (4.202) to the right of the axis.

4.4.3 Determination of force against a fictitious perpendicular wall

Calculation depth $a = 1,00 \text{ m}$ is specified for calculating the weight force. Determination of the partial forces from the weight force is not necessary, because they can be supplemented in accordance with Versions A and B in Section 4.3.2. (see Fig. 95 below).

To be calculated are:

Width bou

$$bou = (hm + hz) / \tan \beta_e = (8,80 + 5,55) / 0,771 = 18,60 \quad \text{m} \quad 4.203$$

Area Aou

$$Aou = bou \cdot (hm + hz) / 2 = 18,60 \cdot 14,35 / 2 = 133,5 \quad \text{m}^2 \quad 4.204$$

Volume $Vou \rightarrow$ with calculation depth $a = 1,00 \text{ m}$

$$Vou = Aou \cdot a = 133,5 \cdot 1,00 = 133,5 \quad \text{m}^3 \quad 4.205$$

Weight $Ge' \rightarrow$ with density $pnwg = 1,466 \text{ t/m}^3$ (4.178)

$$Ge' = Vou \cdot pnwg \cdot g = 133,5 \cdot 1,466 \cdot g = 1919 \quad \text{kN} \quad 4.206$$

Force index gin

$$gin = bou \cdot a \cdot ptg \cdot g / 2$$

$$gin = 18,60 \cdot 1,00 \cdot 1,466 \cdot 9,807 / 2 = 133,7 \quad \text{kN/dm}^2 \quad 4.207$$

The calculated dimensions are shown to scale in Fig. 95.

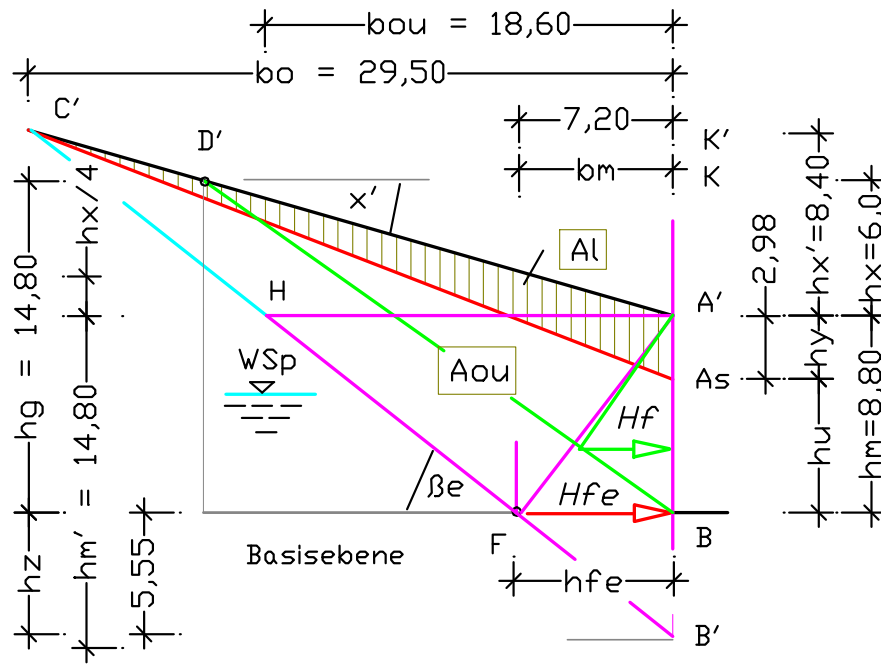


Fig. 95: Area A_{ou} (H-A'-B'), which is decisive for force determination, if the soil is held back by a wall (A'-B').

Conclusions for Section 4.4:

For determining the inclination and shear angles under load with layers of different soils, the volumes of the upper layers must be adapted to the volume of the lowest layer by means of the soil parameters. This adaptation creates a fictitious soil body, which can be returned to the lowest layer after determining the force by means of the soil parameters. In the case of a soil body with inclined surface, the terrain plane's elevation angle changes from x to x' (see Fig. 93).

Inclination angle β_e under load can be calculated, if a horizontal plane (H-A') with its starting point A' on the inclined surface is first located on the reference axis, and an earth block is placed below this plane. Block height hm' can be determined by means of width bx and the natural inclination angle of the lowest soil layer. In this case, i.e. with an upward sloping terrain plane, height $hx/4$ must be placed on block height hm' at a distance of width bx from the reference axis, thereby forming height $hm' + hx/4$. Height hx represents the distance between Points K and A' on the reference axis. The tangent of inclination angle β_e under load results from $\tan \beta_e = (hm' + hx/4) / bx$. All the other soil body dimensions can be calculated by means of this angle.

4.5 Soil sliding on inclined/level rock layer, Test 10

Test 10 was designed to investigate the behaviour of soils resting on an inclined basal plane (rock layer) after they lose their hold on the imaginary wall (reference axis) and slide down.

It has already been shown in Section 2.4.1. that vertical forces applied to a soil body are converted into horizontal forces, if the soil body is resting on a firm base (see Figs. 23 to 25, page 46). Moreover, Tests 9.2 and 9.3 show that additional horizontal forces can be created in a soil body, if the adjacent soil body with inclined surface is divided into an earth block and a superimposed earth wedge (also see Section 4.3.3).

For the test, a dry loam/sand mix was prepared in a container, and then filled onto the wooden ramp in the left-hand chamber of the glass container up to filling height $h = 2,26$ dm, and the surface smoothed. The wooden ramp is intended to represent an inclined rock layer. Ramp height $h_{uu} = 1,00$ dm was measured at the left-hand chamber wall, and height $h_s = 0,12$ dm was measured at the separating glass pane. The base area of ramp $A_{k_l} = 7,08$ dm² (3.33) was calculated by means of width $b_{k_l} = 2,44$ dm and depth $a = 2,90$ dm (see Section 3.1.1, page 57ff).



Fig. 96: Glass container with built-in wooden ramp, whose surface represents an inclined rock layer.

A mixture of sand with volume $V_a = 10,00$ dm³ and density $ptg_a = 1,645$ kg/dm³, and loam with volume $V_b = 2,00$ dm³ and density $ptg_b = 1,175$ kg/dm³ was used for the filling material. All other properties of the mixture were calculated by means of total volume $V_I = V_a + V_b = 12,00$ dm³, and the densities of sand and loam.

Calculation of soil properties

The following values are used for calculation:

Sand	Loam
Volume $V_a = 10,0 \text{ dm}^3$	Volume $V_b = 2,00 \text{ dm}^3$
Density $ptg_a = 1,645 \text{ kg/dm}^3$	Density $ptg_b = 1,175 \text{ kg/dm}^3$
Area $Ak_l = 7,08 \text{ dm}^2$ (3.33)	Filling height $h = 2,26 \text{ dm}$
Mean ramp height $hm = (1,00 + 0,12) / 2 = 0,56 \text{ dm}$	

Calculation:

Filling volume V

$$V = Ak_l \cdot (h - hm) = 7,08 \cdot (2,26 - 0,56) = 12,00 \quad \text{dm}^3 \quad 4.208$$

Solids volume Vf_a of the sand

$$Vf_a = Vf_{90} \cdot ptg_a / p_{90} = 1,0 \cdot 1,645 / 3,0 = 0,548 \quad \text{dm}^3 \quad 4.209$$

Pore volume Vl_a of the sand

$$Vl_a = Vp - Vf_a = 1,000 - 0,548 = 0,452 \quad \text{dm}^3 \quad 4.210$$

Solids volume Vf_b of the loam

$$Vf_b = Vf_{90} \cdot ptg_b / p_{90} = 1,0 \cdot 1,175 / 3,0 = 0,392 \quad \text{dm}^3 \quad 4.211$$

Pore volume Vl_b of the loam

$$Vl_b = Vp - Vf_b = 1,000 - 0,392 = 0,608 \quad \text{dm}^3 \quad 4.212$$

Solids volume Vf_l (mixture)

$$Vf_l = (V_a \cdot Vf_a + V_b \cdot Vf_b) / (V_a + V_b)$$

$$Vf_l = (10,0 \cdot 0,548 + 2,0 \cdot 0,392) / 12,0 = 0,522 \quad \text{dm}^3 \quad 4.213$$

Pore volume Vl_l (mixture)

$$Vl_l = Vp - Vf_l = 1,000 - 0,522 = 0,478 \quad \text{dm}^3 \quad 4.214$$

Dry density ptg_l (mixture)

$$ptg_l = Vf_l \cdot p_{90} / Vf_{90} = 0,522 \cdot 3,00 / 1 = 1,566 \quad \text{kg/dm}^3 \quad 4.215$$

Inclination angle βt (mixture)

$$\tan \beta t = Vf_l / Vl_l = 0,522 / 0,478 = 1,092 \quad 4.216$$

$$\beta t = 47,5^\circ \quad [-] \quad 4.217$$

Shear angle st

$$\tan st = (\tan \beta t) / 2 = 1,092 / 2 = 0,546 \quad 4.218$$

$$st = 28,6^\circ \quad [-] \quad 4.219$$

Results:

The dry mixture has the following properties:

Sand/loam mixture	
Solids volume $Vf_l = 0,522 \text{ dm}^3$ (4.213)	Volume $V = 12,0 \text{ dm}^3$
Pore volume $Vl_l = 0,478 \text{ dm}^3$ (4.214)	Inclination angle $\beta t = 47,5^\circ$ (4.217)
Density $ptg_l = 1,566 \text{ kg/dm}^3$ (4.215)	Shear angle $st = 28,6^\circ$ (4.219)

Calculation of soil body

Volume $V = 12,00 \text{ dm}^3$ (4.159), base area $Ak_l = 7,08 \text{ dm}^2$ (3.33), and filling height $h = 2,26 \text{ dm}$ are already known for the further calculations. Different shear planes are formed to the left and right of the reference axis after the glass pane is pulled and the soil has slipped down.

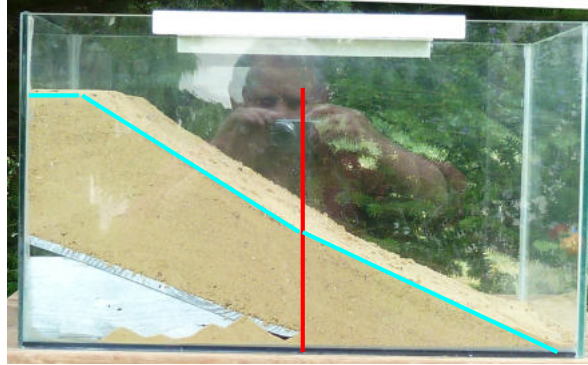


Fig. 97: After the mixture has slipped down, a slope with two different shear angles is created.

The upper shear plane started at filling height $h = 2,26 \text{ dm}$, and went down to the reference axis across width $bl = 0,49 \text{ dm}$, where it reached height $hmu = 1,06 \text{ dm}$. The right-hand shear plane started at height hmu , and ended at the glass bottom at a distance of $br = 0,22 \text{ dm}$ from the right-hand container wall. Because all previous tests resulted in straight shear planes, the reason for this deviation will be examined. For this, the right-hand chamber floor will be raised fictively by the amount of ramp offset $hs = 0,12 \text{ dm}$, and the position of the natural shear plane calculated.

Dimensions of lying earth wedge and ramp:	
Volume $V = 12,0 \text{ dm}^3$	Area $Ak_l = 7,08 \text{ dm}^2$
Filling height $h = 2,26 \text{ dm}$	Depth $a = 2,90 \text{ dm}$
Height $h_{uu} = 1,00 \text{ dm}$	Width $bk_l = 2,44 \text{ dm}$
Height $h_s = 0,12 \text{ dm}$	Width $bl = 0,49 \text{ dm}$
Height $h_{mu} = 1,06 \text{ dm}$	Width $br = 0,22 \text{ dm}$

Calculation:

Area A

$$A = V/a = 12,0/2,90 = 4,14 \quad \text{dm}^2 \quad 4.220$$

Height hb

$$hb = h - h_s = 2,26 - 0,12 = 2,14 \quad \text{dm} \quad 4.221$$

Width $bo' \rightarrow$ with $\tan \beta t = 1,092$ (4.216)

$$bo' = hb / \tan \beta t = 2,14/1,092 = 1,96 \quad \text{dm} \quad 4.222$$

Width bl'

$$bl' = bk_l - bo' = 2,44 - 1,96 = 0,48 \quad \text{dm} \quad 4.223$$

Height $ho' = hmu' \rightarrow$ with $\tan st = 0,546$ (4.218)

$$ho' = bo' \cdot \tan st = 1,96 \cdot 0,546 = 1,07 \quad \text{dm} \quad 4.224$$

Width bu'

$$bu' = ho' / \tan s_l = 1,07 / 0,546 = 1,96 \quad \text{dm} \quad 4.225$$

Width brr

$$brr = bk_l - bu' = 2,44 - 1,96 = 0,48 \quad \text{dm} \quad 4.226$$

Area $Az \rightarrow$ of ramp, reduced by height $hs = 0,12$ dm

$$Az = (huu' - hs) \cdot bk_l / 2$$

$$Az = (1,00 - 0,12) \cdot 2,44 / 2 = 1,074 \quad \text{dm}^2 \quad 4.227$$

Area $AA' \rightarrow$ of soil body after the mixture has slipped down

$$AA' = hp \cdot bl' + (hp + hmu') \cdot bo' / 2 + hmu' \cdot bu' / 2 - Az$$

$$AA' = 2,14 \cdot 0,48 + (2,14 + 1,07) \cdot 1,96 / 2 + 1,07 \cdot 1,96 / 2 - Az$$

$$AA' = 1,027 + 3,146 + 1,049 - 1,074 = 4,15 \quad \text{dm}^2 \quad 4.228$$

Results:

The equality of surfaces $A = 4,14 \text{ dm}^2$ (4.220) and $AA' = 4,15 \text{ dm}^2$ (4.228) permits the conclusion that the wooden ramp fitted into the left-hand chamber of the glass container neither influences the sliding behaviour of the filling material nor the formation of a natural shear plane in the dry loam/sand mixture.

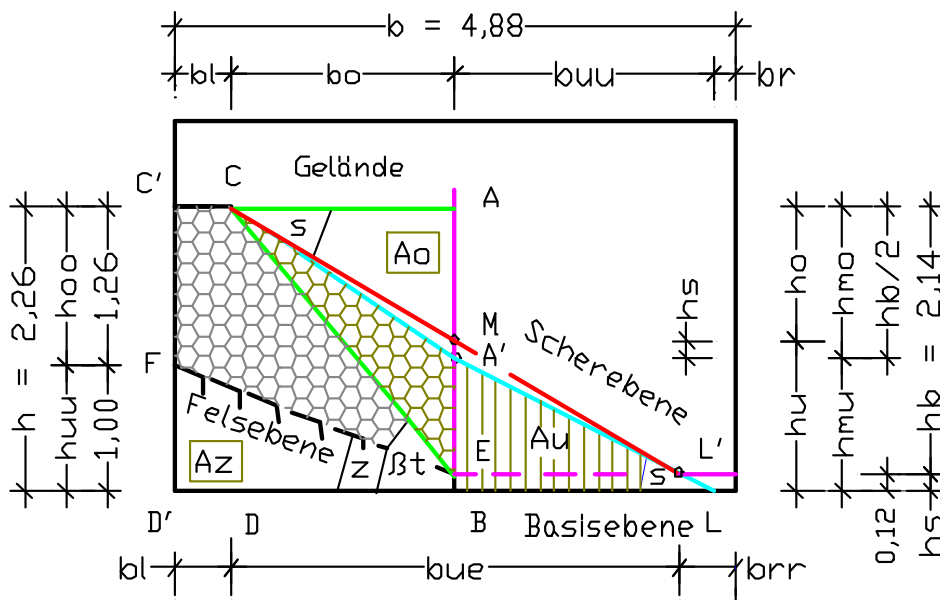


Fig. 98: Shown above the concave planes (cyan) is the shear plane of the mixture (red), which would have been formed without height offset hs .

The calculations show that the concave shear plane visible in Fig. 98 is causally related to the height offset hs between the wooden ramp and the glass

bottom of the right-hand chamber. Without this height offset, a linear shear plane (red) would have been formed (compare Figs. 96 and 97 with Fig. 98). Because no difference is seen in the movement of earth masses, whether they slide down a wooden ramp or an inclined rock layer, the findings of Test 10 can be applied for the movement of soils on an inclined rock layer. Also see the following calculation examples as well as Figs. 99 to 101.

4.6 Soil sliding on a rock layer with continuous incline

The previous tests showed that if an earth mass loses its hold on a reference axis, it will continue to move until its forces in the ground have been equalized. Additional examples will illustrate the subject of "Sliding behaviour of soils".

Example 1: Here, soil resting on an inclined plane will slide down onto a horizontal plane (B–L'), where it will stabilize.

Example 2: The soil resting on an inclined rock plane will start to slide down the incline, and then find a new hold.

Example 3: Investigates the behaviour of a loaded soil sliding down an inclined rock plane. For this, the dimensions determined in Section 4.5. will be used.

Example 1

For this example, the calculation used in the previous Section will be used, i.e. soil volume $V = 12,0 \text{ dm}^3$, area $A = 4,14 \text{ dm}^2$ (4.208), calculations height $hb = h - hs = 2,14 \text{ dm}$ (4.220), and shear angle $st = 28,6^\circ$ (4.219). Elevation angle z of the rock corresponds to the inclination of the wooden ramp.

Elevation angle z

$$\tan z = (huu - hs) / bk_l = (1,00 - 0,12) / 2,44 = 0,361 \quad 4.229$$

$$z = 19,8^\circ \quad [-] \quad 4.230$$

Possible loosening of the soil as it slides down is not taken into account. The soil body's position on the inclined basal plane will be calculated.

Diagonal $fs \rightarrow$ distance (B–E)

$$fs = hb \cdot \cos st / 2 = 0,878 \cdot 2,14/2 = 0,94 \quad \text{m} \quad 4.231$$

Length $fr \rightarrow$ of shear plane

$$fr = bu \cdot \cos st = 1,96 \cdot 0,878 = 1,72 \quad \text{m} \quad 4.232$$

Length $fl \rightarrow$ of shear plane

$$fl = hb / \sin st - fr = 2,14/0,479 - 1,72 = 2,75 \quad \text{m} \quad 4.233$$

Result of Example 1:

The calculated dimensions are shown in Fig. 99.

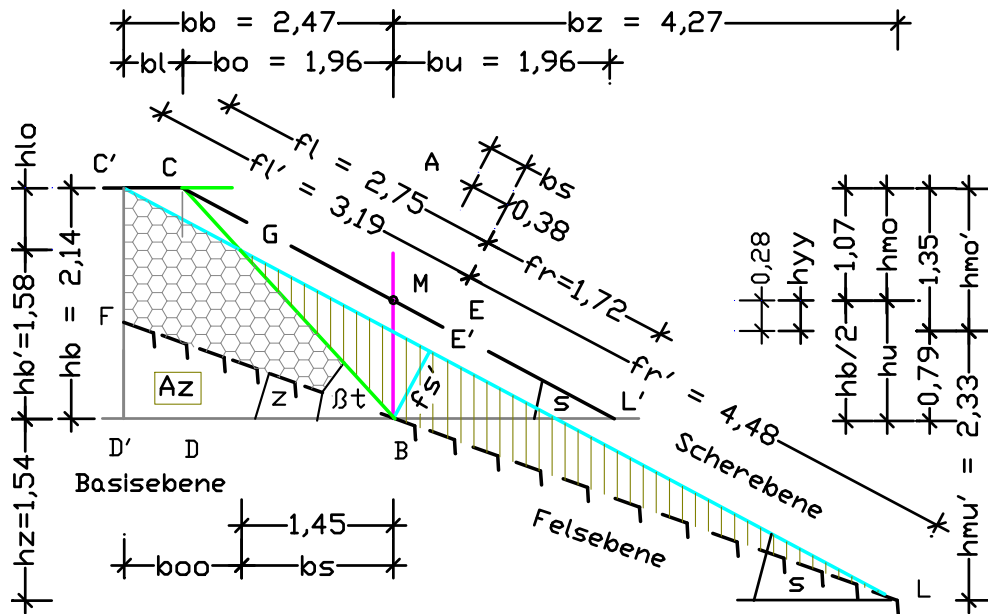


Fig. 99: Lowering of the shear plane due to the continuous inclined rock layer.

Example 2

The behaviour of the soil to the left of the reference axis is examined, which slides down an inclined rock layer instead of a horizontal plane. For this, the angle of the inclined rock layer is defined as $z = 13,0^\circ$. To be calculated are the lowering of the 'shear plane under load' by the amount hyy , and the soil's distribution after it has moved down on the inclined rock layer.

As shown in Fig. 99, larger amounts of soil than in Example 1 are moved, leading to the lowering of the natural shear plane by height hyy . Height hyy can be calculated by means of height $ho = hb / 2 = 1,07$ dm (4.221), shear angle $st = 28,6^\circ$ (4.219), and the angle of the rock slope $z = 19,8^\circ$ (4.230).

Height hyy

$$\begin{aligned} (ho + hyy)^2 / \tan st &= (hu - hyy)^2 / (\tan st - \tan z) \\ (1,07 + hyy)^2 / 0,546 &= (1,07 - hyy)^2 / (0,545 - 0,361) \\ (1,07 + hyy) &= (1,07 - hyy) \cdot \sqrt{0,546/0,185} \\ hyy &= 0,77 / 2,72 = 0,28 && \text{dm} \quad 4.234 \end{aligned}$$

Height hmo'

$$hmo' = hmo + hyy = 1,07 + 0,28 = 1,35 \quad \text{dm} \quad 4.235$$

Height hu'

$$hu' = hu - hyy = 1,07 - 0,28 = 0,79 \quad \text{dm} \quad 4.236$$

Width bb

$$bb = hmo' / \tan st = 1,35 / 0,546 = 2,47 \quad \text{dm} \quad 4.237$$

Width $bz \rightarrow$ with angle $z = 19,8^\circ$ (4.181)		
$bz = hu' / (\tan st - \tan z)$		
$bz = 0,79 / (0,546 - 0,361) = 4,27$	dm	4.238
Height $hz \rightarrow$ with angle $z = 19,8^\circ$ (4.181)		
$hz = bz \cdot \sin z = 4,27 \cdot 0,361 = 1,54$	dm	4.239
Height hmu'		
$hmu' = hu' + hz = 0,79 + 1,54 = 2,33$	dm	4.240
Height hb'		
$hb' = hu' / (\tan \beta t / \tan st) = 0,79 \cdot 2 = 1,58$	dm	4.241
Width bs		
$bs = hb' / \tan \beta t = 1,58 / 1,092 = 1,45$	dm	4.241
Area Aoo		
$Aoo = bb \cdot hmo' / 2 = 2,47 \cdot 1,35 / 2 = 1,67$	dm ²	4.243
Area Auu		
$Auu = bz \cdot hu' / 2 = 4,27 \cdot 0,79 / 2 = 1,68$	dm ²	4.244
Diagonal fs'		
$fs' = hu' \cdot \cos st = 0,79 \cdot 0,878 = 0,69$	dm	4.245
Width bs		
$bs = hu' \cdot \sin st = 0,79 \cdot 0,479 = 0,38$	dm	4.246
Length $fr' \rightarrow$ of shear plane under angle $st = 28,6^\circ$ (4.219)		
$fr' = bz / \cos st - bs = 4,27 / 0,878 - 0,38 = 4,48$	dm	4.247
Length $fl' \rightarrow$ of shear plane		
$fl' = bb / \cos st + bs = 2,47 / 0,878 + 0,38 = 3,19$	dm	4.248

Result of Example 2:

As before, the calculated dimensions have been entered in Fig. 99. The calculation reveals that the shear angle remains the same, regardless of whether the soil slides on a horizontal plane (Example 1) or on a continuous inclined rock layer (Example 2). In order to equalize the areas $Aoo = Auu$ between the slid-down soil to the left of the reference axis, and the piled up soil to the right, the natural shear plane had to be lowered by height $hyy = 0,28$ dm (4.234).

Example 3

As in the previous examples, the sliding of earth masses on a continuous inclined rock layer is calculated, whereby the soil is also subjected to a load. To simplify the calculation, the example with different soil types is selected, and the corresponding specifications are used to determine soil movement (see Section 4.4, page 126).

The following values from Section 4.4 are used:

Shear angle $se = 21,1^\circ$ (4.192)	Height $hx = 6,00$ m (4.186)
Angle $x' = 15,9^\circ$ (4.184)	Height $hg = 14,80$ m (4.187)
Width $bx = 21,15$ m (4.185)	Height $hm = 8,80$ m (4.188)

Height hyy is calculated by means of height hm , shear angle $se = 21,1^\circ$ (4.143), elevation angle $x' = 15,9^\circ$ of the inclined surface, and the angle of rock slope $z = 13,0^\circ$ with $\tan z = 0,231$.

Height hyy

$$\begin{aligned}
 hyy^2 / [2 \cdot (\tan se - \tan x')] &= (hm - hyy)^2 / [2 \cdot (\tan se - \tan z)] \\
 hyy^2 / [2 \cdot (0,385 - 0,284)] &= (8,80 - hyy)^2 / [2 \cdot (0,385 - 0,231)] \\
 hyy^2 &= (8,80 - hyy)^2 \cdot 0,202 / 0,308 \\
 hyy &= \sqrt{0,656 \cdot (8,80 - hyy)} \quad hyy + 0,810 hyy - 7,127 = 0 \\
 hyy &= 7,127 / 1,81 = 3,94 \quad \text{m} \quad 4.249
 \end{aligned}$$

Fig. 100 below corresponds to Fig. 99, except that the new position of the shear plane has been inserted.

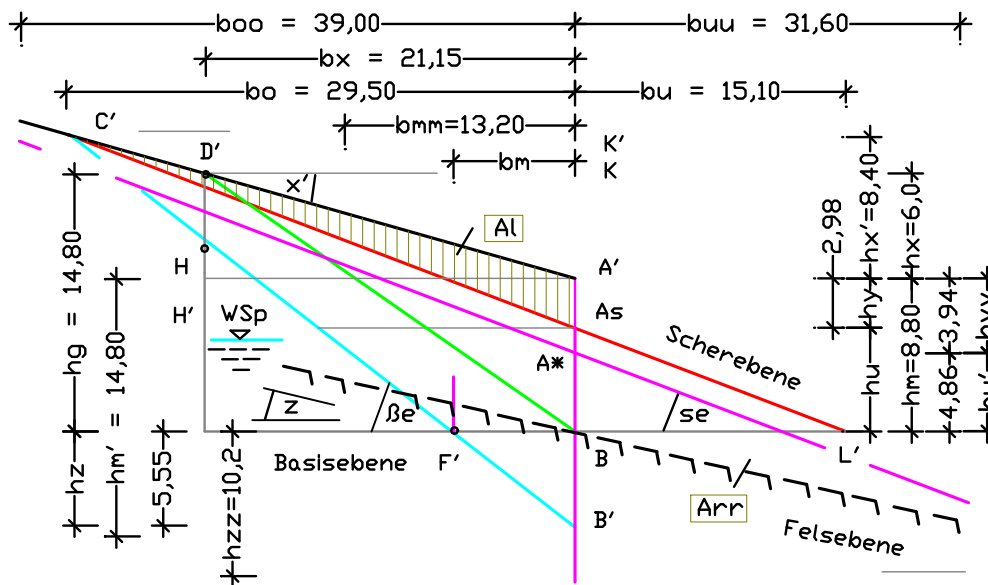


Fig. 100: Additional lowering of the shear plane due to soil distribution on a continuous inclined rock layer.

Height hu'

$$hu' = hm - hyy = 8,80 - 3,94 = 4,86 \quad \text{m} \quad 4.250$$

Width boo

$$\begin{aligned}
 boo &= hyy / (\tan se - \tan x') = \\
 boo &= 3,94 / (0,385 - 0,284) = 39,0 \quad \text{m} \quad 4.251
 \end{aligned}$$

Width buu

$$buu = hu' / \tan se = 4,86 / (0,385 - 0,231) = 31,6 \quad \text{m} \quad 4.252$$

Height h_{xx}

$$h_{xx} = b_{oo} \cdot \tan x' = 39,0 \cdot 0,284 \sim 11,0 \quad \text{m} \quad 4.253$$

Height h_{gg}

$$h_{gg} = b_{oo} \cdot \tan \beta_e = 39,0 \cdot 0,771 \sim 30,0 \quad \text{m} \quad 4.254$$

Height h_{zz}

$$h_{zz} = h_{gg} - h_{xx} - h_m = 30,0 - 11,0 - 8,80 = 10,2 \quad \text{m} \quad 4.255$$

Width b_{mm}

$$b_{mm} = h_{zz} / \tan \beta_e = 10,2 / 0,771 = 13,20 \quad \text{dm} \quad 4.256$$

Area A_l

$$A_l = (b_{oo} \cdot h_{yy}) / 2 = (39,0 \cdot 3,94) / 2 = 76,8 \quad \text{m}^2 \quad 4.257$$

Area A_r

$$A_r = (b_{uu} \cdot h_{u'}) / 2 = (31,6 \cdot 4,86) / 2 = 76,8 \quad \text{m}^2 \quad 4.258$$

Area $A_l = 76,8 \text{ m}^2$ (4.257) covers the soil mass resting on the shear plane under load. If the soil loses its hold at the reference axis, it slides down the shear plane with angle $se = 21,1^\circ$ (4.192), and forms an earth wedge with area $A_r = 76,8 \text{ m}^2$ (4.258) to the right of the axis.

Result of Example 3:

As a result of further lowering of the shear plane under load, width $bm = 7,2 \text{ m}$ (4.200) is increased to width $b_{mm} = 13,2 \text{ m}$ (4.256), thereby increasing the horizontal force H_{fe} on the inclined rock plane against the reference axis, i.e. it contributes significantly to a landslide (see Fig. 101).

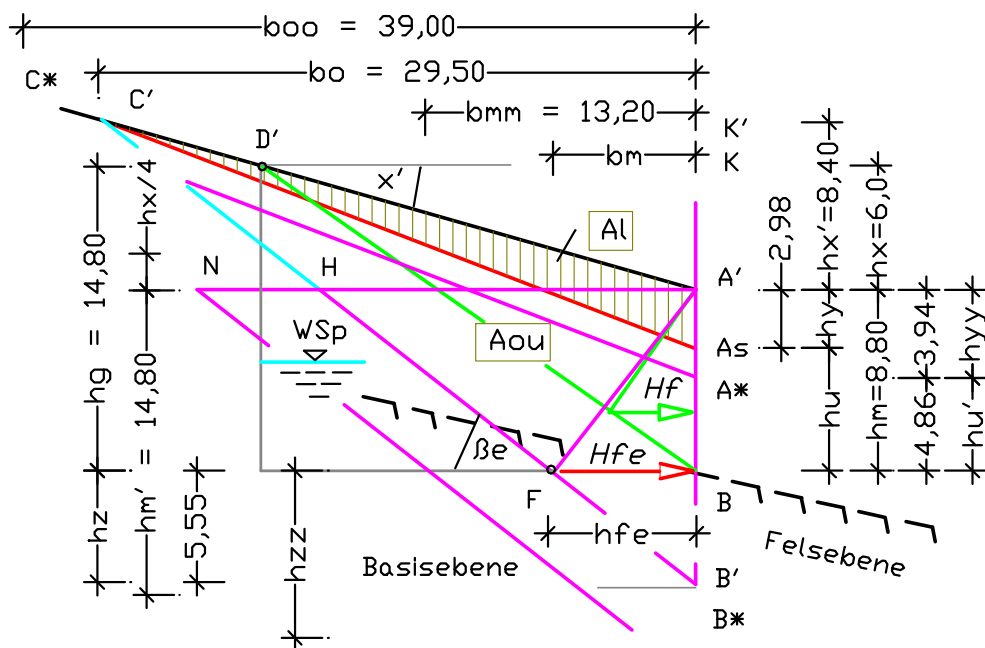


Fig. 101: Force area (H-A'-B') of Fig. 91, and its increase (N-A'-B*) due to further lowering of the shear plane.

Tests 9.2 and 9.3 and the three examples show that the sliding of soil masses from a slope is subjected to numerous conditions, such as varying soil properties, horizontal and inclined surfaces, horizontal and inclined basal planes, as well as continuously inclined basal planes (rock layers). But the examples also showed that the New Earth Pressure Theory permits the earth movements in a slope as well as landslides to be calculated. As further proof of this thesis, the possible causes leading to the landslide in Nachterstedt will be investigated (see Section 5.2).

4.7 Earth pressure on underground pipes and tunnels

In order to determine the load on underground pipes or tunnel runs, a system of coordinates is recommended, whereby an earth block with area $A = b_o \cdot h = 100 \text{ m}^2$ is inserted in every quadrant. If the structure to be calculated is then placed at the center of the system, the maximum forces against the structure can be determined by means of the force field value of 400 m^2 and calculation depth $a = 1,00 \text{ m}$ (see center of Fig. 3, page 12). Because the height/side ratio h/b_o of the earth blocks also corresponds to the tangent of the inclination angle, the side view A of the block can be divided into active and reactive force areas by means of the inclined plane (see Section 4.2).

In Fig. 102 below, a pipe is inserted at the central force point, whereby the forces acting on the pipe are indicated by arrows.

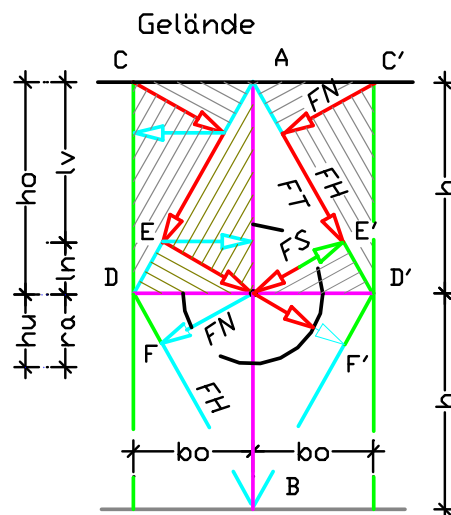


Fig. 102: Coordinate axes, the pipe, and the four quadrants.

From this, it can be derived that the pipe is loaded via force area (A–D'–D), and the force is dispersed into the ground via area (D–D'–B). Consequently, the horizontal coordinate axis (D–D') must support the earth load from both

the 50 m² large earth wedges of the upper earth blocks. If the pipe or tunnel diameter does not fill the distance (E–F') or (E'–F), the loaded structure only has to take up the forces of the earth wedges and disperse them via the walls, which would otherwise have had to be dispersed by the displaced soil.

Below the coordinate axis (D–D'), the forces of the earth load and the structure – consisting of own dead weight, interior work, and traffic loads – must be dispersed by force area (D–D'–B). If the structure's diameter exceeds the dimension (E–F'), the force area will be increased beyond the max. permissible amount. This overload of the substratum can lead to subsidence of the structure (see Section 4.2.3).

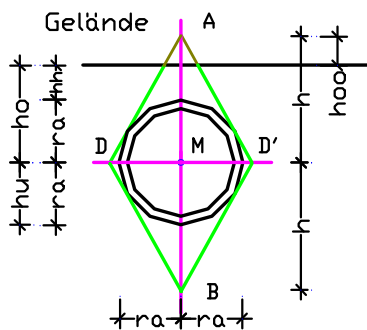


Fig. 103: Minimization of loaded wedge area.

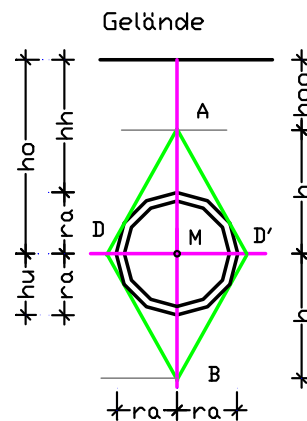


Fig. 104: Wedge area lowered by height *hoo*.

Moreover, the distance between natural force area and terrain plane can be influenced by height *hoo* (see Figs. 103 and 104). If height *h* of the maximum earth load force field (A–D'–D) is reduced by height *hoo*, the structural load is also reduced. However, if height *hoo* acts above height *h*, the forces from this earth layer will not load the structure, because they are deflected sideways past the pipe or tunnel cross-section via the inclined planes. As already mentioned in the pipe statics, additional forces from stationary or traffic loads can act on pipes installed nearer to the surface.

Test 11 was conducted in view of the “Survey on the status of sewer systems in Germany” [2], according to which a major portion of the calculated annual sewer renovation demand is due to shifted axes and sags in the pipes, cracks, breaks, faults in the connections to buildings, and 'lane grooves' in the road surface. For this, the glass container industrial cotton wool was filled into the container instead of easily formable soil, up to a layer height of 1,0 dm Subse-

quently, the separating glass pane was fixed in the container by means of a board (length = 2,44 dm; width = 1,0 dm) from the left, so that basalt grit could be filled into the left-hand chamber, and more cotton wool into the right-hand chamber. When the basalt layer in the left-hand chamber had reached a height of about 0,8 dm, the board was removed, and basalt grit and cotton wool were filled into the container up to its top edge. After pulling out the separating glass pane, the basalt grit spread out into the fringe areas of the cotton wool.

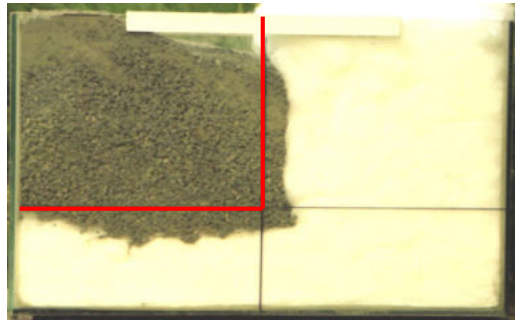


Fig. 105: Model with different soil types in the sewer trench.

The test showed that if soil with a higher density is filled into a trench, any adjacent soil with lower density at the bottom and the sides of the trench can be displaced. Because the New Earth Pressure Theory permits earth movements at the contact faces of two different soil types to be calculated, many of the kinds of pipe damage listed above could be prevented, if the current specifications for pipe statics were adapted accordingly.

Determining the earth forces on an installed DN 1800 Sb sewer pipe

To be calculated are the forces acting against a DN 1800 Sb pipe that is to be installed in an open trench in 'stony ground' with a bedding height $hb = 0,22$ m, whereby the trench is to be filled with the same material after the pipe has been laid. A trench depth of $hs = 5,00$ m is specified. The 'stony ground' has a moist density of $\rho_{ig} = 1,992$ t/m³, and an inclination angle of $\beta_i = 58,0^\circ$. First of all, the trench dimensions and then the force fields as well as the earth forces acting against the pipe are to be determined by means of nominal pipe diameter DN 1800 ($d_i = 1,80$ m), wall thickness $s = 0,18$ m, and a sheeting panel thickness of $vd = 0,12$ m. The loads resulting from road traffic are not taken into account with this example.

The following table summarizes the specified dimensions:

Trench	Pipe DN 1800 mm
Trench depth $hs = 5,00$ m	Inside diameter $di = 1,80$ m
Bedding height $hb = 0,22$ m	Outside diameter $da = 2,16$ m
Sheeting thickness $vd = 0,12$ m	Pipe wall thickness $s = 0,18$ m
Density $pig = 1,992$ t/m ³	Inclination angle $\beta i = 58,0^\circ$

Trench depth $hg = hs + s + hb$ and trench width can be calculated by means of the pipe's nominal diameter, whereby width bg results from addition of the pipe's outside diameter da , two work spaces $ar = 0,50$ m, and two sheeting thicknesses vd , i.e. $bg = da + 2 \cdot (ar + vd)$. The half outside diameter da is indicated by height ra , so that earth block height and calculation height can be determined by means of $h = hs + s - ra$.

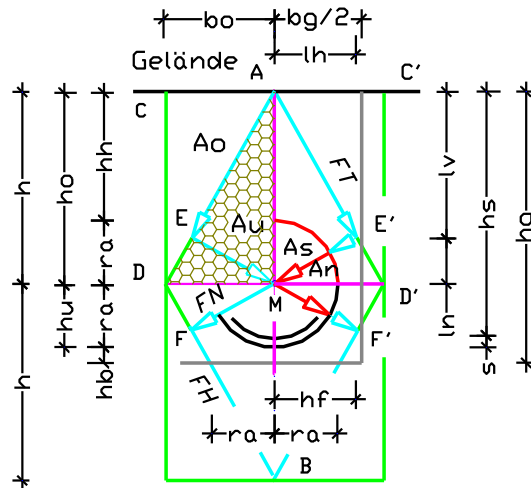


Fig. 106: Pipe and the hatched block area $Au = A - Ao$.

The following values are specified for determining the force due to the filling material: calculation depth $a = 1,00$ m, moist density $pig = 1,992$ t/m³, and angle $\beta i = 58,0^\circ$. To be determined are wedge width bo and wedge area Au , plus the areas As and An , which are separated from area Au by the pipe radius.

Calculation:

Outer pipe radius ra

$$ra = da/2 = 2,16/2 = 1,08 \quad \text{m} \quad 4.259$$

Block height h

$$h = hs + s - ra = 5,00 + 0,18 - 1,08 = 4,10 \quad \text{m} \quad 4.260$$

Trench depth hg

$$hg = hs + s + hb = 5,00 + 0,18 + 0,22 = 5,40 \quad \text{m} \quad 4.261$$

Trench width bg

$$bg = da + 2 \cdot (ar + vd) = 2,16 + 2 \cdot 0,62 = 3,40 \quad \text{m} \quad 4.262$$

Wedge width bo	$bo = bu = h / \tan \beta_{i58} = 4,10/1,600 = 2,56$	m	4.263
Wedge area Au	$Au = Ao = h \cdot bu/2 = 4,10 \cdot 2,56/2 = 5,25$	m ²	4.264
Height $lv \rightarrow$ angle $\beta_i = 58,0^\circ$	$lv = h \cdot \sin^2 \beta_i = 4,10 \cdot 0,719 = 2,95$	m	4.265
Height ln	$ln = h \cdot \cos^2 \beta_i = 4,10 \cdot 0,281 = 1,15$	m	4.266
Width lh	$lh = h \cdot \sin \beta_i \cdot \cos \beta_i = 4,10 \cdot 0,450 = 1,84$	m	4.267
Area As	$As = d^2 \cdot \pi \cdot 58/360 \cdot 4 = 2,16^2 \cdot \pi \cdot 0,04 = 0,590$	m ²	4.268
Area An	$An = d^2 \cdot \pi \cdot 32 /360 \cdot 4 = 2,16^2 \cdot \pi \cdot 0,022 = 0,326$	m ²	4.269

The calculated force area $Au = 5,25 \text{ m}^2$ (4.264) lies far below the max. permissible force area of $Au' = 50,0 \text{ m}^2$. An overload of the substratum due to forces from the calculated force area will not occur, if the adjacent soil has a similar density as the filling material. Because force determination is done for one half at a time, the calculation results must be adapted accordingly when dimensioning the pipe. Regarding the following calculation, it must be noted that it might be advantageous to determine the force meters lv , ln and lh first, and subsequently convert the force meters into forces using force index gi (see Fig. 106).

Weight $G \rightarrow$ with $g = 9,807 \text{ m/s}^2$	$G = Au \cdot \rho_{ig} \cdot g = 5,25 \cdot 1,992 \cdot 9,807 = 102,6$	kN	4.270
Force FL	$FL = G \cdot \cos \beta_{i58} = 102,6 \cdot 0,530 = 54,3$	kN	4.271
Force FT	$FT = G \cdot \sin \beta_{i58} = 102,6 \cdot 0,848 = 87,0$	kN	4.272
Force Lv	$Lv = G \cdot \sin^2 \beta_{i58} = 102,6 \cdot 0,719 = 73,8$	kN	4.273
Force Ln	$Ln = G \cdot \cos^2 \beta_{i58} = 102,6 \cdot 0,281 = 28,8$	kN	4.274
Force Lh	$Lh = G \cdot \sin \beta_{i58} \cdot \cos \beta_{i58} = 102,6 \cdot 0,448 = 46,1$	kN	4.275
Force index gi	$gi = bu \cdot \rho_{ig} \cdot g / 2 = 2,56 \cdot 1,992 \cdot 9,807/2 = 25,0$	kN/m	4.276
Force meter fl	$fl = FL/gi = 54,4/25,00 = 2,18$	m	4.277

Force meter ft

$$ft = FT/gi = 87,0/25,00 = 3,48 \quad \text{m} \quad 4.278$$

Force meter lv

$$lv = Lv/gi = 73,8/25,00 = 2,95 \quad \text{m} \quad 4.279$$

Force meter ln

$$ln = Ln/gi = 28,8/25,00 = 1,15 \quad \text{m} \quad 4.280$$

Force meter lh

$$lh = Lh/gi = 46,1/25,00 = 1,84 \quad \text{m} \quad 4.281$$

Vertical force $Lv = 73,8$ kN (4.273) must be assigned to force area (A–E'–M), and force $Ln = 28,8$ kN (4.274) must be assigned to force area (E'–D'–M), whereby the letter M describes the center of the pipe.

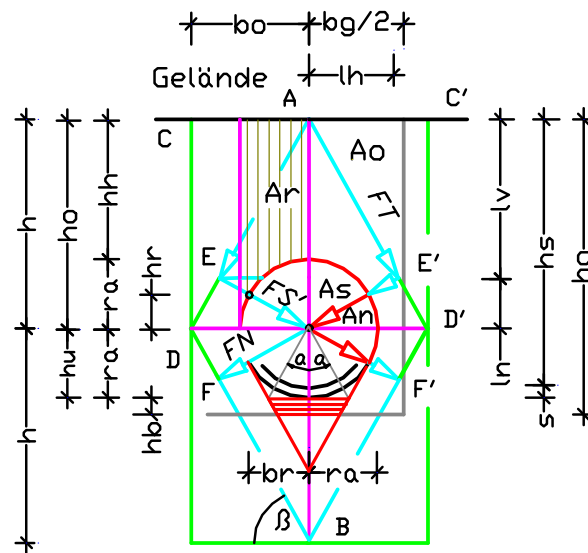


Fig. 107: Force area Ar , force FL' , and the pipe bedding (red) under angle $2 \cdot \alpha$ of the soil under the pipe.

As force Lv in particular only loads the pipe cross-section partially, the above forces and force areas must be adapted to the partial areas Ar , As and An when dimensioning the pipe. Vertical force Lv (which must be determined from area $Ar = (h - ln) \cdot ra$, and possibly spread over the pipe diameter $da = 2,16$ m as a distributed load) acts on the top of the pipe on both sides of the reference axis. Force FS acts against the pipe in planes (E–M) and (E'–M) at height hr and under angle $\alpha = 90^\circ - \beta i = 90^\circ - 58^\circ = 32^\circ$. Because force FL occupies the distance (E–M), it must be reduced by the force amount that lies within the pipe. This reduction can be achieved by means of the radius ra multiplied with force index gi , thereby creating force $FL^* = FL - ra \cdot g$.

The following is calculated:

Area Ar

$$Ar = h \cdot ra - As - An = 4,10 \cdot 1,08 - 0,916 = 3,51 \quad \text{m}^2 \quad 4.282$$

Height hr

$$hr = ra \cdot \sin 32^\circ = 1,08 \cdot 0,530 = 0,57 \quad \text{m} \quad 4.283$$

Width br

$$br = ra \cdot \cos 32^\circ = 1,08 \cdot 0,848 = 0,92 \quad \text{m} \quad 4.284$$

Diagonal fl' → in plane (E–M)

$$fl' = \sqrt{h^2 + br^2} = \sqrt{0,57^2 + 0,92^2} = 1,08 = ra \quad \text{m} \quad 4.285$$

Force Lv^* → from area $Ar \cdot a = Vr$ with $a = 1,00$ m

$$Lv^* = Vr \cdot pig \cdot g = 3,51 \cdot 1,992 \cdot 9,807 = 68,6 \quad \text{kN} \quad 4.286$$

Force FL'

$$FL' = fl' \cdot gi = 1,08 \cdot 25,0 = 27,0 \quad \text{kN} \quad 4.287$$

Results:

In order to dimension the pipe, the vertical forces $2 \cdot Lv^*$ must be spread over the pipe diameter $da = 2,16$ m as a distributed load, and force $FL = 27,0$ kN/m applied against the pipe in planes (E–M) and (E'–M). The above forces can be mirrored for force dispersal, especially if the weight of the pipe and its filled volume correspond to the weight of the soil displaced by the pipe. Decisive for force dispersal into the substratum are the properties and angles of the adjacent soil. The pipe's bedding area with angle 2α is shown hatched (red) in Fig. 107. The load capacity of soils has already been discussed in Section 4.2.

Overloads of the substratum lead to pipe subsidence.

4.8 Earth pressure on single piles

In general, piles are used to disperse large loads in soils that are not very firm. The kinds of pile foundations, pile manufacturing, and the terminology will be taken from DIN 1054, and will not be commented here (also see "Deep foundations, piles, and anchors" [1: N]).

Different to the specifications in DIN 1054, a calculation system consisting of eight earth blocks is used for load dispersal into the adjacent ground via piles. The pile is placed in the vertical axis of the cube, so that the forces of the four upper earth blocks clamp the pile from all sides. In this way, the load applied to the pile head can be dispersed into the adjacent ground via the pile skin. The four earth blocks of the lower plane transfer the forces dispersed into the ground via the pile foot. The volumes and dimensions of the earth blocks as well as the calculations for the load bearing capacity of soils were described in Section 4.2.

The data provided there are based on a calculation depth $a = 1,00$ m, so that height h' and width $b' = \sqrt{4 \cdot a \cdot b}$ of the soil cube's square base area can be determined via volume $V = 4 \cdot V^* = 400$ m³ and inclination angle β of the selected soil type. As for all earth pressure calculations, the inclination angle β of the respective selected soil type β_t , β_i , β_n , β_{iw} or β_{nw} indicated in the Figs. must also be adapted here. Moreover, any force that is to be applied to the pile must be converted into a load area by means of the dry density $ptg_n = Vf_n \cdot ptg_{90}$ of the adjacent soil. I.e., during this conversion, the actual densities of moist or wet soils above and below water, as well as gravitation are not taken into account. This approach using dry density is considered to be correct, because in free nature any water under pressure in the ground will give way, and is therefore not available for load dispersal. Only if forces from soils under water acting against structures must be determined, not the dry density must be used in the statics, but the actual densities of the soils under water ($piwg$ or $pnwg$) as well as apparent gravity g .

By means of volume Vr of the circular cone multiplied with dry density ptg it is possible to determine load Ee , weight $Ge = Ee \cdot g$, and the partial forces Lv , Ln and Lh . Moreover, the soil's dead weight must be taken into account for load dispersal under the pile foot. This can be determined via the pile foot diameter \emptyset , angle β , and density ptg of the adjacent soil. The load and the soil's dead weight must be dispersed via the earth cone with height hg and radius rg .

Loading and load dispersal of a single pile

To be calculated is the payload of a pile with diameter $\emptyset = 0,60$ m without foot widening, that is to be constructed of in-situ concrete with density $p_{pf} = 2,30$ t/m³. The pile's dead weight is to be dispersed entirely by the soil under the pile using the permissible soil pressure. Dry density $ptg = 1,764$ t/m³ (3.9) and inclination angle $\beta_t = 55^\circ$ are assigned to the adjacent soil. The soil pressure $\sigma_{Dzul} = 206,7$ kN/m² (4.5) has already been calculated from the soil column with load area $Ad^* = 1,00$ m² and volume $V^* = 100$ m³ with one-sided force expansion using height $h = 11,95$ m (4.1) and width $b = 8,37$ m (4.2) (see page 95ff).

The following table lists the starting values for the calculations:

Ground	Reinforced pile
Angle $\beta_t = 55,0^\circ$	Diameter $\emptyset = 0,60$ m
Density $ptg = 1,764$ t/m ³	Pile density $p_{pf} = 2,30$ t/m ³
Force field height $h = 11,95$ m	Pile height $h_p = h'$
Force field width $b = 8,37$ m	$\sigma_{Dzul} = 206,7$ kN/m ²

Height h' and width b' of the force field can be determined via inclination angle $\beta t = 55^\circ$ and volume $4 \cdot V^* = 400 \text{ m}^3$ of the upper plane.

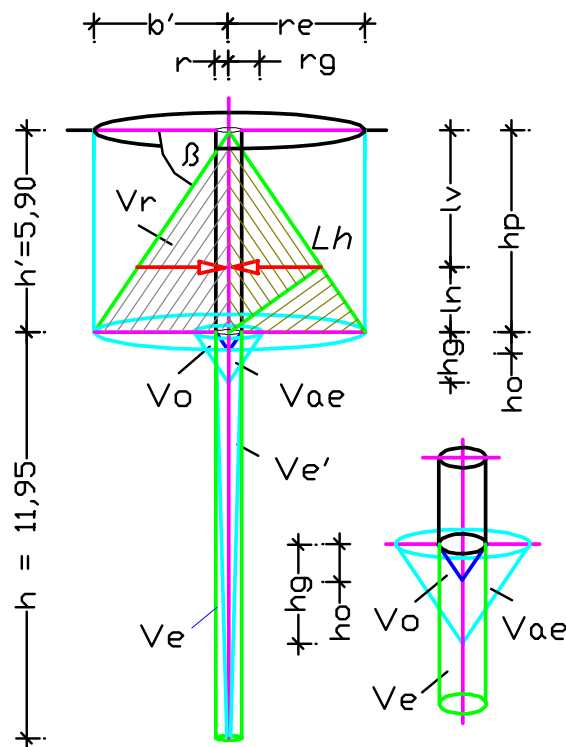


Fig. 108: Section through the soil column with position and description of the individual volumes.

Width b' and height h' describe a soil cube with a square base area. Because the forces acting against a circular pile are to be determined in this case, a force cone with radius $re = b'$ and height h' must be inserted into the soil cube (see Fig. 108). Further explanations regarding the determination of forces against the pile will be provided in the calculation example.

Dimensions of the soil cube

As already described, width b' and height h of the soil cube are calculated by means of volume $V^* = 100 \text{ m}^3$ of a soil column, and inclination angle $\beta t = 55,0^\circ$ of the selected soil type.

Width b'

$$b' = \sqrt[3]{(V^* \cdot 8 / \tan \beta t)} = \sqrt[3]{(100 \cdot 8 / 1,428)} = 8,24 \quad \text{m} \quad 4.239$$

Height h'

$$h' = (b' \cdot \tan \beta t) / 2 = 8,24 \cdot 1,428 / 2 \sim 5,90 \quad \text{m} \quad 4.240$$

Height $h = 11,95 \text{ m}$ (4.1) – which was used to calculate the permissible soil pressure – is still decisive for dispersal of the pile's dead weight.

Maximum permissible load dispersal under the pile foot

With the requirement that the permissible soil pressure under the pile may not be exceeded, height $h = 11,95$ m, density $ptg = 1,764$ t/m³, and pile diameter $\varnothing = d = 0,60$ m are used to calculate the permissible load Eu and its dispersal in the ground.

Load area Ad^*

$$Ad^* = \pi \cdot d^2/4 = \pi \cdot 0,60^2/4 = 0,283 \quad \text{m}^2 \quad 4.290$$

Circumference U

$$U = \pi \cdot d = \pi \cdot 0,60 = 1,88 \quad \text{m} \quad 4.291$$

Volume Ve

$$Ve = h \cdot Ad^* = 11,95 \cdot 0,283 = 3,382 \quad \text{m}^3 \quad 4.292$$

Load Eu

$$Eu = Ve \cdot ptg = 3,382 \cdot 1,764 = 5,97 \quad \text{t} \quad 4.293$$

Weight $Gu =$ weight Gp of the pile

$$Gu = Eu \cdot g = 5,97 \cdot 9,807 = 58,5 \quad \text{kN} \quad 4.294$$

Load Eu or force Gu are dispersed in the ground via the total volume Ve . Hereby, volume Ve is divided into the active volume $Ve' = Ve/3$ and the reactive volume $Ve^* = 2/3$. For determination of the pile load, volume Vo must be added to active volume Ve' , which is calculated from the load-dispersing soil cone under the pile foot. Height hg and radius rg of the cone can then be determined from volume $Vae = Vo + Ve'$ and inclination angle βt .

Calculation:

Height ho

$$ho = 0,5 \cdot d \cdot \tan \beta t_{55} = 0,5 \cdot 0,60 \cdot 1,428 = 0,43 \quad \text{m} \quad 4.295$$

Volume Vo

$$Vo = Ad \cdot ho/3 = 0,283 \cdot 0,43/3 = 0,041 \quad \text{m}^3 \quad 4.296$$

Volume Vae

$$Vae = Vo + Ve/3 = 0,041 + 3,382/3 = 1,168 \quad \text{m}^3 \quad 4.297$$

Radius rg

$$rg = \sqrt[3]{(3 \cdot Vae/\pi \cdot \tan \beta t_{55})}$$
$$rg = \sqrt[3]{(3 \cdot 1,168/\pi \cdot 1,428)} = 0,92 \quad \text{m} \quad 4.298$$

Height hg

$$hg = \sqrt[3]{(3 \cdot Vae \cdot \tan^2 \beta t_{55} / \pi)}$$
$$hg = \sqrt[3]{(3 \cdot 1,168 \cdot 1,428^2 / \pi)} = 1,32 \quad \text{m} \quad 4.299$$

In accordance with the specification that the soil of the lower force plane disperses the pile's dead weight, the possible pile height hp^* is calculated by

means of permissible load $Eu = 5,97 \text{ t}$ (4.293), area $Ad^* = 0,283 \text{ m}^2$ (4.290), and pile density p_{pf} .

Pile height hp^*

$$hp^* = Eu/Ad \cdot p_{pf} = 5,966/0,283 \cdot 2,30 = 9,16 \quad \text{m} \quad 4.300$$

Because height $h' = 5,90 \text{ m}$ (4.240) of the upper force plane must correspond to pile height hp , the reduced dead weight of the pile can be used to increase the pile's payload if a shorter pile is used.

Determining the forces against the pile skin

The force values against the pile are specified by means of width $b' = 8,24 \text{ m}$ (4.288) and height $h' = hp = 5,90 \text{ m}$ (4.289) of the upper soil cube. In accordance with the pile cross-section, a circular soil column with radius $re = b'$ must be entered in the square base area of the cube. A reactive soil cone with volume $Vr = 4 \cdot V^*/3$ is formed in the column's lower area, whereby force areas Ar are assigned to the left and right of the pile axis for the purpose of force determination.

If the force areas Ar are shifted horizontally from the pile's axis to the pile skin, a new cone is formed with radius $ree = re + d/2$ and height $hl' = hp + ho$. Conversion of the cone size results in volume Vr' , which can be changed back to the original cone volume Vr by deducting the pile volume Vp .

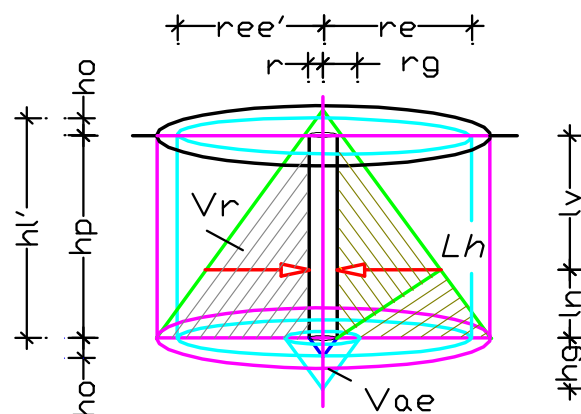


Fig. 109: Upper soil cone with volume Vr , and the lower cone, which disperses the pile's dead weight via volume Vae .

Weight G and the forces Lv , Ln and Lh can be determined via the reduced cone volume (see Fig. 109).

Calculation:

Height $hl' \rightarrow hp = h' = 5,90 \text{ m}$ (4.289)

$$hl' = hp + ho = 5,90 + 0,43 = 6,33 \quad \text{m} \quad 4.301$$

Radius re	$re = b'/2 = 8,24/2 = 4,12$	m	4.302
Radius $ree = boo$	$ree = re + d/2 = 4,12 + 0,60/2 = 4,42$	m	4.303
Volume Vr	$Vr = hl' \cdot ree^2 \cdot \pi/3 = 6,33 \cdot 4,42^2 \cdot \pi/3 = 129,5$	m ³	4.304
Volume Vp	$Vp = (hp+ho/3) \cdot Ad^* = (5,90 + 0,43/3) \cdot 0,283 = 1,7$	m ³	4.305
Volume Vr'	$Vr' = Vr - Vp = 129,5 - 1,7 = 127,8$	m ³	4.306
Weight $G \rightarrow$ of the soil cone	$G = Vr' \cdot ptg_{55} \cdot g = 127,8 \cdot 1,764 \cdot 9,807 = 2210$	kN	4.307

Because counter-acting horizontal forces are formed within the soil cone, weight G must be halved for the determination of force Lh , after which force Lh must be distributed across half the pile skin's circumference.

Weight G'	$G' = G/2 = 2210/2 = 1105$	kN	4.308
-------------	----------------------------	----	-------

Horizontal force Lh against the pile skin, and vertical force Lv on the skin can be determined easily by means of force index git multiplied with the force meter of the forces.

Force index $git \rightarrow$ via pile height $hp = h' = 5.90$ m (4.289)	$git = G'/hp \cdot a = 1105/5,90 \cdot 1,00 = 187,3$	kN/m ²	4.309
Force meter $lv = -rv \rightarrow$ same position, but opposite direction	$lv = hp \cdot \sin^2 \beta_{t55} = 5,90 \cdot 0,671 = 3,96$	m	4.310
Force meter ln	$ln = hp \cdot \cos^2 \beta_{t55} = 5,90 \cdot 0,329 = 1,94$	m	4.311
Force meter $lh = -rh \rightarrow$ same position, but opposite direction	$lh = hp \cdot \sin \beta_{t55} \cdot \cos \beta_{t55} = 5,90 \cdot 0,470 = 2,77$	m	4.312

The following forces are directed onto the pile skin.

Force Lv	$Lv = lv \cdot git = 3,96 \cdot 187,3 = 741,7$	kN	4.313
Force Lh	$Lh = lh \cdot git = 2,77 \cdot 187,3 = 518,8$	kN	4.314
Force $Rv \rightarrow$ reactive force from the load	$-Rv = Lv = 741,7$	kN	4.315
Weight $Ge_{zul} \rightarrow$ with which the pile can be loaded	$Ge_{zul} = 2 \cdot Lv = 2 \cdot 741,7 = 1483$	kN	4.316

Skin area $Am \rightarrow$ of the pile, with height $hp = 5,90$ m (4.289)

$$Am = hp \cdot d \cdot \pi = 5,90 \cdot 0,60 \cdot \pi = 11,12 \quad \text{m}^2 \quad 4.317$$

Skin pressure $\sigma_m \rightarrow$ on both sides, due to force Lh

$$\sigma_m = 2 \cdot Lh/Am = 2 \cdot 518,8/11,12 = 93,3 \quad \text{kN/m}^2 \quad 4.318$$

As mentioned above for pile height $hp^* = 9,16$ m (4.300), the pile's dead weight, which results from the height difference between hp^* and $hp = 5,90$ m, can be used to increase the permissible weight Ge_{zul} .

Weight $Ge^* \rightarrow (hp^* - hp) = 9,16 - 5,90 = 3,26$ m

$$Ge^* = Ge_{zul} + (hp^* - hp) \cdot Ad \cdot p_{pf} \cdot g$$

$$Ge^* = 1483 + 3,26 \cdot 0,283 \cdot 2,30 \cdot 9,807 = 1504 \quad \text{kN} \quad 4.319$$

Results:

It was established that the lower soil layer with height $h = 11,95$ m (4.1) is able to disperse weight $Gu = 58,5$ kN (4.294) without overloading the soil. Equalization of force Gu with the force of the pile's dead weight resulted in the permissible pile height $hp^* = 9,16$ m (4.300).

By means of the soil cone of the upper plane, which was specified in the soil cube with width $b' = 8,24$ m (4.239) and height $hp = 5,90$ m (4.289), it was possible to calculate force $Ge_{zul} = 1483$ kN (4.316), with which the pile can be loaded. By changing the pile's dead weight Gu from pile height $hp^* = 9,16$ m to pile height $hp = 5,90$ m, an excess force was created, which resulted in the higher weight $Ge^* = 1504$ kN (4.319). No safety factors were applied for the above calculations. If one compares height $hg = 1,32$ m (4.299) of the cone under the pile foot with height $hp = 5,90$ m (4.289) of the upper plane cone, the height difference indicates a force potential that could result in a greater pile height and an increased payload. This assumption will now be examined.

Forces when changing the pile height

The counter-acting soil cones with height $h = 5,90$ m can be used for the horizontal clamping force of the pile shaft and for force dispersal below the pile foot. Via the lower soil cone, volume $V_{ae} = 1,168$ m³ (4.248) with height $hg = 1,32$ m (4.299) can be used for the maximum permissible load dispersal under the pile, so that the height difference $h' - hg$ of the cone is available for increasing the pile height. Addition of the upper and lower cone heights leads to two mirrored cones with the mean height $hp' = (2 \cdot hp - hg) / 2 = (2 \cdot 5,90 -$

1,32) / 2 = 5,24 m. This increases the pile height from $h_p = 5,90$ m to $h_p'' = 2 \cdot h_p'$ (see Fig. 109, page 152, and Fig. 110 below).

Pile height h_p''

$$h_p'' = 2 \cdot h_p' = 2 \cdot 5,24 = 10,48 \quad \text{m} \quad 4.320$$

Also here, calculation of the forces against the pile skin is carried out by means of the respective cone height h_p' . Hereby, it must be noted that only the dead weight of a pile with height $h_p^* = 9,16$ m (4.300) is handled by the soil cone with volume V_{ae} . The higher pile dead weight that must be taken into account due to an increase $h_p'' - h_p^*$ of the pile height, will have to be deducted from the determined payload that can be applied to the pile.

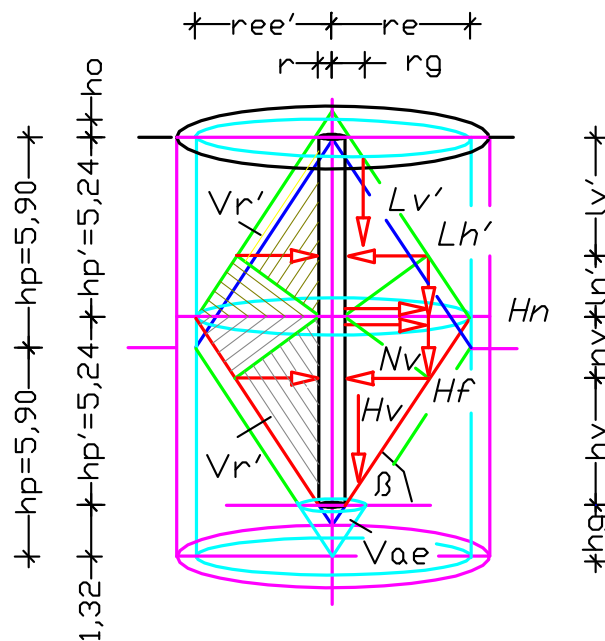


Fig. 110: Soil column and the force cones in both planes with their forces against the pile skin.

The intended determination of the forces against the lengthened pile is carried out by means of the above calculation approach, whereby the descriptions of the dimensions and forces remain unchanged. The previous and new calculation results, in particular for the payload, are summarized in the table below.

But first, the following must be calculated:

Height h_l'

$$h_l' = h_p' + h_o = 5,24 + 0,43 = 5,67 \quad \text{m} \quad 4.321$$

Radius ree'

$$ree' = h_l' / \tan \beta_{t55} = 5,67 / 1,428 = 3,97 \quad \text{m} \quad 4.322$$

Volume V_r

$$V_r = h_l' \cdot ree'^2 \cdot \pi / 3 = 5,67 \cdot 3,97^2 \cdot \pi / 3 = 93,6 \quad \text{m}^3 \quad 4.323$$

Volume $V_p \rightarrow$ pile volume in the area of the upper soil cone

$$V_p = (h_p' + h_o/3) \cdot A_d^* = (5,24 + 0,43/3) \cdot 0,283 = 1,5 \text{ m}^3 \quad 4.324$$

Volume $V_{r'}$

$$V_{r'} = V_r - V_p = 93,6 - 1,5 = 92,1 \text{ m}^3 \quad 4.325$$

Weight G of the soil cone

$$G = V_{r'} \cdot \rho_{t_{55}} \cdot g = 92,1 \cdot 1,764 \cdot 9,807 = 1593 \text{ kN} \quad 4.326$$

Weight G' of half the soil cone

$$G' = G/2 = 1593/2 = 796,5 \text{ kN} \quad 4.327$$

For determining the counter-acting horizontal forces against the pile skin, weight G must be halved and distributed over the cone halves left and right of the reference axis. Subsequently, the horizontal forces $L_h = H_f$ against the pile skin, and the vertical forces $L_v = H_v$ and $L_n = N_v$ are converted into force meters by multiplying them with force index git to obtain a correctly scaled representation.

Force index $git \rightarrow$ via the pile height $h_p' = 5,24 \text{ m}$

$$git = G'/h_p' \cdot a = 796,5/5,24 \cdot 1,00 = 152,0 \text{ kN/m}^2 \quad 4.328$$

Force meter l_v

$$l_v = h_p' \cdot \sin^2 \beta_{t_{55}} = 5,24 \cdot 0,671 = 3,52 \text{ m} \quad 4.329$$

Force meter l_n

$$l_n = h_p' \cdot \cos^2 \beta_{t_{55}} = 5,24 \cdot 0,329 = 1,72 \text{ m} \quad 4.330$$

Force meter $l_h = -r_h$

$$l_h = h_p' \cdot \sin \beta_{t_{55}} \cdot \cos \beta_{t_{55}} = 5,24 \cdot 0,470 = 2,46 \text{ m} \quad 4.331$$

The following forces are directed at the pile skin:

Force $L_v = H_v$

$$L_v = H_v = l_v \cdot git = 3,52 \cdot 152,0 = 535,0 \text{ kN} \quad 4.332$$

Force $L_n = N_v$

$$L_n = N_v = l_n \cdot git = 1,72 \cdot 152,0 = 261,4 \text{ kN} \quad 4.333$$

Force $L_h = H_f$

$$L_h = H_f = l_h \cdot git = 2,46 \cdot 152,0 = 373,9 \text{ kN} \quad 4.334$$

Force $R_v \rightarrow$ reactive force from the load

$$-R_v = L_v + H_v = 535,0 + 535,0 = 1070 \text{ kN} \quad 4.335$$

Weight $G_{ee_{zul}} \rightarrow$ with which the pile can be loaded

$$G_{ee_{zul}} = 2 \cdot L_v = 2 \cdot 1070 = 2140 \text{ kN} \quad 4.336$$

Skin area $A_m^* \rightarrow$ with pile height $h_p'' = 10,48 \text{ m}$ (4.320)

$$A_m^* = h_p'' \cdot d \cdot \pi = 10,48 \cdot 0,60 \cdot \pi = 19,75 \text{ m}^2 \quad 4.337$$

Skin pressure $\sigma_m^* \rightarrow$ on both sides due to force L_h

$$\sigma_m^* = 4 \cdot L_h/A_m^* = 4 \cdot 373,5/19,75 = 75,6 \text{ kN/m}^2 \quad 4.338$$

The pile's dead weight $G_p = 58,5$ kN (4.294) calculated for the pile height $h_p^* = 9,16$ m (4.300) is dispersed into the ground below the pile by means of the soil cone $V_{ae} = 1,168$ m³ (4.297).

Still to be determined and then deducted from weight $G_{ee_{zul}} = 2140$ kN (4.336) is the pile's dead weight for pile height $h_g = 1,32$ m (4.299).

Weight ΔG_p of the pile

$$\Delta G_p = \emptyset \cdot \Delta h_p \cdot p_{pf} \cdot g = 0,283 \cdot 1,32 \cdot 2,3 \cdot 9,807$$

$$\Delta G_p = 8,4 \quad \text{kN} \quad 4.339$$

Weight G_{ee}^*

$$G_{ee}^* = G_{ee} - \Delta G_p = 2140 - 8,4 = 2131,6 \quad \text{kN} \quad 4.340$$

Weight $G_{ee}^* = 2131,6$ kN (4.340) can be applied vertically to the pile with height $h_p'' = 2 \cdot h_p' = 10,48$ m, without causing the pile to subside.

Also this example proves that a pile can be held by horizontal forces in the ground (clamping pressure), and that frictional forces (skin friction forces) only occur when the pile is pulled out or driven deeper into the ground (subsides) due to an excessive load. If a pile is overloaded, the soil under the pile is compacted, thereby forming a steeper inclination angle and lower horizontal forces for load dispersal. If the soil under the pile is unable to follow the changes in the force system, this can lead to pile subsidence, a base failure under the pile, or skewing of the pile. Hereby, the pile skin's surface structure is insignificant (also see "Frictional force" in Section 2.3.1.).

The above determination of permissible pile loading can be also be applied for piles with varying forms of shaft and foot (foot widening). Hereby, only the changed volumes must be taken into account. Not dealt with are eccentric and dynamic loads on piles as well as safety-relevant factors that can influence pile dimensioning.

The table shows the summarized calculation results:

Pile with height $h_p = 5,90$ m	Pile with height $h_p'' = 10,48$ m
Horizontal force $Lh = 518,8$ kN (4.314)	Horizontal force $2Lh = 747,8$ kN (4.334)
Vertical force $Rv = -741,7$ kN (4.315)	Vertical force $Rv = -1070$ kN (4.335)
Skin pressure $\sigma_m = 93,3$ kN/m ² (4.318)	Skin pressure $\sigma_m^* = 75,6$ kN/m ² (4.338)
Weight $Ge^* = 1504$ kN (4.319)	Weight $G_{ee}^* = 2132$ kN (4.340)

4.9 Conclusions for Chapter 4

The New Earth Pressure Theory is based on the assumption that earth stresses are always active, and that stress build-up and relief in the ground is effected

via the inclined plane within earth blocks. If external forces are applied to the terrain or loading plane, the form and size of stress pattern, inclination angle, and possibly the soil density will change. If one isolates an idealized pore-free rock column with a square base area $Ad = 1,00 \text{ m}^2$ from a closed field formation below the terrain plane, the tangent of the inclination angle $\tan \beta t = 100/1 = 100 = \mu$ as well as angle $\beta t = 89,43^\circ$ can be determined by means of the height/side ratio. If one assigns dry density $\rho_{90} = 3,0 \text{ t/m}^3$ and gravity force g to the rock column, a pressure $\sigma_d = 2942 \text{ kN/m}^2$ will be established in the footprint Ad . This pressure will not change, even if the column is moved to the field formation. Consequently, it can be assumed that under comparable conditions, every other soil type will behave in the same way, i.e. an adequate pressure will be generated in the footprint by a soil column with height $h^* = 100 \text{ m}$. However, because under real conditions a soil column would break up under its inclination angle, thereby losing height in favour of area Ad , the larger footprint would also reduce the soil pressure (for further details, see Section 4.2.).

If one returns to the rock column, and replaces the rock below the terrain plane with a soil type, and assuming a permissible one-sided force distribution, its horizontal force will create a force area for its dispersal. In this area with height h' and width b , the inclined plane under angle β will adopt the face diagonal. The soil resting on the inclined plane is described as 'active', and the soil below it is called 'reactive'. If one assigns the calculation width $a = 1,00 \text{ m}$ to force area $A = h' \cdot b$, an earth disk with height h' , footprint $Ad = a \cdot b$, and volume $V^* = 100 \text{ m}^3$ is formed. Because weight G of a 100 m high soil column with footprint $Ad = a^2$ corresponds to weight G of the earth disk with volume $V^* = 100 \text{ m}^3$ and footprint $Ad' = a \cdot b$, it must be possible to calculate the permissible soil pressure from the earth disk's footprint Ad' . From this it can be deduced that every square meter of a specific soil type will be able to support a soil column of the same soil type with height h' , without soil subsidence occurring under the column. In order to calculate load or force dispersals, the loads on soils must first be adapted to the properties of the load-dispersing soil – regardless of whether they consist of an earth mass or an external force. Load dispersal in soil is effected by an increase of the force area of the soil's dead weight and a change of the inclination angle βe under load. In the same way, the natural shear angle s is changed into shear angle se under load. If the load-

dispersing soil is not subjected to an excessive load, the density of this soil remains constant. However, a larger force area in the soil always generates a higher earth pressure force against a wall, or causes the earth mass to slide down an incline more quickly. Force distribution and the angles in the soil can change, if a rock or concrete layer prevents dispersal of the vertical forces due to the load. In this case, the vertical forces are converted into horizontal forces, thereby reducing the inclination angle βe .

Coordinate systems consisting of one, two, four or eight earth blocks are used for determining the force against a structure or to calculate the dispersal of loads applied to structures/components into the adjacent ground. The described volume $V^* = 100 \text{ m}^3$ of an earth block also assists in determining a soil's loading limits. By means of an earth block and calculation depth $a = 1,00 \text{ m}$ it is possible to calculate the load acting on a supporting wall. Two earth blocks are required to observe the force dispersal under a strip foundation. Four earth blocks located in a plane below the surface serve for force dispersal under a single foundation with quadrilateral force distribution.

A vertically arranged coordinate system equipped with four earth blocks serves to determine the force against a pipe or tunnel cross-section, and to calculate force dispersal below the cross-section. Hereby, the central point of the pipe is placed at the center of the coordinate system. The two upper earth blocks load the cross-section, and the two lower blocks disperse the forces downwards into the soil. Eight earth blocks in two planes with four blocks each, form a soil cube whose square base area with width b' replaces the calculation depth a . This coordinate system serves to determine the forces of a single pile, whose axis is placed in the vertical system axis. The forces of the four earth blocks of the upper plane clamp the pile, and the four blocks of the lower plane take up the force that is to be dispersed into the ground via the pile foot.

The calculation examples in this chapter prove that the determined soil properties can be used to calculate the earth forces acting on the most varied structures, and that the dispersal of forces within the adjacent ground can be described.

5 Accidents caused by earth movements

In Germany, there are regular reports in the media about subsidence and structural damage as well as related accidents involving alleged 'unforeseeable' soil movements. Often enough, the search for the causes takes years, until finally the matter remains unsolved and is shelved. But now, new findings about soil behaviour, and the calculation basics provided by the New Earth Pressure Theory open up the possibility to determine soil behaviour precisely. The most well-known accidents in 2009 – subway excavations in Cologne with the collapse of the Historic Archive, and the landslide in Nachterstedt during filling of the Concordia lake, with fatalities and enormous material damage – were selected in order to show that the basics of the New Theory can be used to determine the cause of the damage. Because the public media hardly publish any technical details or relevant facts about the reported damage events, assumptions are made regarding soil parameters and structural dimensions.

5.1 Collapse of Cologne's Historic Archive in 2009

Reports and photo galleries [G] about the collapse of the Historic Archive in Cologne are available in the Internet. The presumed cause of the accident is hydraulic subsurface erosion, which is supposed to have caused a cave-in with a length of 70 m and a width of 50 m. Moreover, pumping reports are mentioned, that provide evidence of excessive water withdrawal with uncontrollably large amounts of sand, which could have caused the soil instability under the archive building.

The press articles “Im ‚Kölner Loch‘ verschwinden Beweise und Millionen” (Evidence and millions vanish in the 'Cologne Hole'), dated 05.03.2011 (*www.zeit.de*), and “Das Kölner Lehrstück” (The Cologne Lesson), dated 24.01.2013 (*www.focus.de*) report that the cause of damage has still not been found. The journal “Kölner Stadtanzeiger” of 30.03.2014 reports: “Cause to be established by end of 2014”.

If one views the enormous weight of the Historic Archive building as a load on the substratum next to the tunnel cross-section, an overload of the right-hand slotted wall must be seen as a possible cause of the damage. This assumption is supported by publications in the Internet regarding the leaning church tower of Sankt Johann Baptist [E].

Determination of earth and building loads (archive) and the dispersal of these loads in the adjacent ground are not new, but there are serious differences between the calculation basics of current earth pressure teachings and the New Theory, which are discussed briefly in Section 2.5, page 43, and are examined in detail in Chapter 4, page 92ff.

Because no plans of the archive building or for the subway excavation site could be acquired for the investigations described below about the cause of the accident, pictures from the photo gallery and the infographic “Cross-section of the Cologne subway route” [B] from the Internet were used in order to reproduce the tunnel cross-section of the cave-in area according to constructional aspects. Fully aware of the numerous necessary assumptions, the following calculations regarding the cause of the accident have been formulated in such a way that they can be reproduced and verified as soon as real figures are known. Also because of the assumptions, the calculation results have been rounded more generously than is usual.

5.1.1 Assumptions on tunnel cross-section and substratum

It is assumed that the slotted retaining walls of the excavation pit measured $hs = 30,0$ m [B] from the street or terrain level (OKG) to the wall foot. The lamellar thickness of the slotted walls is estimated at $d = 1,0$ m, whereby integral steel girders serve to anchor the slotted wall into the ground. The underside of the tunnel floor (reinforced concrete), which is equal to the top level of the underwater concrete, is at height $hss = -25,0$ m measured from the OKG, and the cross-section of the tunnel shell has a clearance width of $bt = 14,50$ m. The long-term groundwater level was defined at height $hw = -5,00$ m below the OKG.

In accordance with the New Earth Pressure Theory, an inclination angle $\beta t = 65^\circ$, and an angle-dependent dry density $ptg = 2,046$ t/m³ were calculated for the quaternary gravel/sand substratum (see Appendix 1). Hereby, it is assumed that the soil can be described as firmly bedded, due to the repeated contact with groundwater, and its volume also remains constant, even if the pore water is removed (see Tests 2 and 3 regarding soil compaction through water (Section 2.4.3 and Figs. 19 to 21, page 42).

Not known are the individual layers of the tunnel floor (concreting process), the connection between tunnel floor and slotted walls, and the constructional

condition of the tunnel floor at the time of the accident. Moreover, it was not possible to find out whether the load required to counteract the uplift due to groundwater was applied exclusively by means of the invert construction, or if additional load dispersal was to be provided via railway platforms, walls, columns, and ceilings.

5.1.1.1 Load assumptions about the archive and residential building

The Historic Archive was a modern 7-floor building with a flat roof (Fig. 111). When scaled against the height of the neighbouring building, the upper floors must have been built with reduced clearance heights. More typical of the standard buildings in the street is the adjacent residential building with four floors and a converted attic. When comparing the construction method and the utilization of the two buildings, it is clear that the archive and its use as a library exerts a far higher load on the substratum than the simple residential building.

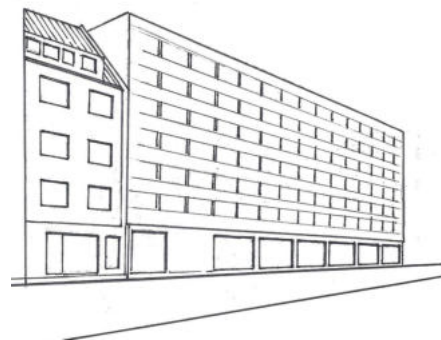


Fig. 111: Street view sketch of the archive with adjacent residential building.

The influences of the different substratum loads will be examined, whereby the following assumptions are made:

The clearance heights of the six upper floors are estimated at $h = 2,3$ m, and those of the ground floor and the cellar at $h = 3,5$ m. For the ground floor, a building width of $b = 13,5$ m is assumed, whereas a width of $b' = 14,0$ m is assumed for all upper floors due to the overhang on the street side. Assumed ceiling thicknesses of $d = 0,30$ m, and an assumed continuous base slab as building foundation with a thickness of 1,10 ms are used to determine the weight and masses below. The building height from the underside of the base plate is calculated by adding all the clearance heights $\sum h = 2 \cdot 3,5 + 6 \cdot 2,3 = 20,8$ m plus the ceilings and the base plate $\sum d = 8 \cdot 0,30 + 1,10 = 3,5$ m. Measured from street level (or OKG) and with the selected groundwater level WSp, the underside of the base plate is located at $\Delta h = hw = -5,0$ m, so that the

archive's height above OKG is $hh = \sum h + \sum d + hw = 20,8 + 3,5 - 5,0 = 19,3$ m. The sidewalk width between the rear edge (HK) of the slotted wall and the archive is estimated at $bb = 3,0$ m. Due to the overhang of the upper floors, the distance to the HK of the slotted wall is reduced to width $bb = 2,5$ m. For the calculations, a vertical reference axis is placed through the archive at a distance of $ble = 3,0 + b'/2 = 3,0 + 14,0/2 = 10,0$ m from the HK of the slotted wall. A calculation depth of $a = 1,00$ m is specified.

Structural weights of the archive

It is further assumed that the archive was built as a reinforced concrete frame construction, and the ceilings are supported by concrete pillars instead of internal walls. For load determination, the outer walls, central pillars, ceiling joists, and haunches of the building shell are given a width of $bw = 1,40$ m, together with a mean density of $p_1 = 2,20$ t/m³. A density of $p_2 = 2,50$ t/m³ is assigned to the reinforced concrete ceiling slabs and the base plate. The forces to be dispersed by the substratum are determined by means of the structural dimensions and the densities p_1 and p_2 .

Weight $Ge_1 \rightarrow$ of the walls with density $p_1 = 2,20$ t/m³

$$Ge_1 = bw \cdot \sum h \cdot p_1 \cdot g = 1,40 \cdot 20,8 \cdot 2,2 \cdot g = 628 \quad \text{kN} \quad 5.1$$

Weight $Ge_2 \rightarrow$ of the ceilings with density $p_2 = 2,50$ t/m³

$$Ge_2 = b' \cdot \sum d \cdot p_2 \cdot g = 14,0 \cdot 3,5 \cdot 2,5 \cdot g = 1201 \quad \text{kN} \quad 5.2$$

Weight Ge_3 , which covers the interior work of the eight floors and the roof, is calculated via the useful building area with width $b^* = b' - bw = 14,0 - 1,4 = 12,6$ m, and the assumed density $p_3 = 0,125$ t/m².

Weight $Ge_3 \rightarrow$ of the interior work with density $p_3 = 0,125$ t/m³

$$Ge_3 = 9 \cdot b^* \cdot p_3 \cdot g = 9 \cdot 12,6 \cdot 0,125 \cdot 9,807 = 139 \quad \text{kN} \quad 5.3$$

Weight $Ge_4 \rightarrow$ from live load $p_v = 5,0$ kN/m² (DIN 1054)

$$Ge_4 = 8 \cdot b^* \cdot p_v = 8 \cdot 12,6 \cdot 5,0 = 504 \quad \text{kN} \quad 5.4$$

Addition of the weight forces Ge_1 to Ge_4 divided by total width $b'' = b' + 2 \cdot 0,50 = 14,0 + 1,0 = 15,0$ m (foundation width plus overhangs) results in weight q_v per m². This force must be adapted to the properties of the loaded soil by means of dry density $ptg = 2,046$ t/m³ and gravity force $g = 9,807$ m/s². Dry density must be used here, because the pore water in the soil escapes under load, so that only the structure of the solids (solids volume) is available for force dispersal into the ground.

Weight q_v

$$q_v = (Ge_1 + Ge_2 + Ge_3 + Ge_4) / b''$$

$$q_v = (628 + 1201 + 139 + 504) / 15,0 = 164,8 \quad \text{kN/m}^2 \quad 5.5$$

Load height $he_1 \rightarrow$ with dry density $ptg = 2,046 \text{ t/m}^3$

$$he_1 = q_v / ptg \cdot g = 164,8 / 2,046 \cdot 9,807 \approx 8,20 \quad \text{m} \quad 5.6$$

Results:

The archive's structural weight including the live load for libraries $p_v = 0,5 \text{ kN/m}^2$ (DIN 1054) has a weight $q_v = 164,8 \text{ kN/m}^2$ (5.5). In order to disperse weight q_v into the soil below the archive, it has been converted into a load area with height $he_1 = 8,2 \text{ m}$ (5.6) and width $b'' = 15,0 \text{ m}$ (see Fig. 112 on page 168).

Structural weights of residential building

In order to obtain an opposing value to the archive's load dispersal, the residential building next to the archive was selected, and placed on the other side of the tunnel. Hereby, it is assumed that 4-floor buildings are predominant along the subway route, and that with its 7 floors the archive is an exception. Consequently, and due to the different building loads to the left and right of the subway cross-section, unequal force fields will act against the slotted walls of the tunnel (see Fig. 112, page 168, and Fig. 113, page 170).

For the fictive residential building on the left of the tunnel, a distance $bb' = 16,5 \text{ m}$ to the front edge of the left-hand slotted wall is selected. Moreover, the following values are used: clear height of the normal floors is $h = 2,50 \text{ m}$, and $h = 2,30 \text{ m}$ for the cellar and attic. Moreover, ceiling slab thickness is given as $d = 0,20 \text{ m}$, and thickness of the continuous base plate is $d = 0,70 \text{ m}$. By means of heights $\sum h = 2 \cdot 2,30 + 4 \cdot 2,75 = 15,6 \text{ m}$ plus the thickness of the six ceiling slabs plus base plate $\sum d = 6 \cdot 0,20 + 0,70 = 1,9 \text{ m}$, it is possible to establish a building height of $hg = 17,5 \text{ m}$ from the underside of the base plate, whereby the ceiling of the attic apartment is valued as part of the ridged roof. The width of the residential building is set at $b = 11,5 \text{ m}$, so that after deduction of the supporting walls with width $b_w = 1,3 \text{ m}$, a useful area width of $b^* = b - b_w = 11,5 - 1,3 = 10,2 \text{ m}$ remains. Live load $p_v = 0,150 \text{ t/m}^2$, and load $p_3 = 0,125 \text{ t/m}^2$ for light transverse walls and other interior work are taken into account by means of width b^* . The underside of the base plate is placed at $\Delta h = -2,80 \text{ m}$ below street level. The above values are used to calculate the weights of the residential building.

Determining the structural weights of the residential building

Weight Ge_1 → of the walls with density $p_4 = 2,00 \text{ t/m}^3$

$$Ge_1 = bw \cdot \sum h \cdot p_4 \cdot g = 1,30 \cdot 15,6 \cdot 2,0 \cdot g = 398 \quad \text{kN} \quad 5.7$$

Weight Ge_2 → of the ceilings with density $p_2 = 2,50 \text{ t/m}^3$

$$Ge_2 = b' \cdot \sum d \cdot p_2 \cdot g = 11,5 \cdot 1,9 \cdot 2,5 \cdot g = 536 \quad \text{kN} \quad 5.8$$

Weight Ge_3 → of the interior work with density $p_3 = 0,125 \text{ t/m}^3$

$$Ge_3 = 6 \cdot b^* \cdot p_3 \cdot g = 6 \cdot 10,2 \cdot 0,125 \cdot 9,807 = 75 \quad \text{kN} \quad 5.9$$

Weight Ge_4 → from live load $p_v = 1,5 \text{ kN/m}^2$ (DIN 1054)

$$Ge_4 = 6 \cdot b^* \cdot p_v = 6 \cdot 10,2 \cdot 1,5 = 92 \quad \text{kN} \quad 5.10$$

Adding the weight forces and then dividing the sum by the foundation width plus foundation overhang $b'' = 11,5 + 0,5 = 12,0 \text{ m}$, results in a weight per m^2 that must be adapted to the properties of the substratum as above.

Weight q_v

$$q_v = (Ge_1 + Ge_2 + Ge_3 + Ge_4) / b''$$

$$q_v = (398 + 536 + 75 + 92) / 12,0 = 91,8 \quad \text{kN/m}^2 \quad 5.11$$

Load height he_2 → with dry density $ptg = 2,046 \text{ t/m}^3$

$$he_2 = q_v / ptg \cdot g = 91,8 / (2,046 \cdot 9,807) = 4,6 \quad \text{m} \quad 5.12$$

Results:

The residential building including the live load $p_v = 1,5 \text{ kN/m}^2$ (DIN 1054) has a weight of $q_v = 91,8 \text{ kN/m}^2$ (5.11), which results in a load height $he_2 = 4,6 \text{ m}$ (5.12) after conversion with the characteristics of the adjacent soil. Load height he_2 must be applied over the entire width $b'' = 12,0 \text{ m}$ (Fig. 113, page 170). If one compares load height $he_1 = 8,2 \text{ m}$ (5.6) of the archive (Fig. 112, page 168) with load height $he_2 = 4,6 \text{ m}$ (5.12) of the residential building, the different loads on the substratum and thereby on the slotted walls are obvious.

5.1.1.2 Assumptions for soil properties

The infographic “Cross-section of the Cologne subway route” [B] shows quaternary gravels/sands as substratum. This soil type is used as the basis for determining the other properties for the individual soil conditions (see Chapter 3, page 54).

If one imagines the quaternary gravel/sand in a dried state for the following calculations, it is possible to convert the dry soil into a moist soil, a wet soil, or a 'soil under water' simply by adding water. Every soil, whether in the dry, moist, or wet state, represents a specific soil type with own parameters. The different inclination angles and densities of the soils enable the forces next to

and under the tunnel cross-section to be investigated, and assign them to the individual structural components.

Moreover, Tests 2 and 3 in Sections 2.4.2 and 2.4.3 showed that the volume of a 'wet soil under water' does not change, if the water is removed from the soil and subsequently introduced again. For the soil volume under the buildings, this permits the deduction that the soil volume is not influenced simply by removing the water during the process of lowering the groundwater level. Also if fine particles (sand) were removed from the adjacent soil when pumping off the groundwater, this should hardly have affected the stability of the soil under the buildings. Moreover, it is possible that the inflow of groundwater from more distant regions could have flushed new fine particles into the soil below the buildings.

Properties of dry gravel

According to the New Earth Pressure Theory, a dry density $ptg = 2,046 \text{ t/m}^3$ and an inclination angle $\beta t = 65,0^\circ$ can be assigned to quaternary gravel/sand, from which the following additional soil properties can be calculated:

Dry density $ptg = 2,046 \text{ t/m}^3 \rightarrow$ via the inclination angle $\beta t = 65^\circ$

$$ptg = p_{90} / (1 / \tan \beta t + 1) = 3 / (1/2,146 + 1) = 2,046 \text{ t/m}^3 \quad 5.13$$

Solids volume Vf

$$Vf = ptg \cdot Vp_{90} / p_{90} = 2,046 \cdot 1,000 / 3,0 = 0,682 \text{ m}^3 \quad 5.14$$

Pore volume Vl

$$Vl = Vp_{90} - Vf = 1,000 - 0,682 = 0,318 \text{ m}^3 \quad 5.15$$

Properties of wet gravel with completely water-filled pores:

Weight of pore water $pwg = 1,00 \text{ t/m}^3$

$$pwg = Vl \cdot pwg / Vp_{90} = 0,318 \cdot 1,0 / 1,0 = 0,318 \text{ t/m}^3 \quad 5.16$$

Wet density png

$$png = ptg + pwg = 2,046 + 0,318 = 2,364 \text{ t/m}^3 \quad 5.17$$

Inclination angle $\beta n \rightarrow ptg_{90} = 3,00 \text{ t/m}^3$

$$\tan \beta n = Vf / (Vl + Vl \cdot pwg / ptg_{90})$$

$$\tan \beta n = 0,682 / (0,318 + 0,318 \cdot 1,0 / 3,0) = 1,609 \quad 5.18$$

$$\beta n = 58,1^\circ \quad [-] \quad 5.19$$

Properties of wet gravel under water

Conversion of a dry soil into a wet soil under water has been described in Section 3.2.1.

Solids volume Vfw

$$Vfw = 2 \cdot Vf / 3 = 2 \cdot 0,682 / 3 = 0,455 \text{ m}^3 \quad 5.20$$

Uplift volume Vfa

$$Vfa = Vf/3 = 0,682/3 = 0,227 \quad \text{m}^3 \quad 5.21$$

Fictitious dry density under water $ptwg$

$$ptwg = Vf_w \cdot ptg_{90}/Vp_{90} = 0,455 \cdot 3,0/1,0 = 1,364 \quad \text{t/m}^3 \quad 5.22$$

Wet density under water $pnwg$

$$pnwg = ptwg + p_w = 1,364 + 0,318 = 1,682 \quad \text{t/m}^3 \quad 5.23$$

Density $pawg \rightarrow$ to determine the uplift force

$$pawg = Vfa \cdot ptg_{90}/Vp_{90} = 0,227 \cdot 3,0/1,0 = 0,682 \quad \text{t/m}^3 \quad 5.24$$

Inclination angle β_{nw}

$$\tan \beta_{nw} = Vf_w / (Vl + Vl/3 - Vl/2)$$

$$\tan \beta_{nw} = 0,455 / (0,318 - 0,318/6) = 1,717 \quad 5.25$$

$$\beta_{nw} = 59,8^\circ \quad [-] \quad 5.26$$

Results:

The following properties were calculated for the quaternary gravel:

Wet gravel	Wet gravel under water
Wet density $p_{ng} = 2,364 \text{ t/m}^3$ (5.17)	Wet density $p_{nwg} = 1,682 \text{ t/m}^3$ (5.23)
Inclination angle $\beta_n = 58,1^\circ$ (5.19)	Inclination angle $\beta_{nw} = 59,8^\circ$ (5.26)
Under water: Uplift density $p_{awg} = 0,682 \text{ t/m}^3$ (5.24)	

During the above calculations, a possible reduction of solids volume that might have occurred through the removal of fine particles from the substratum during lowering of the groundwater level, was not taken into account.

5.1.2 Load on substratum due to the building weights

The archive and the residential building must be seen as loads on the substratum, which are represented by the substitute load height he and foundation width b'' as load area Ae , and act on the foundation bed (underside of base plate). In order to trace the force dispersals in the ground, a vertical reference axis is placed centrally in area $Ae = he \cdot b''$, and the wedge area of the soil's dead weight $Ao = bo \cdot ho/2$ is placed to the left and right of the axis with width $bo = b''/2$ and height ho . Wedge height ho can be determined via width bo and inclination angle $\beta_n = 58,1^\circ$ (5.19). Height he of load area Ae below area Ao must be arranged so that equal halves of load area Ae are located to the left and right of the axis. The partial areas $Ae/2$ must be divided diagonally into active area Aa and reactive area Ar , whereby the diagonal within area $Ae/2$ must be seen as a new inclined plane with angle β_e . For force determination, the active area Ao of the soil's dead weight and the active area Aa of the structural weight

must be added to area $Ac = Ao + Aa$. Next, weight Ge across area Ac is multiplied with wet density $png = 2,364 \text{ t/m}^3$ (5.17) and gravity force $g = 9,807 \text{ m/s}^2$ (see Section 2.5).

Wet density png and inclination angle βn were selected for force determination because it is unlikely that in spite of the mentioned 'excessively high water removal' during tunnel construction, the originally wet gravel has been converted into a moist, partially saturated gravel. Moreover, it would only be possible to establish the soil's pore water by taking unaffected samples on site.

Force areas under the archive

The following data are available for calculation:

Properties of wet gravel	Dimensions of archive
Wet density $png = 2,364 \text{ t/m}^3$ (5.17)	Height $he_l = 8,2 \text{ m}$ (5.6)
Inclination angle $\beta n = 58,1^\circ$ (5.19)	Height $\Delta h = -5,0 \text{ m}$
Slotted wall height $hs = 30,0 \text{ m}$	Width $b'' = 15,0 \text{ m}$
Distance width $ble = 10,0 \text{ m}$ (rear of slotted wall to reference axis)	
Groundwater lowered to underside of tunnel floor $hss = -25,0 \text{ m}$	

The dimensions to be determined are shown in Fig. 112 below.

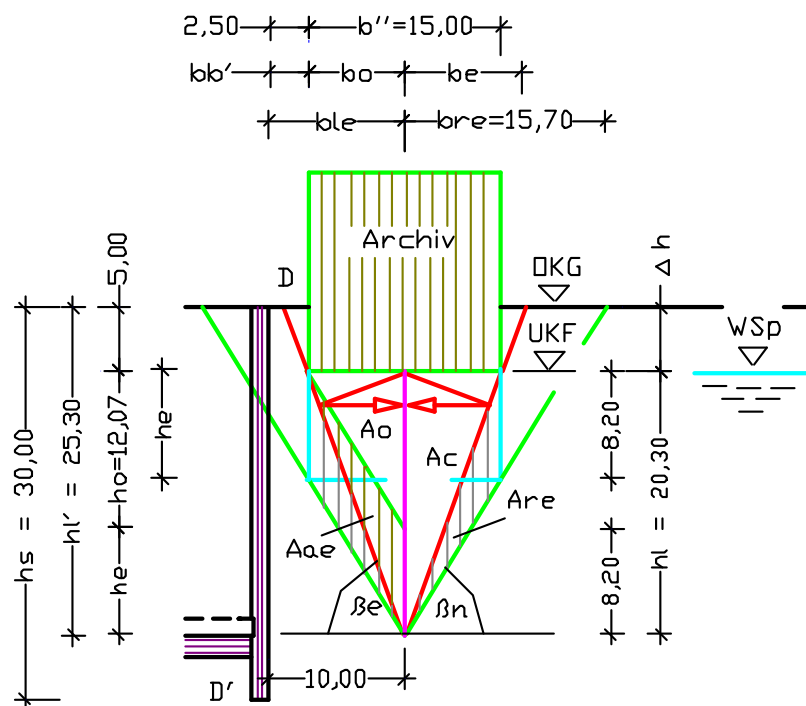


Fig. 112: Force fields for load dispersal in the ground under the archive.

Calculation:

Width bo

$$bo = b''/2 = 15,00/2 = 7,50$$

m 5.27

Height h_o	$h_o = b_o \cdot \tan \beta_n = 7,50 \cdot 1,609 = 12,07$	m	5.28
Load area A_o	$A_o = b_o \cdot h_o/2 = 7,50 \cdot 12,07/2 = 45,26$	m ²	5.29
Load area A_e	$A_e = b_o \cdot h_e/2 = 7,50 \cdot 8,20/2 = 30,75$	m ²	5.30
Height h_l	$h_l = h_o + h_e = 12,07 + 8,20 = 20,27$	m	5.31
Active load area A_c	$A_c = b_o \cdot h_l/2 = 7,50 \cdot 20,27/2 = 76,01$	m ²	5.32
Height $h_l' \rightarrow$ terrain level up to tip of the force field	$h_l' = h_l + \Delta h = 20,27 + 5,00 = 25,27$	m	5.33
Inclination angle β_e	$\tan \beta_e = h_l/b_o = 20,27/7,50 = 2,703$		5.34
	$\beta_e = 69,7^\circ$	[-]	5.35
Width b_e	$b_e = h_l' / \tan \beta_e = 25,27/2,703 = 9,35$	m	5.36
Width b_{re}	$b_{re} = h_l' / \tan \beta_n = 25,27/1,609 = 15,72 \sim 15,7$	m	5.37

The inclination angle β_e can be reproduced mathematically by means of the loaded soil volumes. For this, areas $A_o = 45,26 \text{ m}^2$ (5.29) and $A_e = 30,75 \text{ m}^2$ (5.30) must first be converted into the volumes V_o and V_e by means of calculation depth $a = 1,00 \text{ m}$, after which their volumes can be determined. Already known are volumes $V_f = 0,682 \text{ m}^3$ (5.14) and $V_l = 0,318 \text{ m}^3$ (5.15) of the dry soil. If volume V_o is multiplied with the volumes V_f and V_l , the volumes $\sum V_{fo}$ and $\sum V_{lo}$ are obtained. Moreover, volume V_o is subjected to the substitute load of the archive, whose active part has been determined on both sides of the vertical reference axis by means of area $A_e = 30,75 \text{ m}^2$ (5.30) and volume V_e . Volume $\sum V_{fe}$ is determined by means of volumes V_e and V_f . The angle function of the wet soil is available for calculating $\tan \beta_e$.

Volume $\sum V_f$	$\sum V_f = A_c \cdot a \cdot V_f = 76,01 \cdot 1,0 \cdot 0,682 = 51,84$	m ³	5.38
Volume $\sum V_l$	$\sum V_l = A_o \cdot a \cdot V_l = 45,26 \cdot 1,0 \cdot 0,318 = 14,39$	m ³	5.39
Inclination angle β_e^*	$\tan \beta_e^* = \sum V_f / 1,333 \cdot \sum V_l = 51,84 / 1,333 \cdot 14,39 = 2,703$		5.40
	$\beta_e^* = 69,7^\circ$	[-]	5.41

Results for the archive:

Width $bo = 7,50$ m (5.27)	Height $ho = 12,07$ m (5.28)
Width $be = 9,35$ m (5.36)	Height $hl = 20,27$ m (5.31)
Width $bre = 15,70$ m (5.37)	Height $hl' = 25,27$ m (5.33)
Inclination angle $\beta e = 69,7^\circ$	Area $Ac = 76,0$ m ² (5.32)

Moreover, the equal angles βe and $\beta e^* = 69,7^\circ$ show that loads and their dispersal into the ground can be traced by means of the soil volumes.

Force areas under the residential building

The following data are available for calculation:

Wet gravel	Residential building
Wet density $\rho_{ng} = 2,364$ t/m ³	Height $he_1 = 4,60$ m (5.12)
Inclination angle $\beta n = 58,1^\circ$	Height $\Delta h = -2,80$ m
Slotted wall height $hs = 30$ m	Width $b'' = 12,00$ m
Distance width $bre = 15,70$ m (reference axis to slotted wall)	

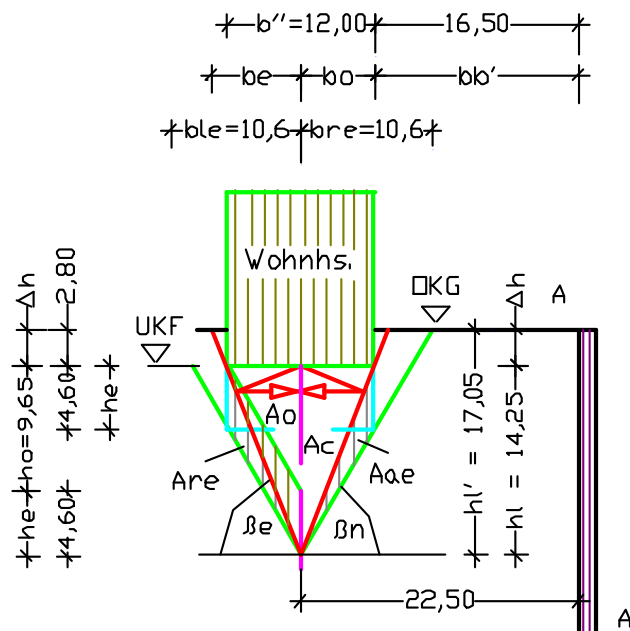


Fig. 113: Force fields for load dispersal in the ground under the residential building.

Calculation:

Width bo

$$bo = b''/2 = 12,00/2 = 6,00 \quad \text{m} \quad 5.42$$

Height ho

$$ho = bo \cdot \tan \beta n = 6,00 \cdot 1,609 = 9,65 \quad \text{m} \quad 5.43$$

Height hl

$$hl = ho + he = 9,65 + 4,60 = 14,25 \quad \text{m} \quad 5.44$$

Height hl' → terrain level up to tip of the force field

$$hl' = hl + \Delta h = 14,25 + 2,80 = 17,05 \quad \text{m} \quad 5.45$$

Inclination angle β_{ne}

$$\tan \beta_{ne} = hl/bo = 14,25/6,00 = 2,375 \quad 5.46$$

$$\beta_{ne} = 67,2^\circ \quad [-] \quad 5.47$$

Width be

$$be = hl' / \tan \beta_{ne} = 17,05/2,375 = 7,18 \quad \text{m} \quad 5.48$$

Width ble → $\tan \beta_n = 1,609$ (5.18)

$$ble = hl' / \tan \beta_n = 17,05/1,609 = 10,60 \quad \text{m} \quad 5.49$$

Load area Ae

$$Ae = 2 \cdot bo \cdot he = 2 \cdot 6,00 \cdot 4,60 = 55,2 \quad \text{m}^2 \quad 5.50$$

Active load area Ac

$$Ac = bo \cdot hl/2 = 6,00 \cdot 14,25/2 = 42,8 \quad \text{m}^2 \quad 5.51$$

Results for residential building:

Width $bo = 6,00$ m (5.42)	Height $hl = 14,25$ m (5.44)
Width $be = 7,18$ m (5.48)	Height $hl' = 17,05$ m (5.45)
Inclination angle $\beta_e = 67,2^\circ$	Area $Ac = 42,8$ m ² (5.51)

5.1.3 Forces from the substratum against the tunnel cross-section

Fig. 114 below shows the earth wedges with their areas A_{ol} and A_{or} , which load the 30 m high slotted walls, whereby the groundwater level has been lowered to height $h_{ss} = 25$ m (upper side of underwater concrete). Initially, the building weights (archive and residential building) are not taken into account.

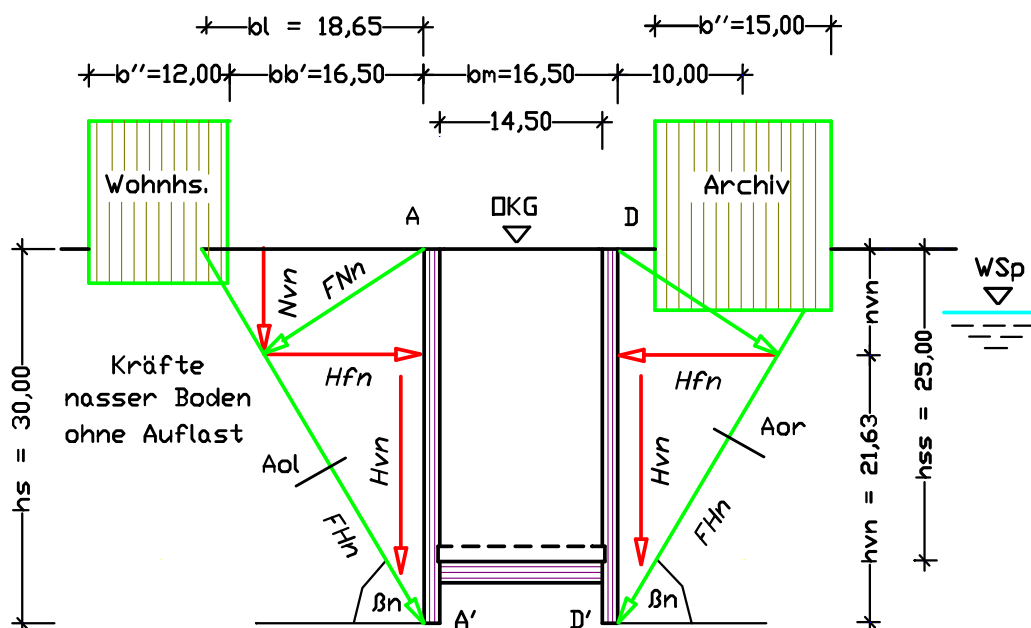


Fig. 114: Active force areas of the wet soil against the slotted walls, but without the influence of building weights and groundwater.

Forces against the slotted walls (only earth loads)

Available for calculation are: Slotted wall height $h_s = 30,00$ m, wet density $p_{ng} = 2,364$ t/m³ (5.17), and inclination angle $\beta_n = 58,1^\circ$ (5.19). The load areas and the forces against the walls are to be determined.

Forces from area $A_{ol} = A_{or}$

Width bl

$$bl = h_s / \tan \beta_n = 30,00 / 1,609 = 18,65 \quad \text{m} \quad 5.52$$

Load area $A_{ol} = A_{or}$

$$A_{ol} = A_{or} = h_s \cdot bl / 2 = 30,00 \cdot 18,65 / 2 = 279,8 \quad \text{m}^2 \quad 5.53$$

Weight G_{tl}

$$G_{tl} = A_{ol} \cdot p_{tg} \cdot g = 279,8 \cdot 2,046 \cdot 9,807 = 5614 \quad \text{kN} \quad 5.54$$

Weight G_{nl}

$$G_{nl} = A_{ol} \cdot p_{ng} \cdot g = 279,8 \cdot 2,364 \cdot 9,807 = 6487 \quad \text{kN} \quad 5.55$$

Force N_{vn}

$$N_{vn} = G_{nl} \cdot \cos^2 \beta_n = 6487 \cdot \cos^2 58,1^\circ = 1811 \quad \text{kN} \quad 5.56$$

Force H_{vn}

$$H_{vn} = G_{nl} \cdot \sin^2 \beta_n = 6487 \cdot \sin^2 58,1^\circ = 4676 \quad \text{kN} \quad 5.57$$

Force H_{fn}

$$H_{fn} = G_{nl} \cdot \sin \beta_n \cdot \cos \beta_n = 6487 \cdot 0,849 \cdot 0,528$$

$$H_{fn} = 2908 \quad \text{kN} \quad 5.58$$

Force index $g_{in} \rightarrow$ for conversion of forces into force meters

$$g_{in} = bol \cdot p_{tg} \cdot g / 2 = 18,65 \cdot 2,364 \cdot g / 2 = 216,2 \quad \text{kN/m}^2 \quad 5.59$$

Force meter n_{vn}

$$n_{vn} = N_{vn} / g_{in} = 1810 / 216,2 = 8,37 \quad \text{m} \quad 5.60$$

Force meter h_{vn}

$$h_{vn} = H_{vn} / g_{in} = 4676 / 216,2 = 21,63 \quad \text{m} \quad 5.61$$

Force meter h_{fn}

$$h_{fn} = H_{fn} / g_{in} = 2908 / 216,2 = 13,45 \quad \text{m} \quad 5.62$$

Forces from area A_{ol}'

Area A_{ol}' is used to determine the forces acting out of the ground against the slotted wall from terrain level down to the underside of the tunnel floor $-25,30$ m = height hl' .

Width $bol' = bor'$

$$bol' = bor' = hl' / \tan \beta_n = 25,27 / 1,609 = 15,70 \quad \text{m} \quad 5.63$$

Area A_{ol}'

$$A_{ol}' = hl' \cdot bol' / 2 = 25,27 \cdot 15,70 / 2 = 198,6 \quad \text{m}^2 \quad 5.64$$

Weight Gnl'

$$Gnl' = Aol' \cdot png \cdot g = 198,6 \cdot 2,364 \cdot 9,807 = 4604 \quad \text{kN} \quad 5.65$$

Force Nvn'

$$Nvn' = Gnl' \cdot \cos^2 \beta n = 4604 \cdot \cos^2 58,1^\circ = 1286 \quad \text{kN} \quad 5.66$$

Force Hvn'

$$Hvn' = Gnl' \cdot \sin^2 \beta n = 4604 \cdot \sin^2 58,1^\circ = 3318 \quad \text{kN} \quad 5.67$$

Force Hfn'

$$Hfn' = Gnl' \cdot \sin \beta n \cdot \cos \beta n = 4604 \cdot 0,849 \cdot 0,528$$

$$Hfn' = 2064 \quad \text{kN} \quad 5.68$$

Force index gin'

$$gin' = bol' \cdot ptg \cdot g / 2 = 15,70 \cdot 2,364 \cdot g / 2 = 182,0 \text{ kN/m}^2 \quad 5.69$$

Force meter $nv n'$

$$nv n' = Nvn' / gin' = 1285 / 182,0 = 7,06 \quad \text{m} \quad 5.70$$

Force meter hvn'

$$hvn' = Hvn' / gin' = 3315 / 182,0 = 18,21 \quad \text{m} \quad 5.71$$

Force meter hfn'

$$hfn' = Hfn' / gin' = 2064 / 182,0 = 11,34 \quad \text{m} \quad 5.72$$

The above calculations do not include the forces acting against the right-hand slotted wall due to the archive's force dispersal. These will be determined in the following Section (see Fig. 115, page 174).

The loads from the residential building are not taken into account, because they do not influence the forces from area Aol against the left-hand supporting wall.

Results:

Calculated forces against the slotted walls, and the different heights:

Forces from area Aol	Forces from area Aol'
Wet density $png = 2,364 \text{ t/m}^3$	Inclination angle $\beta n = 58,1^\circ$
Wedge height $hs = 30,00 \text{ m}$	Wedge height $hl' = 25,27 \text{ m}$ (5.33)
Width $bl = 18,65 \text{ m}$ (5.52)	Width $bol' = 15,70 \text{ m}$ (5.63)
Area $Aol = 279,8 \text{ m}^2$ (5.53)	Area $Aol' = 198,6 \text{ m}^2$ (5.64)
Force $Gnl = 6487 \text{ kN}$ (5.55)	Force $Gnl' = 4604 \text{ kN}$ (5.65)
Force $Nvn = 1811 \text{ kN}$ (5.56)	Force $Nvn' = 1286 \text{ kN}$ (5.66)
Force $Hvn = 4676 \text{ kN}$ (5.57)	Force $Hvn' = 3318 \text{ kN}$ (5.67)
Force $Hfn = 2908 \text{ kN}$ (5.58)	Force $Hfn' = 2064 \text{ kN}$ (5.68)
Force meter $nv n = 8,37 \text{ m}$ (5.60)	Force meter $nv n' = 7,06 \text{ m}$ (5.70)
Force meter $hvn = 21,63 \text{ m}$ (5.61)	Force meter $hvn' = 18,21 \text{ m}$ (5.71)
Force meter $hfn = 13,45 \text{ m}$ (5.62)	Force meter $hfn' = 11,34 \text{ m}$ (5.72)

5.1.4 Forces from archive and substratum against right-hand slotted wall

Due to the merging of force areas from building load dispersal with the pure earth pressure (areas Aol and Aol'), different load diagrams result (Fig. 115). Because the load areas mentioned above do not overlap on the left-hand side of the tunnel cross-section – and depending on load condition – the forces from area Aol (5.53), with wedge height $hs = 30,0$ m, or the forces from area Aol' (5.64), with wedge height $hl' = 25,3$ m (5.33), become decisive for dimensioning the left-hand slotted wall. On the right-hand side of the tunnel cross-section, the pure earth pressure force from area Aor cannot be used for dimensioning the right-hand slotted wall (Fig. 114), because force area Aor is completely superimposed by the force areas Ac of the load dispersals under the archive (Fig. 115). As a result, only area Aco remains for determining the forces acting against the right-hand slotted wall. Because width $be = 9,35$ m (5.36) in the terrain plane – which is measured from the archive's reference axis to Point D – the distances width $ble = 10,00$ m from the reference axis to the rear edge of the slotted wall is not fully covered, a residual width $be' = ble - be = 10,00 - 9,35 = 0,65$ m remains. In order to determine residual width $be' = 0,65$ m by means of area Aco , height hro is determined via width ble and angle βe of the right-hand slotted wall, whereby the wedge area – which is calculated from width be' and height Δh , and exceeds the terrain plane – is not taken into account.

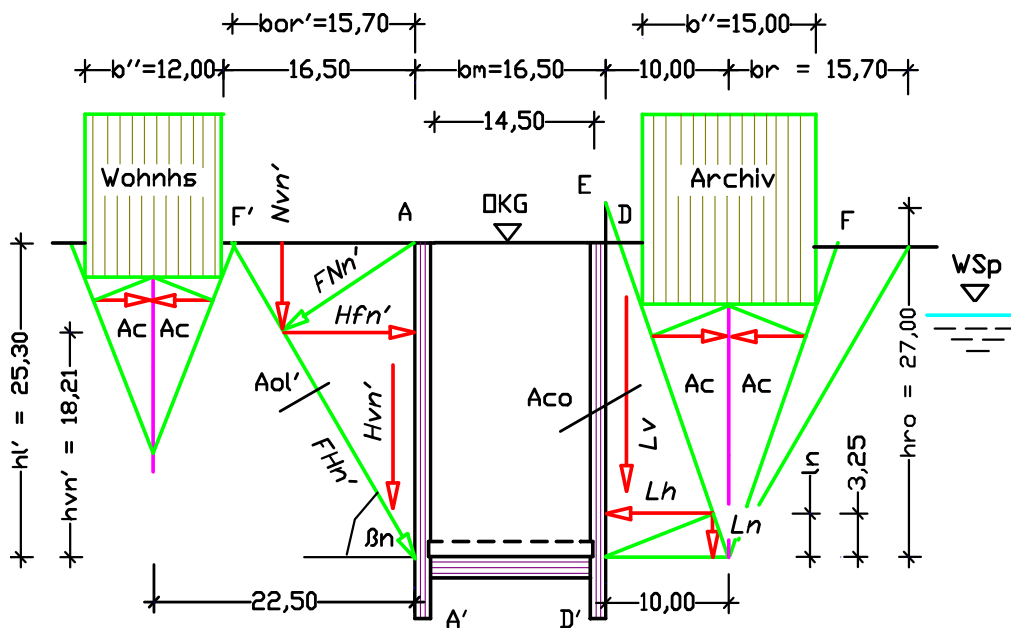


Fig. 115: Load areas at left and right of the tunnel, which are used for dimensioning the slotted walls.

The following are determined:

Height $hro \rightarrow$ with angle $\beta e = 69,7^\circ$ (5.35) $\rightarrow \tan \beta e = 2,703$ (5.34)

$$hro = ble \cdot \tan \beta e = 10,00 \cdot 2,703 = 27,03 \quad \text{m} \quad 5.73$$

Load area Aco

$$Aco = ble \cdot hro/2 = 10,0 \cdot 27,03/2 = 135,0 \quad \text{m}^2 \quad 5.74$$

Weight Gen

$$Gen = Aco \cdot png \cdot g = 135,0 \cdot 2,364 \cdot 9,807 = 3130 \quad \text{kN} \quad 5.75$$

Force Ln

$$Ln = Gen \cdot \cos^2 \beta e = 3130 \cdot 0,120 = 376 \quad \text{kN} \quad 5.76$$

Force Lv

$$Lv = Gen \cdot \sin^2 \beta e = 3130 \cdot 0,880 = 2754 \quad \text{kN} \quad 5.77$$

Force Lh

$$Lh = Gen \cdot \sin \beta e \cdot \cos \beta e$$

$$Lh = 3130 \cdot 0,938 \cdot 0,347 = 1019 \quad \text{kN} \quad 5.78$$

Force index gin

$$gin = ble \cdot png \cdot g/2 = 10,0 \cdot 2,364 \cdot g/2 = 115,9 \text{ kN/m}^2 \quad 5.79$$

Force meter ln

$$ln = Ln/gin = 376/115,9 = 3,25 \quad \text{m} \quad 5.80$$

Force meter lv

$$lv = Lv/gin = 2754/115,9 = 23,75 \quad \text{m} \quad 5.81$$

Force meter lh

$$lh = Lh/gin = 1019/115,9 = 8,80 \quad \text{m} \quad 5.82$$

Results:

The horizontal force $Hfn' = 2064 \text{ kN}$ (5.68) acting against the slotted wall from the wet substratum with thrust height $hvn' = 18,21 \text{ m}$ (5.71), is converted into horizontal force $Lh = 1019 \text{ kN}$ (5.78) with thrust height $ln = 3,25 \text{ m}$ (5.80) due to the load distribution from the archive.

Forces from area Aco	
Wet density $png = 2,364 \text{ t/m}^3$	Inclination angle $\beta ne = 69,7^\circ$
Wedge height $hro = 27,03 \text{ m}$ (5.73)	Wedge width $ble = 10,00 \text{ m}$
Force $Gen = 3130 \text{ kN}$ (5.75)	Area $Aco = 135,0 \text{ m}^2$ (5.74)
Force $Ln = 376 \text{ kN}$ (5.76)	Force meter $ln = 3,25 \text{ m}$ (5.80)
Force $Lv = 2754 \text{ kN}$ (5.77)	Force meter $lv = 23,75 \text{ m}$ (5.81)
Force $Lh = 1019 \text{ kN}$ (5.78)	Force meter $lh = 8,80 \text{ m}$ (5.82)

5.1.5 Formation of earth blocks to determine the uplift forces

In order to distribute the forces onto the slotted walls and the tunnel floor, the calculated force areas must be combined into earth blocks. Due to the introduced horizontal calculation level, which simultaneously represents the lowered groundwater level, blocks are formed above and below this plane. Height $hl' = 25,27$ m (5.33) shows the distance from the top of the terrain level down to this plane (see Fig. 116).

The block area above the assumed groundwater level, and to the left of the tunnel is calculated by means of height hl' and width $bol' = 15,7$ m (5.63). The inclined plane with angle $\beta n = 58,1^\circ$ must be assigned to this area. The two earth blocks to the right of the tunnel share the overall width $br = 10,0 + 15,7 = 25,7$ m. Their inclination angles are $\beta ne = 69,7^\circ$ (5.35) and $\beta n = 58,1^\circ$.

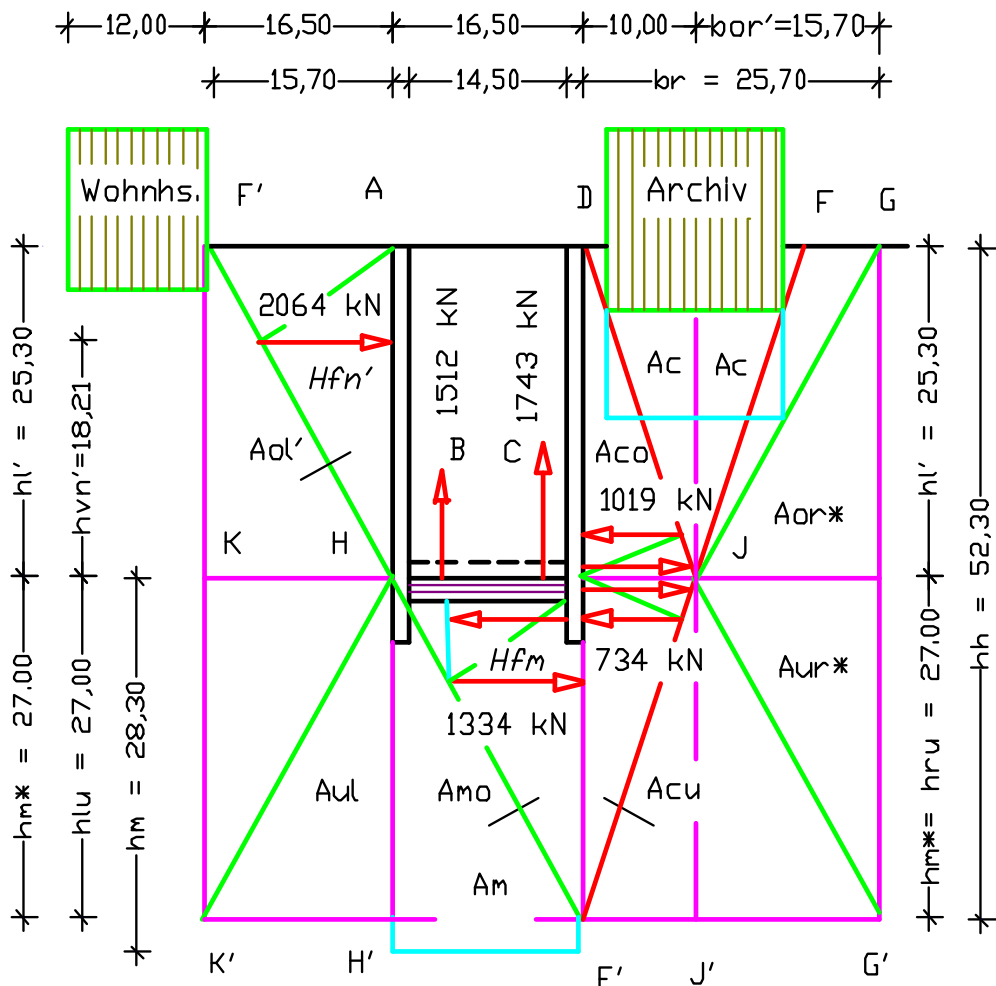


Fig. 116: Load areas of earth blocks above and below the lowered groundwater level (top side of underwater concrete).

Because the blocks below the horizontal calculation level are located in the groundwater area, their soil properties had to be adapted to 'wet soil under

water', and the widths of the upper blocks transferred to the lower blocks. In this way, height hlu of the left-hand earth block can be determined via width $bol' = 15,70$ m (5.63) and angle β_{ew} (5.84).

Normally, i.e. without the dominant load from the archive, the vertical calculation axis for the earth block below the tunnel cross-section would pass centrally through the cross-section. This would permit height hm of the middle earth block to be determined via half of width bm and inclination angle $\beta_{nw} = 59,8^\circ$ (5.26). In this case, the inclination angle $\beta_e = 69,7^\circ$ (5.35) of force area Ac_o on the right-hand side of the tunnel profile indicates that the load from the archive has not yet been dispersed. Consequently, force area Ac_o must be mirrored vertically, thereby creating area Ac_u . Because this force area enters the groundwater, its inclination angle β_e changes to angle β_{ew} (5.84), and its wedge height hro changes to height hru (also see Figs. 114 and 115).

Angle β_{ew} can be calculated from the same volumes as angle β_e (5.40), but here, the formula approach for 'wet soil under water' must be applied. Apart from angle β_{ew} , also width $be = 9,35$ m (5.36) is available for calculating height hru . If one plots height hru vertically downwards below plane (K–H–J), a through-point is obtained, at which the right-hand inclined plane below angles β_{nw} and β_n rises up to the terrain plane, thereby determining the width of the right-hand earth block. On the left-hand tunnel side, the earth block above the lowered groundwater levels has already been determined with height $hl' = 25,3$ m and width $bor = 15,7$ m (5.63). Height hlu of the left-hand earth block under water can be calculated via width bor and angle β_{nw} . Block height hm is established below the tunnel cross-section, which can be determined from width bm and angle β_{nw} . To also enable the uplift forces under water to be calculated via a uniform block height, the different heights hlu , hm , and hru must be adapted under constructional aspects. Further aspects to be taken into account, are seen in the restriction of force flow due to the slotted wall in the rising left-hand inclined plane, and in height $hb = 2,00$ m with underwater concrete.

Apart from the block dimensions, the following densities below and above the lowered groundwater level are available for determining the uplift forces acting below the tunnel floor: dry density $ptg = 2,046$ t/m³ and wet density $png = 2,364$ t/m³ (5.17) above the groundwater level, and fictitious dry density $ptwg = 1,364$ t/m³ (5.22) and wet density $pnwg = 1,682$ t/m³ (5.23) above it.

It must be mentioned that the New Earth Pressure Theory uses the dry soil densities to calculate the uplift forces, and thereby does not follow the calculation method of the teachings using the stationary and non-stationary pore water pressure. Determination of uplift via the pore water pressure is rejected, because in free nature, water under pressure gives way, and is therefore not available for transmitting the earth forces against the tunnel floor. For its force system, the New Earth Pressure Theory uses the solids structures of the adjacent soils, and recognizes that force differences in the earth blocks can lead to soil shifting or soil lifting. Consequently, fluctuating pore water quantities or groundwater variations in the ground are not important for determining the uplift forces. For adaptation of the block heights under water, first the inclination angle β_{ew} , and then heights h_{lu} , h_{m^*} , and h_{ru} are calculated. Volumes $\sum V_f = 51,84 \text{ m}^3$ (5.38) and $\sum V_l = 14,39 \text{ m}^3$ (5.39) as well as the following formula are available for calculating the angle:

$$\tan \beta_{nw} = V_{fw} / (5/6 \cdot \sum V_l) \quad (5.25)$$

When calculating the inclination angle for the soil under water, uplift of the solids is taken into account by reducing the solids volumes by 1/3. Thereby, volume $V_{fw} = 0,667 \cdot V_f$ remains for calculation.

Inclination angle $\beta_{ew} \rightarrow \sum V_f = 51,84 \text{ m}^3$ (5.38) and $\sum V_l = 14,39 \text{ m}^3$ (5.39)

$$\tan \beta_{ew} = 0,667 \cdot \sum V_f / (5/6 \cdot \sum V_l) \quad (5.40)$$

$$\tan \beta_{ew} = 0,667 \cdot 51,84 / (5/6 \cdot 14,39) = 2,883 \quad 5.83$$

$$\beta_{ew} = 70,9^\circ \quad [-] \quad 5.84$$

Height h_{ru}

$$h_{ru} = b_e \cdot \tan \beta_{ew} = 9,35 \cdot 2,883 = 27,0 \quad \text{m} \quad 5.85$$

Height $h_{lu} \rightarrow$ with width $bol' = 15,70 \text{ m}$ (5.63) and $\tan \beta_{nw} = 1,717$ (5.25)

$$h_{lu} = bol' \cdot \tan \beta_{nw} = 15,70 \cdot 1,717 = 27,0 \quad \text{m} \quad 5.86$$

Height $h_m \rightarrow$ with width $bm = 16,50 \text{ m}$ and $\tan \beta_{nw} = 1,717$ (5.25)

$$h_m = bm \cdot \tan \beta_{nw} = 16,50 \cdot 1,717 = 28,3 \quad \text{m} \quad 5.87$$

In general, the uplift against the tunnel floor from the soil volume is calculated via height $h_m = 28,3 \text{ m}$ (5.87). But hereby, several factors influence the uplift. Firstly, the underwater concrete – with estimated height $hb = 2,00 \text{ m}$ – reduces the soil's volume, from which the uplift is generated, and secondly, there is a difference between soil density $ptwg = 1,364 \text{ t/m}^3$ and density $p = 2,400 \text{ t/m}^3$ of the underwater concrete. Moreover, height hb of the underwater concrete is divided by the assumed horizontal calculation level, so that $0,30 \text{ m}$ of height hb

come to rest above, and 1,70 m below the lowered water plane. Taking these factors into account, height hm is recalculated into height hm^* .

Height hm^*

$$hm^* = 28,30 - 1,70 \cdot (2,400 - 1,364) / 1,364 = 27,0 \quad \text{m} \quad 5.88$$

The remaining heights of the lower earth blocks are adapted by means of height hm^* , and the areas and forces of the individual blocks are determined via the widths of the upper blocks.

Area Aol'

Area $Aol' = 198,6 \text{ m}^2$ (5.64) and weight $Gnl' = 4604 \text{ kN}$ (5.65) are known, so that weight Gtl' with dry density $ptg = 2,046 \text{ t/m}^3$ must be calculated

Weight Gtl'

$$Gtl' = Aol' \cdot ptg \cdot g = 198,6 \cdot 2,046 \cdot 9,807 = 3985 \quad \text{kN} \quad 5.89$$

Force Gwl of the pore water is calculated from the difference $Gnl' - Gtl'$:

Weight Gwl

$$Gwl = Gnl' - Gtl' = 4604 - 3985 = 619 \quad \text{kN} \quad 5.90$$

Area Aul

The following data are available for calculation:

Dry density $ptwg = 1,364 \text{ t/m}^3$	Wet density $pnwg = 1,682 \text{ t/m}^3$
Wedge height $hlu = 27,0 \text{ m}$ (5.86)	Wedge width $bol' = 15,7 \text{ m}$ (5.63)

Area Aul

$$Aul = hlu \cdot bol' / 2 = 27,00 \cdot 15,70 / 2 = 212,0 \quad \text{m}^2 \quad 5.91$$

Force $Gtlu \rightarrow$ with $ptwg$

$$Gtlu = Aul \cdot ptwg \cdot g = 212,0 \cdot 1,364 \cdot 9,807 = 2836 \quad \text{kN} \quad 5.92$$

Force $Gnlu \rightarrow$ with $pnwg$

$$Gnlu = Aul \cdot pnwg \cdot g = 212,0 \cdot 1,682 \cdot 9,807 = 3497 \quad \text{kN} \quad 5.93$$

Area Am

The following data are available for calculation:

Dry density $ptwg = 1,364 \text{ t/m}^3$	Wet density $pnwg = 1,682 \text{ t/m}^3$
Wedge height $hm^* = 27,0 \text{ m}$ (5.88)	Wedge width $bm = 16,50 \text{ m}$

Area Am

$$Am = hm^* \cdot bm / 2 = 27,0 \cdot 16,50 / 2 = 223,0 \quad \text{m}^2 \quad 5.94$$

Force $Gtm \rightarrow$ with $ptwg$.

$$Gtm = Am \cdot ptwg \cdot g = 223,0 \cdot 1,364 \cdot 9,807 = 2983 \quad \text{kN} \quad 5.95$$

Force $Gnm \rightarrow$ with $pnwg$.

$$Gnm = Am \cdot pnwg \cdot g = 223,0 \cdot 1,682 \cdot 9,807 = 3678 \quad \text{kN} \quad 5.96$$

Area A_{or}^*

The following data are available for calculation:

Dry density $ptg = 2,046 \text{ t/m}^3$	Wet density $png = 2,364 \text{ t/m}^3$
$\beta n = 58,1^\circ, \tan \beta n = 1,609 \text{ (5.18)}$	$\beta n = 59,8^\circ, \tan \beta nw = 1,717 \text{ (5.25)}$
Wedge height $hl' = 25,30 \text{ m (5.33)}$	Wedge height $hru = 27,0 \text{ m (5.86)}$

Width $br \rightarrow ble =$ width bl under load e

$$br = ble + bor' = 10,00 + 15,70 = 25,70 \quad \text{m} \quad 5.97$$

Area A_{or}^*

$$A_{or}^* = hl' \cdot br/2 = 25,30 \cdot 25,70 / 2 = 325,1 \quad \text{m}^2 \quad 5.98$$

Force $G_{tr} \rightarrow$ with ptg

$$G_{tr} = A_{or}^* \cdot ptg \cdot g = 325,1 \cdot 2,046 \cdot 9,807 = 6523 \quad \text{kN} \quad 5.99$$

Force $G_{nr} \rightarrow$ with png

$$G_{nr} = A_{or}^* \cdot png \cdot g = 325,1 \cdot 2,364 \cdot 9,807 = 7537 \quad \text{kN} \quad 5.100$$

Force G_{wr} of the pore water is calculated from the difference $G_{nr} - G_{tr}$:

Weight G_{wr}

$$G_{wr} = G_{nr} - G_{tr} = 7537 - 6523 = 1014 \quad \text{kN} \quad 5.101$$

Area A_{ur}^*

The following data are available for calculation:

Dry density $ptwg = 1,364 \text{ t/m}^3$	Wet density $pnwg = 1,682 \text{ t/m}^3$
Wedge height $hru = 27,0 \text{ m (5.85)}$	Wedge width $br = 25,70 \text{ m (5.97)}$

Area A_{ur}^*

$$A_{ur}^* = hru \cdot bor'/2 = 27,00 \cdot 25,70/2 = 347,0 \quad \text{m}^2 \quad 5.102$$

Force $G_{tru} \rightarrow$ with $ptwg$

$$G_{tru} = A_{ur}^* \cdot ptwg \cdot g = 347 \cdot 1,364 \cdot 9,807 = 4642 \quad \text{kN} \quad 5.103$$

Force $G_{nru} \rightarrow$ with $pnwg$

$$G_{nru} = A_{ur}^* \cdot pnwg \cdot g = 347 \cdot 1,682 \cdot 9,807 = 5724 \quad \text{kN} \quad 5.104$$

Results:

Areas	Forces
Area $A_{ol}' = 198,6 \text{ m}^2 \text{ (5.64)}$	Force $G_{tl}' = 3985 \text{ kN (5.89)}$
Width $bol' = 15,70 \text{ m (5.63)}$	Force $G_{nl}' = 4604 \text{ kN (5.65)}$
Area $A_{ul} = 212,0 \text{ m}^2 \text{ (5.91)}$	Force $G_{tlu} = 2836 \text{ kN (5.92)}$
Height $hm^* = 27,00 \text{ m (5.88)}$	Force $G_{nlu} = 3497 \text{ kN (5.93)}$
Area $A_m = 223,0 \text{ m}^2 \text{ (5.94)}$	Force $G_{tm} = 2983 \text{ kN (5.95)}$
Width $bm = 16,50 \text{ m}$	Force $G_{nm} = 3678 \text{ kN (5.96)}$
Area $A_{or}^* = 325,1 \text{ m}^2 \text{ (5.98)}$	Force $G_{tr} = 6523 \text{ kN (5.99)}$
Width $br = 25,70 \text{ m (5.97)}$	Force $G_{nr} = 7537 \text{ kN (5.100)}$
Area $A_{ur}^* = 347,0 \text{ m}^2 \text{ (5.102)}$	Force $G_{tru} = 4642 \text{ kN (5.103)}$
	Force $G_{nru} = 5724 \text{ kN (5.104)}$
Force $G_{wl} = 619 \text{ kN (5.90)}$	Force $G_{wr} = 1014 \text{ kN (5.101)}$

5.1.6 Determination of uplift forces against the tunnel floor

By means of the above weight forces, it is possible to calculate uplift forces Rvl and Rvr , and also determine them graphically. For this, a coordinate system was selected, in which block widths bor' , bm , and bor are plotted on the abscissa, and the forces plotted on the ordinate. The ordinates are located on the outer sides of the slotted walls. To determine uplift force Rvl , the forces $Gtlu$, Gtl' , and Gwl must be plotted to the left of the left-hand ordinate above width bol' from bottom to top, and force Gtm plotted at the right below the abscissa (see Fig. 117).

Uplift force Rvr can be calculated from forces $Gtru$, Gtr , and Gwr , which must be assigned above the abscissa width $bor = br = 25,7$ m (5.97). Force Gtm with width $bm = 16,5$ m remains below this plane. Corresponding scales must be selected for the graphical representation of forces and widths. Accordingly, the indicated forces must be put into relation to widths $bor' + bm$ and $bm + bor$ via their force values, so that their connecting planes to the interfaces and thereby lead to the positions of uplift forces Rvl and Rv . The weight forces Gwl and Gwr of the pore water are not required for the further calculations. They are shown in the earth blocks as hatched blue areas (see Figs. 117 and 118 below).

Determining force Rvl

If weight forces $Gtl' + Gtlu$, which must be plotted on the left-hand ordinate, are added to the uplift force Gtm , the total force GTL is obtained.

$$GTL = Gtl' + Gtlu + Gtm$$

$$GTL = 3985 + 2836 + 2983 = 9804 \quad \text{kN} \quad 5.105$$

Width bxl

$$GTL \cdot bxl/blg = Gtlu \cdot bxl/blg + Gtm$$

$$9804 \cdot bxl/32,20 = 2836 \cdot bxl/32,20 + 2983$$

$$bxl = 13,80 \quad \text{m} \quad 5.106$$

The individual forces are shown in Fig. 117, whereby the gradient of the forces of the left-hand block to the central force Gtm is indicated by the red force plane. By means of width $blg = bor' + bm = 15,70 + 16,50 = 32,2$ m, this leads to Point D, which is located on the right-hand ordinate. Another force plane is created between forces $Gtlu$ and Gm . This is shown green in Fig. 117. The red and green planes intersect at the distance width bxl measured from Point D.

Width bll

$$bll = blg - bxl = 32,20 - 13,80 = 18,40 \quad \text{m} \quad 5.107$$

Uplift force Rvl

$$Rvl = Gtl_u \cdot bxl/blg = 2836 \cdot 13,80/32,2 = 1215 \quad \text{kN} \quad 5.108$$

Uplift force Rvl (5.108) is generated by the left-hand earth block. It acts at the distance width $bxl = 13,80$ m (5.106) from Point D.

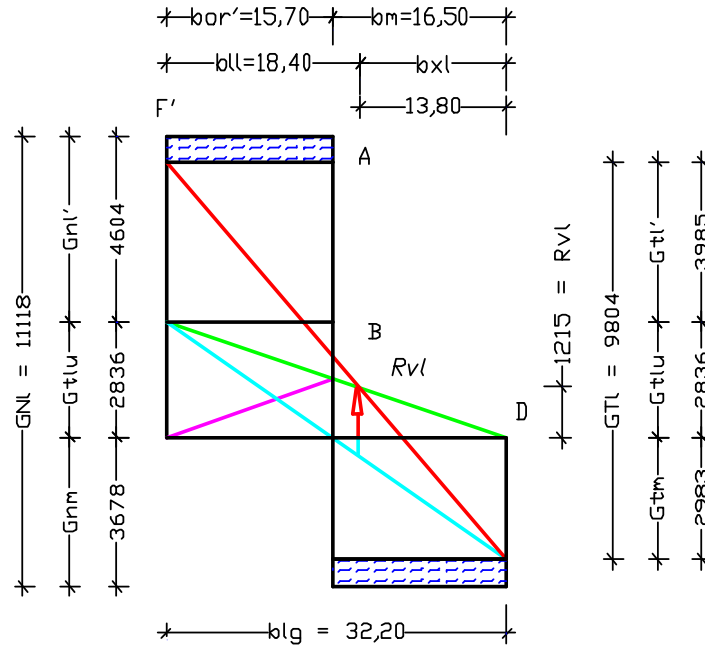


Fig. 117: Force areas acting against the left-hand slotted wall and the tunnel floor, and the resulting uplift force Rvl .

Determining force Rvr

Also here, weight GTr must first be determined via forces $Gtru = 4642$ kN (5.103), $Gtr = 6523$ kN (5.99), and $Gtm = 2983$ kN (5.95). Weight Gwr (5.101) of the pore water is not taken into account.

Weight GTr

$$GTr = Gtr + Gtru + Gtm$$

$$GTr = 6523 + 4642 + 2983 = 14148 \quad \text{kN} \quad 5.109$$

The positions of the forces are shown in Fig. 118 below. Also here, the individual forces must be brought into relation with total width $brg = bm + bor$, i.e. $brg = 16,50 + 25,70 = 42,20$ m.

Width bxr

$$GTr \cdot bxr/brg = Gtru \cdot bxr/brg + Gtm$$

$$14148 \cdot bxr/42,20 = 4642 \cdot bxr/42,20 + 2983$$

$$bxr = 13,20 \quad \text{m} \quad 5.110$$

Width brr

$$brr = brg - bxr = 42,20 - 13,20 = 29,00 \quad \text{m} \quad 5.111$$

Uplift force R_{vr}

$$R_{vr} = G_{tru} \cdot b_{xr}/b_{rg} = 4642 \cdot 13,20/42,20 = 1452 \quad \text{kN} \quad 5.112$$

Uplift force R_{vr} (5.112) is generated by the right-hand earth block. It acts at the distance width $b_{xr} = 13,20$ m (5.110) from Point A. The force planes and their intersections are shown in Fig. 118. As above, the red lines represent the upper and lower force gradients (G_{Tr}/b_{rg} and G_{tm}/b_{rg}), and the green line shows the calculation level. Weight G_{wr} (5.101) of the pore water is shown as a hatched blue area.

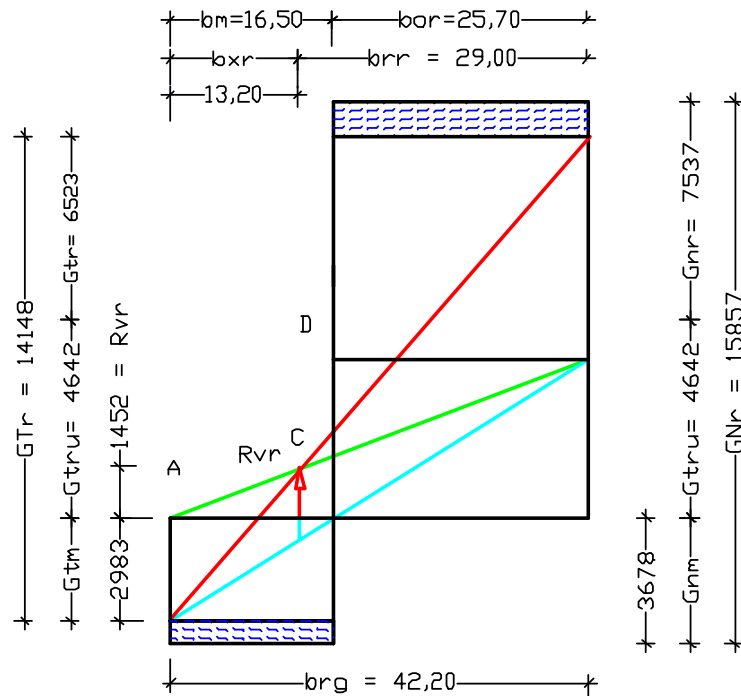


Fig. 118: Force areas acting against the right-hand slotted wall and the tunnel floor, and the resulting uplift force R_{vr} .

Force area of uplift forces R_{vl} and R_{vr}

The force areas of uplift forces R_{vl} and R_{vr} are transferred into Fig. 119 from Figs. 117 and 118, where they rest on the upper side of the underwater concrete. The upper limits of uplift force R_{vl} in Fig. 119 are shown in magenta, and those of force area R_{vr} in green. Due to the overlap of the uplift areas, and thereby also of the forces in these areas, the force area with the blue upper limit is created. The sum of the forces in the vertical planes B and C are shown as red arrows. Consequently, force R_{vl} must be assigned to plane B, and force R_{vr} to plane C. In order to detect the influence of the uplift forces on the tunnel floor and its wall connections, additional sections are established next to the vertical planes B and C. They are designated A and D on the outer sides of the slotted walls, and A' and D' on the inner sides.

Widths $b_{xl} = 13,80$ m (5.106) and $b_{ll} = 18,40$ m (5.107) at the left, and widths $b_{xr} = 13,20$ m (5.110) and $b_{rr} = 29,00$ m (5.109) on the right are available for calculating the uplift forces in the individual planes. By means of the central width $b_m = 16,50$ m minus widths b_{xl} and b_{xr} , it is possible to determine the distances of the planes (A'–B) with 2,70 m, and (C–D') with 3,30 m to the inner sides of the slotted walls. Moreover, the forces in the vertical planes A', B, C, and D' can be converted into force meters using force indices $gitl$ and $gitr$.

With an open floor, i.e. without the concrete base slab between the slotted walls, and in accordance with the principles of laminar flow, the force meters correspond to the heights of the rising earth masses in the tunnel cross-section. Fictitious dry density $ptg = 2,046$ t/m³ (Appendix 1) and $ptwg = 1.36$ t/m³ (5.22), areas $A_{ol}' = 198,6$ m² (5.64), $A_{ul} = 212,0$ m² (5.91), $A_{or}^* = 325,1$ m² (5.98), and $A_{ul}^* = 347,0$ m² (5.102), gravity force $g = 9,807$ m/s², and widths $blg = 32,20$ m and $brg = 42,20$ m are available for determining the force indices.

Force index $gitl$

$$gitl = blg \cdot (ptg \cdot A_{ol}'/A_{ul} + ptwg \cdot A_{ul}/A_{ol}') \cdot g / 4 =$$

$$gitl = 32,2 \cdot (2,046 \cdot 198,6/212,0 + 1,364 \cdot 212,0/198,6) \cdot g / 4 =$$

$$gitl = 32,2 \cdot (1,917 + 1,456) \cdot 9,807 / 4 = 266,3 \quad \text{kN/m}^2 \quad 5.113$$

Force index $gitr$

$$gitr = brg \cdot (ptg \cdot A_{or}^*/A_{ul}^* + ptwg \cdot A_{ul}^*/A_{or}^*) \cdot g / 4 =$$

$$gitr = 42,2 \cdot (2,046 \cdot 325,1/347,0 + 1,364 \cdot 347,0/325,1) \cdot g / 4 =$$

$$gitr = 42,20 \cdot (1,917 + 1,456) \cdot 9,807 / 4 = 349,0 \quad \text{kN/m}^2 \quad 5.114$$

Calculation of force meters

Area of $R_{vl} = 1215$ kN (5.108) / $gitl$

Forces in the vertical planes	$gitl$	Force meter	
A = $1215 \cdot 15,70/18,40 = 1036$ kN	266,3	= 3,89 m	5.115
A' = $1215 \cdot 16,70/18,40 = 1103$ kN	266,3	= 4,14 m	
B = $R_{vl} = 1215$ kN	266,3	= 4,56 m	
C = $1215 \cdot 3,30/13,80 = 291$ kN	266,3	= 1,10 m	
D' = $1215 \cdot 1,00/13,80 = 88$ kN	266,3	= 0,33 m	
D = 0 kN	266,3	= 0,00 m	

Area of $R_{vr} = 1452 \text{ kN} (5.112) / \text{gitr}$

Forces in the vertical planes	gitl	Force meter
$A = 0 \text{ kN}$	349,0	= 0,00 m
$A' = 1452 \cdot 1,00/13,20 = 110 \text{ kN}$	349,0	= 0,32 m
$B = 1452 \cdot 2,70/13,20 = 297 \text{ kN}$	349,0	= 0,85 m
$C = R_{tr} = 1452 \text{ kN}$	349,0	= 4,16 m
$D' = 1452 \cdot 26,70/29,00 = 1337 \text{ kN}$	349,0	= 3,83 m
$D = 1452 \cdot 25,70/29,00 = 1287 \text{ kN}$	349,0	= 3,69 m

5.116

The force meters previously calculated from the uplift forces R_{vl} and R_{vr} are shown in planes A to D of Fig. 119. Addition of the force meters generates the total reactive force area of the uplift against the tunnel floor (see also Results, and the table (5.117) below.

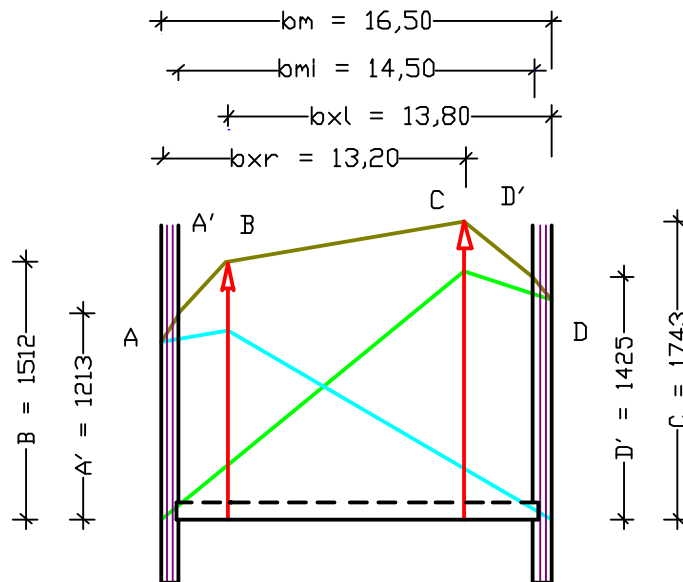


Fig. 119: Force areas of pressure forces R_{vl} and R_{vr} , and the upper contour (A–B–C–D) of the reactive total force area.

Results:

For determining the uplift forces against the tunnel floor, a lowered ground-water level to height $hl' = -25,30 \text{ m}$ was assumed. The calculation results are summarized in the table below.

Uplift pressures $\sum R_{vl}$ and $\sum R_{vr}$	Force meter/height hy
$A = 1036 + 0 = 1036 \text{ kN}$	$3,89 + 0,00 = 3,89 \text{ m}$
$A' = 1103 + 110 = 1213 \text{ kN}$	$4,14 + 0,32 = 4,46 \text{ m}$
$B = 1215 + 297 = 1512 \text{ kN}$	$4,56 + 0,85 = 5,41 \text{ m}$
$C = 291 + 1452 = 1743 \text{ kN}$	$1,10 + 4,16 = 5,26 \text{ m}$
$D' = 88 + 1337 = 1425 \text{ kN}$	$0,33 + 3,83 = 4,16 \text{ m}$
$D = 0 + 1287 = 1287 \text{ kN}$	$0,00 + 3,69 = 3,69 \text{ m}$

5.117

Because planes A and D and their uplift forces lie on the outer sides of the slotted walls, they are not used to determine the uplift under the tunnel floor. Due to the uplift with an open floor (no concrete base slab), the earth masses would rise up to the indicated heights (see Fig. 119).

5.1.7 Determination of horizontal earth forces under water

The forces of the wet soil acting from left to right against the slotted walls above the lowered groundwater level $hl' = 25,30$ m (5.33) have already been determined. Force $Hfn' = 2064$ kN (5.68), which acts against the left-hand slotted wall at height $hvn' = 18,21$ m (5.71), has been determined from area Aol' . Force $Lh = 1019$ kN (5.78) acts against the right-hand slotted wall at height $ln = 3,25$ m (5.80). To be determined on the next pages are the horizontal forces from areas Amo and Acu , whereby area Amo lies above the inclined plane of area Am , and area Acu lies below area Aco (see Fig. 116, page 176).

Forces from area Amo

Area Amo is calculated from height $hmo^* = 27,00$ m (5.88) minus the height of the underwater concrete floor, which lies 1,70 m below the assumed groundwater level, i.e. $hmo = 27,00 - 1,70 = 25,30$ m.

Width $bmo \rightarrow$ with $\tan \betanw = 1,717$ (5.25)

$$bmo = hmo / \tan \betanw = 25,30 / 1,717 = 14,70 \quad \text{m} \quad 5.118$$

Area Amo

$$Amo = hmo \cdot bmo / 2 = 25,30 \cdot 14,70 / 2 = 186,0 \quad \text{m}^2 \quad 5.119$$

Force $Gmo \rightarrow$ with $pnwg = 1,682$ t/m³ (5.23)

$$Gmo = Amo \cdot pnwg \cdot g = 186,0 \cdot 1,682 \cdot 9,807 = 3068 \quad \text{kN} \quad 5.120$$

The other forces in area Amo are determined by means of force Gmo .

Force $Nvm \rightarrow$ with $\betanw = 59,8^\circ$ (5.26)

$$Nvm = Gmo \cdot \cos^2 \betanw = 3068 \cdot 0,253 = 776 \quad \text{kN} \quad 5.121$$

Force Hvm

$$Hvm = Gmo \cdot \sin^2 \betanw = 3068 \cdot 0,747 = 2292 \quad \text{kN} \quad 5.122$$

Force Hfm

$$Hfm = Gmo \cdot \sin \betanw \cdot \cos \betanw$$

$$Hfm = 3068 \cdot 0,864 \cdot 0,503 = 1334 \quad \text{kN} \quad 5.123$$

Force index gim

$$gim = bmo \cdot pnwg \cdot g / 2 = 14,70 \cdot 1,682 \cdot 9,807 / 2 = 121,2 \quad \text{kN/m}^2 \quad 5.124$$

Force meter nvm

$$nvm = Nvm / gim = 776 / 121,2 = 6,40 \quad \text{m} \quad 5.125$$

Force meter hvm

$$hvm = Hvm / gim = 2292 / 121,2 = 18,90 \quad \text{m} \quad 5.126$$

Force meter hfm

$$hfm = Hfm/gim = 1334/121,2 = 11,00 \quad \text{m} \quad 5.127$$

Force meter hfm' → referred to the height of the underside of right-hand slotted wall

$$hfm' = hfm \cdot hb'/nvm = 11,00 \cdot 3,0/6,40 = 5,16 \quad \text{m} \quad 5.128$$

Force Hfm' → horizontal force against the inner side of the slotted wall

$$Hfm' = hfm' \cdot gm = 5,16 \cdot 121,2 = 625 \quad \text{kN} \quad 5.129$$

Forces from area Acu

The following data are available for calculation:

Dry density $ptwg = 1,364 \text{ t/m}^3$	Wet density $pnwg = 1,682 \text{ t/m}^3$
Wedge width $be = 9,35 \text{ m (5.36)}$	Wedge height $hru = 27,00 \text{ m (5.85)}$
Wedge width $be' = 0,65 \text{ m}$	Angle $\betaew = 70,9^\circ \text{ (5.84)}$

To be noted here, is that height hru (5.85) has been determined by means of width be (5.36) and angle βew (5.84). But because area Acu occupies width $ble = 10,00 \text{ m}$ up to the vertical calculation level D, the new wedge height hru' must first be determined in order to include width $be' = ble - be = 0,65 \text{ m}$ in wedge area Acu . That this causes the lower calculation level to be exceeded, is accepted.

Height hru' → $\tan \betaew = 2,883$ (5.83)

$$hru' = ble \cdot \tan \betaew = 10,00 \cdot 2,883 = 28,83 \quad \text{m} \quad 5.130$$

Area Acu

$$Acu = ble \cdot hru'/2 = 10,00 \cdot 28,83/2 = 144,0 \quad \text{m}^2 \quad 5.131$$

Force Gtc → with $ptwg$

$$Gtc = Acu \cdot ptwg \cdot g = 144,0 \cdot 1,364 \cdot 9,807 = 1926 \quad \text{kN} \quad 5.132$$

Force Gnc → with $pnwg$

$$Gnc = Acu \cdot pnwg \cdot g = 144,0 \cdot 1,682 \cdot 9,807 = 2375 \quad \text{kN} \quad 5.133$$

Force Nvw → with Gnc and $\betaew = 70,9^\circ$

$$Nvw = Gnc \cdot \cos^2 \betaew = 2375 \cdot 0,107 = 254 \quad \text{kN} \quad 5.134$$

Force Hvw

$$Hvw = Gnc \cdot \sin^2 \betaew = 2375 \cdot 0,893 = 2121 \quad \text{kN} \quad 5.135$$

Force $Hfwr$

$$Hfwr = Gnc \cdot \sin \betaew \cdot \cos \betaew$$

$$Hfwr = 2375 \cdot 0,945 \cdot 0,327 = 734 \quad \text{kN} \quad 5.136$$

Force index $ginw$

$$ginw = ble \cdot pnwg \cdot g/2 = 10,0 \cdot 1,682 \cdot g/2 = 82,5 \text{ kN/m}^2 \quad 5.137$$

Force meter nvw

$$nvw = Nvw/ginw = 254/82,5 = 3,10 \quad \text{m} \quad 5.138$$

Force meter hvw

$$hvw = Hvw/ginw = 2121/82,5 = 25,70 \quad \text{m} \quad 5.139$$

Force meter $hfwr$

$$hfwr = Hfwr/ginw = 734/82,5 = 8,90 \quad \text{m} \quad 5.140$$

Results:

Area $Acu = 144,0 \text{ m}^2$ (5.131)	Force $Gnc = 2375 \text{ kN}$ (5.133)
Height $nvw = 3,10 \text{ m}$ (5.138)	Force $Hfwr = 734 \text{ kN}$ (5.136)

5.1.8 Balancing the uplift forces with the tunnel's weight pressures

The uplift forces are summarized in Table (5.117) on page 189. The weight forces counteracting the uplift forces are determined from the underwater concrete with density $p_4 = 2,400 \text{ t/m}^3$, partial height $\Delta h' = 2,00 - 1,70 = 0,30 \text{ m}$, the reinforced concrete of the tunnel floor with density $p_2 = 2,500 \text{ t/m}^3$, and height $hbs = 1,50 \text{ m}$ as well as the intermediate ceiling with an estimated height $hz \sim 1,20 \text{ m}$, and the associated internal supports.

Because the slotted walls support part of the ceiling load, and for simplification, distribution of the ceiling load will be reduced to 75%, and distributed over 75% of the clear width $bt = 14,50 \text{ m}$. In this way, the tunnel floor near to the slotted walls, with width $bt' = 0,25 \cdot 14,50/2 = 1,80 \text{ m}$, remains unaffected by the ceiling load. As substitute load for the supports, a height increase of $hz^* = 0,10 \text{ m}$ is assumed for the intermediate ceiling. The following weight forces counteract the uplift forces:

Weight $Gu \rightarrow$ underwater concrete with height $\Delta h' = 0,30 \text{ m}$

$$Gu = bt \cdot \Delta h' \cdot p_4 \cdot g = 14,5 \cdot 0,30 \cdot 2,400 \cdot 9,807 = 102 \quad \text{kN} \quad 5.141$$

Weight $Gs \rightarrow$ tunnel floor

$$Gs = bt \cdot hbs \cdot p_2 \cdot g = 14,5 \cdot 1,50 \cdot 2,500 \cdot 9,807 = 533 \quad \text{kN} \quad 5.142$$

Weight $\sum G_l \rightarrow$ with width $bt = 14,50 \text{ m}$

$$\sum G_l = Gu + Gs = 102 + 533 = 635 \quad \text{kN} \quad 5.143$$

Weight $Gi' \rightarrow$ interior work: heights $hz + hz^* = 1,20 + 0,10 = 1,30 \text{ m}$

$$Gi' = bt' \cdot hh \cdot p_2 \cdot g = 1,80 \cdot 1,30 \cdot 2,50 \cdot 9,807 = 57 \quad \text{kN} \quad 5.144$$

Weight $Gi^* \rightarrow$ interior work: height $hz + hz^* = 1,30 \text{ m}$

$$Gi^* = bt^* \cdot hh \cdot p_2 \cdot g = 10,90 \cdot 1,30 \cdot 2,50 \cdot 9,807 = 348 \quad \text{kN} \quad 5.145$$

Weight $Gsw \rightarrow$ slotted wall: height $hs = 30,0 \text{ m}$

$$Gsw = d \cdot h \cdot p_2 \cdot g = 1,00 \cdot 30,0 \cdot 2,50 \cdot 9,807 = 736 \quad \text{kN} \quad 5.146$$

The calculated uplift forces from the adjoining soil (5.117), and the opposing weight forces (see above) from tunnel construction show that the uplift forces in the vertical calculation planes A' to D' against the tunnel floor cannot be offset completely by the weight forces (see table below).

Offset

of the uplift forces against the weight forces from the tunnel profile:

Uplift pressures	Weight forces from the components	Remaining uplift forces
A = 1036 kN	$-(57 + 736) = -793$ kN	= 243 kN
A' = 1213 kN	-635 kN	= 578 kN
B = 1512 kN	$-635 - 348 = -983$ kN	= 529 kN
C = 1743 kN	$-635 - 348 = -983$ kN	= 760 kN
D' = 1425 kN	-635 kN	= 790 kN
D = 1287 kN	$-(57 + 736) = -793$ kN	= 494 kN

5.147

Forces and their points of application against the tunnel cross-section

As already mentioned, the force determinations are based on assumptions, because corresponding documents, such as construction plans, soil properties, states of construction, etc., could not be obtained. Therefore, the calculations have been formulated in such a way that they can be reproduced and verified as soon as real figures are known. The assumptions made, as well as the force application points against the slotted walls and the tunnel floor, are shown in Fig. 120.

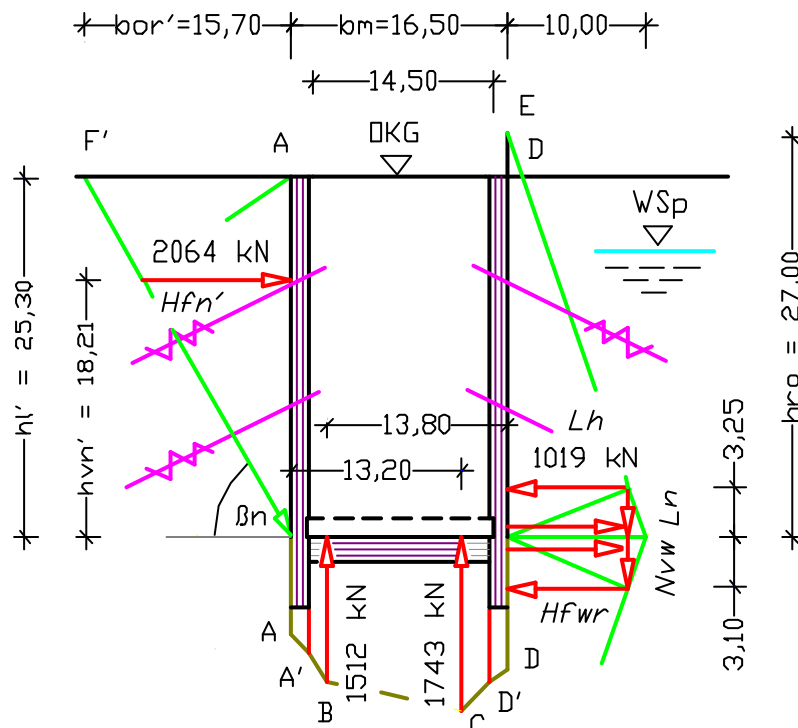


Fig. 120: Tunnel cross-section with the applied forces.

Slotted walls

It was assumed that the excavation pit was initially stabilized by means of slotted walls, ground anchors, internal bracing, and a non-reinforced under-

water concrete slab. A height of $h_s = 30,00$ m, and a thickness of $d = 1,00$ m were assigned to the walls. According to reports in the media, the walls are supposed to have been reinforced with steel girders spaced at approx. 3,50 m, and a light bar reinforcement. Ground anchors in the upper wall regions, and internal bracing against the walls should have kept the construction site free for excavation under water. After reaching an excavation depth of $-27,00$ m, the underwater concrete slab with an assumed thickness $h_b = 2,00$ m could have been installed. By lowering the groundwater level down to height $h_{ss} = -25,00$ m below the terrain level (OKG), the preconditions were provided to install a second layer of ground anchors and the tunnel floor of reinforced concrete with an estimated height $h_{bs} = 1,50$ m. Moreover, it was assumed that connecting reinforcements for the floor/wall interface were installed in the slotted walls, together with cutouts in the walls for the tunnel floor.

When determining the forces acting against the slotted walls, very different load diagrams are shown. While the horizontal force $H_{fn}' = 2064$ kN (5.68) from area A_{ol}' on the left-hand side acts against the slotted wall at height $h_{vn}' = 18,21$ m (5.71) above the calculation level ($hl' \sim -25,30$ m), a completely different load occurs on the right-hand slotted wall due to the structural weight of the archive (see Fig. 120 above).

The archive's structural weight is so dominant that it changes the active force fields of the adjacent soil into reactive fields, and shifts the horizontally acting force $L_h = 1019$ kN (5.78) at height $l_n = 3,25$ m (5.80). Below the calculation level, horizontal force $H_{fwr} = 734$ kN (5.136) acts at height $n_{vw} = 3,10$ m (5.138). This is opposed by force $H_{fm}' = 625$ kN (5.129), which acts from the inside against the foot of the right-hand slotted wall.

Tunnel floor

Based on photos of the tunnel cross-section at the time of the accident, it was deduced that the underwater concrete with selected height $h_b = 2,00$ m, the tunnel floor with assumed height $h_{bs} = 1,50$ m, a few supports, and an intermediate reinforced concrete ceiling had been installed. As the actual tunnel walls were still missing, the ceiling reached from slotted wall to slotted wall. A limited cutout depth and connecting reinforcements in the walls were assumed for the connections between tunnel floor and the slotted walls, which were intended mainly to transfer the uplift forces into the slotted walls. The uplift forces

acting against the tunnel floor were calculated according to the New Earth Pressure Theory by means of the fictitious dry densities of the wet soil above and below water. Hereby, it is assumed that water under pressure gives way in free nature, and is therefore not available for transferring forces, while the solids structure of a soil type remains unchanged under normal pressure conditions (see Section 3.2, page 67).

The uplift forces were determined using the weight forces of earth blocks, which were put into relation to the forces of the adjacent blocks. The balance of forces between the left-hand earth blocks and the middle earth block under the tunnel floor resulted in uplift force $R_{vl} = -1215$ kN (5.108) in plane B, and the balance between the right-hand earth blocks and the middle block resulted in force $R_{vr} = -1452$ kN (5.112) in plane C (see Figs. 117 and 118). The superimposition of forces R_{vl} and R_{vr} is shown in Fig. 119, page 185.

The uplift forces counteract the building loads on the tunnel. In order to distribute these loads realistically over the entire width $bm = 16,50$ m of the tunnel floor, sections with widths $1,00 + 1,70 + 10,30 + 2,50 + 1,00 = 16,50$ m were selected. After reducing the uplift forces by the weight forces of the tunnel floor, the intermediate ceiling, and the supports, uplift force $R_{vC} = -760$ kN remains in plane C, and force $R_{vD}' = -790$ kN in plane D', i.e. on the inside of the right-hand slotted wall (see Table 5.147, page 189).

Possible cause of the accident

The individual forces and their attack planes against the tunnel cross-section are shown in Tables (5.117) and (5.147), and have been transferred into Figs. 119 and 120, pages 185 and 189.

While the left-hand slotted wall is loaded by earth pressure force $Hfn' = 2064$ kN (5.68), and this force is dispersed directly into the ground via the upper position of the ground anchors, the forces against the right-hand slotted wall are concentrated on the connection area of the tunnel floor. In particular, the uplift forces $R_{vC} = -760$ kN and $R_{vD}' = -790$ kN against the tunnel floor, as well as the earth pressure force $Lh = 1019$ kN (5.78) with thrust value $ln = 3,25$ m (5.80) above the selected calculation level ($hl' -25,30$ m) generate a torsion in the floor/wall area, which assisted the upward movement of the tunnel floor and resulted in stresses in the wall being exceeded. The torsional force was

increased by the counteracting horizontal forces Lh and Hf_{we} , which point to the right at the height of the tunnel floor (see Fig. 120, page 189).

If one places force $Lh = 1019 \text{ kN}$ (5.78) with height $ln = 3,25 \text{ m}$ (5.80) above the selected calculation level an ($hl' \sim -25,30 \text{ m}$), and subtracts the height $hbs = 1,50 \text{ m}$ of the concrete floor, the point of attack from the adjacent soil against the slotted wall at a height of about $1,75 \text{ m}$ lies above the concrete floor. The connecting reinforcement for the tunnel floor is likely to be below this point, whereby a special wall reinforcement is not available here to handle the horizontal attack of force Lh . When looking at the connecting reinforcement shown in the photos, it seem unlikely that the uplift forces $RvC = -760 \text{ kN}$ and $RvD' = -790 \text{ kN}$ can be dispersed into the wall via this reinforcement. Based on the calculated uplift forces, it is probable that the right-hand side of the soil slab is raised, leading to a tilt of the slab, and thereby causing compression, rotation, and fractures in the right-hand slotted wall. The possible fractures are shown in Fig. 121 below.

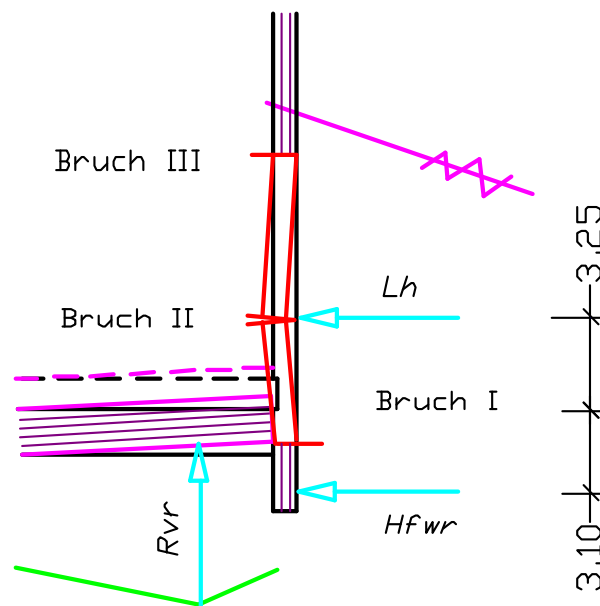


Fig. 121: Possible fractures in the slotted wall.

Because, according to the calculation requirements of current earth pressure teachings, an earth pressure force of $Lh = 1019 \text{ kN}$ (5.78) cannot be expected in the indicated fracture plane II, the author assumes that the installed reinforcement was not dimensioned for this force. Consequently, small wall fractures could arise, which were then widened by the water/sand mixture flowing into the tunnel under high pressure, thereby breaking up the wall's concrete across a

large area. Due to the removal of earth masses from the adjacent substratum, the archive's collapse was inevitable.

The above earth pressure calculations permit the conclusion that the groundwater level in this section of the subway excavation was lowered far more than assumed in this study with height $hl' = -25,30$ m. This surmise is based on the uplift forces shown in Table (5.117), which had to be reduced by the weight forces of the tunnel floor, the columns, and the intermediate ceiling (see Table 5.147). If one considers the situation on the construction site after installation of the underwater concrete and before installation of the tunnel floor, it would have been necessary to take measures that were suited firstly to keep the excavation pit dry for installation of the floor reinforcement, and secondly to reduce the uplift forces caused by the still missing counteracting weight forces. Both of these requirements could only be met by lowering the groundwater level even further. The author is convinced that this would have had no negative effects on the stability of the adjacent building – provided that no solid material is removed from the adjacent ground.

5.1.9 Conclusions about the collapse of the archive in Cologne

The calculations carried out according to the New Earth Pressure Theory permit the assumption that the structural weight of the Historic Archive in Cologne was not taken into account adequately during construction planning. In this respect, a parallel event comes to mind, namely the church tower of Sankt Johann Baptist, which tilted during the subway excavations.

Moreover, the study also reveals that the basics of current earth pressure teachings do not follow the real soil behaviour, but use data related to soil values (shear strength, influence, and density) that is based on empiric values [1: I.19]. In addition, the teachings provide specifications for the dispersal of vertical loads into the substratum [1: P.14], and for determining uplift forces by means of pore water pressure [1:D.1ff.], which can result in significant undersizing in partial areas of the tunnel cross-section (see Section 2.5, page 43).

Because the basics of current earth pressure teachings have been adopted in the standards for earth pressure determination, the archive's collapse can be blamed less on the planners applying these standards, but rather on the authors of the specifications. Planners and executors can decide freely whether to observe the

standards or not, but legal regulations mostly require that application of the specifications in the current teachings as "state-of-the-art" is compulsory.

Knowledge of the disclosed shortcomings in the current rules and standards for earth pressure calculation could even permit the collapse of the Historic Archive in Cologne to be explained with the correct application of currently valid building regulations.

5.2 Landslide into the Concordia lake near Nachterstedt in 2009

Also the landslide in Nachterstedt on 18th July 2009 with three fatalities and high material damage was covered intensively by all media. The landslide occurred in connection with open cast lignite mining, whereby part of the huge pit was to be refilled with overburden, and the far greater part was to be flooded as a lake. The events leading up to the disaster were summarized in the article: “*So entstand das Desaster von Nachterstedt*” [11]. The extent of the landslide is shown in a series of photos [J].

In order to investigate the enormous earth movement with the findings of the New Earth Pressure Theory, the author visited the accident site in Nachterstedt. Hereby, it was intended to take measurements of the different angles in the terrain and the slope (before/after), and to take soil samples. Unfortunately, after discussions with the responsible *Lausitzer und Mitteldeutschen Bergbau-Verwaltungsgesellschaft (LMBV)*, access to the widely cordoned off site was denied. Also denied was the request to view the results of local soil investigations carried out for the LMBV. Consequently, for the investigation described here, it was only possible to assess the slope’s soil type by visual inspection and from photos of the landslide. Should the soil type selected for the investigation be different from the material used to fill the pit, the real soil parameters can be entered in the following calculations without problems.

The photo below, which shows the open cast mining pit before flooding, was taken from Wikipedia/Concordia lake.



Fig. 122: Open cast mine pit before flooding.

There is a proliferation of speculations on the Internet about the cause of the accident. On 18th July 2010, the magazine ‘Spiegel’ reported: *The Lausitzer und Mitteldeutsche Bergbau-Verwaltungsgesellschaft has now published the*

present state of the findings regarding the Nachterstedt case. – Their summary: "Obviously, several influencing factors were involved simultaneously, but in a form and manner that is still unknown to us." And the expert nominated by the Federal State Government expects that evaluation of the accident site will take quite a while longer, because "the entire terrain is in motion".

In the press release PM 030/2012 dated 17.07.2012, the Ministry for Science and Economic Affairs (Saxony-Anhalt) stated: "*Determination of the causes should be completed by middle of next year*". On 04.05.2013, the newspaper "Mitteldeutsche Zeitung" wrote: "*Dispute between experts continues*" [13]. On 13.12.2013, a radio broadcast by the Mitteldeutsche Rundfunk was titled "*Groundwater pressure caused devastating landslide in Nachterstedt*" and reported that expert opinions proved that the landslide had been caused by high groundwater pressure, and that it could not have been predicted. Moreover, an expertise from the LMBV excludes the possibility of previous mining activities being the cause of the accident [14].

In the following, the cause of the Nachterstedt landslide will be investigated using the findings that resulted in the New Earth Pressure Theory. Also the Deutsche Zentrum für Luft- und Raumfahrt (DLR = German Aerospace Center) has kindly permitted the use of their "Comparative Map of Nachterstedt with 'before/after' Section Views" [H]. This document was used to create a system of reference coordinates for the DLR section views, which were then assigned between the widths 5472000 m and 5472500 m of the geodetic length 661450 m. On the one hand, the heights required for the section through the terrain were partially interpolated from the DLR sections, and on the other hand they were supplemented with height data from the "EffJot Forum – Geological maps of Nachterstedt" [12].

In the author's reference coordinate system, the geodetic width is described as 'Station' (Stat). The lowest point of the pit (lake bed) is given with height +42 m a.s.l. at the geodetic width of 5742480 m (Stat. 2480), and rises up to the height of +97 m a.s.l. in the area of width 5742000 m (Stat. 2000). Just before the landslide, the Concordia lake is said to have reached a water level of height +82 m a.s.l. By means of the differences in height resulting from the sloping lake bed, the lake's water level, and the terrain levels, the different properties of the adjacent soil types in the moist or wet state can be calculated. Because

every soil type and every soil state generates different horizontal forces, it is possible to determine the ‘shear plane under load’ in the individual Stations of the slope, and to represent the extent of the landslide mathematically.

5.2.1 Filling material and its properties

A loam/sand mixture is assumed to have been used for the partial refilling of the open cast mine pit, consisting of 60% by vol. of loamy solids with $Vf_b = 0,392 \text{ m}^3$ (4.162), and 40% by vol. of sandy solids with $Vf_a = 0,548 \text{ m}^3$ (4.160) per $1,00 \text{ m}^3$ (see Section 4.5, page 133).

Based on the author’s experience, the filling material is assumed to have had a moisture content of 78 liters of water per $1,00 \text{ m}^3$ before the landslide. Moreover, it is known that no mechanical compaction is used for such refills, contrary to e.g. dam building. From the above assumptions, further properties of the filling material with the soil conditions dry, moist, and wet above/below water can be calculated. The changes in soil properties occur, when more water is added to the filling mixture, or the soil is flooded with water, e.g. due to the rising water level in the Concordia lake.

Characteristics of the dry soil

The assumed overburden material consists of:

Sand	$Vfa = 0,548 \text{ m}^3$	40 %	$Vfa' = 0,219 \text{ m}^3$
Loam	$Vfb = 0,392 \text{ m}^3$	60 %	$Vfb' = 0,235 \text{ m}^3$
Mixture		<u>100 %</u>	$Vf = 0,454 \text{ m}^3$ $Vl = 0,546 \text{ dm}^3$

The changed soil characteristics due to the addition of water are calculated. The volumes of this soil type in the dry state are shown in the soil cube below. They form the basis for the conversions of the soil states.

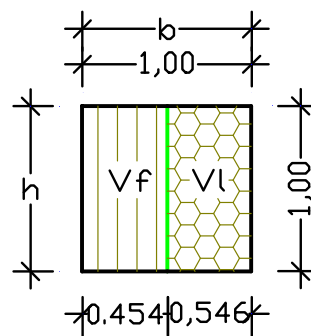


Fig. 123: Soil cube of the loam/sand mixture.

The following is determined:

Dry density ptg

$$ptg = Vf \cdot ptg_{90} / Vp = 0,454 \cdot 3,0 / 1,0 = 1,362 \quad \text{t/m}^3 \quad 5.148$$

Inclination angle βt

$$\tan \beta t = Vf / Vl = 0,454 / 0,546 = 0,832 \quad 5.149$$

$$\beta t = 39,7^\circ \quad [-] \quad 5.150$$

The dry soil properties are changed by the addition of an assumed water quantity of 78 liters ($Vln = 0,078 \text{ m}^3$) and the associated soil compaction (see Section 3.1.4, page 63).

Characteristics of the compacted moist soil mix

Due to the addition of water, the cube of dry soil (Fig. 123) expands by the fictitious solids volume Vfi , so that the original cube with volume $Vp = 1,00 \text{ m}^3$ at calculation depth $a = 1,00 \text{ m}$ has a greater width bb and a smaller height h' . If spreading of the soil is prevented due to its fixed position in the slope, it will be compacted.

The following is determined:

Fictitious solids volume $\rightarrow Vfi$ of the moist soil

$$Vfi = Vln \cdot pwg / ptg_{90} = 0,078 \cdot 1,0 / 3,0 = 0,026 \quad \text{m}^3 \quad 5.151$$

Width bb

$$bb = b + bw = 1,000 + 0,026 = 1,026 \quad \text{m} \quad 5.152$$

Height h'

$$h' = Vp / bb \cdot a = 1,000 / 1,026 \cdot 1,00 = 0,975 \quad \text{m} \quad 5.153$$

If the cube is now filled with the same soil type from height $h' = 0,975 \text{ m}$ up to height $h = 1,00$ and prevents spreading of the soil due to the addition of water, the properties of the moist compacted soil can be calculated as follows (see volumes in Figs. 124 to 126).

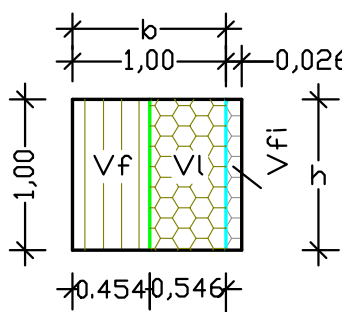


Fig. 124: Widening due to water absorption.

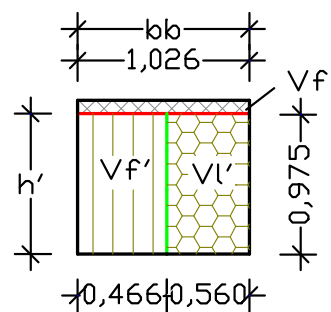


Fig. 125: Loss of height due to soil expansion.

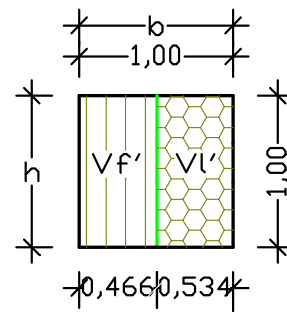


Fig. 126: Volumes of compacted soil.

Solids volume Vf'	$Vf' = Vf/h' = 0,454/0,975 = 0,466$	m^3	5.154
Pore volume Vl'	$Vl' = Vp - Vf' = 1,000 - 0,466 = 0,534$	m^3	5.155
Inclination angle βi	$\tan \beta i = Vf / (Vl + Vf_i) = 0,466 / (0,534 + 0,026) = 0,832$		5.156
	$\beta i = 39,8^\circ$	[-]	5.157
Dry density ptg	$ptg = Vf \cdot ptg_{90}/Vp = 0,466 \cdot 3,00/1,00 = 1,398$	t/m^3	5.158
Parts by weight of water pwg'	$pwg' = Vln \cdot pwg/Vp = 0,078 \cdot 1,00/1,0 = 0,078$	t/m^3	5.159
Moist density pig	$pig = ptg + pwg' = 1,398 + 0,078 = 1,476$	t/m^3	5.160

Every further increase of pore water in the moist soil will change its properties again, and promotes the soil's urge to move. The limits of this conversion are reached, when the soil's pore structure has been completely filled with water. This soil is the described as 'wet', and its properties are determined below.

Characteristics of wet uncompacted soil

A pore volume of $Vl' = 0,534 m^3$ was calculated for the moist compacted mixture (5.155). This permits the soil type to absorb another 534 liters = Vln of water. While determining the properties of the wet soil above water, the approach using the natural compaction by water is not used at first, so that this soil compaction will be investigated later.

Calculation:

Fictitious solids volume $\rightarrow Vfn$ of the wet soil

$$Vfn = Vln \cdot pwg/ptg_{90} = 0,546 \cdot 1,00/3,00 = 0,178 \quad m^3 \quad 5.161$$

Inclination angle βn

$$\tan \beta n = Vf' / (Vl' + Vfn) = 0,466 / (0,534 + 0,178) = 0,655 \quad 5.162$$

$$\beta n = 33,2 \quad [-] \quad 5.163$$

Shear angle sn

$$\tan sn = (\tan \beta n) / 2 = 0,655/2 = 0,327 \quad 5.164$$

$$sn = 18,1^\circ \quad [-] \quad 5.165$$

Dry density ptg'

$$ptg' = Vf' \cdot ptg_{90}/Vp = 0,466 \cdot 3,00/1,00 = 1,398 \quad t/m^3 \quad 5.166$$

Parts by weight of water pwg'

$$pwg' = Vln \cdot pwg/Vp = 0,534 \cdot 1,00/1,00 = 0,534 \quad t/m^3 \quad 5.167$$

Wet density png

$$png = ptg' + pwg' = 1,398 + 0,534 = 1,932 \quad t/m^3 \quad 5.168$$

Characteristics of wet soil in the compacted state

Compaction of the wet soil creates width bb and height h' , and changes the soil cube, as shown in Figs. 127 to 129.

Width $b_w \rightarrow V_{fn} = 0,178 \text{ m}^3$ (5.161)

$$b_w = V_{fn}/h \cdot a = 0,178/1,00 \cdot 1,00 = 0,178 \quad \text{m} \quad 5.169$$

Width bb

$$bb = b + b_w = 1,000 + 0,178 = 1,178 \quad \text{m} \quad 5.170$$

Height h'

$$h' = V_p/bb \cdot a = 1,000/1,178 \cdot 1,00 = 0,849 \quad \text{m} \quad 5.171$$

After standardization of the wet soil to a volume of $V_p = 1,00 \text{ m}^3$, the soil characteristics are as follows:

Solids volume V_{f^*}

$$V_{f^*} = V_{f'}/h' = 0,466/0,849 = 0,549 \quad \text{m}^3 \quad 5.172$$

Pore volume V_{l^*}

$$V_{l^*} = V_p - V_{f^*} = 1,000 - 0,549 = 0,451 \quad \text{m}^3 \quad 5.173$$

Inclination angle β_{n^*}

$$\tan \beta_{n^*} = V_{f^*}/1,333 \cdot V_{l^*} = 0,549/1,333 \cdot 0,451 = 0,913 \quad 5.174$$

$$\beta_{n^*} = 42,4^\circ \quad [-] \quad 5.175$$

Shear angle sn^*

$$\tan sn^* = (\tan \beta_{n^*})/2 = 0,913/2 = 0,456 \quad 5.176$$

$$sn^* = 24,5^\circ \quad [-] \quad 5.177$$

Dry density ptg^*

$$ptg^* = V_{f^*} \cdot ptg_{90}/V_p = 0,549 \cdot 3,00/1,00 = 1,647 \quad \text{t/m}^3 \quad 5.178$$

Parts by weight of water pwg^*

$$pwg^* = V_{ln^*} \cdot pwg/V_p = 0,451 \cdot 1,00/1,0 = 0,451 \quad \text{t/m}^3 \quad 5.179$$

Moist density png^*

$$png^* = ptg^* + pwg^* = 1,647 + 0,451 = 2,098 \quad \text{t/m}^3 \quad 5.180$$

With a wet soil above water, the indicated volume reduction would lead to the following compaction:

$$\lambda = h/h' = 1,00/0,849 = 1,178 \rightarrow 17,8 \quad \% \text{ by vol.} \quad 5.181$$

According to the author's findings from his experiments with different soil types in the dry, moist, and wet states as well as with soils under water, a dry, loosely filled sand can lose about 15% of its volume by the addition of water (see Section 2.4.3, page 41).

In the soil band, the volume change from moist, partially compacted soil to wet compacted soil above water is represented as follows:

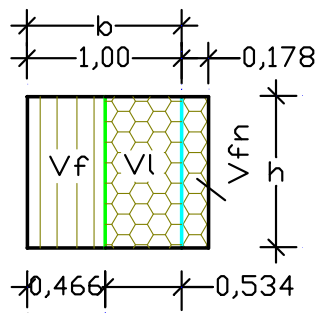


Fig. 127: Widening of the soil cube due to water absorption.

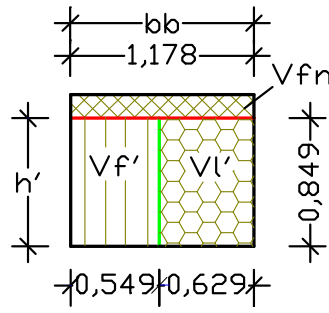


Fig. 128: Before standardization, with loss of height due to compaction.

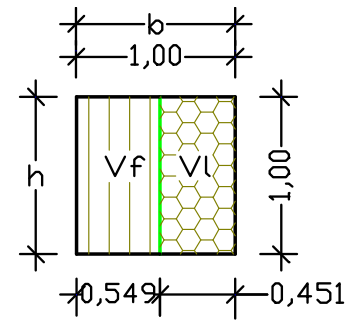


Fig. 129: Volumes of compacted wet soil after standardization.

Characteristics of wet uncompacted soil under water

If one considers that up the time of the landslide, the Concordia lake's water level had risen from a height of 42,0 m a.s.l. up to a height of 82,0 m a.s.l., it can be assumed that the filling material was first flooded by the simultaneously rising groundwater level. As demonstrated by the author's tests, the rising water level must have changed the initially dry uncompacted filling material into a wet compacted soil under water. Moreover, the rising groundwater generated uplift forces in the filling material, which were not present initially, and therefore had to lead to a reduction of soil density and the associated increased risk of a landslide. In order to reproduce the calculations for the properties of wet soils under water more easily when using real soil properties, the unoccupied pore volume $V_{lt} = 0,00 \text{ m}^3$ is used in the corresponding formulas (see "Calculating the properties of moist soils", Section 3.1.4, page 63).

The following volumes are used to determine the properties of the wet soil under water: $V_{f'} = 0,466 \text{ m}^3$ (5.154), $V_{l'} = 0,534 \text{ m}^3$ (5.155), and $V_{ln} = 0,534 \text{ m}^3$.

Volume of uplift $V_{fa} \rightarrow$ with V_{fn} of the wet soil

$$V_{fa} = V_{f'}/3 + V_{lt} = 0,466 \cdot 1/3 + 0,00 = 0,155 \quad \text{m}^3 \quad 5.182$$

Solids volume $V_{fw} \rightarrow$ ratio $p_{wg}/p_{tg90} = 1/3$

$$V_{fw} = 2 \cdot V_{f'}/3 - V_{lt}/3 = 2 \cdot 0,466/3 - 0,0 = 0,311 \quad \text{m}^3 \quad 5.183$$

Inclination angle $\beta_{nw} \rightarrow$ of the wet soil under water

$$\tan \beta_{nw} = V_{fw} / (5 \cdot V_{l'} / 6) = 0,311 / (5 \cdot 0,534 / 6) = 0,698 \quad 5.184$$

$$\beta_{nw} = 34,9^\circ \quad [-] \quad 5.185$$

Shear angle $snw \rightarrow$ of the wet soil under water

$$\tan snw = (\tan \beta_{nw}) / 2 = 0,698/2 = 0,349 \quad 5.186$$

$$snw = 19,3^\circ \quad [-] \quad 5.187$$

Wet density $p_{ngw} \rightarrow$ of the wet soil under water

$$p_{ngw} = (V_{fw} \cdot p_{tg90} + V_{l'} \cdot p_{wg}) / V_{p90}$$

$$p_{ngw} = (0,311 \cdot 3,0 + 0,534 \cdot 1,0) / 1,0 = 1,467 \quad \text{t/m}^3 \quad 5.188$$

Fictitious volume $V_{nw} \rightarrow$ leads to a reduction of width bb (5.191)

$$V_{nw} = V_l' / 6 = 0,534 / 6 = 0,089 \quad \text{m}^3 \quad 5.189$$

Because the water pressure prevents the urge of the wet soil to spread out, volume $V_{nw} = 0,089 \text{ m}^3$ or its width bw' are used with a negative sign in the calculation approach (5.191).

Width $bw' \rightarrow$ equals a at a depth of 1,00 m

$$bw' = V_{nw} / h \cdot a = 0,089 / 1,00 \cdot 1,00 = 0,089 \quad \text{m} \quad 5.190$$

Width $bb \rightarrow$ width reduction

$$bb = b + bw = 1,000 - 0,089 = 0,911 \quad \text{m} \quad 5.191$$

Height h'

$$h' = V_p / bb \cdot a = 1,000 / 0,911 \cdot 1,00 = 1,098 \quad \text{m} \quad 5.192$$

Compaction factor λ

$$\lambda = h / bb = 1,00 / 0,911 = 1,098 \rightarrow 9,8 \quad \% \text{ by vol.} \quad 5.193$$

The volumes of the wet compacted soil under water are shown in the soil band and after standardization in the soil cube (Fig. 131).

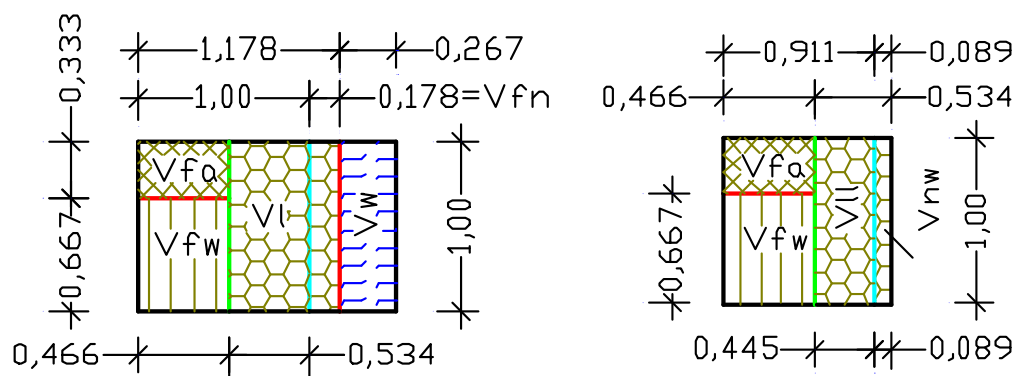


Fig. 130

Fig. 131

Figs. 130 and 131 show the volumes of the wet compacted soil under water before and after standardization.

Summary of the results

According to reports in the media, no significant changes of the terrain surface were observed before the landslide. Consequently, the above calculations indicate that severe force shifts must have occurred in the slope. The calculated compaction factor $\lambda = 1,098$ (5.193) alone would have been able to cause a lowering of the terrain surface in the lake's shore area by the amount of Δh . This height Δh will be calculated by means of the lake's water level height $h^* = 40,0 \text{ m}$.

Height Δh

$$\Delta h = h^* - h^* / \lambda = 40,00 - 40,00 / 1,098 = 3,60 \quad \text{m} \quad 5.194$$

The table below shows that the water stored in the lake caused a considerable change in the properties of the slightly moist loam/sand mix of the different soil conditions.

Summary of the soil characteristics

Soil properties	Moist and uncompacted	Wet and uncompacted	Wet and compacted	Wet under water, uncompacted
Density t/m ³	$p_{ig} = 1,476$ (5.160)	$p_{ng} = 1,932$ (5.168)	$p_{ng}^* = 2,098$ (5.180)	$p_{nwg} = 1,467$ (5.188)
Angle	$\beta_{i} = 39,8^\circ$ (5.157)	$\beta_{n} = 33,2^\circ$ (5.163)	$\beta_{n}^* = 42,4^\circ$ (5.175)	$\beta_{nw} = 34,9^\circ$ (5.185)
Shear angle	$s_{i} = 22,6^\circ$	$s_{n} = 18,1^\circ$ (5.165)	$s_{n}^* = 24,5^\circ$ (5.177)	$s_{nw} = 19,3^\circ$ (5.187)
Compaction			$\lambda = 17,8\%$ by vol. (5.181)	$\lambda = 9,8\%$ by vol. (5.193)

Because, apart from soil compaction, the earth masses on the shear planes of the different soils increase the urge to move in the slope, the influence of the soil loads on the shear planes will be investigated.

5.2.2 Adaptation of loads in soils under water

Loads on soils have been described in Section 2.4.1 and supplemented in Section 4.3. According to the New Earth Pressure Theory, the dispersal of loads in the ground is handled exclusively by the solids structure of the loaded soil. Neither the absorbed pore water nor the adjacent groundwater can be used for load dispersal. To be noted is that the uplift generated by soils under water reduces the solids volume by one third, and thereby has an influence on the inclination and shear angles as well as the soil's drifting apart.

Because the angles for the different soil conditions have already been calculated, a renewed angle calculation due to the load can be omitted, if one increases the load height he – which is present above the groundwater level – in accordance with the ratio of the solids volume V_f'/V_{fw} . For example, with an assumed load height $he = 10,00$ m, the new load height he^* can be calculated by means of the solids volumes $V_f' = 0,466$ m³ (5.154) above, and $V_{fw} = 0,311$ m³ (5.183) under water.

Load height he^*

$$he^* = he \cdot V_f'/V_{fw} = 10,0 \cdot 0,466/0,311 \sim 15,0 \quad \text{m} \quad 5.195$$

Under water, an increased load causes a horizontal expansion of the soil cube by the amount of width $\Delta b = V_f'/3 \cdot h \cdot a$, whereby $h = 1,00$ m corresponds to the cube height. For the calculation of widths and angles, the volume $V_{fa} = V_f'/3$ is introduced, and equated to the uplift volume V_{fa} :

Volume Vla

$$Vla = Vf' / 3 = 0,466 / 3 = 0,155 \quad \text{m}^3 \quad 5.196$$

Inclination angle $\beta_{ew} \rightarrow$ under load (see Section 3.2.1, page 68).

$$\tan \beta_{ew} = Vf_w / (5 \cdot Vl' / 6 + Vla)$$

$$\tan \beta_{ew} = 0,311 / (5 \cdot 0,534 / 6 + 0,155) = 0,518 \quad 5.198$$

$$\beta_{ew} = 27,4^\circ \quad [-] \quad 5.199$$

Shear angle $sew \rightarrow$ under load

$$\tan sew = (\tan \beta_{we}) / 2 = 0,518 / 2 = 0,259 \quad 5.200$$

$$sew = 14,5^\circ \quad [-] \quad 5.201$$

The inclination angle which is reduced by the load, can also be calculated by means of the volumes of the respective soil type. For this, the solids volume Vf_w must be put into relation with the changed pore volume of the soil under water (see equation [3.93] on page 74). In this case, width $\Delta b = 0,155$ m of volume $Vla = 0,155$ m³ (5.196) must be added to width $b_w = 0,178$ m (5.169), which then results in width $b_w^* = 0,333$ m of the soil band (see Fig. 132).

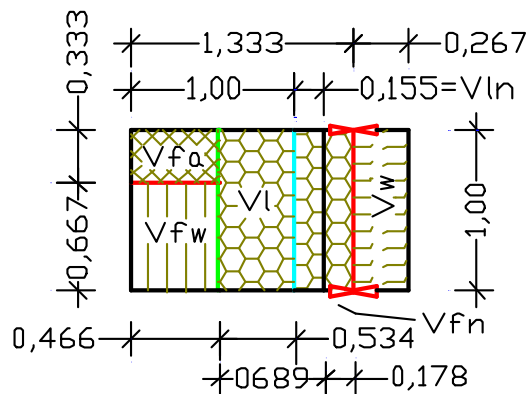


Fig. 132: Soil band under water that has expanded to width $b_w' = 0,333$ m due to the load.

The sectional view (Fig. 133) is available to determine the individual calculation values. Stations (Stat) have been included in the sectional view, which indicate the changes in the terrain levels, and thereby different load conditions in the slope.

5.2.3 Location of shear planes in the respective Stations

The sectional view (Fig. 133) serves to determine the positions of shear planes in the individual Stations. It is based on the site plans kindly provided by the DLR (before/after), and uses the height +40 m a.s.l. as reference. It shows the terrain contour between heights +135,00 m a.s.l. and +42,00 m a.s.l. over a distance of 500 m. In addition, the terrain contour after the landslide (magenta), the original bed of the open cast mine between +97 m a.s.l. and +42 m a.s.l.,

and the stored water level of +82 m a.s.l. in the Concordia lake at the time of the landslide were taken from the DLR site plans. All other heights have been interpolated from the basic data, and vertical reference axes (Stat) inserted at certain points to indicate changes in the slope angle or special features in connection with the groundwater tables. A height/length ratio of 1:0,36 was selected for the graphical representation in Fig. 133, whereby 'Terrain I' indicates the original terrain contour, 'Terrain II' indicates the contour after the landslide, and 'Bottom' indicates the original bed of the open cast pit.

Sectional view at the geodetic length of 661450 m

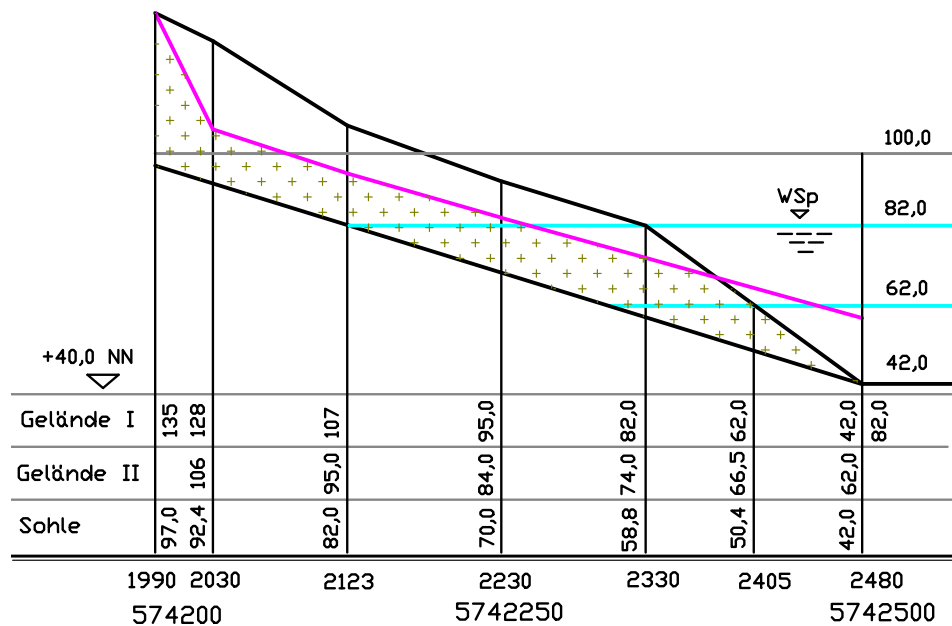


Fig. 133: Sectional view of the terrain contour before the landslide, after the landslide (magenta), and the original bottom of the pit.

Determination of the shear plane under load is done in sections, i.e. at the vertical reference axes. The changing soil properties, the different terrain heights, and the water levels in the lake at +62 m a.s.l. and +82,0 m a.s.l. are taken into account when calculating the shear planes under load. The calculations are made in accordance with the details given in Sections 4.4 to 4.6.

The different slope angles in the terrain contour make it necessary to divide the longitudinal section into five calculation sections. In contrast, the original pit bottom has a continuous incline, so that its angle z can be calculated by means of heights +42,0 m a.s.l. at Stat. 2480, and +97,0 m a.s.l. at Stat. 1990.

Angle z → of pit bottom incline

$$\tan z = (97,0 - 42,0) / (2480 - 1990) = 0,112 \quad 5.202$$

$$z = 6,4^\circ \quad [-] \quad 5.203$$

Volume adaptation of different soil types

For calculating the forces in differently layered soil types, the overall calculation height must first be determined by adding the individual layer heights. Subsequently, the soil properties of the upper layers must be adapted to the soil type of the bottom layer (see Section 4.4, pages 126ff).

This definition starts with the lowest soil layer, whereby height h_u and the real inclination angle β are used to determine wedge width b_u . Provided that the soil layers are in accordance with Fig. 92 (page 127), height h_o on the reference axis, and height h_{oo} at the distance of width b_u indicate the distances to the real terrain contour. In order to adapt the upper soil type to the lower soil type, heights h_o and h_{oo} are multiplied with the previously mentioned ratio factor V_f'/V_{fw} , so that heights h_{oo}' and h_o' are created. The connecting line between heights h_{oo}' and h_o' corresponds to the fictitious terrain contour with angle x' . If one now adds heights h_u and h_o' at the reference axis, and inserts a horizontal line above them, the new wedge with width $b_o = (h_u + h_o') / \tan \beta$ will be located in this plane. Width b_o and height $h_{oo}' = h_x$ define a wedge area whose bottom represents the load resting on the earth wedge with width b_o and height $h_u + h_o'$.

Other dependencies when determining inclination and shear angle under load will be detailed later as appropriate, whereby the heights are marked with letters, and specified in 'm a.s.l.'. In the respective Stations, the original pit bottom is named H_s , and the real terrain height is named H_o , whereby the distance between the two heights is named h_m . As explained in Section 4.3.1, the weight of the soil in the wedge area above width b_o changes the natural angle, thereby creating the inclination and shear angles β_e and s_e under load. Calculation of the angles depends on the respective ratio of angles x and x' of the rising terrain slope to angle s of the natural shear plane. Fig. 78 of Test 9.2 on page 110 shows the determination of shear plane under load, if angle x is steeper than angle s . The other version (angle x is flatter than angle s) is shown in Fig. 81 of test 9.3 on page 113.

As shown in the named Figs., the reference axis is shifted into the slope by the amount of width b_m due to the inclined plane under load. Hereby, the impairment of vertical force dispersal, e.g. due to rock in the basal plane, converts the vertical forces into horizontal forces, which can have an additional positive influence on possible soil movements. If the surface of the assumed rock layer

lies in an inclined plane, the urge to move in the slope is increased, whereby the sliding soil lowers the shear plane under load even further (see Fig. 93, page 129).

In summary, it can be said that in order to disperse the soil load, the natural inclined plane becomes steeper, thereby exceeding the limit value (μ) of the internal soil friction. With an increasing influence on the soil structures, the soil's mobility and its urge to initiate a landslide also grows. The associated calculations of weights and forces are carried out by means of the selected calculation depth $a = 1,00$ m and the areas.

Station 2405

According to the DLR site plans (before/after), the bed of the Concordia lake was at height +42,0 m a.s.l., and the storage water level at the time of the landslide was at height +82 m a.s.l. In order to reproduce the landslide, the first vertical reference axis was placed in Stat. 2405, where half of the storage water level, and the terrain height of the lake shore were at height $Ho_1 +62,0$ m a.s.l. Height $Hs_1 +50,4$ m a.s.l. of the lake bed was determined by means of angle $z = 6,4^\circ$ (5.203) and the distance between Stats. 2480 and 2405. Starting at the lake shore, the terrain contour rises up to height $Ho_2 = +82,0$ m a.s.l. in Stat. 2330. For Stats. 2405 to 2330, angle x of the terrain slope is determined via height $hg = 20,0$ m divided by the section length $lg_1 = 75,0$ m.

Angle $x_1 \rightarrow$ of the real terrain slope

$$\tan x_1 = h / lg_1 = 20,0 / 75,0 = 0,267 \quad 5.204$$

$$x_1 = 14,9^\circ \quad [-] \quad 5.205$$

It is assumed that below the horizontal plane at +62,0 m a.s.l., the moist soil used to fill the pit was changed into a 'wet soil under water' by the water stored in the lake. The calculated soil properties have been entered in the table below.

Properties	
Moist soil above water	Wet soil under water
Density $\rho_{ig} = 1,476$ t/m ³ (5.160)	Density $\rho_{nwg} = 1,467$ t/m ³ (5.188)
Solids volume $Vf'' = 0,466$ m ³ (5.154)	Solids volume $Vfw = 0,311$ m ³ (5.183)
Inclination angle $\beta_i = 39,8^\circ$ (5.157)	Inclination angle $\beta_{nw} = 34,9^\circ$ (5.185)
$\tan \beta_i = 0,832$ (5.156)	$\tan \beta_{nw} = 0,698$ (5.184)
$\tan s_i = 0,832/2 = 0,416$	$\tan s_{nw} = 0,349$ (5.186)
Shear angle $s_i = 22,6^\circ$	Shear angle $s_{nw} = 19,3^\circ$ (5.187)

In order to reproduce the soil movement in the slope, the properties of the moist soil must first be adapted to those of the soil under water, i.e. height h_{oo} in particular must be converted into height h_{oo}' by means of the ratio V_f'/V_{fw} . For this, the wedge width bo must be determined via height hm and the angle of the soil under water (β_{nw}).

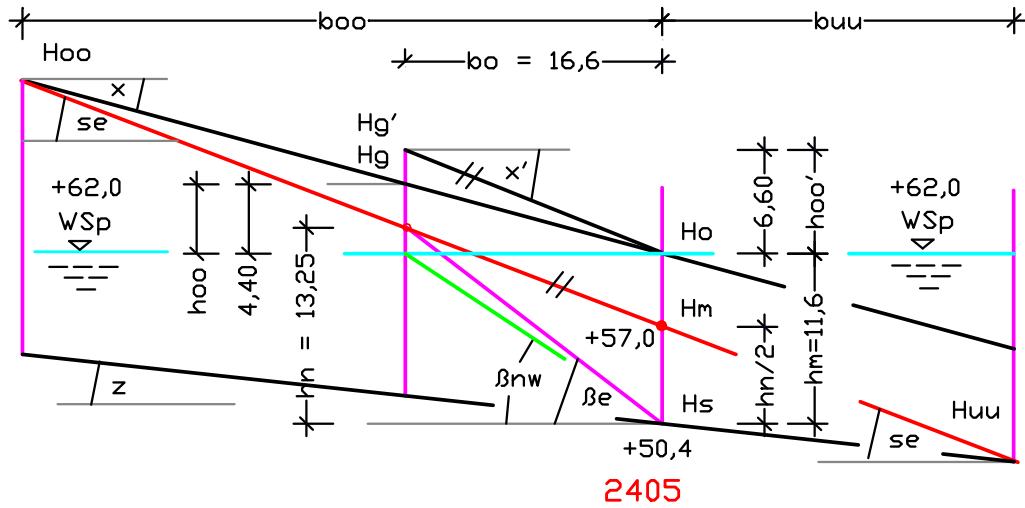


Fig. 134: Shear plane under load (red) between heights H_{oo} and H_{uu} .

The original terrain height H_g and the fictitious height H_g' must be calculated from the reference axis at the distance width bo . In this case, wedge height hx of the soil load on the natural shear plane (green) corresponds to height $h_{oo}' = hx$, so that angle x' of the fictitious slope can be calculated via height hx and width bo . The inclination angle β_e under load can be determined via height $hm = hm + hx/4$ and width bo . Angle se of the shear plane under load can be determined via $\tan se = (\tan \beta_e) / 2$.

Calculation:

Height $hm \rightarrow$ view height of the bottom soil at the reference axis

$$hm = Ho_1 - Hs_1 = 62,0 - 50,4 = 11,6 \quad \text{m} \quad 5.206$$

Width $bo \rightarrow$ with angle $\beta_{nw} = 35^\circ$ and height $hm = 11,60$ m

$$bo = hm / \tan \beta_{nw} = 11,6 / 0,698 = 16,6 \quad \text{m} \quad 5.207$$

Height $h_{oo} \rightarrow$ with angle $x_1 = 14,9^\circ$

$$h_{oo} = bo \cdot \tan x_1 = 16,6 \cdot 0,267 \sim 4,4 \quad \text{m} \quad 5.208$$

Height h_{oo}'

$$h_{oo}' = h_{oo} \cdot V_f'/V_{fw} = 4,4 \cdot 0,466/0,311 = 6,6 \quad \text{m} \quad 5.209$$

Angle x_1'

$$\tan x_1' = h_{oo}' / bo = 6,6 / 16,6 = 0,398 \quad 5.210$$

$$x_1' = 21,7^\circ \quad [-] \quad 5.211$$

Height hm'

$$hm' = hm + h_{oo}' / 4 = 11,6 + 6,6 / 4 \sim 13,25 \quad \text{m} \quad 5.212$$

Inclination angle β_e

$$\tan \beta_e = hm' / bo = 13,25 / 16,6 = 0,798 \quad 5.213$$

$$\beta_e = 38,6^\circ \quad [-] \quad 5.214$$

Shear angle se

$$\tan se = (\tan \beta_e) / 2 = 0,798 / 2 = 0,399 \quad 5.215$$

$$se = 21,8^\circ \quad [-] \quad 5.216$$

In this case, the practically identical angles of fictitious slope $x_l' = 21,7^\circ$ (5.211) and of shear plane under load $se = 21,8^\circ$ (5.216) indicate that no soil loads are resting on the shear plane under load, which could slide and thereby cause earth movements in the slope. Widths boo and buu show the range of influence for this calculation.

Width boo

$$boo = hm / (\tan \beta_e - \tan se) = 11,6 / 0,399 \sim 29,1 \quad \text{m} \quad 5.217$$

Width buu

$$buu = hm / (\tan se - \tan z)$$

$$buu = 11,6 / (0,399 - 0,112) \sim 40,4 \quad \text{m} \quad 5.218$$

Because the slightly moist filling material is exposed to the rising groundwater level for the first time, a soil subsidence with height Δh must be assumed in the above range. This can best be calculated at the reference axis using height hm and compaction factor $\lambda = 17,8\%$ by vol. (see summary of soil characteristics in Section 5.2.1, page 197).

Height Δh

$$\Delta h = hm \cdot \lambda / 100 = 11,6 \cdot 17,8 / 100 \sim 2,1 \quad \text{m} \quad 5.219$$

Results:

Because angles x' and se in the area of Stat. 2405 are equal, and apart from the compaction of the adjacent soil due to the groundwater level increase, no further soil movement will occur, except if such movement is initiated at some other location in the slope.

Station 2330

This Station was selected, because the terrain contour Ho_2 as well as the water level (WSp) in the lake are at height +82,0 m a.s.l. Height HS_2 of the lake bed at +58,8 m a.s.l. was interpolated via angle $z = 6,4^\circ$ (5.203). A change of incline occurs in the terrain contour, whereby angle $x_l = 14,9^\circ$ (5.205) to the right of the reference axis remains, while the terrain to the left of the axis between

Stat. 2330 and Stat. 2123 increases with angle x_2 from height +82,00 m a.s.l. to height +107,0 m a.s.l. along the length $lg_2 = 207$ m.

The following calculations are made to represent the terrain profile:

Angle $x_2 \rightarrow$ via the height difference +107,0 m minus +82,00 m

$$\tan x_2 = (107,0 - 82,0) / lg_2 = 25,0 / 207 = 0,121 \quad 5.220$$

$$x_2 = 6,9^\circ \quad [-] \quad 5.221$$

Height $hm \rightarrow$ view height of the soil at the reference axis

$$hm = Ho_2 - Hs_2 = 82,0 - 58,8 = 23,2 \quad \text{m} \quad 5.222$$

Wedge width $bo \rightarrow$ with $\tan \beta_{nw}$ (5.184)

$$bo = hm / \tan \beta_{nw} = 23,2 / 0,698 \sim 33,2 \quad \text{m} \quad 5.223$$

Height $hoo \rightarrow$ above water

$$hoo = bo \cdot \tan x_2 = 33,2 \cdot 0,121 \sim 4,0 \quad \text{m} \quad 5.224$$

Height $hoo' \rightarrow$ taking factor Vf'/Vfw into account

$$hoo' = hoo \cdot Vf'/Vfw = 4,0 \cdot 0,466 / 0,311 \sim 6,0 \quad \text{m} \quad 5.225$$

Angle $x_2' \rightarrow$ of the fictitious slope

$$\tan x_2' = hoo' / bo = 6,0 / 33,2 = 0,181 \quad 5.226$$

$$x_2' = 10,3^\circ \quad [-] \quad 5.227$$

Height hn

$$hn = hm + hoo' / 4 = 23,2 + 6,0 / 4 = 24,7 \quad \text{m} \quad 5.228$$

Inclination angle β_e

$$\tan \beta_e = hn / bo = 24,7 / 33,2 = 0,744 \quad 5.229$$

$$\beta_e = 36,6^\circ \quad [-] \quad 5.230$$

Shear angle se

$$\tan se = (\tan \beta_e) / 2 = 0,744 / 2 = 0,372 \quad 5.231$$

$$se = 20,4^\circ \quad [-] \quad 5.232$$

Here, the difference between angles se and x_2' shows that the earth weights resting on the shear plane to the left of the reference axis can start to slide if they lose their hold. Height hyy and widths boo and buu can be calculated by means of height $hm = 23,20$ m (5.222) and angles se , x_2' and $z = 6,4^\circ$ (5.203), thereby limiting the possible soil movement in the area of influence around Stat. 2330.

Height hyy

$$hyy^2 / [2 \cdot (\tan se - \tan x_2')] = (hm - hyy)^2 / [2 \cdot (\tan se - \tan z)]$$

$$hyy^2 / [2 \cdot (0,372 - 0,181)] = (23,2 - hyy)^2 / [2 \cdot (0,372 - 0,112)]$$

$$hyy^2 = (23,2 - hyy)^2 \cdot 0,382 / 0,52$$

$$hyy = \sqrt{0,735 \cdot (23,2 - hyy)} \quad hyy + 0,857 hyy - 19,89 = 0$$

$$hyy = 19,89 / 1,857 \sim 10,7 \quad \text{m} \quad 5.233$$

Height hu

$$hu = hm - hyy = 23,2 - 10,7 = 12,5 \quad \text{m} \quad 5.234$$

Width boo

$$boo = hyy / (\tan se - \tan x_2')$$

$$boo = 10,7 / (0,372 - 0,181) = 56,0 \quad \text{m} \quad 5.235$$

Width buu

$$buu = hu / (\tan se - \tan z)$$

$$buu = 12,50 / (0,372 - 0,112) = 48,1 \quad \text{m} \quad 5.236$$

Area Aoo

$$Aoo = boo \cdot hyy / 2 = 56,0 \cdot 10,7 / 2 = 299,7 \quad \text{m}^2 \quad 5.237$$

Area Auu

$$Auu = buu \cdot hu / 2 = 48,1 \cdot 12,50 / 2 = 300,5 \quad \text{m}^2 \quad 5.238$$

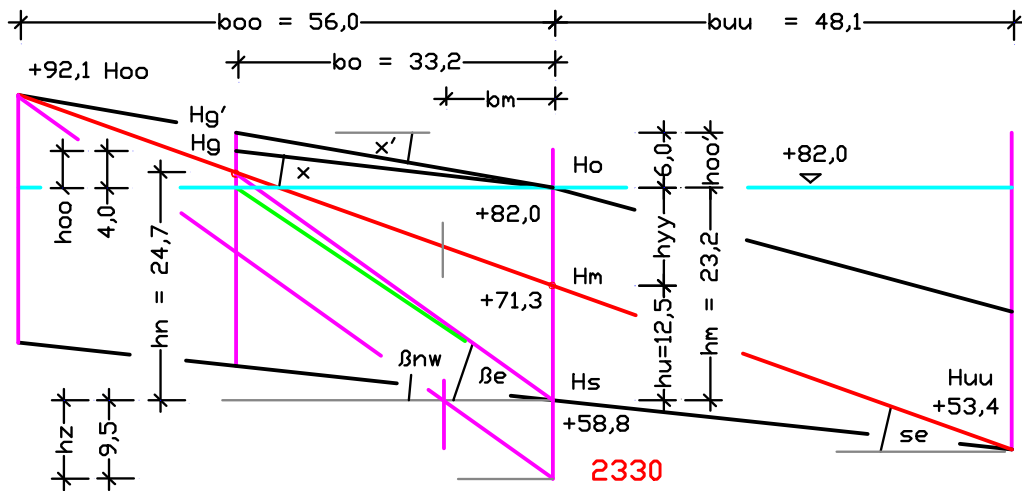


Fig. 135: Heights Hg and Hg' of the terrain contours, and the positions of the inclined planes (magenta) and shear plane under load (red).

For the graphical representation of the force areas and forces acting against the fictitious wall in the reference axis of Stat. 2330, the following heights and widths are determined and then converted into heights a.s.l. and Stations.

Height hh

$$hh = boo \cdot \tan \beta_e = 56,0 \cdot 0,764 = 42,8 \quad \text{m} \quad 5.239$$

Height hxx

$$hxx = boo \cdot \tan x_2' = 56,0 \cdot 0,181 = 10,1 \quad \text{m} \quad 5.240$$

Height hz

$$hz = hh - hxx - hm = 42,8 - 10,1 - 23,2 = 9,5 \quad \text{m} \quad 5.241$$

Height hm'

$$hm' = hh - hxx = 42,8 - 10,1 = 32,7 \quad \text{m} \quad 5.242$$

Width bou

$$bou = hm' / \tan \beta_e = 32,7 / 0,764 = 42,8 \quad \text{m} \quad 5.243$$

Width bou'

$$bou' = (hm' - hyy) / \tan \beta_e$$

$$bou' = (32,7 - 10,7) / 0,764 = 28,8 \quad \text{m} \quad 5.244$$

Width bm	$bm = hz / \tan \beta e = 9,5 / 0,764 = 12,4$	m	5.245
Area Aou	$Aou = (bou \cdot hm') / 2 = (42,8 \cdot 32,7) / 2 = 700,0$	m ²	5.246
Height Hoo	$Hoo = Ho_2 + hxx = 82,0 + 10,1 = 92,1$	m a.s.l.	5.247
Stat. of height Hoo	$\text{Stat. } 2330 - boo = 2330 - 56,0 = \text{Stat. } 2274$		5.248
Height Hm	$Hm = Ho_2 - hyy = 82,0 - 10,7 = 71,3$	m a.s.l.	5.249
Height Hz	$Hz = Ho_2 - hm' = 82,0 - 32,7 = 49,3$	m a.s.l.	5.250
Height Huu	$Huu = Hs_2 - buu \cdot \tan z =$ $Huu = 58,8 - 48,1 \cdot 0,112 = 53,4$	m a.s.l.	5.251
Stat. of height Huu	$\text{Stat. } 2330 + buu = 2330 + 48,1 \sim \text{Stat. } 2378$		5.252

Also here, the slightly moist filling material is subjected to the rising ground-water level, so that a soil subsidence can be determined via height $hm = 23,2$ m (5.222) and compaction factor $\lambda = 17,8\%$ by vol. (see Test 3, page 41, and the summary of soil characteristics in Section 5.2.1, page 197).

Height Δh	$\Delta h = hm \cdot \lambda / 100 = 23,2 \cdot 17,8 / 100 \sim 4,10$	m	5.253
-------------------	---	---	-------

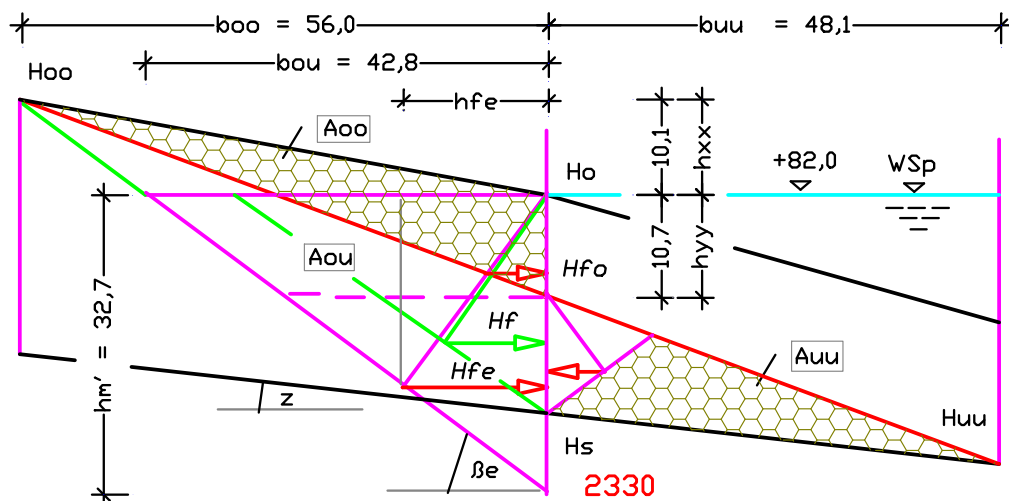


Fig. 136: Position, direction, and force meters of the forces around Stat. 2330, whereby the forces are shown in italics.

Results:

The shear plane under load increases with angle $se = 20,4^\circ$ (5.232) from height $Huu + 53,4$ m a.s.l. at Stat. 2274 via height $Hm + 71,3$ m a.s.l. at the reference

axis, up to height $H_{00} +92,1$ m a.s.l. at Stat. 2378. The soil above this shear plane will start moving as soon as it overcomes the frictional force of the adjacent soil in the area of Stat. 2405. The horizontal force H_{f0} acting from wedge area $A_{00} = 299,7$ m² (5.237) against reference axis of Stat. 2330, can be calculated by means of area $A_{0u} = 700,0$ m² (5.246), density $\rho_{nwg} = 1,467$ t/m³ (5.188), and gravity force. Not taken into account in the above calculations is the soil subsidence to be expected in the determined height $\Delta h = 4,10$ m (5.253). If one includes this subsidence in the earth movement, earth weights in the same amount would be missing, which could provide resistance against the sliding soil.

The force areas shown in Fig. 129 were calculated on the basis of real heights and widths. Force determination based on fictitious terrain heights is possible, but then the results would have to be adapted to the real values using factor $V_{f'}/V_{fw}$. In spite of the different calculation methods, no differences in forces should arise due to the reverse calculation.

Station 2230

The heights $H_{S3} = 70,0$ m a.s.l. of the lake bed and the terrain contour $H_{O3} = +95,0$ m a.s.l., and the distance between the Stations plus the elevation angle $z = 6,4^\circ$ (5.203) of the lake bed or the terrain plane $x_2 = 6,9^\circ$ (5.221) were used to determine the profile section (before). Due to the landslide (afterwards) the original terrain surface was lowered, so that the new lake shore was created at Stat. 2230. Height $H_w +82,0$ m a.s.l. is assigned to the lake shore, as it is assumed that the earth masses which slid down the slope only raised the lake's water level by a few centimeters, and that this increase is negligible for the following calculations.

The following calculations are made to represent the terrain profile:

Height $hm \rightarrow$ view height of the soil at the reference axis

$$hm = H_{O3} - H_{S3} = 95,0 - 70,0 = 25,0 \quad \text{m} \quad 5.254$$

In this case, height hm is divided by the assumed groundwater level $H_w +82,0$ m a.s.l., so that heights h_o and h_{oo} can be determined and then multiplied with factor $V_{f'}/V_{fw}$ to create the fictitious terrain contour. Width bo is calculated via height $h_w = H_w - H_{S3}$.

Height h_w

$$h_w = H_w - H_{S3} = 82,0 - 70,0 = 12,0 \quad \text{m} \quad 5.255$$

- Wedge width $bo \rightarrow$ with $\tan \beta_{nw}$ (5.184)
- $$bo = hu / \tan \beta_{nw} = 12,0 / 0,698 \sim 17,2 \quad \text{m} \quad 5.256$$
- Height $ho \rightarrow$ above water at the reference axis
- $$ho = Ho_3 - Hs_3 = 95,0 - 82,0 = 13,0 \quad \text{m} \quad 5.257$$
- Height $ho' \rightarrow$ above water
- $$ho' = ho \cdot Vf' / Vf_w = 13,0 \cdot 0,466 / 0,311 \sim 19,5 \quad \text{m} \quad 5.258$$
- Height hoo
- $$hoo = ho + bo \cdot \tan x_2 = 13,0 + 17,2 \cdot 0,121 \sim 15,1 \quad \text{m} \quad 5.259$$
- Height hoo'
- $$hoo' = hoo \cdot Vf' / Vf_w = 15,1 \cdot 0,466 / 0,311 \sim 22,6 \quad \text{m} \quad 5.260$$
- Height hx
- $$hx = hoo' - ho' = 22,6 - 19,5 = 3,1 \quad \text{m} \quad 5.261$$
- Angle $x_2' \rightarrow$ of the fictitious terrain slope
- $$\tan x_3' = hx / bo = 3,1 / 17,2 = 0,180 \quad 5.262$$
- $$x_3' = 10,2^\circ \quad [-] \quad 5.263$$
- Height hm^*
- $$hm^* = hw + ho' = 12,0 + 19,5 = 31,5 \quad \text{m} \quad 5.264$$
- Wedge width $bo' \rightarrow$ with $\tan \beta_{nw}$ (5.184)
- $$bo' = hm^* / \tan \beta_{nw} = 31,5 / 0,698 = 45,1 \quad \text{m} \quad 5.265$$
- Height hn
- $$hn = hm^* + hx/4 = 31,5 + 3,1/4 = 32,3 \quad \text{m} \quad 5.266$$
- Inclination angle β_e
- $$\tan \beta_e = hn / bo = 32,3 / 45,1 = 0,716 \quad 5.267$$
- $$\beta_e = 35,6^\circ \quad [-] \quad 5.268$$
- Shear angle se
- $$\tan se = (\tan \beta_e) / 2 = 0,716 / 2 = 0,358 \quad 5.269$$
- $$se = 19,7^\circ \quad [-] \quad 5.270$$

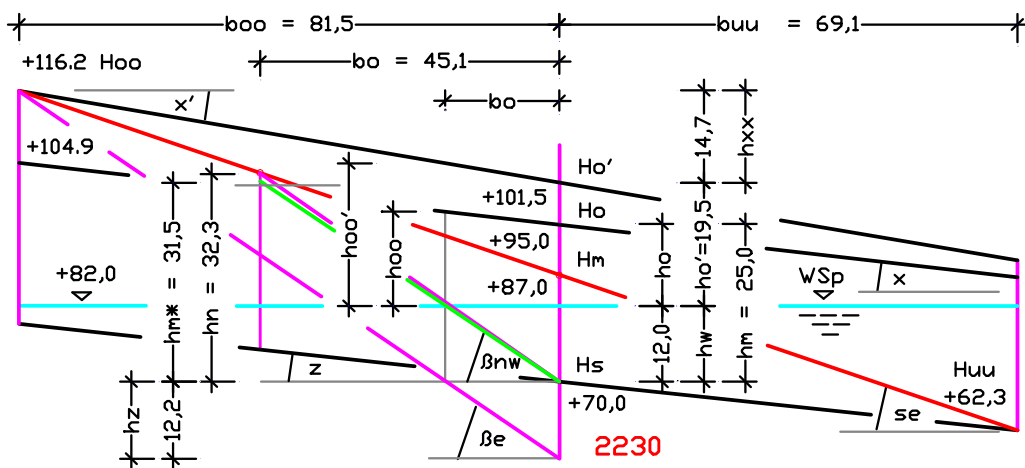


Fig. 137: Development of the inclined plane by means of height hn and width bo and the position of shear plane under load (red).

Also here, the difference between angles se and x_3' indicates that earth weights are resting on the shear plane to the left of the reference axis, which will generate horizontal forces against Stat. 2230 if they lose their hold. By means of height $hm^* = 31,5$ m (5.264) and the angles se , x_3' and z (5.203), it is possible to calculate height hyy as well as widths boo and buu , thereby limiting the possible soil movement in the influence area of Stat. 2230.

Height hyy

$$\begin{aligned} hyy^2 / [2 \cdot (\tan se - \tan x_3')] &= (hm^* - hyy)^2 / [2 \cdot (\tan se - \tan z)] \\ hyy^2 / [2 \cdot (0,358 - 0,180)] &= (31,5 - hyy)^2 / [2 \cdot (0,358 - 0,112)] \\ hyy^2 &= (31,5 - hyy)^2 \cdot 0,356 / 0,492 \quad | \quad hyy = \sqrt{0,724 \cdot (31,5 - hyy)} \\ hyy &= 26,8 / 1,851 \sim 14,5 \quad \text{m} \quad 5.271 \end{aligned}$$

Height hu

$$hu = hm^* - hyy = 31,5 - 14,5 = 17,0 \quad \text{m} \quad 5.272$$

Width boo

$$\begin{aligned} boo &= hyy / (\tan se - \tan x_3') \\ boo &= 14,5 / (0,358 - 0,180) = 81,5 \quad \text{m} \quad 5.273 \end{aligned}$$

Width buu

$$\begin{aligned} buu &= hu / (\tan se - \tan z) \\ buu &= 17,0 / (0,358 - 0,112) = 69,1 \quad \text{m} \quad 5.274 \end{aligned}$$

Area Aoo

$$Aoo = boo \cdot hyy / 2 = 81,5 \cdot 14,5 / 2 = 590,9 \quad \text{m}^2 \quad 5.275$$

Area Auu

$$Auu = buu \cdot hu / 2 = 69,1 \cdot 17,0 / 2 = 587,4 \quad \text{m}^2 \quad 5.276$$

Height hh

$$hh = boo \cdot \tan \beta_e = 81,5 \cdot 0,716 = 58,4 \quad \text{m} \quad 5.277$$

To determine the force areas and forces acting against the fictitious wall in the reference axis of Stat. 2230, the heights and widths are calculated and then converted into heights a.s.l. and Stations.

Height hxx

$$hxx = boo \cdot \tan x_3' = 81,5 \cdot 0,180 = 14,7 \quad \text{m} \quad 5.278$$

Height hz

$$hz = hh - hxx - hm^* = 58,4 - 14,7 - 31,5 = 12,2 \quad \text{m} \quad 5.279$$

Height hm'

$$hm' = hh - hxx = 58,4 - 14,7 = 43,7 \quad \text{m} \quad 5.280$$

Width bou

$$bou = hm' / \tan \beta_e = 43,7 / 0,716 = 61,0 \quad \text{m} \quad 5.281$$

Width bou'

$$\begin{aligned} bou' &= (hm' - hyy) / \tan \beta_e \\ bou' &= (43,7 - 14,5) / 0,716 = 40,8 \quad \text{m} \quad 5.282 \end{aligned}$$

Width bm

$$bm = hz / \tan \beta_e = 12,2 / 0,716 = 17,0 \quad \text{m} \quad 5.283$$

Area Aou

$$Aou = (bou \cdot hm') / 2 = (61,0 \cdot 43,7) / 2 = 1332,9 \quad \text{m}^2 \quad 5.284$$

Height Hoo

$$Hoo = Hs_3 + hm^* + hxx = 70 + 31,5 + 14,7 = 116,2 \quad \text{m a.s.l.} \quad 5.285$$

Stat. of height Hoo

$$\text{Stat. } 2230 - boo = 2230 - 81,5 = \text{Stat. } 2148,5 \quad 5.286$$

Height Hm

$$Hm = Hs_3 + hm^* - hyy = 70,0 + 31,5 - 14,5 = 87,0 \quad \text{m a.s.l.} \quad 5.287$$

Height H_z

$$H_z = Hs_3 - hz = 70,0 - 12,2 = 57,8 \quad \text{m a.s.l.} \quad 5.288$$

Height Huu

$$Huu = Hs_3 - buu \cdot \tan z =$$

$$Huu = 70,0 - 69,1 \cdot 0,112 = 62,3 \quad \text{m a.s.l.} \quad 5.289$$

Stat. of height Huu

$$\text{Stat. } 2230 + buu = 2230 + 69,1 = \text{Stat. } 2299,1 \quad 5.290$$

Here, a soil compaction due to the rising groundwater level at the reference axis must be determined via height $hw = 12,0$ m (5.255) and compaction factor $\lambda = 17,8\%$ by vol. (see Section 5.2.1, page 197).

Height Δh

$$\Delta h = hw \cdot \lambda / 100 = 12,0 \cdot 17,8 / 100 \sim 2,1 \quad \text{m} \quad 5.291$$

In order to better distinguish the forces and their areas from the heights in the Figs., the abbreviations of the forces are shown in italics (see Figs. 138 to 140, and 142).

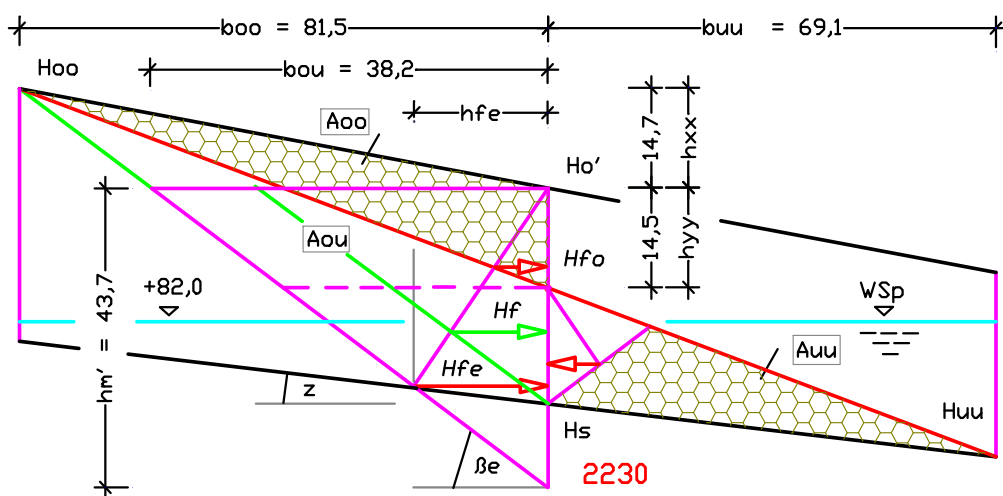


Fig. 138: Position, direction, and force meters of the forces around Stat. 2230, whereby they can be calculated via the area Aou .

Results:

With an angle $se = 19,7^\circ$ (5.270), the shear plane under load runs from height $H_{oo} +116,2$ m a.s.l. in Stat. 2148 through height $H_m +87,0$ m at the reference axis up to height $H_{uu} +62,3$ m in Stat. 2299. Resting on this plane is soil in area $A_{oo} \sim 590$ m³ (5.275), which slides as soon as it loses its hold at the reference axis in Stat. 2230. Moreover, soil subsidence in the amount of height $\Delta h \sim 2,1$ m (5.291) must be expected due to the first contact of the slightly moist soil with the rising groundwater level at the reference axis.

For force determination, the individual heights, widths, and angles are calculated, and the force positions are shown in Fig. 139.

Station 2123

At the time of the landslide, the assumed water plane of the Concordia lake reaches the sloping lake bed in Stat. 2123. This terminates the direct influence of the groundwater on the slightly moist filling material, and heights H_w and H_{s4} are at $+82,0$ m a.s.l.. Simultaneously, the previous volume increase (V_f/V_{fw}) is eliminated, so that height h_x can be calculated directly via width b_o and the angles of the moist soil $si = 22,6^\circ$ or $\beta_i = 39,8^\circ$ (5.157). To the left of the reference axis, the terrain rises from height $H_{o4} +107,0$ m a.s.l. up to height $H_{s5} +128,0$ m a.s.l. along the length $l_{g4} = 93,00$ m. To the right of the axis, the terrain contour falls with angle $x_2 = 6,9^\circ$ (5.221). The lake bed rises further from height $H_{s4} +82,0$ m a.s.l. with angle $z = 6,4^\circ$ (5.203).

Calculation:

Angle x_4

$$\tan x_4 = (128,0 - 107,0) / l_{g4} = 21,0 / 93,00 = 0,226 \quad 5.292$$

$$x_4 = 12,7^\circ \quad [-] \quad 5.293$$

Height hm

$$hm = H_{o4} - H_{s4} = 107,0 - 82,0 = 25,0 \quad \text{m} \quad 5.294$$

Wedge width b_o

$$b_o = hm / \tan \beta_i = 25,0 / 0,832 = 30,0 \quad \text{m} \quad 5.295$$

Height h_x

$$h_x = b_o \cdot \tan x_4 = 30,0 \cdot 0,226 = 6,8 \quad \text{m} \quad 5.296$$

Height hn

$$hn = hm + h_x/4 = 25,0 + 6,8 / 4 = 26,7 \quad \text{m} \quad 5.297$$

Inclination angle β_e

$$\tan \beta_e = hn / b_o = 26,7 / 30,0 = 0,890 \quad 5.298$$

$$\beta_e = 41,7^\circ \quad [-] \quad 5.299$$

Shear angle se

$$\tan se = (\tan \beta e) / 2 = 0,890 / 2 = 0,445 \quad 5.300$$

$$se = 24,0^\circ \quad [-] \quad 5.301$$

Height hyy as well as widths boo and buu are calculated by means of height hm = 26,7 m (5.297) and angles se , x_3 and $z = 6.4^\circ$ (5.203).

Height hyy

$$hyy^2 / [2 \cdot (\tan se - \tan x_4)] = (hm^* - hyy)^2 / [2 \cdot (\tan se - \tan z)]$$

$$hyy^2 / [2 \cdot (0,445 - 0,226)] = (25,0 - hyy)^2 / [2 \cdot (0,445 - 0,112)]$$

$$hyy^2 = (25,0 - hyy)^2 \cdot 0,438 / 0,666 \quad | \quad hyy = \sqrt{0,658 \cdot (25,0 - hyy)}$$

$$hyy = 20,3 / 1,811 \sim 11,2 \quad \text{m} \quad 5.302$$

Height hu

$$hu = hm - hyy = 25,0 - 11,2 = 13,8 \quad \text{m} \quad 5.303$$

Width boo

$$boo = hyy / (\tan se - \tan x_4)$$

$$boo = 11,2 / (0,445 - 0,226) = 51,1 \quad \text{m} \quad 5.304$$

Width buu

$$buu = hu / (\tan se - \tan z)$$

$$buu = 13,8 / (0,445 - 0,112) = 41,5 \quad \text{m} \quad 5.305$$

Area Aoo

$$Aoo = boo \cdot hyy / 2 = 51,1 \cdot 11,2 / 2 = 286,2 \quad \text{m}^2 \quad 5.306$$

Area Auu

$$Auu = buu \cdot hu / 2 = 41,5 \cdot 13,8 / 2 = 286,4 \quad \text{m}^2 \quad 5.307$$

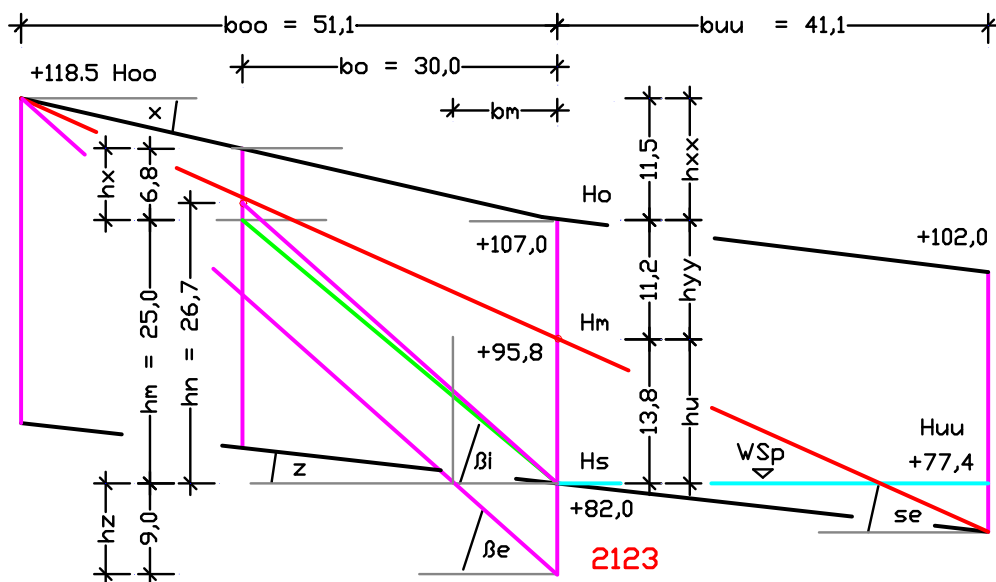


Fig. 139: Heights and the position of shear plane under load (red).

Height hh

$$hh = boo \cdot \tan \beta e = 51,1 \cdot 0,890 = 45,5 \quad \text{m} \quad 5.308$$

The heights and widths of the force areas are determined, which act against the fictitious wall on the reference axis.

Height h_{xx}

$$h_{xx} = b_{oo} \cdot \tan \alpha_4 = 51,1 \cdot 0,226 = 11,5 \quad \text{m} \quad 5.309$$

Height h_z

$$h_z = h_h - h_{xx} - h_m = 45,5 - 11,5 - 25,0 = 9,0 \quad \text{m} \quad 5.310$$

Height h_m'

$$h_m' = h_h - h_{xx} = 45,5 - 11,5 = 34,0 \quad \text{m} \quad 5.311$$

Width b_{ou}

$$b_{ou} = h_m' / \tan \beta_e = 34,0 / 0,890 = 38,2 \quad \text{m} \quad 5.312$$

Width b_{ou}'

$$b_{ou}' = (h_m' - h_{yy}) / \tan \beta_e$$

$$b_{ou}' = (34,0 - 11,2) / 0,890 = 25,6 \quad \text{m} \quad 5.313$$

Width b_m

$$b_m = h_z / \tan \beta_e = 9,0 / 0,890 = 10,1 \quad \text{m} \quad 5.314$$

Area A_{ou}

$$A_{ou} = (b_{ou} \cdot h_m') / 2 = (38,2 \cdot 34,0) / 2 = 649,4 \quad \text{m}^2 \quad 5.315$$

Height H_{oo}

$$H_{oo} = H_{o4} + h_{xx} = 107,0 + 11,5 = 118,5 \quad \text{m} \quad 5.316$$

a.s.l.

Stat. of height H_{oo}

$$\text{Stat. } 2123 - b_{oo} = 2123 - 51,1 = \text{Stat. } 2071,9 \quad 5.317$$

Height H_m

$$H_m = H_{s4} + h_u = 82,0 + 13,8 = 95,8 \quad \text{m a.s.l.} \quad 5.318$$

Height H_z

$$H_z = H_{s4} - h_z = 82,0 - 9,0 = 73,0 \quad \text{m a.s.l.} \quad 5.319$$

Height H_{uu}

$$H_{uu} = H_{s4} - b_{uu} \cdot \tan z =$$

$$H_{uu} = 82,0 - 41,5 \cdot 0,112 = 77,4 \quad \text{m a.s.l.} \quad 5.320$$

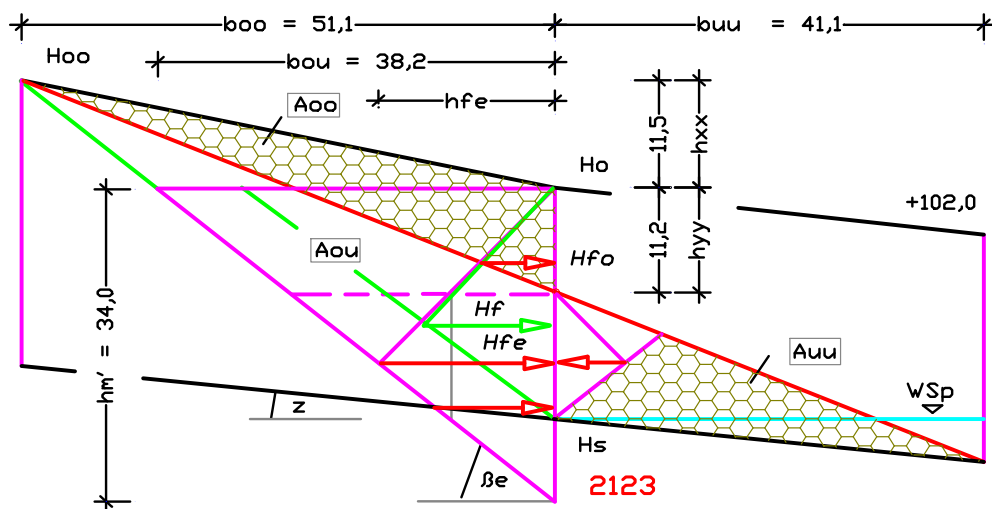


Fig. 140: Position, direction, and force meters of the forces at Stat. 2123.

No soil compaction is assumed at the reference axis Stat. 2123, because the direct influence of the groundwater on the filling material ends here, and the water rising through capillary action can be ignored with this compaction of the soil.

Stat. of height H_{uu}

$$\text{Stat. } 2123 + b_{uu} = 2123 + 41,5 \sim \text{Stat. } 2164 \quad 5.321$$

Results:

With an angle $se = 24,0^\circ$ (5.301), the shear plane under load runs from height $H_{oo} + 118,5$ m a.s.l. in Stat. 2072 through height $H_m + 95,8$ m at the reference axis up to height $H_{uu} + 77,4$ m in Stat. 2164. Resting on this plane is soil in area $A_{oo} \sim 590$ m³ (5.315), which slides as soon as it loses its hold at the reference axis in Stat. 2123. For force determination, the individual heights, widths, and angles are calculated, and the force positions are shown in Fig. 141. There is no soil subsidence due to rising groundwater.

Station 2030

Terrain height $H_{o5} + 128,0$ m a.s.l., lake bed height $H_{s5} + 92,4$ m a.s.l., and the height of the soil layer $hm = 35,60$ m at the reference axis were calculated. Because the terrain contour to the left of the reference axis has different slope angles, height hg is determined by means of load area A . The slope of the lake bed continues to rise with angle $z = 6,4^\circ$ (5.203).

The properties of the moist soil as well as inclination angle $\beta_i = 39,8^\circ$ (5.157) are used for calculating the shear plane under load and its angle se .

Height hm

$$hm = H_{o5} - H_{s5} = 128,0 - 92,4 = 35,6 \quad \text{m} \quad 5.322$$

Wedge width bo

$$bo = hm / \tan \beta_i = 35,6 / 0,832 = 42,8 \quad \text{m} \quad 5.323$$

Height hg → averaged wedge height of load area A

$$hg = [5,0 \cdot 20,0 + (5,0 + 7,0) \cdot 30,0] / 50 = 9,2 \quad \text{m} \quad 5.324$$

Angle x_5 → of the rising terrain slope

$$\tan x_5 = hg / lg_5 = 9,2 / 50,0 = 0,184 \quad 5.325$$

$$x_5 = 10,4^\circ \quad [-] \quad 5.326$$

Height hx

$$hx = bo \cdot \tan x_5 = 42,8 \cdot 0,184 = 7,9 \quad \text{m} \quad 5.327$$

Height hn

$$hn = hm + hx/4 = 35,6 + 7,9 / 4 = 37,6 \quad \text{m} \quad 5.328$$

Inclination angle βe

$$\tan \beta e = hn / bo = 37,6 / 42,8 = 0,878 \quad 5.329$$

$$\beta e = 41,3^\circ \quad [-] \quad 5.330$$

Shear angle se

$$\tan se = (\tan \beta e) / 2 = 0,878 / 2 = 0,439 \quad 5.331$$

$$se = 23,7^\circ \quad [-] \quad 5.332$$

Height hyy as well as widths boo and buu are calculated by means of height $hm = 35,6$ m (5.322) and angles se , x_5 , and $z = 6,4^\circ$ (5.203).

Height hyy

$$hyy^2 / [2 \cdot (\tan se - \tan x_5)] = (hm - hyy)^2 / [2 \cdot (\tan se - \tan z)]$$

$$hyy^2 / [2 \cdot (0,439 - 0,184)] = (35,6 - hyy)^2 / [2 \cdot (0,439 - 0,112)]$$

$$hyy^2 = (35,6 - hyy)^2 \cdot 0,510 / 0,654 \quad | \quad hyy = \sqrt{0,780 \cdot (35,6 - hyy)}$$

$$hyy = 31,4 / 1,883 = 16,7 \quad \text{m} \quad 5.333$$

Height hu

$$hu = hm - hyy = 35,6 - 16,7 = 18,9 \quad \text{m} \quad 5.334$$

Width boo

$$boo = hyy / (\tan se - \tan x_5)$$

Width boo

$$boo = 16,7 / (0,439 - 0,184) = 65,5 \quad \text{m} \quad 5.335$$

Width buu

$$buu = hu / (\tan se - \tan z)$$

$$buu = 18,9 / (0,439 - 0,112) = 57,8 \quad \text{m} \quad 5.336$$

Area Aoo

$$Aoo = boo \cdot hyy / 2 = 65,5 \cdot 16,7 / 2 = 546,9 \quad \text{m}^2 \quad 5.337$$

Area Auu

$$Auu = buu \cdot hu / 2 = 57,8 \cdot 18,9 / 2 = 546,2 \quad \text{m}^2 \quad 5.338$$

Height hh

$$hh = boo \cdot \tan \beta e = 65,5 \cdot 0,878 = 59,5 \quad \text{m} \quad 5.339$$

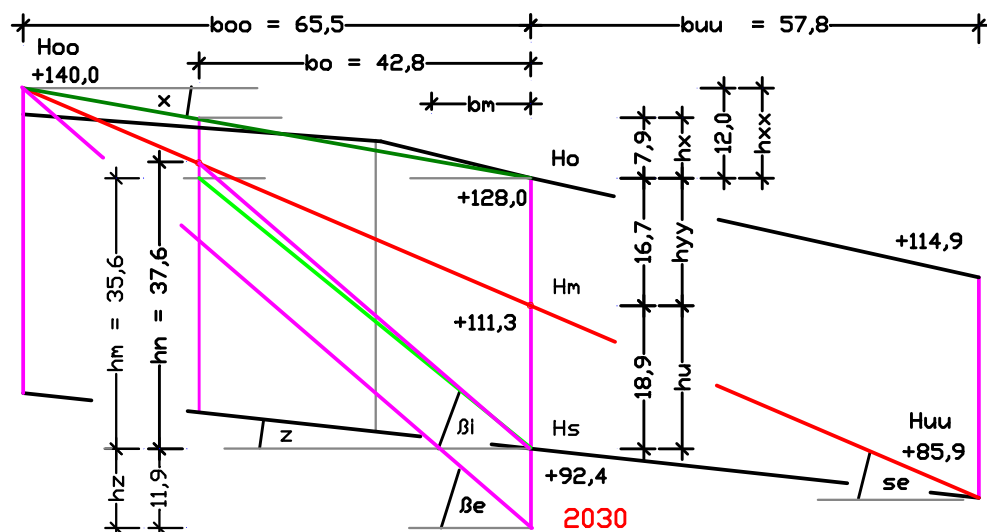


Fig. 141: Heights and the position of shear plane under load (red).

The heights and widths of the force areas are determined, which act against the fictitious wall on the reference axis.

Height h_{xx}

$$h_{xx} = b_{oo} \cdot \tan \alpha_5 = 65,5 \cdot 0,184 = 12,0 \quad \text{m} \quad 5.340$$

Height h_z

$$h_z = h_h - h_{xx} - h_m = 59,5 - 12,0 - 35,6 = 11,9 \quad \text{m} \quad 5.341$$

Height $h_{m'}$

$$h_{m'} = h_h - h_{xx} = 59,5 - 12,0 = 47,5 \quad \text{m} \quad 5.342$$

Width b_{ou}

$$b_{ou} = h_{m'} / \tan \beta_e = 47,5 / 0,878 = 54,1 \quad \text{m} \quad 5.343$$

Width b_{ou}'

$$b_{ou}' = (h_{m'} - h_{yy}) / \tan \beta_e$$

$$b_{ou}' = (47,5 - 16,7) / 0,878 = 35,1 \quad \text{m} \quad 5.344$$

Width b_m

$$b_m = h_z / \tan \beta_e = 11,9 / 0,878 = 13,6 \quad \text{m} \quad 5.345$$

Area A_{ou}

$$A_{ou} = (b_{ou} \cdot h_{m'}) / 2 = (54,1 \cdot 47,5) / 2 = 1285 \quad \text{m}^2 \quad 5.346$$

Height H_{oo}

$$H_{oo} = H_{o5} + h_{xx} = 128,0 + 12,0 = 140,0 \quad \text{m a.s.l.} \quad 5.347$$

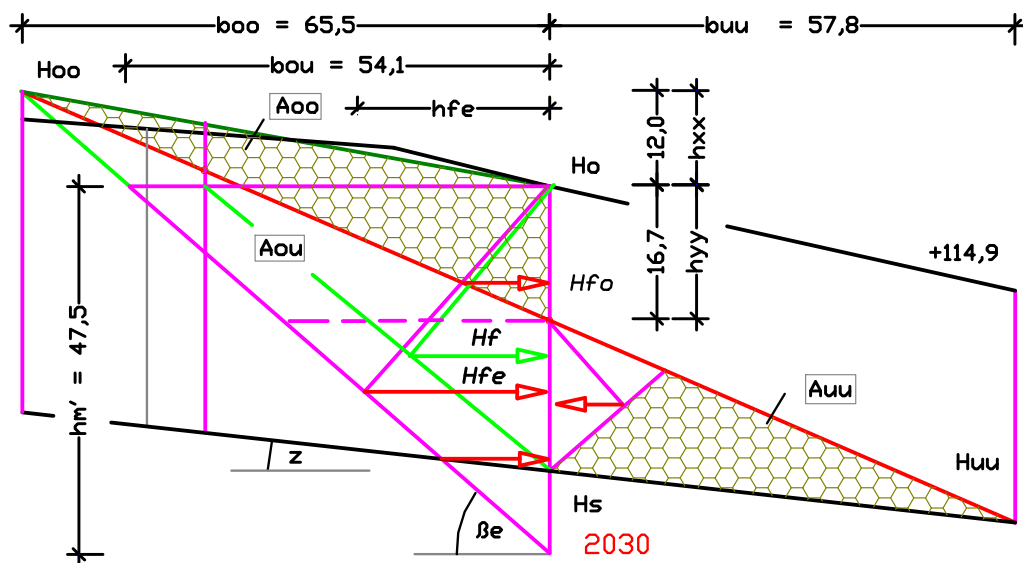


Fig. 142: Position, direction, and force meters of the forces at Stat. 2030.

Stat. of height H_{oo}

$$\text{Stat. 2030} - b_{oo} = 2030 - 65,5 \sim \text{Stat. 1965} \quad 5.348$$

Height H_m

$$H_m = H_{s5} + h_u = 92,4 + 18,9 = 111,3 \quad \text{m a.s.l.} \quad 5.349$$

Height H_z

$$H_z = H_{s5} - h_z = 92,4 - 11,9 = 80,5 \quad \text{m a.s.l.} \quad 5.350$$

Height H_{uu}

$$H_{uu} = H_{s5} - b_{uu} \cdot \tan z =$$

$$H_{uu} = 92,4 - 57,8 \cdot 0,112 = 85,9 \quad \text{m a.s.l.} \quad 5.351$$

Stat. of height H_{uu}

$$\text{Stat. } 2030 + b_{uu} = 2030 + 57,8 \sim \text{Stat. } 2088$$

5.352

Results:

With an angle $se = 23,7^\circ$ (5.332), the shear plane under load runs from height $H_{oo} +140,0$ m a.s.l. in Stat. 1965 through height $H_m +111,3$ m at the reference axis to height $H_{uu} +85,9$ m in Stat. 2088. Resting on this plane is soil in area $A_{oo} \sim 547$ m³ (5.337), which slides as soon as it loses its hold at the reference axis in Stat. 2030. For force determination, the individual heights, widths, and angles are calculated, and the force positions are shown in Fig. 142. There is no soil subsidence due to rising groundwater.

The heights and shear angles se calculated above are assigned to the respective Stats. in the table below, and the transferred to the sectional view in Fig. 143.

Stat	Distance	Angle	Height H_{oo}	b_{oo}	Height H_m	b_{uu}	Height H_{uu}
2480			42,0 m		42,0 m		42,0 m
	75 m						
2405		$se = 21,8^\circ$ (5.216)			57,0 m		
	75 m						
2330		$se = 20,4^\circ$ (5.232)	92,1 m (5.247)	56,0 m (5.235)	71,3 m (5.249)	48,1 m (5.236)	53,4 m (5.251)
	100 m						
2230		$se = 19,7^\circ$ (5.270)	116,2 m (5.285)	81,5 m (5.273)	87,0 m (5.287)	69,1 m (5.274)	62,3 m (5.289)
	107 m						
2123		$se = 24,0^\circ$ (5.301)	118,5 m (5.316)	51,1 m (5.304)	95,8 m (5.318)	41,5 m (5.305)	77,4 m (5.320)
	93 m						
2030		$se = 23,7^\circ$ (5.332)	140,0 m (5.347)	65,5 m (5.335)	111,3 m (5.349)	57,8 m (5.336)	85,9 m (5.351)

5.2.4 Result and conclusions for the landslide in Nachterstedt

The calculations on the landslide are based on own experiments, which show that soils will generate a 'natural shear plane', if they slide down from an earth block without loosening. However, the shear planes change, if earth blocks are loaded with earth wedges (inclined surfaces). An additional force shift occurs, if earth masses rest on a continuous inclined plane (rock layer) instead of on a horizontal plane, particularly when this barrier layer prevents further dispersal of the vertical forces, and converts these undispersed vertical forces into horizontal forces. A rising groundwater level increases the conversion of forces, changes the soil properties, and can thereby create layers of different soil types. The necessary calculations of soil angles (β or s) or forces of soil beddings can be simplified, if one adapts the properties and volumes of the soil layers by

In Fig. 143 above, heights H_m of the calculation sections have been entered in the Stations and connected. The red line shows the position of shear plane under load. It only deviates slightly from the line (magenta) of the landslide, which has been taken from the plans (before/after) supplied by the Deutsche Zentrum für Luft- und Raumfahrt. The green line between Stats. 2230 and 2480 indicates the height of landfill that must have occurred due to the landslide.

The causes leading to the landslide in Nachterstedt, could be due to the following factors:

- Partial filling of the open mine pit with uncompacted soils (overburden material).
- Creation as well as increase of groundwater levels in the slope due to water storage in the Concordia lake.
- First-time immersion of the filling material into the groundwater, with the associated changes of the soil properties, i.e. a reasonably stable and light moist soil changes into a wet soil under water.
- The loss of density of soils under water due to the natural physical uplift increases the soil's natural compaction, thereby lowering the slope's surface.
- Reduction of the earth resistances in the soil, and high instability of the slope due to water absorption by the soil.

The Nachterstedt landslide calculations are based on the findings of Test 3, in which dry sand is compacted by factor $\lambda = 14,2\%$ by volume (2.22) simply by the addition of water (see Section 2.4.3, page 41).

Decisive for the natural change in the soil properties was the first contact of the relatively dry and uncompacted soil of the filling material with the rising water of the Concordia lake. Ultimately, the soil's water absorption resulted in a fully wettened and compacted condition, and the transformation of the shear level in the slope.

An additional flow of groundwater – e.g. from the Harz region – as suggested by geologists as a possible cause of the landslide, can be neglected.

Moreover, the conformity of the actual and calculated shear planes in Fig. 143 shows that the risk potential of a possible landslide can be determined with the specifications provided by the New Earth Pressure Theory. The specifications of current earth pressure teachings cannot provide mathematical evidence for the risk of a landslide in the slope.

6 Summary

The author's own professional experience during many years led to the realization that even the strictest application of standard German rules for the construction business can lead to considerable structural damage. This has already been pointed out by the author in his scientific papers “Earth pressure according to the physical law of the inclined plane” [16] and “Time for a new earth pressure teaching” [17]. Ultimately, it was the collapse of the Historic Archive in Cologne during subway excavations, and the landslide in Nachterstedt after filling the Concordia lake, with fatalities and high material damage, that promoted this study.

Its aim was the detailed investigation of possible discrepancies in calculation basics, thereby pointing out the differences between the theses of the teachings and the new theory. To start with, the definitions of current earth pressure teachings and the New Earth Pressure Theory were introduced and compared (see Chapter 2).

6.1 Basics of earth pressure teachings and new theory

In the case of an obstruction for the transverse contraction in the soil created by its own weight, the teachings state that only vertical forces can arise, and that these forces can only be dissipated vertically in deeper layers. Only if additional forces (weights) are applied on the terrain surface, or if the obstruction (supporting wall) gives way, will the soil be able to move laterally, thereby creating vertical and horizontal stresses. Moreover, the teachings see an imbalance of the earth stresses in the ground, which they compensate by means of the empiric earth pressure factor K_a . They place a horizontal force (earth pressure force) against the supporting wall on the lower third point of the inclined plane (failure line) equally for all soil types, and show that wall friction and a possible cohesion can influence soil stress and angle of the earth pressure force against the wall.

The New Earth Pressure Theory agrees with the teachings that a load applied to rock, concrete, etc. in particular, generates a material load parallel to the perpendicular force direction. However, in all other soil types – with or without load – vertical and horizontal stresses/forces are created. Hereby, it is assumed that soils are more or less decomposition products of primary rock, consisting

of a solids volume and a pore volume. If one takes one cubic meter as solids volume, and adds a known pore volume, this will change the total volume, but not the solids volume. If the increased volume is standardized, a new soil type is created. Consequently, a rock exposed to erosion will exhibit a high solids volume and a low pore volume, whereby the volume ratios are reversed, e.g. with dust as a soil type. In view of this fact, it can be deduced that the relationship between solids volume V_f and pore volume V_l not only enables the soil density, but also the internal friction angle to be determined.

The New Earth Pressure Theory applies the pure basics of physics, and neither requires empiric at-rest earth factors to maintain an equilibrium in the ground, nor the mobilization of horizontal stresses by means of wall rotations or wall shifts.

6.2 Force determination and force distribution

Current earth pressure teachings state that the Mohr-Coulomb failure criterion (shear law) – which is based on Coulomb's and Mohr's theories – is applied for earth pressure determination. Regarding Coulomb's classical earth pressure theory – of which the original sketches exist (Fig. 9, page 23) – the teachings state “*with this approach, the stress distribution is unknown*” (see [1: page P.10] and Section 2.3.3).

Instead, the current earth pressure teachings combine a flow condition – the original of which is unknown to the author – with Mohr's stress circle, and present this combination as the “Mohr-Coulomb failure criterion”. Amongst other things, the teachings use Mohr's stress circle to position the main stress (downhill force $T = FH$) into the horizontal plane, in order to determine the angles δ_x and δ_z , and other values. Hereby, the teachings fail to see that neither weight Ge nor its partial forces, such as normal force FN and downhill force FH , can be rotated (see "calculation example" and Fig. 14, page 36).

What's more, Tests 4 and 5 prove that soil sliding from a standing earth wedge to a lying wedge are not subjected to any flow condition. Moreover, no analogy can be found between failure criterion and "physical plane", as described by the teachings. Similarly, no confirmation was found for the teachings' claim that for all soil types, the earth pressure force acts against the perpendicular wall in the lower third point of the failure line, whereby the force direction can be changed due to wall friction or cohesion (see Sections 2.3.7 and 2.3.8).

Regarding force determination and force distribution as defined by the teachings it must be established that these neither follow Coulomb's classical earth pressure theory, nor do they have a physical basis. Consequently, the current calculation models for determining earth pressure can no longer claim to represent the present state of the art.

However, Coulomb's classical earth pressure theory (Fig. 9, page 23) is still valid, and has been adopted and expanded as the New Earth Pressure Theory. This New Theory shows that – depending on soil type – soils in free nature form an inclination angle βt from $\sim 0,6^\circ$ up to $89,4^\circ$, and the soil's force distribution cannot be enforced under the elevation angle $\alpha < 45^\circ$ of the "inclined plane". Moreover, the earth pressure force always acts horizontally against the wall, whereby thrust height h_v varies in accordance with the different inclination angles, and cannot be fixed at height $h/3$.

6.3 Soil properties and their determination

In order to do without empiric soil parameters when determining earth pressure, tests were carried out with dry, moist, and wet soils in a glass container above and under water. These tests were guided by the specification that an idealized hard basalt rock in the dry state has a density $\rho t g = 3,00 \text{ t/m}^3$, and therefore a solids volume V_f of 100% can be assigned to it [6: page 2.2–2 and 15: page 605]. By adding a pore volume V_l , followed by standardization, a soil type is created, whose density, inclination angle, and shear angle can be calculated. If one fills the soil pores partially or completely with water, moist or wet soils are created, whose characteristics can be determined analogously to those of dry soils. In order to verify this calculation procedure, various tests were conducted in a glass container with different soil types and water.

The results show that friction value μ , inclination angle β , shear angle s , and soil density can be calculated from the ratio of solids volume to pore volume. Enclosures 2 and 3 have been included for a simplified comparison of these results, which are described in more detail in Section 3.4.

This new calculation method for soil parameters would enable the previous classification of soils according to primary rock, grain composition, and grain sizes to be replaced, together with the distinction between non-cohesive and

cohesive soils, and the hardly significant soil descriptions such as solid, rigid, soft, pasty, liquid, silty.

6.4 Applicability of the New Earth Pressure Theory

As demonstrated, the New Earth Pressure Theory follows the pure basics of physics. These specifications enable all components subjected to earth pressure to be determined statically. In order to show that the newly acquired findings from the tests can be applied in practice, the reasons and causes for the landslide in Nachterstedt and the collapse of the Historic Archive in Cologne were investigated mathematically.

- During excavation work for the subway in Cologne, evidence was found for fractures in a slotted wall, which were causal for the archive's collapse (see Figs. 113 and 114, pages 170 and 171, as well as [F] and [G]).
- In Nachterstedt, the rising water of the Concordia lake (a flooded open-cast coal mine) changed the soil properties in the flooded area to such an extent that a landslide was inevitable. According to available records, the pit was partially filled with uncompacted and reasonably dry material. Time-delayed to the rising water level in the lake, the groundwater level in the refilled area also rose, thereby penetrating the reasonably dry uncompacted filling material. According to the Archimedean Principle, this leads to a reduction of soil density, a steeper shear plane, and a lowering of the shear plane within the slope. The calculation method for the landslide is confirmed by the fact that the calculated shear plane and the movement plane shown 'afterwards' in the profile view are practically identical (see Fig. 136, page 212).

The unambiguous results in both cases could not have been obtained by applying the current rules and standards of geotechnical engineering. But even if the rules and standards had been observed, both events would not have been avoidable. Hence, it can be established that force determinations according to the New Earth Pressure Theory not only provide precise calculation basics for dimensioning civil engineering structures, but also open up application areas that go far beyond the scope of present earth pressure teachings,

The findings of this study provide good reason for the professional world to discuss the misinterpretations in the basics of current earth pressure teachings and the calculation guidelines of 'Eurocode 7'.

Moreover, it is remarkable that in spite of the large number of publications on the subject of earth pressure, no inherently consistent earth pressure theory exists, which can also dispense with empiric values. However, the new approach for determining earth pressure presented here, supplements the multi-phase system of solid-state physics and therefore requires no empiric soil characteristics, and is based exclusively on accepted physical basics. With this new theory, the calculated soil forces agree completely with real soil behaviour.

Terminology of the New Earth Pressure Theory

To avoid confusion when comparing the conventional earth pressure teachings with the New Earth Pressure Theory, the author has replaced existing terms with other terms and descriptions. The new terms and their meanings are described below.

Should the New Earth Pressure Theory find acceptance in the expert world, an adaptation of the selected terminology and the abbreviations to existing standards of physics, mathematics, and geology would be a simple matter.

- **Earth** is used as the superordinate term for all soil types – from hard rock down to primordial dust in the dry state or containing adsorption or adhesion water.
- **Primordial dust** describes a soil type that is seen as the end product of hard rock destruction, i.e. 1 m³ rock is converted into a dust amount of 100 m³ (solids content of dust $V_f = 0,01$ m³).
- As opposed to 'solid or rigid bodies' **stable soil bodies** contain a certain pore content V_l , which leads to instability if the soil type and thereby to a build-up of stress in the ground.
- **Volumes** are suitable for disassembling soils into their constituent parts and reshaping them according to the volumes of solid material V_f and pores V_l . Hereby, it becomes clear that every destruction of the original rock changes its volume, thereby creating a new soil type. Because the solids volume remains the same, the pore volume must adapt to the new volume. Consequently, soil compaction or soil loosening is related exclusively to the pore volume. It is also only the pore volume that can absorb or discharge water.
- **Parts by weight** result from the multiplication of a soil's volume with the proportional densities of hard basalt rock $p_{g0} = 3,00$ t/m³, of water $p_w = 1,00$ t/m³, and/or of air $p_0 = 0,00$ t/m³.
- **Density** is calculated from the addition of a soil's parts by weight, whereby the solids volume V_f is multiplied with rock density $p_{g0} = 3,00$ t/m³ and gravity force g , the pore water with water density $p_w = 1,00$ t/m³ and g , and the pores not occupied by water with gas density $p_0 = 0,00$ t/m³.
- **Earth block** represents a soil body whose volume $V = a \cdot b \cdot h$ divided by calculation depth a and side view A ($A = V/a$), and its block height h

divided by block width b results in the tangent of inclination angle β . The natural inclination or frictional plane divides the side view A diagonally, so that the active forces act in the wedge area above the inclined plane, and the reactive forces act in the wedge area below the inclined plane. The active and reactive earth stresses act in opposite directions, thereby maintaining an equilibrium in the earth block.

- **Terrain level** corresponds to the terrain's upper surface, and usually indicates the upper limit of an earth block.
- The **basal plane** represents the lower limit of an earth block, whereby the block or wedge height h determines the distance to the terrain level.
- The **inclination or frictional plane** with inclination angle β divides the soil body's area diagonally into active and reactive earth wedges.
- The **downhill plane** with **downhill force** FH and the counter-acting **reactive force** Rv occupies the lower section of the inclined plane. It begins where the normal force plane touches the inclined plane at right angles, and ends on the basal plane at the base point of the wedge.
- The **normal force plane** in the standing earth wedge begins at the perpendicular wall (reference axis) at the height of the terrain contour, and drops down to the inclined plane with angle $(90^\circ - \beta)$, where it touches the inclined plane at right angles. Normal force is described with FN .
- A **shear plane** is formed in free nature, if the support of the soil within an earth block provided by a supporting wall is removed, and the soil slides down to a lying earth wedge. Provided that the soil is not loosened by its movement, the wedge surface is called the shear plane. Shear angle s is calculated from $\tan s = (\tan \beta) / 2$.
- The **slope plane** represents the upper limit of the lying earth wedge in the same way as the shear plane. The term is used to indicate that the soil's volume has changed due to loosening or compaction.
- **Inclination angle** β is measured between the basal plane and the rising inclined plane. Its tangent corresponds to friction value μ of the respective soil type in the dry state. Natural or artificial influences on the soil's state (loosening or compaction) change the inclination angle in a similar way as the adsorption of pore water or the uplift of soils under water.

- **Shear angle** s is calculated from half the inclination angle's tangent, and thereby stands in direct relationship with the mass of an earth wedge. This means that if soil slides down from a 'standing earth wedge', half of the mass remains in the standing wedge, and the other half moves down the perpendicular wall to the basal plane.
- **Force index** gi is a calculation value with which forces within an earth wedge can be converted into force meters **or** force meters converted into forces, and can be represented true-to scale. The supplementary letters git , gii , gin , and giw are assigned to the force index.

The many application possibilities for the New Earth Pressure Theory make it necessary to extend the numerous terms by means of letters or sequences of letters. For example, the respective soil state is represented by the letter t = dry, i = infiltrated with water, and n = wet, i.e. pores are completely saturated with water. For example: dry density ptg , moist density pig , wet density png , moist density under water $piwg$, and wet density under water $pnwg$.

Other letters are: hard rock = f , water = w , and gases/air = l . Supplementary letters indicate the position of dimensions, areas or forces in the calculation system (left l , middle m , right r , top o , and bottom u). The letter e shows that a load/substitute load acts on an earth wedge.

Further terms are introduced at the relevant locations.

References

Sources used

The following papers from the Technische Universität München (TUM) were selected preferentially to represent the “earth pressure teachings”.

- [1] TUM München, Lehrstuhl für Grundbau, Bodenmechanik, Felsmechanik und Tunnelbau – Zentrum Geotechnik, <http://www.lrz.de/> (PDFs)
 - E** Klassifikation von Boden und Fels
 - G** Flachgründungen (DIN 1054:2005)
 - I** Scherfestigkeit
 - J** Grundlagen geotechnischer Entwürfe und Ausführungen
 - K** Einfache Flachgründungen
 - N** Tiefgründungen, Pfähle und Anker
 - P** Erddruck
 - S** Statik von Tunnelbauwerken
- [2] Christian Berger u. Johannes Lohaus (2004), Zustand der Kanalisation – Ergebnisse der DWA-Umfrage; Korrespondenz Abwasser Abfall; ISSN: 1616–430X; Jg. 52, Nr. 5, 2005, S. 528-539 (10).
- [3] Christian Berger u. Christian Falk (2009), Deutsche Vereinigung für Wasserwirtschaft, Abwasser und Abfall e.V. (DWA), Zustand der Kanalisation in Deutschland – Ergebnisse der DWA-Umfrage 2009’, http://de.dwa.de/tl_files/_media/content/PDFs/Abteilung_AuG/Zustand-der-Kanalisation-in-Deutschland-2009.pdf.
- [4] Wolfgang Fellin (2007), Bodenmechanik und Grundbau, Übung 1, Skript, Universität Innsbruck, <ftp://ftp.uibk.ac.at/pub/uni-innsbruck/igt/skripten/bmgb1.pdf>
- [5] H. Frank (6:2001), Bodenmechanik und Erddruckberechnung, Skript, Technische Hochschule Mittelhessen (Gießen – Friedberg), <http://homepages.thm.de/~hg8195/Skripte/Boden.pdf>
- [6] Technische Universität Darmstadt, Werkstoffe und Mechanik im Bauwesen, (3:2003), http://www.iwmb.tu-darmstadt.de/media/iwmb/l/boden_ufm/Kap_2_-_Bodenphysik.pdf
- [7] Frank Jablonski, Mohr’scher Spannungskreis (Seiten 385-412), Skript, Uni Bremen, Natur und Technik, <http://www.mechanik.uni-bremen.de>
- [8] Theodor Triantafyllidis (4:2011), Formelsammlung zur Vorlesung Bodenmechanik 1, Karlsruher Institut für Technologie, http://www.ibf.uni-karlsruhe.de/downloads/skripten/bm1_formeln.pdf
- [9] Heiner Siedel (3:2012), Einführung Technische Gesteinskunde, Skript, TU Dresden, http://www.tu-dresden.de/die_tu_dresden/fakultaeten/fakultaet_bauingenieurwesen/geotechnik/geologie/studium/vorlesungen/geologie/dateien/gestkunde/abschnitt1.pdf
- [10] Heiner Siedel (3:2012), Technische Eigenschaften von Naturstein und Prüfverfahren, Skript, TU Dresden, http://tu-dresden.de/die_tu_dresden/fakultaeten/fakultaet_bauingenieurwesen/geotechnik/geologie/studium/vorlesungen/geologie/dateien/gestkunde/abschnitt3.pdf
- [11] So entwickelte sich das Desaster von Nachterstedt, Zentrum für Satellitengestützte Kriseninformation, Vorbereitung of the Tagebaurestloches Nachterstedt/Schadeleben für die Flutung, <http://www.ecm-ing.com/ursachen/> und <http://www.ecm-ing.com/grundbruch/>
- [12] EffJot (7:2009), Geologische Karten zu Nachterstedt, <http://blog.effjot.net/2009/07/geologische-karten-zu-nachterstedt/>

- [13] Mitteldeutsche Zeitung (04.05.2013), Gutachterstreit schwelt weiter, Artikel
www.mz-web.de/Unfall-Nachterstedt
- [14] Mitteldeutsche Zeitung (29.11.2013), LMBV-Gutachten schließt Altbergbau als Unglücksursache aus, Artikel mit Hinweisen auf Lagerungsdichte of the Verfüllmaterials und Grundwasserströme,
http://www.mdr.de/nachrichten/gutachten-nachterstedt100_zc-e9a9d57e_zs-6c4417e7.htm
- [15] Horst Kuchling (2001), Taschenbuch der Physik, 17. Auflage, Buchverlag Leipzig
ISBN 3-446-21760-6.
- [16] Norbert Giesler (3:2005), Erddruck nach dem physikalischen Gesetz der ‚inclined Ebene‘, Artikel, tis – Tiefbau – Ingenieurbau – Straßenbau,
six4.bauverlag.de/sixcms_4/sixcms_upload/media/.../giesler_0305.pdferddruck
- [17] Norbert Giesler (3:2010), Zeit für eine neue Erddruck-Lehre, Artikel, tis – Tiefbau – Ingenieurbau – Straßenbau, www.unitracc.de/aktuelles/artikel/zeit-fuer-eine-neue-erddruck-lehre?

Contemporary literature

Contemporary literature on earth pressure that refers to the **earth pressure factor K_a** or the **Mohr-Coulomb failure criterion** was taken into account by the author, but not followed up, as both terms indicate an unchanged adoption of current earth pressure teachings.

Although the contemporary literature listed here contains supplements on earth pressure teachings, in the author's view they do not represent anything new regarding the earth pressure theory.

Bernd Schuppener (3:2013), Grundlagen für geotechnische Nachweise im Verkehrswasserbau, Bundesanstalt für Wasserbau, Normen-Handbuch zu Eurocode 7 und DIN 1054:2010,
http://vzb.baw.de/publikationen.php?file=mitteilungsblaetter/0/schuppener_Normen-Handbuch.pdf

Christian Moormann (4:2010), Die geotechnische Normung auf dem Weg zum Eurocode 7, Universität Stuttgart, <http://www.uni-stuttgart.de/igs/content/publications/191.pdf>

Other literature

Aktionsgemeinschaft Impulse per Kanalbau München (4:2013); Forderungskatalog – Impulse per Kanalbau, <http://www.impulse-pro-kanalbau.de/app>

Jean-Pierre Burg (2008/2009), Festigkeitsprofile der Lithosphäre, Skript, Eidgenössische Technische Hochschule Zürich, Struktural Geologie und Tektonik,
http://www.structuralgeology.ethz.ch/BurgJeanPierre_rheolprof.pdf

H. Czurda u. R. Biehl (3:2000), Erd- und grundbautechnische Aspekte beim Bau von Logistikhallen, Skript, Ingenieur-Gemeinschaft ICP, Karlsruhe, www.icp-ing.de

Fabian Kirsch (2:2012), Auswahl-Kriterien, Risiken sowie Prüf- und Sanierungsmöglichkeiten bei der Anwendung von Tiefbaugründungen im Brückenbau (Pfahlgründungen), Skript, Technische Universität Braunschweig sowie Consult GmbH Braunschweig,
http://www.gudconsult.de/uploads/media/00128_d.pdf

H. S. Müller u. M. Beitzel (5:2006), Neue Erkenntnisse zum Frischbetonverhalten, Skript, Uni Karlsruhe, Institut für Massivbau und Baustofftechnologie
<http://digbib.ubka.uni-karlsruhe.de/volltexte/documents/559965>

Rolf Katzenbach (2:2009), Erddruck IV, Skript, Institut und Versuchsanstalt für Geotechnik der TU Darmstadt, http://www.geotechnik.tu-darmstadt.de/media/institut_und_versuchsanstalt_fuer_geotechnik/studiumundlehre_1/musterloesungen/umweltgeotechnik_3/06_-_Erddruck_12-02-09.pdf

Additional literature

Günter Kunze (2012), Einführung in die bodenphysikalischen Grundlagen, Skript, Technische Universität Dresden, Professur für Baumaschinen- und Fördertechnik,
www.springer.com/cda/content/.../cda.../9783834815927-c1.pdf?...0...

Christian Moormann (11:2012), Bauliche Maßnahmen zur Bergung der Archivalien und zur Erkundung der Schadensursache, Baugrundtagung; Einsturz of the Stadtarchivs in Köln; Artikel, Institut für Geotechnik der Universität Stuttgart,
http://www.uni-stuttgart.de/igs/content/publications/221_CM_Baugrundtagung.pdf

Dr.-Ing. Bernhard Odenwald (3:2013), Einwirkungen und Beanspruchungen aus Grundwasser und Oberflächenwasser, Skript, Bundesanstalt für Wasserbau Karlsruhe, BAW-Kolloquium, Neue Normen und Regelwerke in der Geotechnik,
<http://vzb.baw.de/publikationen/kolloquien/0/Odenwald%20Einwirkungen.pdf>

Thomas Richter (2:2011), Neue Bemessungskonzepte – DIN 1054, Skript, Geotechnik und Dynamik Consult GmbH, Brandenburgische Ingenieurkammer,
http://www.gudconsult.de/uploads/media/00081_d.pdf

Ulrich Simon u. Mathias Bernhard Wieland (2011/2012), Spannungs- und Dehnungstransformation, (Mohr'scher Spannungskreis), Skript, Statik Universität Ulm und Ulmer Zentrum für wissenschaftliches Rechnen; Mathematische Modellbildung und Simulation in der Mechanik,
http://www.uni-ulm.de/fileadmin/website_uni_ulm/uzwr/mmsm/mmsm1-ws1112/Skript-MMSM1.pdf,
http://www.uni-magdeburg.de/ifme/l-dynamik/grundkurs/Matrikel_11/Semester_2/Vorlesung/festigkeit_s176-204.pdf

Vertiefungsblock Ökologische Bodenphysik (WS/2003), Skript, Albert-Ludwigs-Universität Freiburg, Professur für Bodenökologie; Bodenphysik,
<http://www.bodenkunde.uni-freiburg.de/objekte/blockphys>

DIN 1054 (2010-12): Baugrund – Sicherheitsnachweise im Erd- und Grundbau

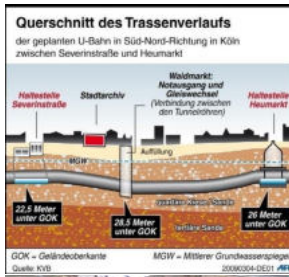
DIN 1926 (2007-03): Prüfverfahren für Naturstein – Bestimmung der einachsigen Druckfestigkeit

DIN 4085 (2011-05) und DIN E 4085: Baugrund – Berechnung of the Erddrucks

DIN 18196 (2009-03), DIN 18300 (2008-09), DIN 18301 (2012-09) u. DIN 18311 (2008-09).

Graphics

[B]



Panorama infographic: Cross-section of the Cologne subway route.

<http://www.n24.de/n24/Nachrichten/Panorama/d/636592/infografik--querschnitt-der-koelner-u-bahntrasse.html>

[C]



Köln Nachrichten: **North-South Subway**: koeln-nachrichten.de

View into the excavation pit on the Waidmarkt before installation of the rescue and inspection scaffolds. Photo: Archiv Köln Nachrichten

http://www.koeln-nachrichten.de/assets/images/Lokales/2010/Maerz/02032010_NordSuedstadtbahn2_kl.jpg

[D]



Excavation pit with intermediate ceiling.

http://www1.wdr.de/themen/archiv/sp_stadtarchiv_ubahn/archiveinsturz548_v-TeaserAufmacher.jpg

[E]



Church tower of St. Johann Baptist in Cologne.

The leaning tower of Cologne; Photo:

http://www.koeln-magazin.info/uploads/pics/schiefer_turm.jpg

[F]



EXPRESS shows two details from the appraisal film, for example a severely damaged slotted wall – directly where the archive building stood, and gravel was able to penetrate. Photo: KVB

http://lh5.ggpht.com/mfKFLSkAXmaC3qbC8L3244MKtGFZqpngfpG7Xd_ZLLaXm-FaEJt-f4ymogIqBhzppnvr6g=s113

[G]



Photo series about the collapse of the archive in Cologne:

<http://koeln-magazin-info/stadtarchiv-koeln.html>

<http://Querschnitt-N24.de/Infografik:Querschnitt-der-Koelner-U-Bahntrasse>.

[H]

Deutsches Zentrum für Luft- und Raumfahrt (DLR); High-precision aerial photos of the Nachterstedt landslide area “Comparison map of Nachterstedt, profile sections before and after”.

<http://www.zki.dlr.de/de/article/936> and

[http://www.dlr.de/desktopdefault.aspx/tabid-5105/8598_read-18849/24.07.2009 – Luftbild-Vergleichskarte Nachterstedt, vorher und nachher](http://www.dlr.de/desktopdefault.aspx/tabid-5105/8598_read-18849/24.07.2009-Luftbild-Vergleichskarte-Nachterstedt-vorher-und-nachher).

[J]

Nachterstedt photo series under: <http://www.n-tv.de/mediathek/bilderserien/nachterstedt>.

Anlage 1

Raum- und Gewichtsteile von Böden

Bodenarten entstehen durch den Zerfall von Felssteinen
 Bodeneigenschaften bestimmen sich über das Verhältnis
 von Feststoff- zu Porenvolumen

Berechnungen

bezogen auf die Körpertiefe $a = 1,00 \text{ m}$.

Bodenarten von Fels bis Urstaub und Urstaub unter Wasser	Ermittlung der Raumteile										Gewichtsteile			Winkel			Winkel nasser Böden unter Wasser			
	h	b	Δb	Vo	ΔV	Vp	Vf	Vf	VI	ptg	png	ptwg	pnwg	tan βn	sn	sn	an βnw	βnw	snw	g
	m	m	m	m ³	m ³	m ³	m ³	m ³	m ³	m ³	t/m ³	t/m ³	t/m ³	t/m ³	t/m ³	t/m ³	t/m ³	t/m ³	t/m ³	m/s ²
Fels, hart fest	1,00	1,00	0,01	1,00	0,01	1,01	0,99	0,01	2,97	0,01	2,98	1,98	1,99	71,62	89,2	88,4	76,42	89,3	88,5	9,807
Fels, schwer lösbar	1,00	1,00	0,09	1,00	0,09	1,09	0,92	0,08	2,76	0,08	2,84	1,84	1,92	8,573	83,3	76,9	9,148	83,8	77,7	9,807
Fels, normal lösbar	1,00	1,00	0,18	1,00	0,18	1,18	0,85	0,15	2,55	0,15	2,70	1,70	1,85	4,253	76,8	64,8	4,539	77,6	66,2	9,807
Geröll, dicht gelagert	1,00	1,00	0,27	1,00	0,27	1,27	0,79	0,21	2,37	0,21	2,58	1,58	1,79	2,799	70,3	54,5	2,987	71,5	56,2	9,807
Geröll, lose gelagert	1,00	1,00	0,36	1,00	0,36	1,36	0,73	0,27	2,20	0,27	2,47	1,47	1,73	2,081	64,1	45,9	2,199	65,5	47,7	9,807
Kies, fest gelagert	1,00	1,00	0,47	1,00	0,47	1,47	0,68	0,32	2,05	0,32	2,36	1,36	1,68	1,608	58,1	38,8	1,716	59,8	40,6	9,807
Kies, lose gelagert	1,00	1,00	0,58	1,00	0,58	1,58	0,63	0,37	1,90	0,37	2,27	1,27	1,63	1,299	52,4	33,0	1,386	54,2	34,7	9,807
Kies, schluffig	1,00	1,00	0,70	1,00	0,70	1,70	0,59	0,41	1,76	0,41	2,18	1,18	1,59	1,071	47,0	28,2	1,143	48,8	29,7	9,807
Boden, bindig plast.	1,00	1,00	0,84	1,00	0,84	1,84	0,54	0,46	1,63	0,46	2,09	1,09	1,54	0,894	41,8	24,1	0,954	43,6	25,5	9,807
Boden, bindig weich	1,00	1,00	1,00	1,00	1,00	2,00	0,50	0,50	1,50	0,50	2,00	1,00	1,50	0,750	36,9	20,6	0,800	38,7	21,8	9,807
Boden, bindig breiig	1,00	1,00	1,19	1,00	1,19	2,19	0,46	0,54	1,37	0,54	1,91	0,91	1,46	0,629	32,2	17,5	0,672	33,9	18,6	9,807
Löß, breiig	1,00	1,00	1,43	1,00	1,43	2,43	0,41	0,59	1,24	0,59	1,82	0,82	1,41	0,525	27,7	14,7	0,560	29,3	15,7	9,807
Löß, fließfähig	1,00	1,00	1,73	1,00	1,73	2,73	0,37	0,63	1,10	0,63	1,73	0,73	1,37	0,433	23,4	12,2	0,462	24,8	13,0	9,807
Löß, wässrig	1,00	1,00	2,14	1,00	2,14	3,14	0,32	0,68	0,95	0,68	1,64	0,64	1,32	0,350	19,3	9,92	0,373	20,5	10,6	9,807
Urstaub u. Wasser	1,00	1,00	2,75	1,00	2,75	3,75	0,27	0,73	0,80	0,73	1,53	0,53	1,27	0,273	15,3	7,77	0,291	16,2	8,29	9,807
Urstaub u. Wasser	1,00	1,00	3,73	1,00	3,73	4,73	0,21	0,79	0,63	0,79	1,42	0,42	1,21	0,201	11,4	5,74	0,214	12,1	6,12	9,807
Urstaub u. Wasser	1,00	1,00	5,67	1,00	5,67	6,67	0,15	0,85	0,45	0,85	1,30	0,30	1,15	0,132	7,53	3,78	0,141	8,03	4,04	9,807
Urstaub u. Wasser	1,00	1,00	11,4	1,00	11,4	12,4	0,08	0,92	0,24	0,92	1,16	0,16	1,08	0,066	3,75	1,88	0,070	4,01	2,01	9,807
Urstaub u. Wasser	1,00	1,00	95,5	1,00	95,5	96,5	0,01	0,99	0,03	0,99	1,02	0,02	1,01	0,008	0,45	0,23	0,008	0,48	0,24	9,807
Urstaub u. Wasser	1,00	1,00	573	1,00	573	574	0,00	1,00	0,01	1,00	1,00	0,00	1,00	0,001	0,08	0,04	0,001	0,08	0,04	9,807

Anlage 3

Kräfte und Kraftmeter von nassen Böden

gegen eine 10,0 m hohe Wand.
Ermittelt nach physikalischer Ebene
und den Ergänzungen ($\beta < 45^\circ$).

Berechnungen

bezogen auf die Körpertiefe $a = 1,00$ m.

Bodenarten von Fels bis Urstaub und Urstaub unter Wasser	Neigungs- winkel	Ermittlung der Gewichtskraft Gn Höhe	Breite bo	Fläche Ao	Dichte png	Kraft Gn	Ermittlung der Kräfte										Ermittlung der Kraftmeter											
							sin β	cos β	sin ² β	cos ² β	sin β cos β	FN	FH	Hv	Nv	Hf	gin	fn	fh	fv	nv	hf	kn/m ²	m	m	m	m	m
Fels, hart fest	89,2	71,62	10,00	0,140	0,698	2,979	20,40	1,000	0,014	1,000	0,000	0,014	0,28	20,4	20,4	0,00	0,28	2,04	0,14	10,00	10,00	0,00	0,00	0,14	10,00	10,00	0,00	0,14
Fels, schwer lösbar	83,3	8,573	10,00	1,167	5,833	2,839	162,4	0,993	0,116	0,987	0,013	0,115	18,8	161	160	2,18	18,7	16,24	1,16	9,93	9,87	0,13	1,15	1,16	9,93	9,87	0,13	1,15
Fels, normal lösbar	76,8	4,253	10,00	2,351	11,76	2,700	311,3	0,973	0,229	0,948	0,052	0,223	71,2	303	295	16,3	69,4	31,13	2,29	9,73	9,48	0,52	2,23	2,29	9,73	9,48	0,52	2,23
Geröll, dicht gelagert	70,3	2,799	10,00	3,573	17,86	2,577	451,5	0,942	0,336	0,887	0,113	0,317	152	425	400	51,1	143	45,15	3,36	9,42	8,87	1,13	3,17	3,36	9,42	8,87	1,13	3,17
Geröll, lose gelagert	64,1	2,061	10,00	4,853	24,26	2,466	586,9	0,900	0,437	0,809	0,191	0,393	256	528	475	112	231	58,69	4,37	9,00	8,09	1,91	3,93	4,37	9,00	8,09	1,91	3,93
Kies, fest gelagert	58,1	1,608	10,00	6,217	31,09	2,364	720,7	0,849	0,528	0,721	0,279	0,448	381	612	520	201	323	72,07	5,28	8,49	7,21	2,79	4,48	5,28	8,49	7,21	2,79	4,48
Kies, lose gelagert	52,4	1,299	10,00	7,698	38,49	2,268	856,1	0,792	0,610	0,628	0,372	0,483	522	678	538	319	414	85,61	6,10	7,92	6,28	3,72	4,83	6,10	7,92	6,28	3,72	4,83
Kies, schluffig	47,0	1,071	10,00	9,336	46,68	2,176	996,3	0,731	0,682	0,534	0,466	0,499	680	728	532	464	497	99,63	6,82	7,31	5,34	4,66	4,99	6,82	7,31	5,34	4,66	4,99
Boden, bindig plast.	41,8	0,894	10,00	11,19	55,94	2,087	1145	0,666	0,746	0,444	0,556	0,497	854	763	509	637	569	114,5	7,46	6,66	4,44	5,56	4,97	7,46	6,66	4,44	5,56	4,97
Boden, bindig weich	36,9	0,750	10,00	13,33	66,67	2,000	1308	0,600	0,800	0,360	0,640	0,480	1046	785	471	837	628	130,8	8,00	6,00	3,60	6,40	4,80	8,00	6,00	3,60	6,40	4,80
Boden, bindig breiig	32,2	0,629	10,00	15,89	79,45	1,913	1490	0,533	0,846	0,284	0,716	0,451	1261	794	423	1067	672	149,0	8,46	5,33	2,84	7,16	4,51	8,46	5,33	2,84	7,16	4,51
Löß, breiig	27,7	0,525	10,00	19,04	95,21	1,824	1703	0,465	0,885	0,216	0,784	0,412	1508	792	368	1335	701	170,3	8,85	4,65	2,16	7,84	4,12	8,85	4,65	2,16	7,84	4,12
Löß, fließfähig	23,4	0,433	10,00	23,09	115,5	1,732	1961	0,397	0,918	0,158	0,842	0,365	1800	779	310	1652	715	196,1	9,18	3,97	1,58	8,42	3,65	9,18	3,97	1,58	8,42	3,65
Löß, wässrig	19,3	0,350	10,00	28,59	143,0	1,636	2294	0,330	0,944	0,109	0,891	0,312	2165	757	250	2044	715	229,4	9,44	3,30	1,09	8,91	3,12	9,44	3,30	1,09	8,91	3,12
Urstaub u. Wasser	15,3	0,273	10,00	36,63	183,2	1,534	2755	0,263	0,965	0,069	0,931	0,254	2658	726	191	2564	700	275,5	9,65	2,63	0,69	9,31	2,54	9,65	2,63	0,69	9,31	2,54
Urstaub u. Wasser	11,4	0,201	10,00	49,76	248,8	1,423	3471	0,197	0,980	0,039	0,961	0,193	3403	684	135	3337	671	347,1	9,80	1,97	0,39	9,61	1,93	9,80	1,97	0,39	9,61	1,93
Urstaub u. Wasser	7,53	0,132	10,00	75,62	378,1	1,300	4819	0,131	0,991	0,017	0,983	0,130	4778	632	82,8	4737	626	481,9	9,91	1,31	0,17	9,83	1,30	9,91	1,31	0,17	9,83	1,30
Urstaub u. Wasser	3,75	0,066	10,00	152,4	762,0	1,161	8675	0,065	0,998	0,004	0,996	0,065	8657	568	37,2	8638	567	868	9,98	0,65	0,04	9,96	0,65	9,98	0,65	0,04	9,96	0,65
Urstaub u. Wasser	0,45	0,008	10,00	1273	6366	1,021	63725	0,008	1,000	0,000	1,000	0,008	63723	500	3,93	63721	500	6373	10,00	0,08	0,00	10,00	0,08	10,00	0,08	0,00	10,00	0,08
Urstaub u. Wasser	0,08	0,001	10,00	7639	38197	1,003	375905	0,001	1,000	0,000	1,000	0,001	####	492	0,64	####	492	37590	10,00	0,01	0,00	10,00	0,01	10,00	0,01	0,00	10,00	0,01